

NORTHWESTERN UNIVERSITY

Cell Culture Systems Inspired by the Hematopoietic Stem Cell Niche

A DISSERTATION

SUBMITTED TO THE GRADUATE SCHOOL  
IN PARTIAL FULFILLMENT OF THE REQUIREMENTS

for the degree

DOCTOR OF PHILOSOPHY

Field of Chemical Engineering

By

James A. King

Evanston, Illinois

December 2007



## ABSTRACT

### Cell Culture Systems Inspired by the Hematopoietic Stem Cell Niche

James A. King

The hematopoietic stem cell (HSC) niche is the site where HSCs reside in vivo. The HSC niche is formed by supporting cells that provide structure and appropriate environmental cues for HSCs. In this study, three components of the HSC niche were evaluated for their influence on HSC expansion ex vivo: (1) culture in reduced oxygen tension, (2) presentation of TPO-mimetic (TPOm) lipid-peptide constructs in a hybrid-bilayer membrane, and (3) immobilization of stem cell factor (SCF) for cell culture.

The HSC niche is localized to areas of reduced oxygen tension and others have shown that reduced  $pO_2$  cultures enhance the maintenance of HSCs. We hypothesized that a detailed analysis of HSC division would clarify how reduced oxygen tension alters HSC maintenance. However, using CFSE-labeled CD34<sup>+</sup> cells, our results showed little difference in cell division profile, overall cellular expansion, or expansion/retention of CD34<sup>+</sup>Thy1<sup>+</sup> cells between low oxygen tension and normoxia.

Three forms of TPOm were synthesized: PEGylated TPOm (TPOm-PEG) and two forms of lipid-tethered TPOm (TPOm-L). Using M07e cells, we determined that TPOm-PEG and TPOm-L elicited similar activation of the signaling molecules ERK 1,2 and STAT5. Studies evaluating the expansion of HSCs showed similar levels of overall expansion and fraction of

CD34<sup>+</sup>Thy1<sup>+</sup> cells for TPOM-L and TPOM-PEG. Thus, TPOM-L did elicit cellular responses, but did not enhance expansion of HSCs as compared to soluble TPOM-PEG.

In vivo, SCF is presented in both membrane-associated and soluble forms. Membrane-associated SCF has been shown to promote HSC self-renewal, while soluble SCF promotes the expansion of lineage-committed progenitors. Two different systems with biotin-binding molecules were used to evaluate our hypothesis that immobilization of SCF would improve HSC expansion. Investigation of the first system (commercially-available NeutrAvidin-coated plates) indicated that biotinylated-SCF released from the surface; therefore, the results could not be attributed directly to immobilized SCF. The second system incorporated a non-fouling, biotinylated poly(ethylene glycol) (PEG) molecules anchored to TiO<sub>2</sub>-coated surfaces via 2,4-dihydroxyphenylalanine (DOPA). Biotinylated-SCF was immobilized to the surface via an avidin bridge to biotin-DOPA-PEG. Surfaces characterized using M07e cells showed that immobilized biotinylated-SCF can elicit a specific adhesive interaction, activate ERK 1/2, and promote cell growth.

## ACKNOWLEDGEMENTS

I would like to acknowledge all of the help I have received during my time at Northwestern. For their help and advice in the undertaking of my many different projects I would like to thank Bill, Phil, and Terry. With the many different project that I worked on it was not always smooth sailing, but I would like to thank Bill for standing by me and giving me the encouragement that was needed to complete this work. Many people helped me immeasurably in the lab. I would like to thank Dominic and Tor for teaching me the basics of mammalian cell culture, showing me how to do research, and working with me to get my thesis projects started. Peter and Lisa for all of their help, insightful comments, and encouragement along the way. Members of Phil's lab—Marsha, Bi-Huang, Simonida, Jeff, Haeshin, and Andrea—for sharing their knowledge of synthesis and characterization and not treating me like an outsider in their labs. Finally, I would like to thank Rico, Shara, and Sofia for all of their help creating/characterizing surfaces and all of their help down the final stretch.

For the non-technical part of this thesis, i.e. life in the real world, I would like to thank my family and friends for all their support and encouragement. Specifically, I would like to thank my parents for instilling in me the desire to improve myself through education and their financial support to accomplish this goal. Roger and Merilee for their encouragement and unending support. Peter and Angie for their willingness to help me with tough decisions and their company on many Saturday nights allowing me to 'escape' from the lab. Jamie and Christa for always lending a sympathetic ear and providing perspective on the challenges I faced. Most of all would like to thank Lora; I cannot describe in words what you have meant to me during this endeavor. Your constant encouragement and unending support got me through the tough times

and your enthusiasm and smile made the good times that much better. Without all of your sacrifices there is no way that I would have completed this.

**LIST OF ABBREVIATIONS**

7-AAD	7-Aminoactinomycetes
Ac <sub>2</sub>	Diacetyl
ACN	Acetonitrile
Ala, A	Alanine
Ar	Argon
Arg, R	Arginine
BFU-E	Burst forming unit-Erythrocyte
BM	Bone Marrow
BOP	benzotriazole-1-yl-oxy-tris(dimethylamino) phosphonium hexafluorophosphate
BP	biotin to protein ratio
BSA	Bovine serum albumin
biotin-SCF	Biotinylated stem cell factor
CAMs	Cell adhesion molecules
CB	Cord Blood
CFSE	Carboxyfluorescein diacetate, succinimidyl ester
CFU	Colony Forming Unit
CFU-GM	Colony Forming Unit-Granulocyte Macrophage
CFU-Mix	Colony Forming Unit-
CFSE	carboxyfluorescein diacetate, succinimidyl ester
CHO	Chinese Hamster Ovary
CLP	Common lymphoid progenitors

CMP	Common myeloid progenitors
Da	Dalton ~ atomic mass unit
DCC	<i>N,N'</i> -dicyclohexylcarbodiimide
DCM	Dichloromethane
DIEA	diisopropylethylamine
DMAP	4-Dimethylaminopyridine
DMF	dimethylformamide
DOPA	2,4-dihydroxyphenylalanine
DP	DOPA <sub>3</sub> PEG <sub>2000</sub>
DPb	DOPA <sub>3</sub> PEG <sub>3400</sub> biotin
DPG	1,2-dipalmitoyl- <i>sn</i> -glycerol
DPG-Su	1,2-dipalmitoyl- <i>sn</i> -glycerol-succinic anhydride
DPPC	1,2-Dipalmitoyl- <i>sn</i> -Glycero-3-Phosphatidylcholine
DPPE	1,2-Dipalmitoyl- <i>sn</i> -Glycero-3-Phosphoethanolamine
EDTA	Ethylenediamine tetraacetic acid
Et <sub>2</sub> O	Diethyl ether
EPO	Erythropoietin
FBS	Fetal bovine serum
FL	Flt-3 ligand
G-CSF	Granulocyte Colony Stimulating Factor
Glu, E	Glutamic Acid
Gln, Q	Glutamine

Gly, G	Glycine
GM-CSF	Granulocyte/Macrophage Colony Stimulating Factor
HABA	2-hydroxyazobenzene-4'-carboxylic acid
HBM	Hybrid bilayer membrane
HBSS	Hank's balanced salt solution
HBF	Hank's balanced salt solution with 20% FBS
HEPES	4-(2-hydroxyethyl)-1-piperazineethanesulfonic acid
HGF	High growth factors
HMPB	4-(4-Hydroxymethyl-3-methoxyphenoxy)-butyric acid
HOBt	<i>N</i> -hydroxybenzotriazole
HPC	Hematopoietic progenitor cell
HSC	Hematopoietic stem cell
IgG	Immunoglobulin
IL-3	Interleukin-3
IL-6	Interleukin-6
Ile, I	Isoleucine
IMDM	Iscove's modified Dulbecco's medium
JAK	Janus family kinase
kDa	kilo-Dalton
LC	Long chain
Leu, L	Leucine
Lys, K	Lysine

MALDI-TOF	Matrix assisted laser desorption/ionization time-of-flight
MAPK	Mitogen activated protein kinase
MFI	Mean Fluorescence Intensity
MGDF	Megakaryocyte Growth and Development Factor
MIP-1 $\alpha$	Macrophage inflammatory protein 1 $\alpha$
mPB	Mobilized Peripheral Blood
MS	Mass spectrometry
MWCO	Molecular weight cutoff
NCA	<i>N</i> -carboxyanhydride
NHS	<i>N</i> -hydroxysuccinimide
NMP	1-Methyl-2-pyrrolidinone
NOD/SCID	Non-Obese Diabetic/Severe combined immunodeficiency
OTS	Octaldecyltrichlorosilane
PAB	PBS/0.05% Sodium azide/0.1% BSA
PBS	Phosphate buffered saline
PBS-B	PBS supplemented with 1.0 % wt. BSA
PDGF	Platelet derived growth factor
PE	Phycoerythrin
PEB	PBS with 0.5% BSA and 2mM EDTA
PEG	Poly(ethylene glycol)
PerCP	Peridinin chlorophyll protein
PI	Propidium Iodide

PI3-K	Phosphatidylinositol 3-kinase
pO <sub>2</sub>	partial pressure due to Oxygen, Oxygen tension
Pro, P	Proline
rhTPO	recombinant human TPO
ROS	Reactive oxygen species
RTK	Receptor tyrosine kinase
SCF	Stem cell factor
SFM	Serum free media
STAT	signal transducers and activators of transcription
TCPS	Tissue culture polystyrene
TFA	Trifluoroacetic acid
TGF- $\beta$	Transforming growth factor- $\beta$
Thr, T	Threonine
TIS	Triisopropylsilane
TPO	Thrombopoietin
TPOm	Thrombopoietin mimetic peptide
TPOm-PEG	Thrombopoietin mimetic peptide, PEGylated
TPOm-1L	Thrombopoietin mimetic peptide, PEGylated with one lipid chain
TPOm-2L	Thrombopoietin mimetic peptide, PEGylated with two lipid chains
TPOm-L	Thrombopoietin mimetic peptide, PEGylated with lipid
Trp, W	Tryptophan

	12
<b>ABSTRACT</b> .....	3
<b>ACKNOWLEDGMENTS</b> .....	5
<b>LIST OF ABBREVIATIONS</b> .....	7
<b>CHAPTER 1: INTRODUCTION AND SPECIFIC AIMS</b> .....	23
1.1 Introduction.....	23
1.2 Aims and objectives.....	27
1.2.1 Aim 1: Exploration of reduced oxygen tensions for HSC self-renewal .....	27
1.2.2 Aim 2: Exploration of immobilized SCF for increased HSC self-renewal .....	28
1.2.3 Aim 3: Exploration of TPOm for increased HSC self-renewal .....	29
<b>CHAPTER 2: BACKGROUD</b> .....	31
2.1 Hematopoiesis and the hematopoietic stem cell .....	31
2.1.1 HSC cell sources .....	32
2.1.2 Identification and isolation of HSCs.....	33
2.2 The hematopoietic microenvironment .....	34
2.2.1 Important cells and growth factors within the hematopoietic microenvironment .....	34
2.2.2 Physiochemical characteristics of the bone marrow microenvironment .....	35
2.3 Ex vivo expansion of HSCs .....	35
2.3.1 Common culture techniques .....	36
2.3.2 Influence of culture environmental cells.....	37
2.4 Characteristics of SCF and its receptor, c-Kit .....	39
2.4.1 SCF .....	39
2.4.2 Membrane-associated and soluble SCF.....	42

	13
2.4.3 c-Kit .....	46
2.4.4 Cellular activation and signal transduction.....	46
2.5 Characteristics of TPO and its receptor cMpl.....	48
2.5.1 TPO .....	48
2.5.2 cMpl, cellular activation, and signal transduction .....	52
2.6 Immobilization proteins and peptides to surfaces.....	54
2.6.1 Protein immobilization.....	54
2.6.1.1 Considerations for the immobilization of SCF .....	55
2.6.1.2 SCF Immobilization strategy .....	55
2.6.2 Peptide immobilization .....	56
2.6.2.1 Considerations for the immobilization of TPOM.....	56
2.6.2.2 Hybrid bilayer membranes.....	57
<b>CHAPTER 3: MATERIALS AND METHODS .....</b>	<b>58</b>
3.1 Synthetic methods.....	58
3.1.1 Lipopeptide synthesis.....	58
3.1.2 Lipopeptide purification and analysis.....	62
3.1.3 Synthesis of DOPA <sub>3</sub> PEG .....	62
3.1.4 Synthesis of DOPA <sub>3</sub> PEG-biotin .....	65
3.1.5 Biotinylation of SCF .....	67
3.1.6 Determination of molar ratios of biotin incorporated into SCF.....	69
3.1.6.1 MALDI-TOF MS of bSCF .....	69
3.1.6.2 HABA assay.....	69

	14
3.2 Surface preparation .....	69
3.2.1 Silanization of glass surfaces .....	69
3.2.2 Preparation of culture cassettes and supported lipid monolayers .....	70
3.2.3 Vesicle preparation and deposition .....	70
3.2.4 Immobilization of bSCF to NeutrAvidin-coated surfaces .....	71
3.2.5 Preparation of DOPA-PEG surfaces in culture cassettes .....	71
3.2.6 Immobilization of bSCF to DOPA-PEG-biotin surfaces .....	72
3.3 General cell culture methods .....	73
3.3.1 Cell counts .....	73
3.3.2 Culture of M07e cells .....	73
3.3.3 Culture of TF-1 cells .....	74
3.3.4 Culture of KG-1a cells .....	74
3.3.5 Culture of CD34+ selected cells .....	74
3.3.5.1 Culture in NeutrAvidin-coated polystyrene plates with biotinylated SCF .....	74
3.3.5.2 Primitive cell expansion and maintenance with TPOM .....	75
3.3.5.3 Megakaryocyte differentiation experiments with TPOM .....	75
3.3.6 Colony forming cell assay .....	75
3.4 Cell characterization .....	76
3.4.1 Flow cytometry .....	76
3.4.1.1 Apoptosis .....	76
3.4.1.2 Cell cycle .....	77
3.4.1.3 CD34 and Thy1 expression .....	77

	15
3.4.1.4 Flow cytometry for the analysis of Mk cells .....	77
3.4.1.5 Cell signaling assay.....	78
3.4.1.6 Carboxyfluorescein diacetate, succinimidyl ester (CFSE) labeling of cells.....	79
3.4.2 Adhesion assay.....	80
<b>CHAPTER 4:</b>	
<b>EXPLORATION OF REDUCED OXYGEN TENSION FOR HSC SELF-RENEWAL .....</b>	<b>81</b>
4.1 Introduction.....	81
4.2 Development of tools for analysis of cellular processes.....	82
4.2.1 Cell division tracking protocol development.....	82
4.2.2 Development of flow cytometric cell signaling assays.....	89
4.3 Primary cell cultures at 5% and 20% O <sub>2</sub> .....	91
4.4 Discussion of primary cell experiments with low oxygen tension .....	101
<b>CHAPTER 5: STUDIES WITH TPO MIMETIC PEPTIDE AND LIPOPEPTIDES .....</b>	<b>102</b>
5.1 Introduction.....	102
5.2 Results.....	105
5.2.1 Synthesis of TPOm lipopeptides.....	105
5.2.2 Activation studies using M07e cells .....	105
5.2.2.1 Activation of ERK 1,2 and STAT5 with soluble TPOm .....	105
5.2.2.2 Immobilized TPOm lipopeptides induce activation of STAT5 and ERK 1,2 at similar levels as soluble material .....	113
5.2.2.3 Activation of STAT5 and ERK 1,2 is enhanced in M07e cells stimulated by TPOm- 1L and SCF .....	119
5.2.2.4 Stimulatory effect of carrier lipids.....	121

	16
5.2.2.5 Release of TPOm-lipopeptides from lipid surfaces .....	123
5.2.3 Cell cultures with TPOm .....	126
5.2.3.1 M07e cell culture with TPOm.....	126
5.2.3.2 Culture of CD34+ selected cells in cocktail containing SCF and FL.....	130
5.2.3.3 Culture of CD34+ selected cells with only TPOm .....	142
5.3 Discussion.....	147
5.3.1 Synthesis of TPOm .....	147
5.3.2 Activation of ERK 1,2 and STAT5 with TPOm stimulation.....	147
5.3.3 Culture of human CD34+ selected cells with TPOm molecules .....	148
<b>CHAPTER 6: EXPERIMENTS WITH BIOTINYLATED SCF .....</b>	<b>150</b>
6.1 Introduction.....	150
6.2 Results for the biotinylation of SCF .....	152
6.3 Results with biotin-SCF immobilized on NeutrAvidin-coated plates .....	158
6.3.1 Immobilized biotin-SCF on NeutrAvidin-coated plates.....	158
6.3.2 Adhesion of M07e cells to immobilized biotin-SCF on NeutrAvidin-coated plates.....	161
6.3.3 Confounding effects due to release of surface-immobilized biotin-SCF.....	163
6.3.4 Immobilized biotin-SCF on NeutrAvidin-coated plates influence on proliferation and differentiation of CD34+ cells .....	166
6.4 Results for DOPA-PEG Surfaces for biotin-SCF Presentation .....	175
6.4.1 Synthesis of DOPA-PEG and DOPA-PEG-biotin.....	176
6.4.2 Characterization of DP and DPb surfaces.....	176
6.4.3 biotin-SCF Supports M07e Cell Adhesion and ERK Activation.....	180

	17
6.4.4 Release of biotin-SCF from DPb surfaces .....	187
6.4.4.1 Release of biotin-SCF from DPb surfaces analyzed by cell signaling assays .....	187
6.4.4.2 Release of biotin-SCF from DPb surfaces by cultures with conditioned media.....	190
6.4.5 CD34+ cell cultures on DP and DPb-NeutrAvidin-biotin-SCF surfaces .....	195
6.5 Discussion .....	205
6.5.1 Biotinylation of SCF .....	205
6.5.2 Comparison of commercially available NeutrAvidin-coated wells and DPb surfaces..	205
6.5.3 Cultures on commercially available NeutrAvidin-coated surfaces .....	207
6.5.4 Characterization of DP and DPb surfaces.....	208
6.5.5 Cultures on DOPA-PEG surfaces .....	209
<b>CHAPTER 7: CONCLUSIONS AND RECOMMENDATIONS</b> .....	<b>211</b>
7.1 Studies with reduced oxygen tension.....	211
7.1.1 Conclusions.....	211
7.1.2 Recommendations for future reduced oxygen cultures .....	211
7.2 Studies with TPO mimetic molecules.....	212
7.2.1 Conclusions.....	212
7.2.2 Recommendations.....	213
7.3 Studies with immobilized biotin-SCF on surfaces with biotin-binding molecules .....	214
7.3.1 Conclusions.....	214
7.3.2 Recommendations for DOPA-PEG-biotin surfaces and biotinylated SCF.....	215
7.4 Overall recommendations .....	218
<b>REFERENCES</b> .....	<b>220</b>

## LIST OF TABLES

Table 2.4.1: SCF amino acid sequence.....	41
Table 2.5.1: TPO amino acid sequence .....	50
Table 4.3.1: Conditions summary for three-day cultures of BM CD34+cells.....	93
Table 5.2.1: Concentrations of TPOM-PEG and rhTPO in dose response experiment shown in Figure 5.2.13.....	127
Table 5.2.2: Conditions evaluated in six-day expansion cultures of BM CD34+ cells with TPOM-2L as shown in Figure 5.2.15 .....	132
Table 5.2.3: Conditions evaluated in six-day expansion cultures of BM CD34+ cells with TPOM-1L as shown in Figures 5.2.16 and 5.2.17 .....	137
Table 6.3.1: Biotin-SCF immobilized on NeutrAvidin-coated surfaces.....	159

## LIST OF FIGURES

Figure 1.1.1: Hematopoietic hierarchy of differentiation .....	26
Figure 2.4.1: Schematic representation of SCF .....	45
Figure 2.5.1: Schematic representation of TPO.....	51
Figure 2.5.2: TPO signaling cascade .....	53
Figure 3.1.1: Schematic of TPOMimetic molecules.....	61
Figure 3.1.2: Schematic of mPEG-DOPA <sub>3</sub> .....	64
Figure 3.1.3: Schematic of biotin-PEG-DOPA <sub>3</sub> .....	66
Figure 3.1.4: Schematic of sulfo-NHS-LC biotin.....	68
Figure 4.2.1: Cell division tracking of a dual positive population K <sub>g</sub> -la cells for 10 days .....	84

	19
Figure 4.2.2: Development of a ‘no division’ control .....	87.
Figure 4.2.3: Development of flow cytometric cell signaling assays for phosphorylated ERK and Akt .....	90
Figure 4.3.1: Overall expansion of BM CD34+ cells in three-day reduced oxygen tension cultures .....	94
Figure 4.3.2: Expansion of CD34+ cells in three-day reduced oxygen tension cultures.....	95
Figure 4.3.3: Expansion of CD34+Thy1+ cells in three-day reduced oxygen tension cultures ....	96
Figure 4.3.4: Cell density of BM CD34+ cells cultured in reduced oxygen tension or elevated growth factor concentrations for three days.....	97
Figure 4.3.5: Expansion of CD34+Thy1+ cells cultured in reduced oxygen tension or elevated growth factor concentrations for three days .....	98
Figure 4.3.6: Overall cell division pattern of CD34+ cells cultured for three days .....	99
Figure 4.3.7: Cell division pattern of CD34+Thy1+ cells cultured for three days .....	100
Figure 5.2.1: Effect of cell density during starvation .....	107
Figure 5.2.2: Effects of high cell density on pERK 1,2 basal levels in unstimulated cells .....	109
Figure 5.2.3: Representative histograms showing results from cell-signaling assay .....	110
Figure 5.2.4: Phosphorylation of ERK 1,2 and STAT5 in M07e cells stimulated by TPOM-PEG.....	111
Figure 5.2.5: Comparison of ERK 1,2 activation induced by rhTPO and TPOM-PEG in M07e cells.....	112
Figure 5.2.6: Fraction of M07e cells adherent to TPOM-lipopeptides .....	114

Figure 5.2.7: Activation of ERK 1,2 and STAT5 in M07e cells stimulated on DPPC surfaces with various amounts of TPOm-1L .....	115
Figure 5.2.8: Activation of ERK 1,2 and STAT5 in M07e cells stimulated on DPPC surfaces with various amounts of TPOm-2L .....	116
Figure 5.2.9: Time course cell signaling activation studies.....	117
Figure 5.2.10: Activation of ERK 1,2 and STAT5 in M07e cells when stimulated with 10 ng/mL soluble SCF immobilized TPOm-1L .....	120
Figure 5.2.11: Unstimulated M07e cell activation on various carrier lipids .....	122
Figure 5.2.12: pERK and pSTAT5 levels in M07e cells activated by supernatants removed from surfaces .....	124
Figure 5.2.13: Dose-dependent M07e cell expansion after seven days.....	128
Figure 5.2.14: Expansion of M07e cells on lipid surfaces.....	129
Figure 5.2.15: Representative CD34 vs. Thy1 dot plots.....	133
Figure 5.2.16: Expansion of BM CD34+ cells cultured on TPOm-2L surfaces.....	135
Figure 5.2.17: Expansion of BM CD34+ cells cultured on TPOm-1L surfaces.....	138
Figure 5.2.18: Expansion of BM CD34+ cells cultured on TPOm-1L surfaces supplemented with IL-3 .....	140
Figure 5.2.19: Results of TPO only culture of mPB CD34+ cells.....	143
Figure 5.2.20: Results of TPO only culture of BM CD34+ cells .....	144
Figure 6.2.1: MALDI-MS spectra of biotin-SCF biotinylated at BP ratio of 2:1.....	154
Figure 6.2.2: MALDI-MS spectra of biotin-SCF biotinylated at BP ratio of 100:1.....	155
Figure 6.2.3: Location of the biotinylated lysine when a single LC-biotin is added to SCF.....	156

Figure 6.2.4: MALDI-MS spectra for SCF biotinylated with new and old sulfo-NHS-LC-biotin reagent .....	157
Figure 6.3.1: Proliferation of M07e cells in four-day cultures on biotin-SCF-modified NeutrAvidin-coated surfaces .....	160
Figure 6.3.2: Fraction of M07e cells adherent to biotin-SCF-modified NeutrAvidin-coated surfaces .....	162
Figure 6.3.3: Biotin-SCF released from NeutrAvidin-coated surfaces support M07e cell expansion .....	164
Figure 6.3.4: mPB CD34+ cells cultured for nine-day on biotin-SCF-modified NeutrAvidin-coated surfaces .....	168
Figure 6.3.5: Cell expansion in nine-day BM CD34+ cell cultures on biotin-SCF-modified NeutrAvidin-coated surfaces .....	169
Figure 6.3.6: Percentage of CD34+ and CD34+Thy1+ cells from a nine-day BM CD34+ cell culture .....	172
Figure 6.3.7: Number of CFU-GM and BFU-E per input cell from a nine-day BM CD34+ cell culture .....	173
Figure 6.4.1: Streptavidin adsorption onto DPb/DP surfaces .....	178
Figure 6.4.2: Sequential adsorption of NeutrAvidin and biotin SCF onto DPb/DP-coated surfaces .....	179
Figure 6.4.3: Fraction of M07e cells adherent to biotin-SCF-modified DPb surfaces .....	182
Figure 6.4.4: Soluble competition using SCF and the fraction of M07e cells adherent to biotin-SCF-modified DPb surfaces .....	183

Figure 6.4.5: Activation of ERK 1,2 in M07e cells stimulated on biotin-SCF-modified DPb surfaces .....	184
Figure 6.4.6: Comparison of ERK 1,2 activation in M07e cells stimulated on biotin-SCF-modified DPb and with soluble SCF in TCPS wells .....	185
Figure 6.4.7: ERK 1,2 activation of M07e cells by supernatants removed from 2.5% DPb surfaces .....	188
Figure 6.4.8: Biotin-SCF released from DPb surfaces .....	192
Figure 6.4.9: Dose response to SCF for M07e cell expansion in TCPS wells and on DP surfaces .....	193
Figure 6.4.10: Expansion and differentiation of mPB CD34+ cells on DP surfaces.....	198
Figure 6.4.11: Expansion of two separate mPB CD34+ cell samples on surfaces with various concentrations of DPb modified with biotin-SCF .....	201
Figure 6.4.12: Six-day M07e cell expansion on DPb, DP, and TCPS surfaces.....	203
Figure 6.4.13: Comparison of M07e cell expansion when expanded with SCF, SCF + NeutrAvidin, and biotin-SCF .....	204

## **CHAPTER 1: INTRODUCTION AND SPECIFIC AIMS**

### **1.1 INTRODUCTION**

Hematopoiesis is the process of generating the various types of mature blood cells. Most of these mature cells are short lived and must be replaced continuously throughout life. Each day, the average human produces approximately 400 billion mature blood cells [1] classified as either lymphoid or myeloid lineages. Each cell lineage has specific roles and functions that it is specialized to perform.

The development of mature cells can be ordered into a hierarchy of differentiation (Figure 1.1.1, [1]). The totipotent hematopoietic stem cell (HSC) is at the top of the hierarchy. A single totipotent HSC has the potential of producing all hematopoietic cell types. These cells are capable of self-renewal as well as differentiating into committed stem cells (common myeloid progenitors, CMP or common lymphoid progenitors, CLP). The regulation of the HSC's decision to self-renew or differentiate is not very well understood [2] and likely governed by multiple processes including cell-cell, cell-matrix, and growth factor-receptor interactions; environmental conditions; and modulation of intrinsic mechanisms [3]. Once the HSC has differentiated, it loses its self-renewal capacity. The pluripotent stem cells give rise to highly proliferative, differentiated progenitors known as colony forming units (CFU). CFUs continue to differentiate until they no longer are capable of division and mature into the end stage cells.

Ex vivo expansion of hematopoietic stem and progenitor cells holds great potential in a variety of therapeutic applications. HSC transplants are widely used as a treatment for hematological malignancies [4]. It is believed that ex vivo expansion of the small population of HSCs (approximately 1 per 15,000 bone marrow cells [5]) could lead to the mitigation of many

side effects associated with chemotherapy. Current treatment for neutropenia is bone marrow transplantation. Cells for bone marrow transplants are often obtained by mobilizing HSCs from the bone marrow into the peripheral blood for collection. For successful engraftment, each bone marrow transplant must contain approximately  $2 \times 10^7$  total nucleated cells [6] and  $1.5 \times 10^5$  CD34+ cells/kg [7]. Expanding the stem cell pool ex vivo would allow the harvest size to be decreased. This would allow patients not able to mobilize large numbers of cells to serve as their own bone marrow donors. Additionally, the ability to expand HSCs ex vivo would allow for the use of a single cord blood sample ( $\sim 1/10$  the number of HSCs as compared to bone marrow samples [8]) to be used for adult bone marrow transplants [5].

Clinically feasible techniques for ex vivo expansion of HSCs have not been established. Several growth factors have been identified as important to the maintenance of HSCs, including stem cell factor (SCF), Flt-3 ligand (FL), and thrombopoietin (TPO) [9-15]. HSC division in culture is typically associated with differentiation into cells with more limited proliferative potential, even in cultures where these cytokines act on primitive cells.

The lack of ex vivo expansion of HSCs contrasts with the extensive HSC self-renewal in vivo, which has been attributed to HSC residence in a stem cell 'niche'. The niche is comprised of numerous supporting cells and extracellular matrix interactions that provide structure and appropriate environmental cues to the stem cells [16, 17]. These cues come in various forms including cell-cell interactions and binding to membrane-bound or soluble cytokines [18]. The physiochemical conditions are an additional set of important variables that should be controlled. In the body, most cells (excluding lung and brain tissue) are designed to function in about 5%

oxygen [19]. However, most ex vivo studies of hematopoietic cells are conducted in atmospheric oxygen environments, which is likely much higher than the in vivo niche [20-23].

Our hypothesis is that by mimicking key components of the in vivo stem cell niche, we can improve upon the results from established techniques. Developing a better understanding of the processes involved in ex vivo HSC expansion will allow tailoring of cell culture techniques to achieve the desired end product, whether they are undifferentiated or mature cells. The objective of this research is to evaluate different niche components—both the physiochemical environment and the presentation of growth factors—to improve existing methods for the ex vivo expansion of HSCs. To accomplish the goal of improving culture outcomes, we have investigated three strategies to mimic the in vivo niche: culture in reduced oxygen tension, presentation of SCF bound to surfaces, and presentation of TPO mimetic (TPOm) lipid-peptide (lipopeptide) constructs in a hybrid bilayer membrane (HBM).

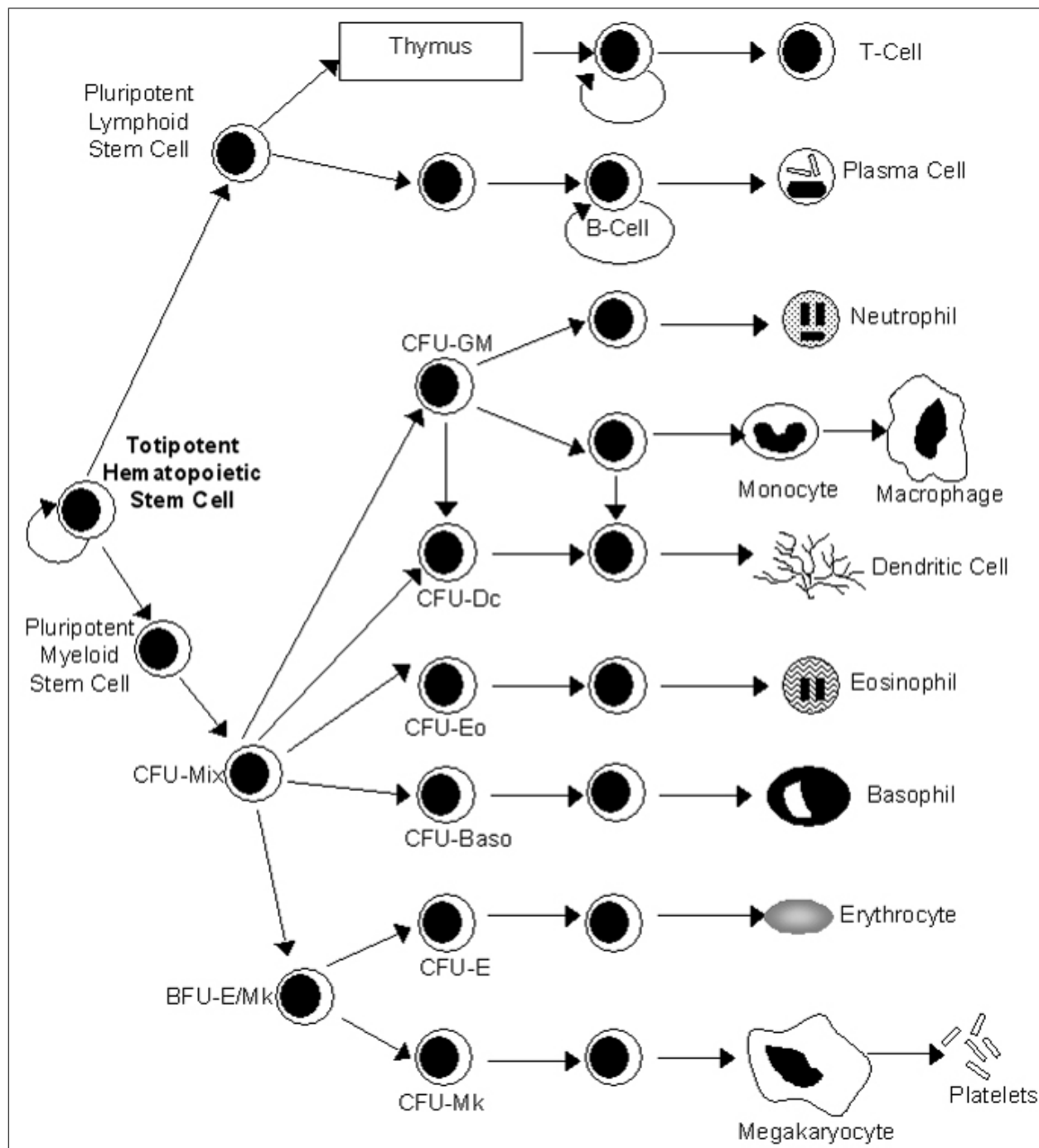


**Figure 1.1.1:** Hematopoietic hierarchy of differentiation.

## **1.2 AIMS AND OBJECTIVES**

### **1.2.1 Aim 1: Exploration of reduced oxygen tensions for HSC self-renewal**

Ex vivo studies of hematopoietic cells in reduced oxygen tension cultures indicate that oxygen is a key parameter in the maintenance of HSC activity [24-29]. Many of these studies have focused on the influence of oxygen tension on specific lineages, rather than HSC self-renewal [30-32].

The few studies focused on self-renewal in lowered oxygen tension used cytokine cocktails that may not be optimized for self-renewal, and could promote differentiation [24-26, 33, 34]. In reduced oxygen tension cultures of mouse bone marrow cells, Cipolleschi and coworkers showed a preferential maintenance of the most primitive cells—cells capable of repopulating mouse bone marrow [24]. Three separate studies by Ivanovic et al. showed that mouse bone marrow CD34+ cells and human mobilized peripheral blood CD34+ cells grown at 1% O<sub>2</sub> maintained stem cell potential (evidenced by repopulating assays), while cultures at 20% O<sub>2</sub> did not [25-27]. These and other studies do not address questions relating to the divisional history of the most immature cells. Under the direction of Drs. William M. Miller and E. Terry Papoutsakis the effects of reduced oxygen tension on HSC culture was evaluated. We hypothesized that a more detailed analysis of cell division history using secondary markers to track the primitive cells would clarify how reduced oxygen tension alters the maintenance of the most primitive cells. However, our results showed little difference in cell division tracking profiles, overall cellular expansion, or expansion/retention of CD34+ progenitors between low oxygen tension and normoxia. Ultimately, the differences between cultures in low oxygen compared to normoxia did not warrant the expense of more detailed analyses.

### **1.2.2 Aim 2: Exploration of immobilized SCF for increased HSC self-renewal**

In the body, SCF is presented in membrane-associated and soluble forms [35-37]. Genetic engineering of mice confirmed that membrane-associated and soluble forms of SCF have different physiological roles [38, 39]. In ex vivo cultures, differential effects of membrane-associated vs. soluble SCF have been demonstrated in studies with stromal cells [40]. Stromal cells exclusively expressing membrane-associated SCF support prolonged human bone marrow mononuclear cell expansion, while stromal cells producing only soluble SCF support extensive amplification of CFUs. It is thought that prolonged activation of c-kit due to decreased internalization explains the differential responses between membrane-associated and soluble SCF [38, 41].

The use of engineered stromal cells is not clinically feasible due to problems associated with contamination and purification of the stem cell product. To combine the benefits of membrane-associated SCF in a more desirable presentation format, we chemically modified SCF with a biotin linker. By modifying a surface with avidin in a non-adhesive background, the biotin-linked SCF can be presented to cells in a surface-bound format. This allows for testing of the hypothesis that immobilized SCF can mimic effects induced by membrane-associated SCF to generate greater numbers of HSCs. We have explored two different systems to evaluate this hypothesis. The first system was developed by Dr. Dominic Chow and employed the use of commercially available NeutrAvidin-coated plates. HSCs expansion on immobilized bSCF surfaces was delayed, but extended as compared to soluble SCF controls. However, control experiments performed later suggested bSCF continually released from the surface, therefore the results could not attributed directly to immobilized SCF. The second system for biotinylated

SCF immobilization was built upon a non-fouling layer of PEG anchored to the surface via the amino acid 2,4-dihydroxyphenylalanine (DOPA). This system was pioneered in Dr. Phil Messersmith's laboratory. In conjunction with Dr. Rico Gunawan, we have been working to expand the functionality of DOPA-PEG surfaces by specifically presenting molecules important in cell culture applications. Characterization of DOPA-PEG-biotin surfaces using M07e cells has shown immobilized bSCF can elicit a specific adhesive interaction, activate ERK 1,2, and promote cell growth.

### **1.2.3 Aim 3: Exploration of TPOM for increased HSC self-renewal**

TPO acts in conjunction with SCF, FL, and other early acting hematopoietic growth factors, such as IL-3, to stimulate the proliferation and maintenance of hematopoietic progenitor cells [9-15]. Many different cytokines are presented in membrane-associated and soluble forms. As noted with SCF, different forms of presentation can have different physiological roles. TPO is not known to be presented in a membrane-associated form. However, the benefits of immobilization are not limited to growth factors that naturally occur in membrane-associated forms. Studies with artificially immobilized insulin—a protein that is not naturally membrane associated—show increased and extended mitogenic signals as compared to soluble insulin in cultures of CHO cells [42].

In contrast to SCF, a peptide mimetic of TPO has been identified [43]. Using phage display, Cwirla and co-workers identified a 14-amino-acid sequence that specifically binds to the TPO receptor c-Mpl, but shares no common sequence homology with full length recombinant human TPO (rhTPO) [43]. Joining two chains of the 14-amino-acid sequence to form a branched peptide dimer—TPO mimetic (TPOM)—creates a molecule that binds c-Mpl with a

much greater affinity than the monomer and is as potent as rhTPO in megakaryocyte (Mk) production from human CD34+ cells [43]. Identifying small molecule mimetics of growth factors allows for custom design of growth factor mimetic molecules for surface presentation. By synthesizing TPOM and conjugating it to lipid, we were able to present this molecule in a hybrid bilayer membrane (HBM).

HBMs have several advantages, including biocompatibility and oriented presentation of ligands. Previously, HBMs have been used by our group and others to examine the interaction with cell adhesion molecules (CAMs) on surfaces [44-47]. In this study we have adapted the cell-membrane-mimetic surfaces developed to investigate cellular interactions with cell adhesion molecule (CAM) ligands to a cytokine mimetic of TPO. This allows for the oriented display of immobilized TPOM lipopeptides (TPOM-L) at low loading densities and controlled ratios. Using HBMs to display TPOM-L, we have studied whether or not the immobilized presentation of TPO alters its ability to expand HSCs. We report on the similar activities of soluble and lipid-immobilized TPOM molecules. Our results show that TPOM-L did elicit cellular responses, but they did not provide enhanced expansion of HSCs.

## **CHAPTER 2: BACKGROUND**

### **2.1 HEMATOPOIESIS AND THE HEMATOPOIETIC STEM CELL**

Mature cells in blood have a finite lifespan and must be continuously replaced. The process of generating various mature blood cell types is known as hematopoiesis. Humans produce approximately 400 billion mature blood cells daily [1]. End term, mature blood cells are not capable of replication and belong to either lymphoid or myeloid lineages. Natural killer cells, B cells, and T cells comprise the lymphoid lineage, while the myeloid line is comprised of the erythrocytic, granulocytic, megakaryocytic, eosinophilic, basophilic, monocytic, and dendritic lineages. Each cell lineage has a specific role and function that it is specialized to perform.

A single totipotent hematopoietic stem cell (HSC) has the potential of producing all hematopoietic cell types (Figure 1.1.1, [1]). HSCs are low frequency cells. The majority of these cells are quiescent residing in the  $G_0$  phase of the cell cycle [48]. When HSCs divide, they can self-renew or differentiate into committed pluripotent stem cells (myeloid or lymphoid pluripotent stem cells). Thus, stem cells are required to make decisions to either self-renew and maintain the stem cell pool, or to differentiate into mature cells and lose the ability to self-renew. The pluripotent stem cells give rise to highly proliferative, committed progenitors known as colony forming units (CFUs). CFUs continue to differentiate until they are no longer capable of division and become mature end-term cells. As cells differentiate and become committed progenitors they begin to express surface markers such as CD33, CD38, HLA-DR. They also express lineage specific markers such as CD2, CD3, CD4, CD8 (T-cells), CD11b, CD15 (granulocyte/monocyte), CD19 (B-cells), CD41a (megakaryocyte), glycophorin A and CD71 (erythrocyte).

The regulation of the balance between self-renewal and differentiation is not well understood [2]. It is unclear whether the decision to self-renew or differentiate is governed by a purely intrinsic/stochastic mechanism, extrinsic signals, or a combination of both [3, 49]. Ultimately, regulation is likely determined by multiple processes including cell-cell interactions, cell-matrix interactions, growth factor-receptor interactions, environmental conditions, and modulation of intrinsic mechanisms [3].

### **2.1.1 HSC cell sources**

There are three main sources of adult HSCs: bone marrow (BM), mobilized peripheral blood (MPB), and cord blood (CB) [50]. Bone marrow is the classic source of HSCs. For years, doctors have performed bone marrow transplants by harvesting the bone marrow of a donor. For the donor, this is an invasive and painful process involving puncturing the bone—typically the hip or sternum—many times and withdrawing bone marrow using a syringe. It is typically performed under general anesthesia [51, 52]. MPB is the preferred cell source for transplantation due to the ease of collection and earlier neutrophil and platelet recovery in patients [53]. Several days prior to collection donors are treated with cytokines such as granulocyte-colony stimulating factor (G-CSF) or SCF, which increases the number of circulating HSCs. For collection of cells, donors are connected to an intravenous line and the cells are isolated via leukaphoresis [52]. MPB however, is the most susceptible to variations due to the preparations used in obtaining the sample and the variability among donors [54].

There are many advantages to using cord blood as a source of HSCs. It is easily accessible with non-invasive procedures and contains a large portion of progenitor cells. Cord blood samples have a lower viral burden of common contaminants such as Epstein-Barr virus

and CMV and lower risk of graft-versus-host disease [52]. Cord blood stem cells have the highest expansion potential [55], but the main disadvantage is the small number of cells collected. The small number of HSCs in cord blood accounts for the longer time to engraft when compared to BM or MPB transplants [51].

### **2.1.2 Identification and isolation of HSCs**

HSCs are primarily defined by their ability to repopulate the blood system of lethally irradiated NOD/SCID mice [56]. Due to the retrospective nature of this assessment, this is not a practical means of isolation. Isolation of cells based on a surface marker is much more practical because cells can be classified, separated, and immediately studied. However, there is not a recognized phenotype that identifies human HSCs. The most widely accepted marker for stem cell activity is the surface sialomucin CD34. Cell separation based on the expression of CD34 has been used to enrich the stem cells within samples [57, 58]. There is heterogeneity among CD34+ cells: some are capable of multiple self-renewal divisions while others are committed progenitors that only produce cells of a specific lineage.

Secondary markers have been used to improve the isolation of HSCs. These markers include the presence of Thy1 or CD133, or the absence of HLA-DR, CD38, and other lineage markers (including glycoporphin A, CD2, CD3, CD4, CD8, CD14, CD15, CD16, CD19, CD20, CD56 and CD66b). The CD34+CD38- subfraction contains an enriched population of primitive HSCs. Several studies show that CD38 expression is down-regulated in culture [59, 60]. Therefore, simply tracking the expansion of CD34+CD38- cells as an indicator of the number of HSCs in culture could be misleading. For the CD34+Thy1+ subpopulation, several studies cite enrichment in multi-potential progenitors [59, 61]. One recent study compared several

secondary markers on mPB cells and concluded that the CD34<sup>+</sup>Thy1<sup>+</sup> subfraction gave the best indication of long-term stem cell activity, based on their repopulating activity in NOD/SCID mice [59]. Another study indicated that Thy1 expression is down-regulated as cells differentiate, not during culture [62]. Given these various findings, CD34<sup>+</sup>Thy1<sup>+</sup> cells were tracked as candidate HSCs in culture in this work.

## **2.2 THE HEMATOPOIETIC MICROENVIRONMENT**

A stem cell niche is a site within the body where stem cells reside. The niche is formed by numerous supporting cells that provide structure and appropriate environmental cues for stem cells [16, 17, 63]. These cues may be interactions with other cells, growth factors, or physiochemical surroundings of the stem cells. In adults, the hematopoietic stem cell niche resides within the bone marrow (BM).

### **2.2.1 Important cells and growth factors within the hematopoietic microenvironment**

The BM is comprised of a heterogeneous mix of hematopoietic cells, non-hematopoietic support cells (known as stroma) and blood vessels. Stromal cells include osteoblasts, adipocytes, macrophages, endothelial and adventitial reticular cells [16, 17]. They provide hematopoietic cells the with growth factors and other signals needed for survival and differentiation [63].

A large volume of experimental evidence suggests that HSCs interact closely with osteoblasts located near the endosteum. The endosteum is located at the interface between the bone marrow and the inner surface of the bone [17]. Examination of lineage-negative murine BM cells labeled with (5 and 6)-carboxyfluorescein diacetate, succinimidyl ester (CFSE) showed preferential homing to the BM endosteal surface [64]. Additionally, using genetic manipulation to artificially increase the number of osteoblasts, two independent research groups presented a

direct correlation between an increase of HSCs and increased numbers of osteoblasts [65, 66]. This, coupled with studies showing that specific ablation of osteoblasts results in depletion of HSCs, [67] implicates that osteoblasts are important in maintaining HSCs.

### **2.2.2 Physiochemical characteristics of the bone marrow microenvironment**

To supply the bone marrow with nutrients, arterial vessels flow into the BM cavity through the foramina nutrica [68] and divide into arterioles. Small arterioles and capillaries supply interconnected sinusoids [20, 23, 69-71]. Arterial blood flowing into the sinus has a  $pO_2$  of 95 mmHg and pH 7.4, while venous blood flowing out of the sinus has a  $pO_2$  of about 40 mmHg and pH 7.35 [72]. As noted above, experimental evidence suggests HSCs interact with osteoblasts located near the endosteum at the interface between the bone marrow and the inner surface of the bone. This region is the furthest away from the central sinuses supplying nutrients. It has been demonstrated experimentally that  $pO_2$  falls approximately 16 mmHg  $30 \mu\text{m}$  ( $\sim 3$  cell diameters, assuming an average cell diameter of  $10 \mu\text{m}$ ) away from a blood vessel and continues to decrease as distance from the vessel increases [73]. Thus, HSCs reside in areas of the bone marrow with subvascular  $pO_2$ .

### **2.3 EX VIVO EXPANSION OF HSCs**

Ex vivo expansion of hematopoietic cells is exceptionally challenging due to numerous variations in key factors influencing culture outcomes. Variability of donor cells can affect how quickly the cells differentiate and add to the unpredictability of the culture outcome. This variability is a result of the complex nature of the maturation process. The complex in vivo environment in which the cells develop adds to this heterogeneity.

Despite the challenging nature of ex vivo HSC culture, there are numerous potential uses for these cells. The uses can be divided into two groups: 1) patients receiving transplants to treat complications of malignant disorders and the chemotherapy that is used in their treatment and (2) treatments for abnormal marrow conditions where the native marrow is deliberately destroyed to treat non-malignant disorders [51].

### **2.3.1 Common culture techniques**

Several paradigms are commonly used in the ex vivo expansion of HSCs. Cultures of HSCs were first established with a feeder layer of irradiated stroma cells (Dexter culture) [74]. These co-culture systems closely resemble the in vivo environment. HSCs co-cultured with supportive stroma can be maintained for weeks at a time [75]. However, in a clinical setting, the use of supporting stromal cells is not acceptable because of the risks of the transmission of animal-borne adventitious agents [76]. Other problems that make these cultures clinically unfeasible co-culture systems include heterogeneity of the feeder layer, variability of the HSC's response to the stromal layer, and the separation of HSCs from feeder cells.

Stroma-free cultures are known as suspension cultures. These cultures require the addition of exogenous hematopoietic growth factors for HSC survival and expansion. Many cytokine combinations have been investigated for the expansion of HSC. 'Optimal' cytokine cocktails vary widely due to differences in cell source, degree of purification, and culture method employed. However, the combination of SCF, FL, and TPO has consistently been shown to induce proliferation while maintaining stem cell activity in BM, MPB, and CB CD34+ cells [9, 10, 12, 62, 77]. As previously noted, a combination of growth factors that increase the frequency of HSCs in ex vivo culture has not been identified.

Another consideration for ex vivo culture of HSCs is the use of bovine serum in media. Serum can be used to support HSCs because of the many hormones and growth factors it contains [78]. Serum is a poorly defined natural product and has large variations in composition and quality. In addition, it is a potential source of bacterial, mycoplasmal, and viral contamination. Serum can contain transforming growth factor- $\beta$  (TGF- $\beta$ ) and macrophage inflammatory protein 1 $\alpha$  (MIP-1 $\alpha$ ), which inhibit proliferation of hematopoietic progenitors [51]. Due to variability and its xenogenic source, the use of serum is not desired in clinical applications. To better conform to clinical regulations, a stroma-free/serum-free media was used for the ex vivo expansion of HSCs in this study.

### **2.3.2 Influence of culture environmental cells**

The environment that cells are grown in is key to the culture outcome. As noted, HSCs reside in a reduced oxygen environment. However, these cells are typically grown in atmospheric oxygen concentration—far from the physiological oxygen tension they experience within the body. Elevated oxygen concentrations (above those in the body) can lead to the production of reactive oxygen species (ROS) [79]. ROS—whether produced internally by normal functions of the cell (ex. aerobic respiration) or from external sources (ex. high  $pO_2$ )—pose a constant threat to living cells, as excessive ROS concentrations can cause damage to DNA, proteins, and lipids [80]. ROS have been specifically indicated in inhibiting the proliferation of primitive hematopoietic progenitors [81], promoting erythroid differentiation in the cell line K562 [82], and monocytic differentiation in HL-60 cells [83]. By lowering the external oxygen concentration, the amount of ROS generated should decrease, and thus the attack of cellular components via ROS attacks would also decrease.

In non-hematopoietic cells types, oxygen tension has been shown to regulate differentiation. The reduction of oxygen tension (3% O<sub>2</sub>) in cultures of CNS precursor cells increased the percentage of dopaminergic neurons compared to normoxia (~ 21% O<sub>2</sub>) [84]. Reduced oxygen tension also increased cell proliferation and protected CNS precursor cells from undergoing apoptosis. Together this yielded a ninefold improvement in the number of dopaminergic neurons. Lin and coworkers recently showed that culture at 1% O<sub>2</sub> maintained preadipocytes in an undifferentiated state [85]. Preadipocytes treated with adipogenic hormones did not lose their precursor phenotype under hypoxic culture conditions. Additionally, these cells did not lose their differentiation potential, as the cultured cells were able to commit to adipogenic differentiation once they were returned to normoxia. Cultures of embryonic stem cells had similar proliferation rates in 3% and 21% oxygen [86]. However, the appearance of differentiated cells was decreased in low oxygen cultures.

Research has established that cells have a different gene expression profile under hypoxia (1 to 5 % O<sub>2</sub> or pO<sub>2</sub> ~ 7.6 to 38 mmHg) vs. normoxia [87-90]. Cells experiencing reduced oxygen tension decrease their total RNA synthesis by 50-70%, while simultaneously upregulating a set of genes to respond to the reduced oxygen environment [91]. Hypoxia-inducible factor (HIF-1 $\alpha$ ) and p53 are transcription factors upregulated under hypoxic conditions. HIF-1 $\alpha$  activates the transcription of genes that increase the delivery of O<sub>2</sub> (VEGF, Epo) and alters the metabolic state to one more suited to a reduced oxygen environment (increased glucose-transport, glycolytic enzymes).

## **2.4 CHARACTERISTICS OF SCF AND ITS RECEPTOR, C-KIT**

Multiple signaling and adhesion molecules are involved with interactions between HSCs and their niche. The interactions between stem cell factor (SCF) and its receptor, c-Kit, are among the most important and well studied. SCF has been shown to be crucial in the maintenance and expansion of HSCs [92]. SCF interaction with c-Kit leads to signaling promoting survival and proliferation of HSCs.

### **2.4.1 SCF**

SCF (also known as Steel factor, Kit ligand, and mast cell growth factor) is a multi-lineage growth factor that acts on HSCs and committed progenitors. SCF can act alone to maintain CD34<sup>+</sup> cells [93], but typically acts on primitive cells in combination with many other growth factors [94, 95]. The mechanisms underlying the synergy are not fully understood, but the synergistic interactions with GM-CSF, IL-3, IL-6, and Epo are not due to changes in their receptors levels [96, 97]. In addition to its importance in the hematopoietic system, SCF also regulates non-hematopoietic cell types including: germ cells [35, 98], interstitial cells of Cajal in intestines [99], melanocytes [100, 101], and neuronal cells [102, 103].

SCF is encoded at the *Steel* locus (*Sl*) on mouse chromosome 10 [36, 94, 104] and on human chromosome 12q22-12q24 [105, 106]. Human SCF cDNA encodes 273 amino acids (Table 2.4.1); the first 25 are a hydrophobic signal sequence, the following 164 amino acids correspond to the isolated soluble SCF protein, and the remaining residues include a hydrophobic transmembrane region [107]. The secondary structure of SCF includes  $\alpha$ -helices and  $\beta$ -sheets, as well as intermolecular disulfide bounds between residue Cys<sup>4</sup> and Cys<sup>89</sup> and between Cys<sup>43</sup> and Cys<sup>138</sup> [108, 109]. The two intermolecular disulfide bounds are an absolute requirement for

bioactivity [109, 110]. Human SCF has four potential N-linked glycosylation sites (positions 65, 72, 93, and 120) and is heavily glycosylated with both N-linked and O-linked sugars when produced in CHO cells [111], although glycosylation is not critical for activity [109, 112].

Spectroscopic analysis comparing SCF derived from *E. Coli* and CHO cells confirms an identical secondary structure conformation, indicating that glycosylation has no effect on SCF structure [107].

**Table 2.4.1:** SCF amino acid sequence.

Number	1									10										20
1	M <sup>1</sup>	K	K	T	Q	T	W	I	L	T	C	I	Y	L	Q	L	L	L	F	N
21	P	L	V	K	T	E	G	I	C	R	N	R	V	T	N	N	V	K	D	V
41	T	K	L	V	A	N	L	P	K	D	Y	M	I	T	L	K	Y	V	P	G
61	M	D	V	L	P	S	H	C	W	I	S	E	M	V	V	Q	L	S	D	S
81	L	T	D	L	L	D	K	F	S	N	I	S	E	G	L	S	N	Y	S	I
101	I	D	K	L	V	N	I	V	D	D	L	V	E	C	V	K	E	N	S	S
121	K	D	L	K	K	S	F	K	S	P	E	P	R	L	F	T	P	E	E	F
141	F	R	I	F	N	R	S	I <sup>2</sup>	D	A	F	K	D	F	V	V	A	S	E	T
161	S	D	C	V	V	S	S	T	L	S	P	E	K	D	S	R	V	S	V	T
181	K	P	F	M	L	P	P	V	A	A	S <sup>3</sup>	S	L	R	N	D	S	S	S	S
201	N	R	K	A	K	N	P	P	G	D	S	S	L	H	W	A	A	M	A	L
221	P	A	L	F	S	L	I	I	G	F	A	F	G	A	L	Y	W	K	K	R
241	Q	P	S	L	T	R	A	V	E	N	I	Q	I	N	E	E	D	N	E	I
261	S	M	L	Q	E	K	E	R	E	F	Q	E	V							

Amino acid sequence from reference [112]

- 1.: Amino Acids in the hydrophobic signal sequence (1-25) are cleaved in processing
- 2.: Amino Acids 149-177 are replaced by a single glycine in membrane-associated SCF
- 3.: Amino Acids beyond 165 are remain associated with the cell when soluble SCF is formed through proteolytic cleavage

### 2.4.2 Membrane-associated and soluble SCF

In the body, SCF is normally both found in transmembrane and soluble forms [37, 113]. The two different forms are a result of alternative splicing of SCF cDNA (Figure 2.4.1). The full-length transcript includes a protein cleavage site in exon 6. SCF<sup>248</sup> (248 amino acids in length) can be proteolytically cleaved and results in soluble SCF comprised of amino acids 1-164 of the original protein. Amino acids 1-164 give a predicted molecular mass of 18,600 Da [107]. In the serum soluble SCF exists mainly as a monomer due to its low concentration (~3 ng/mL, [114]). When the concentration of soluble SCF is above approximately 10 ng/mL, it spontaneously forms a non-covalent homodimer [113, 115]. Crystallization studies show the approximate dimensions of the dimer are 87 Å x 32 Å x 25 Å [116]. The alternate spliced version (SCF<sup>220</sup>, 220 amino acids) is shorter in length and codes for membrane-associated SCF. This version does not contain the proteolytic cleavage site contained within amino acids 147-177 in SCF 248 (encoded by exon 6) [106].

Researchers have shown that membrane-associated and soluble SCF have different physiological roles. In mice, the absence of the *Sl* locus (*Sl<sup>d</sup>*) results in death in utero or in the prenatal period due to severe macrocytic anemia [35, 106]. *Sl<sup>d</sup>* mice only express soluble SCF and suffer from severe defects in germ-line, hematopoietic, and pigmentry cells [39]. The reintroduction of membrane-restricted SCF into *Sl<sup>d</sup>* mice corrected these defects [38]. It is known that membrane-associated SCF also dimerizes [38, 117] and the intracellular region of SCF is important in this dimerization [117]. A mutation that alters amino acids 238-273 of the cytoplasmic region (*Sl<sup>17</sup>*) are associated with defects in hematopoiesis [117, 118].

Membrane-associated SCF has also been examined using genetically-engineered stromal cells [40, 119-121]. The proliferation of human bone marrow mononuclear cells and the duration of cell expansion were greatly enhanced by the presence of membrane-associated SCF [40]. Stromal cells expressing membrane-associated SCF were also more effective in maintaining human bone marrow CD34<sup>+</sup> cells than those expressing only soluble SCF [121]. Furthermore, fibroblasts from *Sl<sup>d</sup>* mice are unable to support the survival of the growth-factor-dependent cell line FDC-P1, while fibroblasts from wild type mice (with transmembrane SCF) are able to do so [122].

Several studies have been performed evaluating chemical immobilization of SCF and anti-c-Kit antibodies to surfaces [123-126]. Kurosawa and coworkers demonstrated that an immobilized monoclonal antibody (YB5.B8) could substitute for SCF as an activator of c-Kit in M07e cells [123]. In its soluble form YB5.B8 inhibited the proliferation of M07e cells, but when immobilized it promoted proliferation and synergized with GM-CSF for M07e cell proliferation. In contrast to these results, an immobilized fusion protein between IgG<sub>1</sub> and rat SCF (rSCF-IgG<sub>1</sub>) decreased the maximum growth potential of M07e cells [126]. Doheny et al., used a fusion protein combining the cellulose-binding domain of cellulase Cex to present immobilized SCF (SCF-CBD) on cellulose surfaces [124]. SCF-CBD surfaces supported enhanced SCF-dependent proliferation as compared to soluble SCF in proliferation assays using M07e, TF-1, and mouse B6SutA cell lines. Immobilized SCF-CBD fusion proteins were found to be 7-fold more potent at stimulating the proliferation of M07e and TF-1 cells than the soluble form and native SCF [124]. Additional characterization of SCF-CBD surfaces using mouse B6SutA cells showed extended c-Kit phosphorylation [125]. In contrast to SCF-CBD, an immobilized fusion

protein between IgG<sub>1</sub> and rat SCF (rSCF-IgG<sub>1</sub>) decreased the maximum growth potential of M07e cells, but induced adhesion dependent shape change in factor dependent CS-1 cells [126].

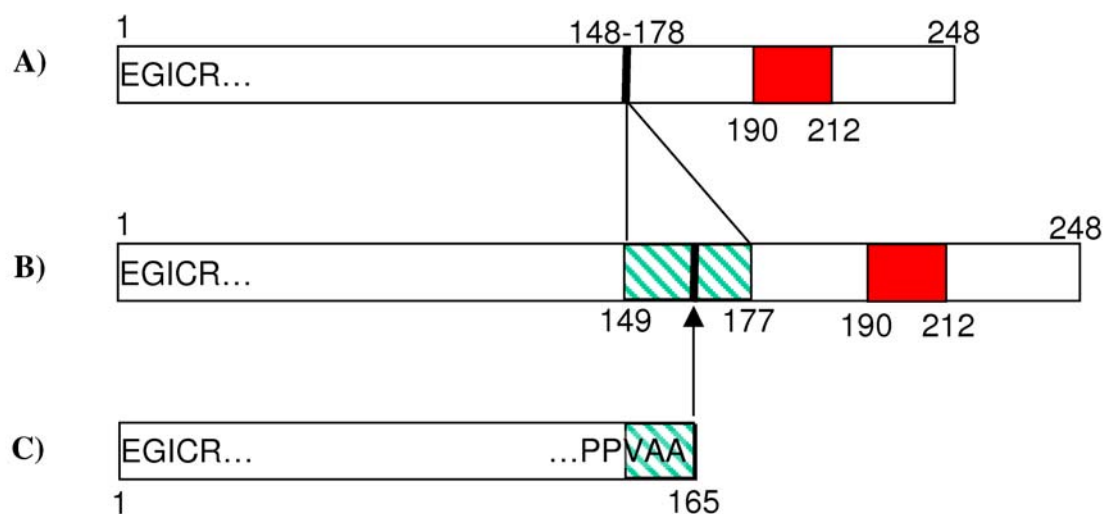


**Figure 2.4.1:** Schematic representation of SCF. **A)** Alternatively spliced membrane-associated SCF with transmembrane region as a solid band. Amino acids 149-177 are replaced by a single glycine due to the absence of exon 6. **B)** Precursor form of soluble SCF. Exon 6 is shown with diagonal stripes. **C)** Soluble SCF after proteolytic cleavage at residue 165. Redrawn from [109].

### **2.4.3 c-Kit**

c-Kit (also known as SCF receptor and CD117) is a receptor tyrosine kinase (RTK) family member [127]. c-Kit is encoded on chromosome 5 at the dominant white spotting locus (*W*) in mice and is found on chromosome 4 in humans [128]. The full-length human protein contains 976 amino acids. The extracellular binding domain is approximately 500 amino acids and includes five immunoglobulin (IgG)-like structures [129]. The first three IgG-like domains are involved in the ligand-receptor binding, and the fourth IgG-like domain is responsible for receptor dimerization [130]. The intracellular domain contains approximately 400 amino acids and is connected to the extracellular domain by a short hydrophobic section spanning the cell membrane. c-Kit is expressed on approximately 70% of all CD34+ cells, including lineage restricted progenitors [131, 132] and is down regulated as cells differentiate [133].

### **2.4.4 Cellular activation and signal transduction**

The binding of SCF causes the rapid homodimerization of c-Kit and induces conformational changes resulting in phosphorylation of tyrosine residues [129]. Although a detailed mechanism for the formation of the SCF-c-Kit complex is not fully understood, a model has been proposed. This model suggests that binding of dimerized SCF initiates c-kit dimerization [113, 130, 134]. This theory is consistent with the fact that SCF dimers show greater biological activity than the monomeric form of SCF [111, 113, 135]. As with other RTKs, dimerization of the receptor activates a variety of biochemical signaling pathways including: Ras/Raf/MAP kinase cascade, phosphatidylinositol 3-kinase (PI3-K), Janus family kinase (JAK)/signal transducers and activators of transcription (STAT), and Src families [136] and the subsequent downstream signaling cascade.

The recruitment of SH2 proteins to the phosphorylated tyrosines of c-Kit activate Ras/Raf/MAP kinase and PI3-K pathways [136, 137]. SH2 domain-containing tyrosine kinases such as Ras, p85, and phospholipase C- $\gamma$  (PLC- $\gamma$ ) are directly recruited to the receptor or by adaptor proteins. In the MAP Kinase pathway, activated Ras then activates the serine-threonine kinase Raf-1. Raf-1 then phosphorylates MEK, which in turn activates ERK1,2 [137]. PI3-K is composed of a heterodimer of an 85 kDa unit (p85) and 110 kDa unit [137]. Phosphorylation of c-Kit activates PI3-K by recruiting p85 and localizing the 110 kDa subunit to activated p85. PI3-K then activates a number of downstream proteins important in protection from apoptosis and activating the mitogenic response including Akt, c-Cbl, and Crkl [136, 137].

SCF has been reported to activate JAK2 in the JAK/STAT signaling pathway [138-140]. JAK2 was found to associate with c-Kit and be transiently activated after SCF stimulation. Activation of JAK2 leads to the activation STAT1, STAT3, and STAT5 [137]. Membrane associated and soluble SCF have different effects on signaling cascades. One differences is the duration of c-Kit tyrosine activation [38, 41]. Studies showed that when stimulated with membrane-associated SCF, c-kit on M07e cells remained phosphorylated for two hours. In contrast, c-Kit on M07e cells stimulated with soluble SCF returned to basal phosphorylation levels in one hour [41]. This difference may be attributed to the cells inability to internalize c-Kit for signal down regulation when stimulated by membrane-associated SCF, compared to soluble SCF. Studies from Stuart Berger's lab indicate that PLC- $\gamma$  is required for the differential effect seen in membrane-associated and soluble SCF [92, 141, 142]. They demonstrated that in primary bone marrow-derived mast cells treatment with the PLC- $\gamma$  antagonist could preferentially suppress mast cell activation by membrane-associated SCF as

compared to soluble SCF [142]. This resulted in c-kit positive cells not being maintained by membrane-associated SCF [92]. Others have attributed the increased proliferation in G1E-ER2 cells stimulated by membrane-associated SCF to sustained and enhanced p38 and ERK 1,2 activation [143].

## **2.5 CHARACTERISTICS OF TPO AND ITS RECEPTOR cMPL**

Experimental evidence indicates that TPO plays a vital and non-redundant role in the self-renewal and expansion of HSCs [144]. The TPO receptor, cMpl, is expressed on all primitive HSCs [145], and removal of cMpl by genetic manipulation leads to significant reduction in the numbers of HSCs [145, 146]. TPO acts in conjunction with SCF, FL, and other early acting hematopoietic growth factors, such as IL-3, to stimulate the proliferation and maintenance of hematopoietic progenitor cells [9, 10, 12].

In addition to its effects on HSCs, TPO is the primary regulatory of megakaryopoiesis and platelet production. TPO influences megakaryocyte (Mk) growth and development by increasing the size and number of Mks. This stimulates the expression of Mk-specific markers (such as CD41 and CD61), and promotes the polyploidization of committed Mks [147]. TPO is also a potent stimulator of Mk colony formation [148].

### **2.5.1 TPO**

The TPO cDNA sequence codes for a protein 353 amino acids in length (Table 2.5.1) and produces a precursor protein with a molecular weight of 36 kDa [147, 149]. After removal of a 21-amino-acid signal peptide, the remaining 332 amino acids undergo glycosylation producing a protein with an apparent molecular weight of 80-90 kDa by SDS-PAGE and ~ 57.5 kDa by mass spectrometry [150]. The mature full-length protein can be divided into two domains based on

homology with EPO (Figure 2.5.1) [151]. The amino acid sequence of the amino terminal domain is similar to that of EPO, sharing 20% homology and an additional 25% similarity [152]. This domain binds to and activates cMpl [147]. The carboxyl-terminal 177 residues show no homology with EPO, and contain multiple N- and O- sites for glycosylation. Deleting this region does not alter activity, but its removal substantially reduces the stability of the molecule [153]. TPO is produced in several organs including the kidneys, skeletal muscle, and the marrow stroma. However, the liver is responsible for up to 50% of the steady state production of TPO [154].

**Table 2.5.1:** TPO amino acid sequence.

Number	1								10										20	
1	M <sup>1</sup>	E	L	T	E	L	L	L	V	V	M	L	L	P	T	A	R	L	T	L
21	S	S	P	A	P	P	A	C	D	L	R	V	L	S	K	L	L	R	D	S
41	H	V	L	H	S	K	L	S	Q	C	P	E	V	H	P	L	P	T	P	V
61	L	L	P	A	V	D	F	S	L	G	E	W	K	T	Q	M	E	E	T	K
81	A	Q	D	I	L	G	A	V	T	L	L	L	E	G	V	M	A	A	R	G
101	Q	L	G	P	T	C	L	S	S	L	L	G	Q	L	S	E	Q	V	R	L
121	L	L	G	A	L	Q	S	L	L	G	T	Q	L	P	P	Q	G	R	T	T
141	A	H	K	D	P	N	A	I	F	L	S	F	Q	H	L	L	R	G	K	V
161	R	F	L	M	L	V	G	G	S	T	L	C	V	R	R <sup>2</sup>	A	P	P	T	T
181	A	V	P	S	R	T	S	L	V	L	T	L	N	E	L	P	N	R	T	S
201	G	L	L	E	T	N	F	T	A	S	A	R	T	T	G	S	G	L	L	K
221	W	Q	Q	G	F	R	A	K	I	P	G	L	L	N	Q	T	S	R	S	L
241	D	Q	I	P	G	Y	L	N	R	I	H	E	L	L	N	G	T	R	G	L
261	F	P	G	P	S	R	R	T	L	G	A	P	D	I	S	S	G	T	S	D
281	T	G	S	L	P	P	N	L	Q	P	G	Y	S	P	S	P	T	H	P	P
301	T	G	Q	Y	T	L	F	P	L	P	P	T	L	P	T	P	V	V	Q	L
321	H	P	L	L	P	D	P	S	A	P	T	P	T	P	T	S	P	L	L	N
341	T	S	Y	T	H	S	Q	N	L	S	Q	E	G							

Amino acid sequence from reference [153].

- 1.: Amino Acids in the signal peptide (1-21) are cleaved in processing.
- 2.: Carbohydrate-rich domain

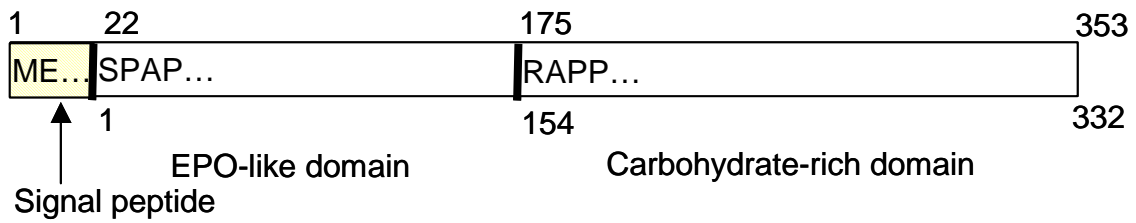


**Figure 2.5.1:** Schematic representation of TPO. Precursor form of TPO with signal peptide, EPO-like domain, and carbohydrate-rich domain. Adapted from references [147] and [151].

### **2.5.2 cMpl, cellular activation, and signal transduction**

TPO influences hematopoietic cells through interactions with its receptor, cMpl. cMpl belongs to the type I hematopoietic cytokine receptor family that includes receptors for G-CSF, EPO, and growth hormone [155]. Upon interaction with TPO cytoplasmic domains of cMpl are not directly phosphorylated. Instead, signaling is activated when cMpl homodimers activate JAK2 kinase molecules tethered to specific amino acid sequences known as Box1 and Box2 [155]. Similar to RTKs such as c-Kit, activation of JAK2 leads to the subsequent recruitment of several signaling molecules [148]. The pathways activated by JAK2 include STAT3, STAT5, Ras/MAPK, PI3-K, and protein kinase c (PKC) (Figure 2.5.2) [148, 156, 157]. The activation of these pathways leads to the upregulation of several target genes important in self-renewal and expansion. For example Kirito and coworkers showed that TPO stimulation led to a two-to-three-fold increase in the levels of HOXB4 mRNA, which enhanced self-renewal in murine HSCs [158]. Additionally, Kirito showed that TPO stimulation increased mRNA levels of HOXA9 [159], which is instrumental in the expansion of primitive HSCs [160, 161].

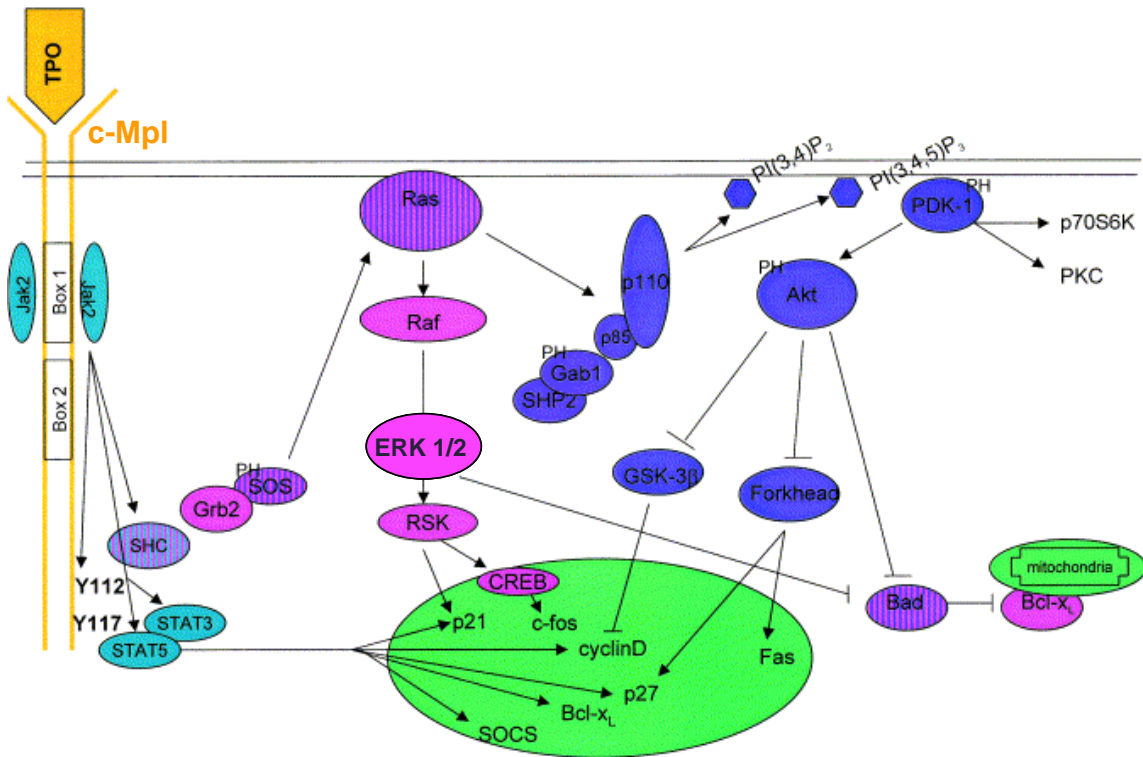


**Figure 2.5.2:** TPO signaling cascade adapted from [148].

## **2.6 IMMOBILIZATION PROTEINS AND PEPTIDES TO SURFACES**

Numerous problems are associated with the immobilization of peptides and proteins. Methods must be devised to orient the immobilized molecules in such a way that they are accessible to cells. This is particularly important since molecules physically constrained to surfaces cannot accommodate cell surface receptors by changing their orientation. Randomly oriented peptides or proteins may have the receptor's binding site near the surface, thus hindering binding to the ligand [162]. Additionally, proteins are particularly susceptible to denaturing and conformational changes when in close contact with surfaces [163]. The sum of these problems result in lower binding efficiency and capacity compared with their soluble counterparts.

### **2.6.1 Protein immobilization**

An important aspect of the stem cell niche involves the presentation of cytokines in an immobilized form (Section 2.2.1). Proteins can be attached to surfaces using a variety of conjugation chemistries. These strategies include: chemical reactions with functional groups such as amines, carboxylic acids, sulfhydryl groups, and carbohydrates (for glycosylated proteins), immobilization via histidine tags [164-166], and biotin-avidin interactions [167, 168]. In many cases, protein modification methods factor into the activity of the immobilized molecules due to targeting strategies. For example, approaches could non-specifically target the amine groups of lysine, resulting in randomly oriented molecules or the inactivation of the molecule—if the lysine is important in receptor interactions. Further, proteins (and all other biomolecules) are fragile, which constrains how they can be chemically manipulated [169].

### ***2.6.1.1 Considerations for the immobilization of SCF***

In order to mimic the membrane-associated form of SCF, a method to specifically attach and orient the molecule must be developed. The first 141 amino acids (from the amino terminus) are important for the activity and binding of SCF [109], therefore it would be beneficial to manipulate the C-terminus amino acids (residues 142-165). If the full-length soluble protein is used (SCF<sup>248</sup>) modification beyond Ser<sup>165</sup> may not yield an immobilized form of SCF due to the presence of a cleavage site. Additionally, dimerization is key to the ability of SCF to induce c-kit activation [134], consequently the residues involved with dimerization should not be modified. Finally, to maintain SCF activity the two intermolecular disulfide bonds must not be disrupted [109, 110]. Therefore the use of reducing agents and thiol chemistries are not suitable for modification of SCF.

### ***2.6.1.2 SCF Immobilization strategy***

To combine the benefits of membrane-associated SCF in a more desirable presentation format, we have chemically modified SCF with a biotin linker. Two different platforms for the immobilization of biotinylated SCF (bSCF) were explored. The first system was developed by Dr. Dominic Chow and utilized commercially available NeutrAvidin (NA) coated plates. Several primary cell experiments were performed to compare immobilized bSCF with soluble SCF. However, control experiments performed later showed that bSCF continually released from the surface; therefore, the results attributed to ‘immobilized’ SCF could not be substantiated.

The second system was developed with Dr. Rico Gunawan and built upon a non-fouling layer of poly(ethylene glycol) (PEG) anchored to the surface via the adhesive amino acid 2,4-

dihydroxyphenylalanine (DOPA). This system was pioneered in Dr. Phil Messersmith's lab. Grafting of nontoxic, uncharged PEG to surfaces is a technique commonly used to generate non-fouling surfaces [170-172]. The non-fouling properties of PEG have been attributed to osmotic repulsion, steric hindrance, and hydrophilicity [173, 174]. To build in the ability to specifically present molecules from the surface, DOPA-PEG molecules were functionalized with biotin. Thus bSCF could be specifically displayed on the DOPA-PEG-biotin surface through an avidin bridge.

### **2.6.2 Peptide immobilization**

Methods employed to immobilize peptides to surfaces are similar to those used for protein immobilization. However, the difference in molecular size compared to proteins makes peptides more amenable to chemical synthesis. This allows for the insertion of amino acid sequences or other functional groups used for conjugation to surfaces.

#### ***2.6.2.1 Considerations for the immobilization of TPOm***

In contrast to SCF, several different peptide [43, 175] and non-peptidyl [176-179] mimics of TPO have been identified. Using phage display, Cwirla and coworkers identified a 14 amino acid sequence (Ile-Glu-Gly-Pro-Thr-Leu-Arg-Gln-Trp-Leu-Ala-Ala-Arg-Ala) that specifically binds to the TPO receptor c-Mpl, but shares no common sequence homology with full-length recombinant human TPO (rhTPO) [43]. By using the  $\epsilon$ -amino group of a Lysine modified at the  $\alpha$ -amino group by  $\beta$ -Alanine, they created a pseudosymmetrical dimeric peptide. This branched peptide dimer, TPO mimetic (TPOm), binds c-Mpl with a much greater affinity than the monomer and was shown as equally potent as rhTPO in the promotion of Mk production [43].

Due to its smaller size, the chemical synthesis of TPOM is much easier than full-length proteins. A specific linkage site can be built into the molecule by manually synthesizing TPOM. The region of TPOM that interacts with cMpl has been characterized [43], therefore TPOM can be linked to a surface in a defined, active conformation. We hypothesize that linking TPOM to a phospholipid analog and incorporating it into a hybrid bilayer membrane (HBM, detailed below in section 2.6.2.1.2) would yield an oriented peptide presented in a non-fouling biocompatible surface.

#### ***2.6.2.2 Hybrid bilayer membranes***

HBMs are supported lipid monolayers created by the deposition of lipids onto a hydrophobic surface. The hydrophobic surfaces are formed by treating silicon or glass with alkylsilanes or gold-coated surfaces with alkylthiols. Lipids can be deposited using the Langmuir-Blodgett technique, but the spontaneous adsorption of lipid vesicles to a hydrophobic surface is more appropriate for larger surface areas and non-planar geometries [44]. Vesicle deposition also allows for the rapid formation of replicate surfaces. HBMs were developed to mimic the conditions at the surface of a cell membrane [180, 181] and have been used to study various cell binding events [44, 181-183]. Our group has used HBMs to explore the interaction of cell adhesion molecules (CAMs) and their ligands [47, 184].

## CHAPTER 3: MATERIALS AND METHODS

### 3.1 SYNTHETIC METHODS

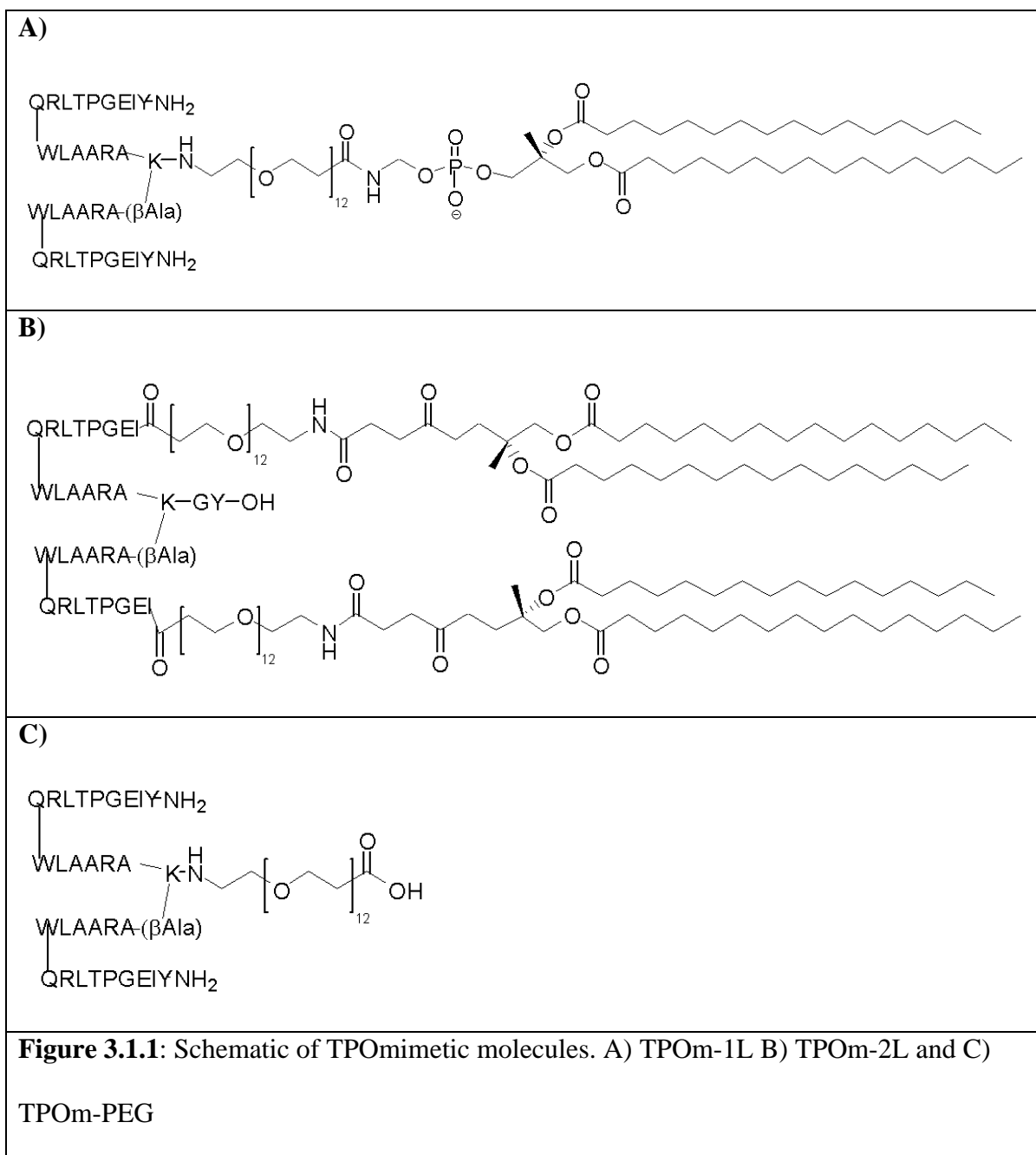
#### 3.1.1 Lipopeptide synthesis

Reagents and solvents for peptide synthesis were purchased from NovaBiochem (San Diego, CA) and Advanced ChemTech (Louisville, KY). Rink amide AM, Chlortrityl, Rink amide PEGA, and PEGA amine resins were evaluated for the manual solid-phase synthesis of thrombopoietin mimetic peptides (TPOm) based on the sequence published by Cwirla et al. [43]. Synthesis on PEGA amine resin yielded the best results for the synthesis of this branched peptide. Two different lipopeptide conjugates were synthesized using different strategies. The strategy for TPOm with one lipid tail (TPOm-1L; Figure 3.1.1A) involved solid-phase peptide synthesis followed by free solution conjugation of the side-chain-protected peptide acid to a single lipid molecule. First, an O-(N-Fmoc-2-aminoethyl)-O'-(2-carboxyethyl)-undecaethyleneglycol (PEG, NovaBiochem) was attached to 4-(4-Hydroxymethyl-3-methoxyphenoxy)-butyric acid (HMPB, NovaBiochem) modified PEGA resin (Polymer Laboratories; Amherst, MA) using *N,N'*-dicyclohexylcarbodiimide (DCC) activation catalyzed by 4-Dimethylaminopyridine (DMAP). The branch point of the peptide was synthesized using Lys(Dde) and  $\beta$ -Ala for symmetry. After lysine and  $\beta$ -Ala addition, the side chain-protecting group (Dde) on Lys and Fmoc on  $\beta$ -Ala were removed with a solution of hydrazine in NMP. Fmoc and Dde groups were removed to provide two amine groups for the extension of the peptide, thus forming the pseudo-symmetrical dimer. The remaining amino acids were added via typical Fmoc solid phase peptide synthesis methods, using a coupling mixture of benzotriazole-1-yl-oxy-tris(dimethylamino) phosphonium hexafluorophosphate (BOP)/*N*-hydroxybenzotriazole

(HOBt)/diisopropylethylamine (DIEA) in dichloromethane (DCM) with a 10 minute preactivation step before coupling. After coupling of the last amino acid, the N<sup>α</sup>-Fmoc protecting group was removed and a small sample was cleaved with 96% TFA /4% triisopropylsilane (TIS) to verify the peptide sequence by MALDI-TOF-MS. The peptide was cleaved from the resin with a solution of 2% trifluoroacetic acid (TFA) in DCM. To ensure that the acid-labile side-chain-protecting groups remained attached to the peptide acid during cleavage, the solution was neutralized by purging into a flask containing 10% pyridine in methanol. The protected TPOM-PEG acid was reacted with 1,2-Dipalmitoyl-*sn*-Glycero-3-Phosphoethanolamine (DPPE, Avanti Lipids) to form the lipopeptide, TPOM-1L. The product was collected by precipitation in acetic acid and the side chain protecting groups were removed by treatment with TFA:Isopropanol:Water (96:2:2). Product was concentrated, precipitated in diethyl ether, and purified using RP-HPLC.

The synthesis of TPOM with two lipid tails (TPOM-2L; Figure 3.1.1B) was performed entirely on the PEGA amine resin. Fmoc-protected tyrosine was added directly to the HMPB linker using DCC activation catalyzed DMAP. This was followed by Glycine, Lys(Dde) and β-Ala for the branching point. The addition of the remaining amino acid monomers to form the branched peptide was similar to that for TPOM-1L. After completing the amino acid addition, PEG was added to the N-termini of each arm of the branched peptide using a mixture of BOP/HOBt/DIEA in DCM. Separately, the acid terminal glycerolipid 1,2-dipalmitoyl-*sn*-glycerol-succinic anhydride (DPG-Su) was formed by reacting 1,2-dipalmitoyl-*sn*-glycerol (DPG; Sigma) with succinic anhydride in the presence of pyridine in DCM. DPG-Su was then reacted with the N-termini of the PEGylated peptide on the resin using BOP/HOBt/DIEA in

DCM. The product was cleaved and side-chain-deprotected in one step using 96% TFA and 4% TIS. As for TPOM-1L, crude products were analyzed and purified by RP-HPLC and their structures were confirmed by MALDI-TOF MS. A PEGylated control peptide with no lipid tail, TPOM-PEG, was also synthesized (Figure 3.1.1C).



### 3.1.2 Lipopeptide purification and analysis

PEGylated peptides were analyzed on a C18 analytical column (GraceVydac; Hesperia, CA), while lipopeptides were analyzed using a C4 analytical column. Products were purified using semi-preparative scale C18 or C4 columns (GraceVydac). All gradients were linear from time 0 to 30 minutes (analytical samples) or from 0 to 120 minutes (semi-preparative samples).

Molecular weights of resulting purified products TPOM-PEG (4272.5 Da), TPOM-1L (4946.7 Da), and TPOM-2L (6066.2 Da) were determined by matrix assisted laser desorption/ionization time-of-flight (MALDI-TOF) mass spectrometry (MS) on a Voyager DE Spectrometer (PerSpective Biosystems; Foster City, CA) in linear and reflector modes. Laser intensity, voltage, and other settings were individually adjusted to optimize the signals for each sample. Saturated sinapinic acid in 50:50 v/v acetonitrile (ACN):water was used as a matrix for all peptides and modified peptides.

### 3.1.3 Synthesis of DOPA<sub>3</sub>PEG

The synthetic methods for DOPA<sub>3</sub>PEG (DP, Figure 3.1.2) were developed by Dr. Bruce Lee in the Messersmith lab and Dr. Zhongqiang Liu performed the synthesis. Diacetyl-DOPA *N*-carboxyanhydride (NCA) was prepared by following published procedures [185]. Methoxy-PEG-NH<sub>2</sub> (2000 MW PEG; Nektar Therapeutics; Huntsville, AL) was dissolved in anhydrous THF and purged with argon (Ar) in a round bottom flask. DOPA(Ac<sub>2</sub>)-NCA was added and the mixture was stirred at room temperature for five days. The polymer solution was added to diethyl ether (Et<sub>2</sub>O) and the precipitate was vacuum filtered and dried in a dessicator to yield Ac<sub>2</sub>DOPA<sub>3</sub>PEG. The diacetyl groups were removed by the addition of piperidine to Ac<sub>2</sub>DOPA<sub>3</sub>PEG in dimethylformamide (DMF). The mixture was rotary evaporated to remove

excess piperidine and precipitated in Et<sub>2</sub>O. After drying in a desiccators, a pale yellow solid was obtained. Using UV-vis as described [186], the number of PEG-bound DOPA was determined to be 3.0.

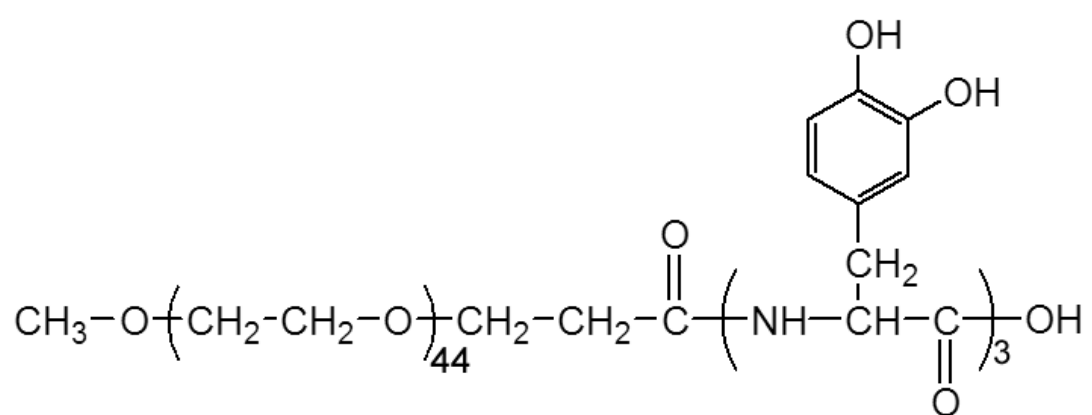


**Figure 3.1.2:** Schematic of mPEG-DOPA<sub>3</sub> (DP)

### 3.1.4 Synthesis of DOPA<sub>3</sub>PEG-biotin

The synthetic methods for DOPA<sub>3</sub>PEG-biotin (DPb, Figure 3.1.3) were developed by Dr. Bruce Lee in the Messersmith lab and and Dr. Zhongqiang Liu performed the synthesis. The conversion was accomplished by reacting Boc-ED (1.37 mmol) and diisopropylethylamine (DIEA) in of chloroform. Biotin-PEG<sub>3400</sub>NHS was added and the mixture stirred at room temperature for two hours. The polymer solution was added to 100 mL of Et<sub>2</sub>O. The precipitate was vacuum filtered and dried to yield Biotin-PEG-Boc-ED.

Biotin-PEG-Boc-ED was dissolved in chloroform and 4N HCl in dioxane. The reaction mixture was stirred at room temperature for 15 minutes and HCl was removed through rotary evaporation. The solution was added to 50 mL of Et<sub>2</sub>O and the precipitate was vacuum filtered and dried to yield 488 mg of Biotin-PEG-NH<sub>2</sub>. <sup>1</sup>H NMR revealed that Boc was completely removed.

Biotin-PEG-NH<sub>2</sub> was dissolved in 10 mL of THF. DOPA(Ac<sub>2</sub>)-NCA and DIEA (0.132 mmol) were then added and the reaction mixture was stirred at room temperature for three days. The polymer solution was precipitated with Et<sub>2</sub>O and the precipitate was vacuum filtered and dried. The peptide-coupled PEG was dissolved in 2.5 mL of DMF and bubbled with Ar for 10 min. Pyridine was added and the solution was stirred for 15 minutes with Ar bubbling. The mixture was rotary evaporated to remove excess pyridine and precipitated again in Et<sub>2</sub>O. After drying in a dessicator, a pale yellow solid was obtained. The number of DOPA molecules per PEG<sub>3400</sub>biotin was determined as described [186]. The average number of DOPA molecules bound to PEG was 2.9.

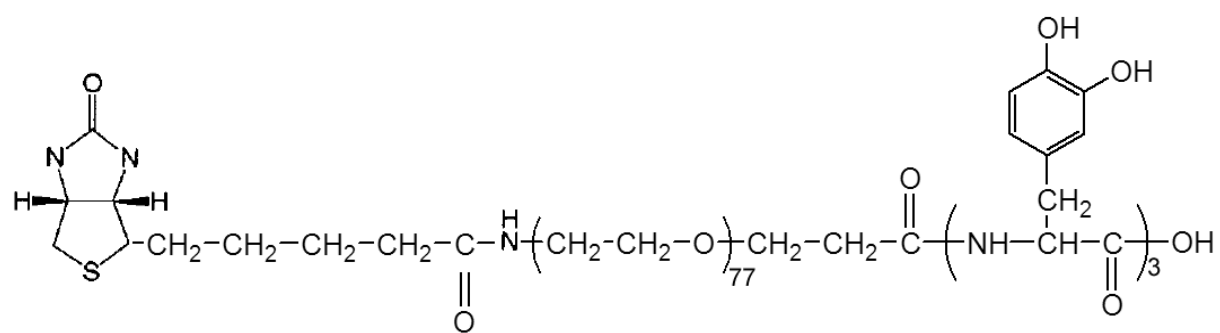


**Figure 3.1.3:** Schematic of biotin-PEG-DOPA<sub>3</sub> (DPb).

### **3.1.5 Biotinylation of SCF**

Recombinant human SCF (Amgen, Thousand Oaks, CA) [112] was conjugated biotin with sulfo-NHS-LC-biotin (LC = long chain, Figure 3.1.4) from Pierce (Rockford, IL) to form biotinylated SCF (biotin-SCF). Sulfo-NHS-LC-biotin was reacted with 200  $\mu\text{g}$  SCF (at 0.5 mg/mL) at different biotin-to-protein (BP) molar ratios (2:1, 5:1, 10:1, and 100:1). Reactions were carried out at room temperature for 30, 60, 90, or 120 minutes with or without vortexing. Following biotinylation, the product was dialyzed overnight against phosphate-buffered saline (PBS) in a dialysis cassette with a molecular weight cutoff of 7,000 Da.

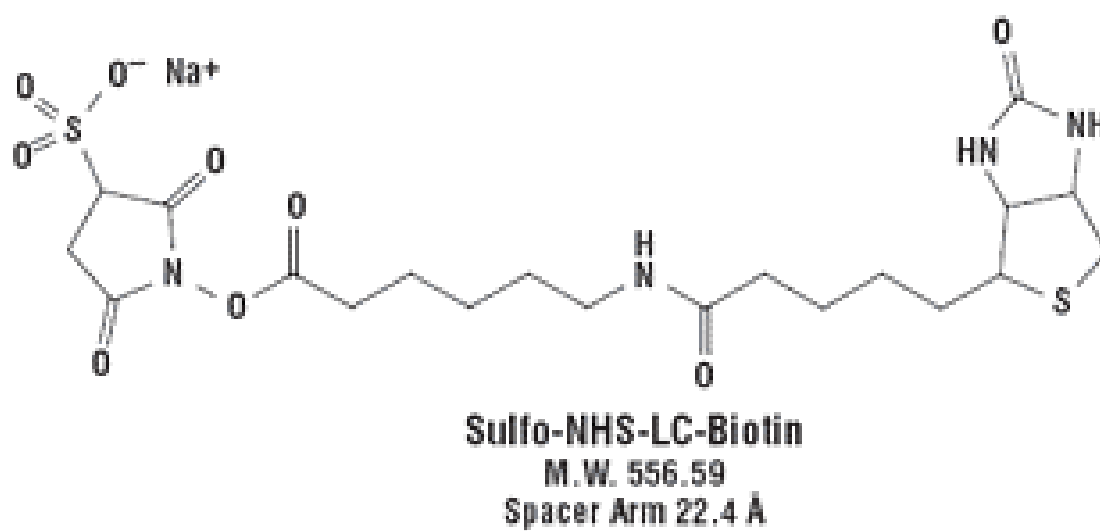


**Figure 3.1.4:** Schematic of sulfo-NHS-LC biotin. From [www.piercenet.com](http://www.piercenet.com)

### **3.1.6 Determination of molar ratios of biotin incorporated into SCF**

#### ***3.1.6.1 MALDI-TOF MS of bSCF***

Molecular weight of bSCF was determined using MALDI-TOF MS in linear mode. Sinapinic acid or  $\alpha$ -cyano-4-hydroxycinnamic acid (CHCA, Sigma) at 10 mg/ml in 50:50 (v/v) acetonitrile (ACN):2% aqueous TFA was used as the matrix for SCF. Various ratios of sample to matrix were prepared and analyzed to optimize for variations in the signal strength. Laser intensity, voltage, and other settings were also individually adjusted to optimize the signals of each sample.

#### ***3.1.6.2 HABA assay***

The molar ratio of biotin incorporated into SCF was determined by the HABA-avidin method. 2-hydroxyazobenzene-4'-carboxylic acid (HABA) (Pierce) forms a complex that absorbs at 500 nm when it binds with avidin. Biotin groups conjugated on SCF displace the HABA dye from the complex, which decreases  $A_{500}$ . A standard curve can be obtained using free biotin to estimate the number of moles of biotin incorporated after the biotinylation of SCF. The molar ratio (biotin to SCF) could then be calculated, once the concentration of SCF was determined by the absorbance at 280 nm.

### **3.2 SURFACE PREPARATION**

#### **3.2.1 Silanization of glass surfaces**

The methods used for the preparation of hydrophobic surfaces, lipid vesicles, and culture cassettes are similar to those previously described [47]. Briefly, glass microscope slides (3"x1", Fisher Scientific) were cleaned by immersion in 1:1 mixture of HCl:methanol for 30 minutes, rinsed with 18 M $\Omega$  water (Millipore; Billerica, MA), and dried in a convection oven at 55° C. The dried slides were then immersed in sulfuric acid for 30 minutes, rinsed with 18 M $\Omega$  water,

and dried in a convection oven at 55° C. The glass was silanized with 12 mM octaldecyltrichlorosilane (OTS) in a 45:3:2 solution of hexadecane:water-saturated carbon tetrachloride:water-saturated chloroform. Clean glass slides were immersed in the coating solution in an ultrasonic bath for 1.5 minutes. Hydrophobic slides were then rinsed three times by sonication in chloroform for a total of 10 minutes. They were then rinsed with 18 MΩ water and dried in a convection oven at 55° C for approximately 10 minutes.

### **3.2.2 Preparation of culture cassettes and supported lipid monolayers**

Culture cassettes were prepared by adhering Lab-Tek (Nalgene-Nunc International; Rochester, NY) 16-well chambers to hydrophobic glass surfaces using silastic (T-2; Dow Corning; Midland, MI). The upper portion of the Lab-Tek chamber are molded with a track that allows for the injection of silastic. The culture cassettes were assembled and held in place with four medium binder clips. In order to have the silastic adhere to the hydrophobic glass, the gasket tracks were injected with 5N NaOH and incubated for three hours. This treatment was followed by neutralization with 1N HCl and thorough washing with 18 MΩ water. Silastic was injected into the etched gasket tracks and cured overnight before use in short-term assays or long-term culture. For long-term culture the cassette was sterilized by 30-minute exposure to 254 nm UV light.

### **3.2.3 Vesicle preparation and deposition**

Dipalmitoylphosphatidylcholine (DPPC; Avanti Lipids) was used as a carrier lipid for the TPOM lipopeptides. DPPC and TPOM lipopeptides were resuspended in chloroform at appropriate molar ratios (0.01 to 5 mol% TPOM lipopeptide) in glass vials and mixed together. Chloroform was evaporated under a stream of nitrogen and the lipids were stored under vacuum overnight to remove residual chloroform. The lipid mixture was then resuspended to 0.5 mg/mL in 18 MΩ

water and heated to 55° C, which is above the melt transition temperature of DPPC (42° C). To produce small unilamellar vesicles, the mixture was tip sonicated for two minutes, filtered through a 0.22 µm filter (Millipore), and immediately deposited into the cell culture cassette. Lipid vesicles were allowed to deposit for 1.5 hours in a convection oven set at 55° C. The lipid surface was then washed via dilution rinses with water and equilibrated media. It is important to note that once formed, the supported lipid monolayers remained under liquid at all times to ensure their integrity. The cassettes were equilibrated in a humidified incubator at 37° C and 5% CO<sub>2</sub> for 30 minutes prior to the inoculation of cells for culture or adhesion assays.

#### **3.2.4 Immobilization of bSCF to NeutrAvidin-coated surfaces**

NeutrAvidin-coated (NA) surfaces pre-blocked with superbloc were obtained from Pierce. Thirty microliters of biotin-SCF in PBS were added to wells of a 96-well plate and incubated for two hours at room temperature. Incubation was followed by eight rinses with PBS. After the final rinse, the surfaces were sterilized by exposure to UV light (254 nm, 40 mW/cm<sup>2</sup>) for 30 minutes.

#### **3.2.5 Preparation of DOPA-PEG surfaces in culture cassettes**

Microscope glass slides (3"x1", Fisher Scientific) were cleaned overnight by emersion in piranha solution (7:3 H<sub>2</sub>SO<sub>4</sub>:H<sub>2</sub>O<sub>2</sub>). The slides were then rinsed with 18 MΩ water and dried inside a 55°C oven. The glass slides were then coated with a 10 nm-thick TiO<sub>2</sub> layer inside an EB3 electron beam evaporation unit (Edwards). Before polymer modification, TiO<sub>2</sub>-coated glass slides were sonicated in isopropanol, dried with N<sub>2</sub> and cleaned in an oxygen plasma chamber (Harrick Scientific, Ossining, NY) for three minutes. Culture cassettes similar to those for lipid surfaces were prepared for cell adhesion, cell signaling, and cell culture assays. The upper

portion of a 16-well Lab-Tek chamber slide was removed from its base and bound to TiO<sub>2</sub>-coated glass slides using injected silastic resin (T-2, Dow Corning). The silastic resin was allowed to cure for at least four hours before the TiO<sub>2</sub> surfaces inside each well were modified with DPb/DP solutions. For long-term culture the cassette was sterilized by 30-minute exposure to 254 nm UV light prior to modification with DPb/DP solutions.

Surfaces were modified with 0.1 mL DP/DPb solutions at a polymer concentration of 1 mg/mL in a cloud-point buffer (CP buffer, 0.1 M MOPS with 0.6 M K<sub>2</sub>SO<sub>4</sub>, pH = 6.0) overnight at 50° C while stirring. For mixed DOPA<sub>3</sub>PEG<sub>77</sub>biotin (DPb) and DP surfaces, solutions of DPb and DP were prepared in the CP buffer with a molar ratio of DPb to DP ranging from 0.01 to 0.15. After polymer modification, surfaces were rinsed with water. To ensure their integrity, DPb/DP coated surfaces remained under liquid at all times.

### **3.2.6 Immobilization of bSCF to DOPA-PEG-biotin surfaces**

After polymer modification, the upper portion and any defects on the microscope slide were blocked by incubation for 30 minutes with PBS supplemented with 1.0 % wt. BSA (PBS-B). Next, PBS-B was removed, and 100 µL of a 0.1 mg/mL solution of NeutrAvidin (Pierce) in PBS-B was incubated inside the wells for 1 hour with gentle mixing at 37° C. The wells were then rinsed with five dilution rinses of PBS-B. Biotinylated SCF was added at 0.01 mg/ml in PBS-B for 1 hour with gentle mixing at 37° C. The wells were then rinsed 15 times with PBS followed by three rinses with equilibrated media. For cassettes used in cell culture, assembled culture cassettes were sterilized by exposed to UV light (254 nm, 40 mW/cm<sup>2</sup>) for 30 minutes prior to polymer modification. Following sterilization, cassettes were kept in sterile tip boxes

and all materials added to the cassette were sterile-filtered using a 0.22  $\mu\text{m}$  syringe filter to maintain sterility.

### **3.3 GENERAL CELL CULTURE METHODS**

All cultures were maintained in a humidified incubator at 37° C containing 5% CO<sub>2</sub> in air, unless otherwise noted.

#### **3.3.1 Cell counts**

Nucleated cell densities were determined in 3 % (w/v) cetrimide solution (Sigma) using a Coulter Multisizer 3 (Coulter Corporation; Miami, FL). Cell viability was assessed using the trypan blue exclusion assay with a hemacytometer.

#### **3.3.2 Culture of M07e cells**

M07e cells, a human acute megakaryoblastic leukemic cell line, were obtained from the German Collection of Microorganisms and Cell Cultures (DSMZ; Braunschweig, Germany). M07e cells responded to SCF, GM-CSF, interleukin-3 (IL-3), IL-6, and TPO. The cell line was initially cultured in Iscove's modified Dulbecco's medium (IMDM; Sigma, St Louis, MO) supplemented with 20% fetal bovine serum (FBS; Hyclone; Logan, UT) and 100 U/ml GM-CSF (Immunex; Seattle, WA). The cell line was adapted to grow in a low-serum medium (2.5% FBS) by gradually reducing the serum concentration over several weeks. The optimal cell density is 0.5 to 1.0 x 10<sup>6</sup> cells/ml and the doubling time is about 32–46 hours. Cells were used between passages 6–12 after adaptation for all experiments. To prepare cells for cell proliferation and stimulation studies, M07e cells were washed twice with PBS. After PBS rinsing the cells were placed in IMDM + 2.5% FBS without growth factors for 18 hours.

### **3.3.3 Culture of TF-1 cells**

TF-1 cells, a human erythroleukemia cell line, were obtained from the ATCC (Manassas, VA). TF-1 cells are completely dependent on IL-3 or GM-CSF for long-term growth and respond to stimulation with SCF, TPO, IL-6, and other hematopoietic cytokines. The cell line was maintained in RPMI 1640 medium (Sigma) adjusted to contain 2 mM L-glutamine, 1.5 g/L sodium bicarbonate, 4.5 g/L glucose, 10 mM HEPES, and 1.0 mM sodium pyruvate. For culture, RPMI 1640 media was supplemented with 10% FBS and 2 ng/mL GM-CSF. The optimal cell density was  $3 \times 10^4$  to  $5 \times 10^5$  cells/mL, which gave a doubling time of approximately 24 hours.

### **3.3.4 Culture of KG-1a cells**

KG-1a cells are a human acute myelogenous leukemia cell line and were obtained from ATCC. KG-1a cells are cytokine independent and were initially maintained in IMDM adjusted to contain 4 mM L-glutamine, 1.5 g/L sodium bicarbonate, and 20% FBS. The cell line was adapted to grow in a 5% FBS by gradually reducing the serum concentration over several weeks. Cultures were maintained between  $0.5$  and  $1 \times 10^6$  cells/mL.

### **3.3.5 Culture of CD34+ selected cells**

CD34+ selected cells were purchased from AllCells (Berkeley, CA). AllCells obtained informed consent from volunteers before donors provided cells.

#### ***3.3.5.1 Culture in NeutrAvidin-coated polystyrene plates with biotinylated SCF***

Mobilized peripheral blood CD34+ cells were cultured in the presence of soluble SCF (100 ng/mL) or surface-immobilized biotinylated SCF in serum-free medium, X-VIVO 15 (Cambrex BioScience; Walkersville, MD). The media also included 100 ng/mL FL ligand (R&D Systems;

Minneapolis, MN) and 50 ng/mL TPO (R&D systems). Cells were maintained at 37 °C in a humidified incubator under 5% O<sub>2</sub>, 5% CO<sub>2</sub>, and the balance N<sub>2</sub>.

#### ***3.3.5.2 Primitive cell expansion and maintenance with TPOM***

Experiments with cytokine cocktails used frozen BM CD34<sup>+</sup> selected cells thawed according to the supplier's instructions. Cells were cultured in StemPro 34 (Invitrogen; Carlsbad, CA) media with 100 ng/mL stem cell factor (SCF) and 100 ng/mL Flt-3 ligand (FL). TPOM-PEG (5 nM) or rhTPO (50 ng/mL) was added to cultures not performed on lipopeptide surfaces with 1% TPOM-2L. Cells were seeded at 200,000 cells/mL and cultured for six days.

#### ***3.3.5.3 Megakaryocyte differentiation experiments with TPOM***

Frozen mobilized peripheral blood (MPB) or bone marrow (BM) CD34<sup>+</sup> selected cells were thawed according to supplier's instructions and placed in basal medium of X-VIVO 20 (Cambrex BioScience). Cultures were initiated at cell densities between 80,000 and 125,000 cells/mL. Cultures were carried out for up to 14 days, and simulated with either 5 nM TPOM-PEG or on DPPC surfaces containing 1% TPOM-1L. Cultures were fed by replacement of 25% of the media and soluble growth factors beginning on day 7 and continuing every other day until the end of culture; cultures stimulated with TPOM-1L lipopeptides received only media. Control cultures in tissue culture polystyrene plates received 100 ng/mL rhTPO (R&D Systems; Minneapolis, MN) or 5nM TPOM-PEG. Cellular expansion and culture densities were determined as noted above using nucleated cell counts.

#### **3.3.6 Colony forming cell assay**

Colony assays were performed as described [187]. Methylcellulose media (StemCell Technologies) was supplemented with IL-3 (R&D Systems), IL-6 (Peprotech; Cherry Hill, NJ),

granulocyte colony stimulating factor (G-CSF, Amgen), granulocyte-macrophage colony stimulating factor (GM-CSF, Amgen), erythropoietin (EPO, Amgen), and SCF (Amgen). Plating densities ranged from 500 freshly selected CD34<sup>+</sup> cells per mL on day 0 to 3,000 cultured cells per mL on day nine. A drop in cloning efficiency was expected as the total number of cells expanded, therefore the plating densities increased as the cultures expanded [31]. The methylcellulose cultures were incubated 14 days under 5% O<sub>2</sub>. After the 14-day period, colonies were enumerated and classified as CFU-GM, BFU-E, or CFU-Mix through a dark-field stereomicroscope (Zeiss; Batavia, IL). Colonies with less than 50 cells were excluded from counts.

### **3.4 CELL CHARACTERIZATION**

#### **3.4.1 Flow cytometry**

##### ***3.4.1.1 Apoptosis***

The level of apoptosis of factor-starved M07e cells was evaluated with flow cytometry via Annexin V-FITC as previously described [32]. Briefly, 5x10<sup>5</sup> cells were washed twice in PBS supplemented with 2 mM EDTA and 0.1% BSA (PEB). Cells were then incubated in Annexin V-FITC (BD-Pharmingen, San Diego, CA) and propidium iodide (PI, Sigma) in Annexin V binding buffer (10 mM HEPES, 140 mM NaCl, 2.5 mM CaCl<sub>2</sub>, pH 7.4). Fluorescence intensities for Annexin-V and PI were acquired using a FACScan flow cytometer (BD Immunocytometry Systems; San Jose, CA) and the data were then analyzed with CellQuest software (BD Immunocytometry Systems). Unstained cells were used to set flow cytometer PMTs prior to data acquisition. Since a portion of the emission spectra of FITC and PE overlaps

each other, cells stained with either FITC or PE were used to compensate for the overlapping fluorescence signals.

#### ***3.4.1.2 Cell cycle***

Cellular DNA content was analyzed to determine their position in the cell cycle as previously described [188]. Briefly, one million cells were washed twice in PEB and were fixed in 75% ethanol on ice for 30 minutes. The cells were then washed twice with PEB before resuspending in staining solution containing 50 µg/mL PI, 30 µg/mL ribonuclease A and 0.1% (v/v) Triton X-100. Cells were stained for 30 minutes prior to collection of data on the FACScan flow cytometer. At least 10,000 events were collected in duplicate. The data were analyzed using ModFit LT software (Verity Software House, Topsham, ME).

#### ***3.4.1.3 CD34 and Thy1 expression***

The presence of cell surface markers, CD34 and Thy1, was determined using flow cytometry with cells stained with FITC-conjugated anti-CD34 antibody and phycoerythrin (PE)-conjugated anti-Thy1 antibody. Cells (~100,000) were washed twice with 0.5 ml PBS supplemented with 0.05% (w/v) Sodium Azide and 0.1% BSA (PAB). Ten microliters of each antibody was added to cells and incubated at room temperature for 30 minutes. After staining, cells were washed twice with 0.5 ml PAB. Prior to acquisition, 7-AAD or DAPI was added to exclude dead cells. Data were collected and analyzed as described above.

#### ***3.4.1.4 Flow cytometry for the analysis of Mk cells***

To assess the viable Mks undergoing apoptosis, cells were stained simultaneously for the expression of CD41, Annexin V, and 7-AAD as previously described [189]. Briefly, cells were washed with PEB and incubated with PE-conjugated anti-CD41 antibody (Immunotech;

Fullerton, CA). After washing, cells were resuspended in Annexin V binding buffer containing FITC-conjugated Annexin V and 7-AAD (Sigma) and analyzed by flow cytometry. Cells undergoing apoptosis are Annexin V<sup>+</sup> and 7-AAD<sup>-</sup>. To determine the extent of polyploidization, cells were labeled with FITC-conjugated anti-CD41 antibody (Immunotech; Fullerton, CA) and fixed with 0.5% paraformaldehyde for 15 minutes at room temperature followed by permeabilization with cold 70% methanol on ice for 1 hour. Cells were then treated with RNase followed by 50 µg/mL propidium iodide (to stain DNA), and analyzed by flow cytometry.

#### ***3.4.1.5 Cell signaling assay***

M07e cells were removed from growth-factor-containing media and placed in IMDM supplemented with 2.5% FBS for 18 hours prior to stimulation. The cells were then resuspended in fresh IMDM supplemented with 2.5% FBS and with growth factors or mimetic peptides, as noted, and immediately seeded at approximately 80,000 cells/well in culture cassettes or 96-well plates for stimulation. Growth factor starved M07e cells were stimulated with rhTPO or TPOM on various surfaces for 20 minutes. A published flow cytometric method [190] was adapted for measuring phosphorylated ERK1/2 and STAT5. Briefly, cells were harvested and fixed with 2% paraformaldehyde, at 4° C. Next, the cells were permeabilized by the addition of ice cold 90% methanol solution and placed on ice. Samples were rinsed once with PBS-B followed by blocking for 30 minutes at 4°C with the same solution. Samples were then stained with a phosphospecific ERK1/2 rabbit monoclonal antibody (Cell Signaling Technologies; Beverly, MA) and a phosphospecific STAT5a mouse monoclonal antibody conjugated to AlexaFluor 488 (BD Pharmingen) at room temperature and rinsed twice with PBS-B. Samples were then stained with PE conjugated goat anti-rabbit secondary antibody (Jackson ImmunoResearch; West

Grove, PA) for 20 minutes at room temperature, washed twice with PBS-B and resuspended in PBS-B for acquisition. Data was acquired using FACScan or LSR-II flow cytometer (BD Immunocytometry Systems) and analyzed with CellQuest or FACS-DIVA software. The fold-over-isotype method was used to normalize the data for experiment-to-experiment variation. To calculate this value, the mean fluorescence intensity (MFI) of a sample was divided by the MFI of an isotype-matched control that was performed on the same day.

#### ***3.4.1.6 Carboxyfluorescein diacetate, succinimidyl ester (CFSE) labeling of cells***

The method used for staining cells was based on those previously described [191, 192]. Briefly, cells were washed twice with SFM and resuspended at  $5 \times 10^6$  cells per mL in PBS. Carboxyfluorescein diacetate, succinimidyl ester (CFSE, Invitrogen; Carlsbad, CA) was added in DMSO to a final concentration of 2  $\mu\text{mol/L}$ . The mixture was incubated in a water bath at 37° C for 10 minutes. Subsequent uptake of the dye was stopped by the addition of ten volumes of ice cold HBSS supplemented with 20% FBS (HBF). The cells were washed once in HBF followed by one wash in HBSS and resuspended at  $5 \times 10^5$  cells/mL in StemPro 34 Media. Cells were cultured overnight at 37° C to allow CFSE not stably bound to intercellular proteins to move outside of the cells.

Following overnight culture, cells were washed twice with HBSS supplemented with 2% FBS. A portion of the cells were removed for further analysis via flow cytometry and the remaining cells were placed into culture. Cells used in flow cytometry analysis were stained with either PE-conjugated anti-CD34 or anti-Thy1 (BD Pharmingen) for 30 minutes at 4° C. After incubation, cells were washed twice in PAB and 0.05  $\mu\text{g}$  PI was added to each tube. Data was acquired on a FACScan and analyzed using CellQuest (BD Immunocytometry Systems; San

Jose, CA) and ModFit LT Software. Cells expressing high levels of PI were gated out as dead cells.

### **3.4.2 Adhesion assay**

Cell adhesion to DOPA-PEG-biotin or lipopeptide containing surfaces was determined by counting fluorescently labeled cells before and after centrifugation. M07e cells were dyed with CFSE or Calcein AM (Invitrogen) and incubated in wells coated with surfaces containing various concentrations of TPOm lipopeptides for two hours at 37°C and 5% CO<sub>2</sub>. A fluorescence microscope at 5x magnification was used to take three images at defined places in each well. Non-adherent cells were removed via normal force centrifugation of cassettes in bags filled with PBS at 30 rcf for 5 minutes. To ensure surface integrity, the cassettes remained submerged under liquid at all times. After centrifugation, wells were re-imaged at the same three defined positions. Metamorph software (Molecular Devices; Sunnyvale, CA) was used to count the number of cells in each field. The values obtained from the three images were averaged for each well and the fraction of adherent cells was calculated by dividing the number of cells in the post-centrifugation images by the number of cells in the pre-centrifugation images.

## **CHAPTER 4: EXPLORATION OF REDUCED OXYGEN TENSION FOR HSC SELF-RENEWAL**

### **4.1 INTRODUCTION**

The bone marrow (BM) is the primary site of HSCs within the body, and experimental evidence suggests HSCs interact with osteoblasts located near the endosteum [64-66, 193]. The endosteum is located at the interface between the bone marrow and the inner surface of the bone [17]. This region is the furthest away from the central sinuses supplying nutrients. It has been demonstrated experimentally that  $pO_2$  falls approximately 16 mmHg 30  $\mu\text{m}$  (~3 cell diameters) away from a blood vessel and continues to decrease as distance from the vessel increases [73]. Thus, HSCs reside in areas of the BM with subvascular  $pO_2$ .

Previous studies have revealed oxygen tension to be an important determinate of proliferation and differentiation in the culture of hematopoietic cells. In low oxygen cultures (~5%, 38 mmHg) the production of erythrocyte, megakaryocyte, and granulocyte/monocyte progenitors are enhanced [30, 194-196], while an elevated  $pO_2$  can accelerate the maturation of erythrocytes and megakaryocytes [32, 196]. Reduced oxygen tension has also been examined in the expansion of primitive hematopoietic cells. Results show that culture at 1%–5%  $O_2$  preserves human CB and BM HSCs better than at 20%  $O_2$  [26, 28, 29].

Several techniques were developed to better understand the important cellular processes occurring in cultures of HSCs. These techniques employed the use of flow cytometry and include cell division tracking with (5 and 6)-carboxyfluorescein diacetate, succinimidyl ester (CFSE, Section 4.2.1) and the detection of phosphorylated molecules in the MAPK and Akt signaling pathways (section 4.2.2). Methods were adapted from previously established protocols using cell lines to reduce the expense of method development on primary cells.

Cell division tracking was used to analyze cultures of BM and mobilized peripheral blood (mPB) CD34<sup>+</sup> selected cells. These cultures were performed in low oxygen environments (5% and 2% O<sub>2</sub>) and compared to control conditions performed at 20% O<sub>2</sub> (Section 4.3). Our results indicated enhancement in expansion of CD34<sup>+</sup>Thy1<sup>+</sup> cells in 2% O<sub>2</sub> with elevated growth factor concentrations. Nevertheless, due to the small differences seen between conditions and the likelihood that many expensive primary cell samples would be necessary to show statistically significant differences, this line of research was not continued.

## **4.2 DEVELOPMENT OF TOOLS FOR ANALYSIS OF CELLULAR PROCESSES**

### **4.2.1 Cell division tracking protocol development**

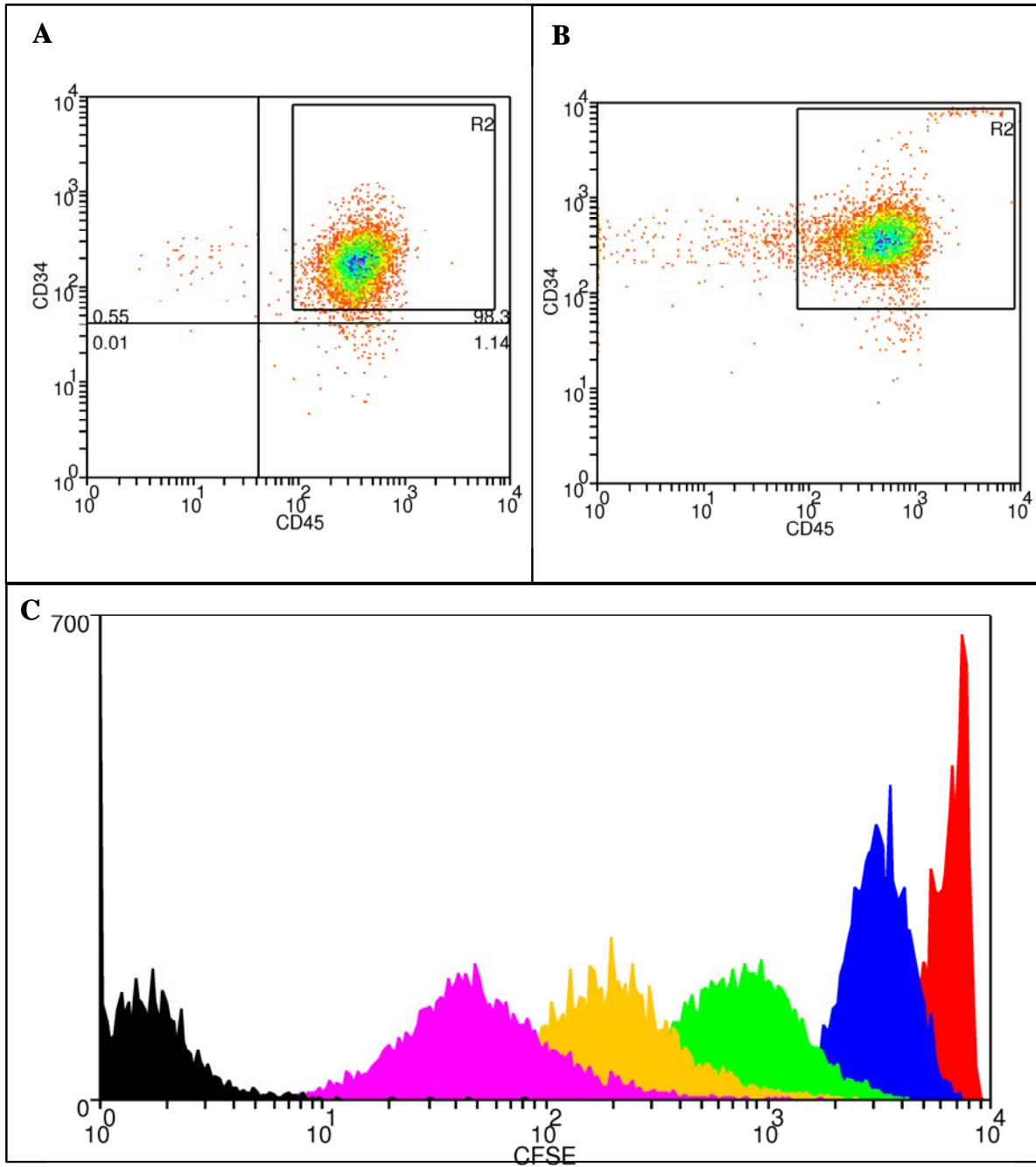
CFSE was used to directly assess the division history of cell lines and primitive cells. To stain cells, the non-fluorescent CFSE molecule is allowed to passively diffuse into cells. Once inside, cellular esterases cleave acetate groups creating a fluorescent molecule. The cleavage process exposes the succinimidyl ester, allowing it to covalently bind to free amines on intracellular proteins and create long-lived fluorescent adducts. The covalent linkage prevents the diffusion of the fluorescent molecules out of the cell. With each successive division, the fluorescence intensity decreases by ½ due to the partitioning of labeled proteins. The protocol for cell division tracking using CFSE was adapted from a previously established protocol [192].

Methods were modified for three-color staining to track the cell division history of CD34<sup>+</sup>Thy1<sup>+</sup> cells. The published protocol did not allow for three-color staining due to the intense staining of CFSE. When analyzing these cells, the fluorescence due to CFSE was so bright it ‘bled’ into additional channels and could not be removed by compensation. This prohibits the observation of additional fluorescent markers. By reducing the initial staining concentration from 10 μM to

2  $\mu$ M, it was possible to observe dual positive (CD34+CD45+) cells, while tracking the division of the cell line Kg-1a for up to 10 days (Figure 4.2.1). This method can also be used to track other cell populations stained with antibodies that are linked to phycoerythrin (PE) and Peridinin chlorophyll protein (PerCP).

Even in cells that do not divide, a small fraction of CFSE naturally moves out of the cell over time [192, 197]. Therefore, the use of initial results for comparison to later time points is not desirable. To track the number of divisions occurring at different time points, a ‘no division’ control was developed. Several options for the ‘no division’ control were explored using the M07e cell line: culture at 4° C, culture without growth factors, and culture in the presence of the cell cycle inhibitor colcemid (0.1  $\mu$ g/mL). Analysis showed that both colcemid and culture at 4°C inhibited cell division to a similar degree (Figure 4.2.2A). However, trypan blue exclusion assays in subsequent experiments showed that the viability of cells cultured at 4° C decreased to a much greater extent (Figure 4.2.2B). Therefore, colcemid was chosen as the ‘no division’ control.

**Figure 4.2.1:** Tracking cell division of a dual positive population of Kg-1a cells for 10 days. Kg-1a cells were labeled with 2  $\mu$ mol/L CFSE. Cell divisions and the cell surface expression of CD34 and CD45 were followed for 10 days in culture. Gating strategy for the isolation of Kg-1a cells positive for CD34 and CD45 on day 10 for 2  $\mu$ M (**A**) and on day 7 for 10  $\mu$ M (**B**). Histogram showing the cell division profile of CD34+CD45+ cells stained with 2  $\mu$ M CFSE cultured for 10 days (**C**) and CD34+CD45+ cells stained with 10  $\mu$ M CFSE cultured for 10 days (**D**). CFSE fluorescence is shown for day 0 (right most), day 2, day 5, day 7, and day 10. The population nearest the left axis is an isotype control performed on day 10 (C) or day 7 (D).



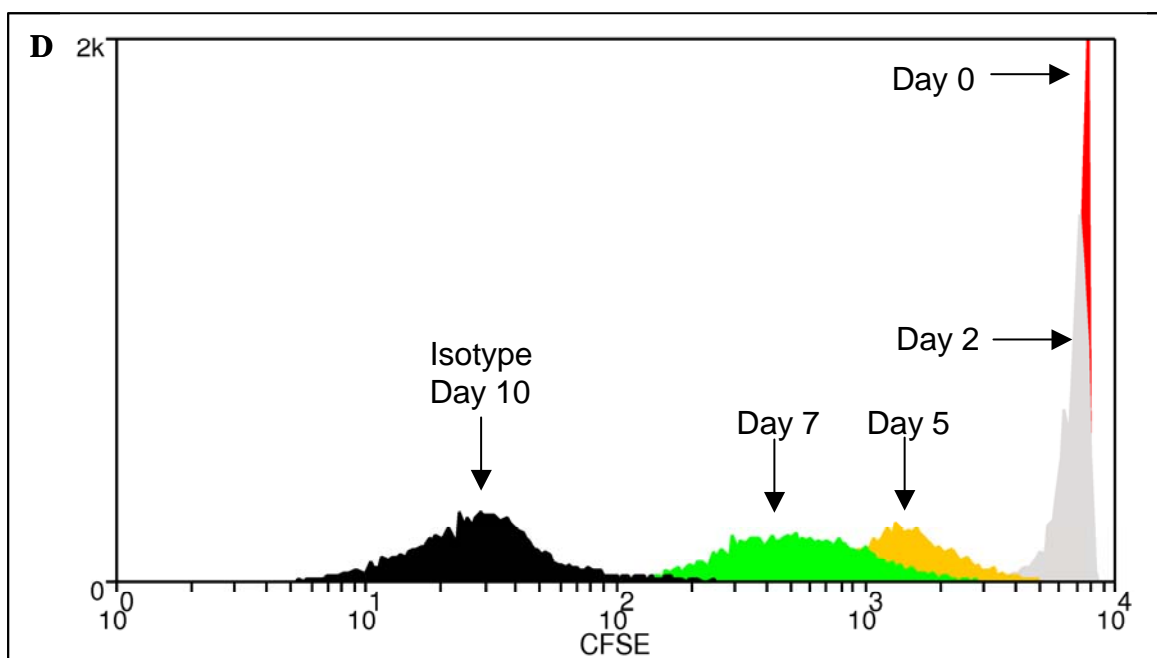
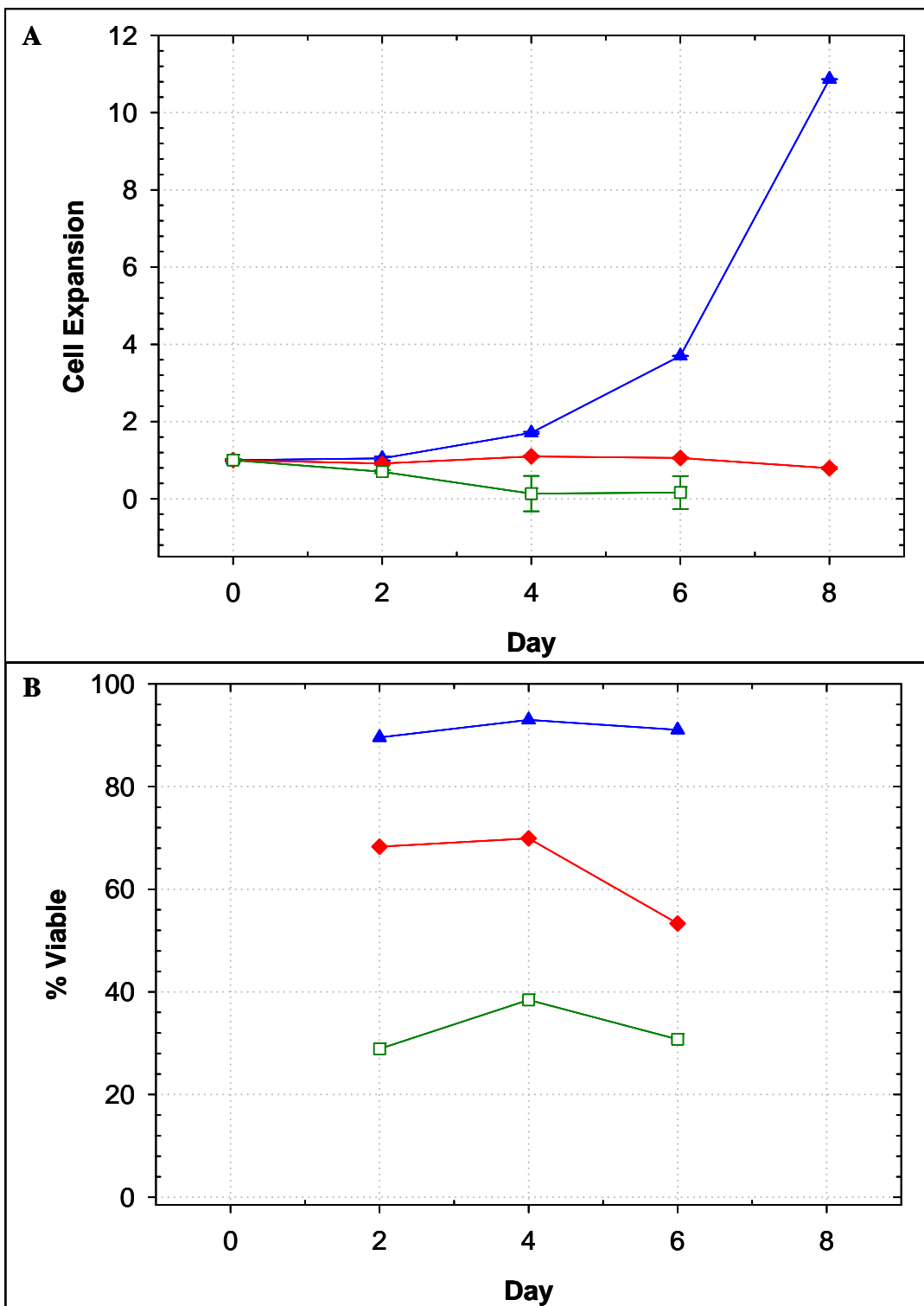


**Figure 4.2.2:** Development of a ‘no division’ control. M07e cells were cultured in IMDM + 2.5% FBS. Cells were cultured at 37° C in the absence (triangles) or presence (diamonds) of 0.1  $\mu$ g/mL colcemide or at 4° C (open squares) for six days. **(A)** Expansion of cells relative to day 0 and **(B)** viability as determined by trypan blue exclusion. Data is representative of two separate experiments.



#### **4.2.2 Development of flow cytometric cell signaling assays**

Recent advances in the ability to detect phosphorylated proteins in permeabilized cells have enabled the study of signal transduction processes via flow cytometry [198]. The use of flow cytometric methods for analysis of signal transduction processes has several advantages over traditional methods such as Western blots and ELISA assays. Flow cytometry analyses are faster, require fewer cells, and provide information about individual cells and population distributions, rather than the mean value for a population of cells. These assays can also be multiplexed and allow the detection of multiple signaling molecules in a single cell. SCF-stimulated M07e cells were used to develop flow cytometric assays for the detection of total and phosphorylated ERK 1,2 and Akt. Results show significant differences between stimulated cells and unstimulated controls, with greater separation for phosphorylated ERK 1,2 (Figure 4.2.3). We have shown the average response of M07e cells to SCF measured using flow cytometry was similar to that measured using Western blots [184].

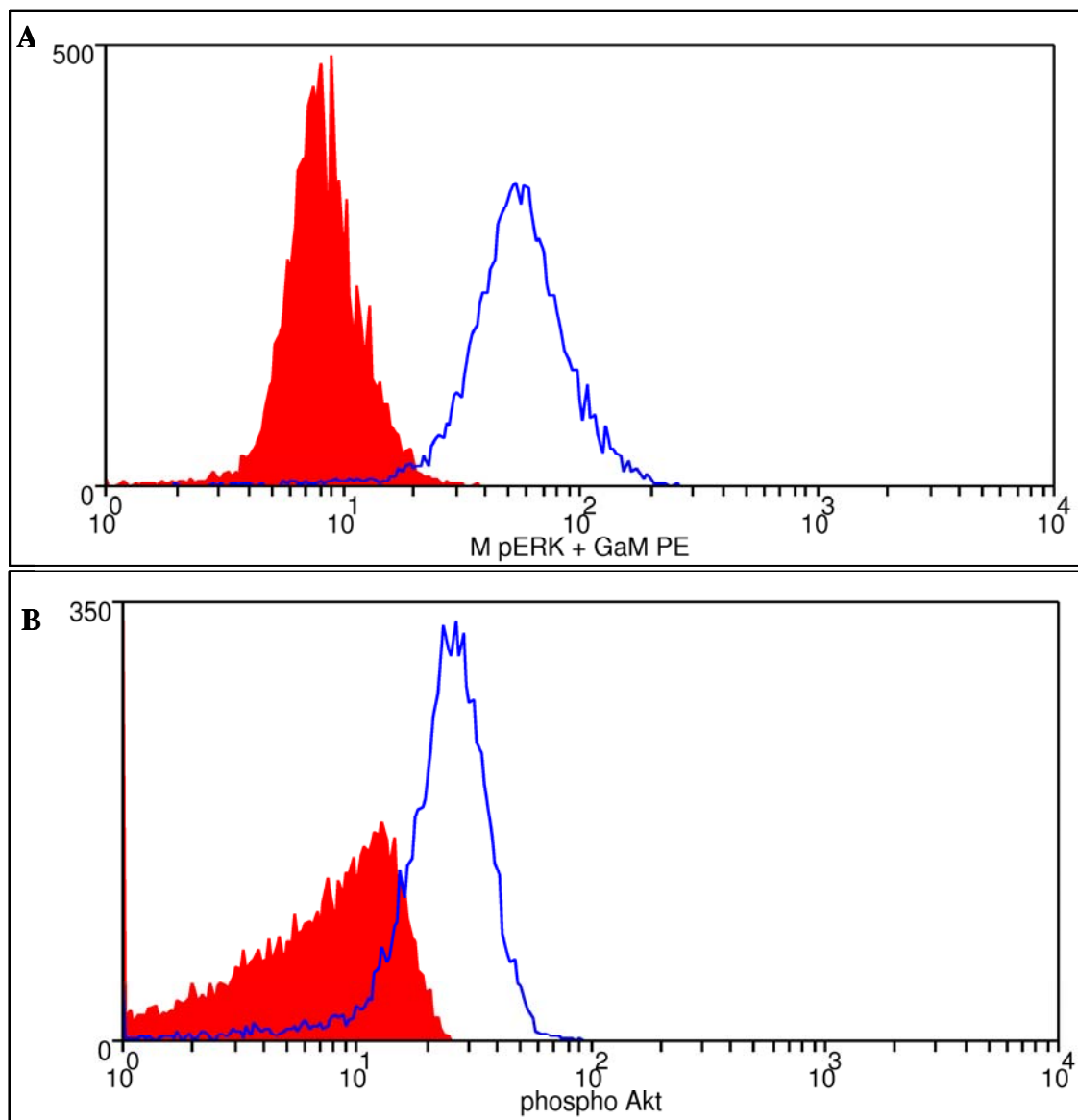


**Figure 4.2.3:** Development of flow cytometric cell signaling assays for phosphorylated ERK and Akt. M07e cells were starved overnight and stimulated in serum-containing media (IMDM + 2.5% FBS) for 15 minutes in TPCS plates followed by processing according to a cell-signaling protocol (Section 3.4.1.5). Unstimulated cells are shown in filled histograms, while cells stimulated with 50 ng/mL SCF are shown as unfilled histograms (line) for cells stained with **A**) anti-phospho-ERK and **B**) anti-phospho-Akt antibodies. Data is representative of at least three separate experiments.

### **4.3 PRIMARY CELL CULTURES AT 5% AND 20% O<sub>2</sub>**

Several experiments were performed using CD34<sup>+</sup> selected BM cells to evaluate the effects of oxygen tension on the culture outcome. Previous experience with primary CD34<sup>+</sup> selected cells indicates that the majority of CD34<sup>+</sup>Thy1<sup>+</sup> primitive cells are lost by the fourth day in culture. To focus on the culture of the candidate HSCs, we chose to conduct short-term three-day cultures. In these cultures the overall cellular expansion, as well as expansion and retention of CD34<sup>+</sup> and CD34<sup>+</sup>Thy1<sup>+</sup> cells were evaluated for a total of seven different conditions (Table 4.3.1). Six of the conditions were evaluated in low oxygen environments (5% and 2% O<sub>2</sub>) and compared to a single condition in normoxia (20% O<sub>2</sub>). Two of the low O<sub>2</sub> conditions served as controls for cell division tracking studies detailed below. Reports suggest that high levels of cytokines increase the maintenance of the most primitive cells [199, 200]. Therefore, two different cytokine doses were also evaluated: five of the seven conditions were supplemented with our normal levels of cytokines (100 ng/mL SCF, 100 ng/mL FL, and 50 ng/mL TPO) and the two remaining conditions received three-fold greater concentrations of growth factors (HGF; 300 ng/mL SCF, 300 ng/mL FL, and 150 ng/mL TPO). Cells not stained with CFSE were grown under 5% O<sub>2</sub> and used as a control to determine if CFSE staining negatively influenced overall expansion. All conditions employed the serum free media, StemPro 34.

After three days in culture, there was no statistical difference in the overall expansion of cells in cultures at 5 and 20 % O<sub>2</sub> ( $p = 0.536$ ). On average, these cultures had only recovered to the input number of cells after an initial decrease (Figure 4.3.1). Additionally, statistically significant differences were not seen between cultures at 5 and 20 % O<sub>2</sub> in the ability to retain CD34<sup>+</sup> cells (day 3  $p = 0.53$ , Figure 4.3.2) or CD34<sup>+</sup>Thy1<sup>+</sup> cells (day 3  $p = 0.22$ , Figure 4.3.3).

Comparison of control unstained cells to CFSE stained cells showed CFSE did not alter overall expansion ( $p = 0.703$ , Figure 4.3.1) or expansion of CD34+Thy1+ cells ( $p = 0.472$ , Figure 4.3.3). Cultures under 2% O<sub>2</sub> or with HGF were evaluated in a single experiment and sampled only on day three. Results from this experiment showed that 5% O<sub>2</sub> with HGF gave an improvement in overall expansion compared to cultures under 5% O<sub>2</sub> with normal cytokine levels ( $p = 0.03$ , Figure 4.3.4). HGF 5% O<sub>2</sub> cultures also exhibited an advantage in the expansion of CD34+Thy1+ cells (Figure 4.3.5). Cultures at 2% O<sub>2</sub> showed a small decrease in the density of cells, but the addition of HGF improved cell density to a level equivalent to that seen in conditions at 5% O<sub>2</sub> (Figure 4.3.4). HGF cultures in 2% O<sub>2</sub> also produced a significantly greater number of CD34+Thy1+ cells as compared to 2% O<sub>2</sub> ( $p < 0.005$ , Figure 4.3.5).

The cell division profiles for the same six conditions were also compared. Figure 4.3.6 shows a representative example of the overall pattern of cell divisions at day three in culture. Cultures in 20% and 5% oxygen environments behaved similarly with respect to the number of divisions, but cultures in 2% oxygen had a larger percentage of cells with 0 or 1 division. Analysis of the division pattern of CD34+Thy1+ cells shows that some portion of cells from all conditions had undergone at least one division by day three, and in some conditions cells had undergone as many as four divisions (Figure 4.3.7). The benefit of high growth factor concentrations is also shown in Figure 4.3.7, with a greater retention of CD34+Thy1+ cells after division as compared to normal growth factors under the same O<sub>2</sub> environment. The HGF conditions also had a greater percentage of CD34+Thy1+ cells per division.

**Table 4.3.1:** Summary of the conditions evaluated in three-day cultures of BM CD34+ cells.

	Condition Name	Growth Factors	Other
1	20% O <sub>2</sub>	Normal <sup>1</sup>	
2	5% O <sub>2</sub>	Normal	
3	5% O <sub>2</sub> HGF	HGF <sup>2</sup>	
4	2% O <sub>2</sub>	Normal	
5	2% O <sub>2</sub> HGF	HGF	
6	5% O <sub>2</sub> Colce.	Normal	With 0.1 µg/mL colcemide
7	5% O <sub>2</sub> Mock	Normal	No CFSE added <sup>3</sup>

<sup>1</sup> 100 ng/mL SCF, 100 ng/mL FL, and 50 ng/mL TPO

<sup>2</sup> 300 ng/mL SCF, 300 ng/mL FL, and 150 ng/mL TPO

<sup>3</sup> Cells for all of the other conditions were stained with CFSE

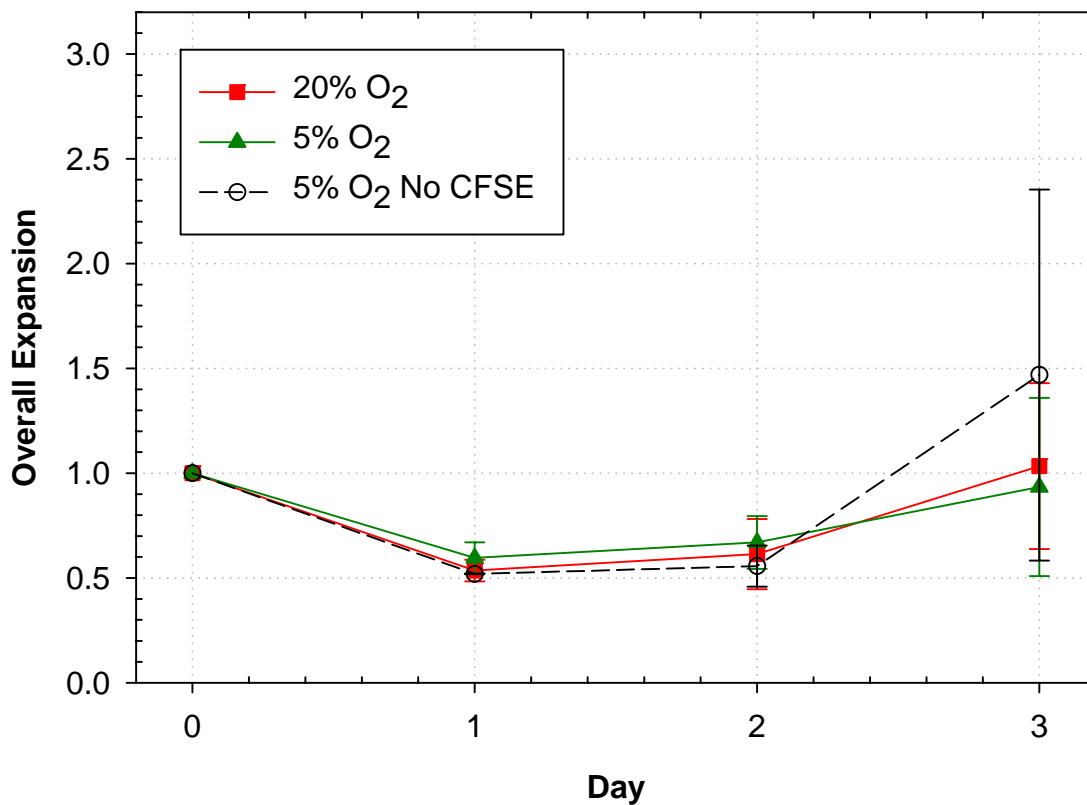


**Figure 4.3.1:** Overall expansion of BM CD34<sup>+</sup> cells in three day cultures. CFSE stained cells (Section 3.4.1.6) were seeded at ~200,000 cells/mL into 24-well plates with serum-free media and 100 ng/mL SCF, 100 ng/mL FL, and 50 ng/mL TPO. Cultures were grown in two different humidified, 5% CO<sub>2</sub> incubators: one with atmospheric oxygen concentration (20% O<sub>2</sub>, solid squares) and the other with 5% O<sub>2</sub> (solid triangles); the balance was N<sub>2</sub>. Unstained cells (No CFSE, open circles dashed line) were cultured under 5% O<sub>2</sub>. Sample wells were sacrificed on days 1, 2, and 3 and the cell density determined using a Coulter counter. Expansion was calculated by dividing the overall cell density on day X by the initial cell density. Data shown are the average of two experiments  $\pm$  S.E.M.

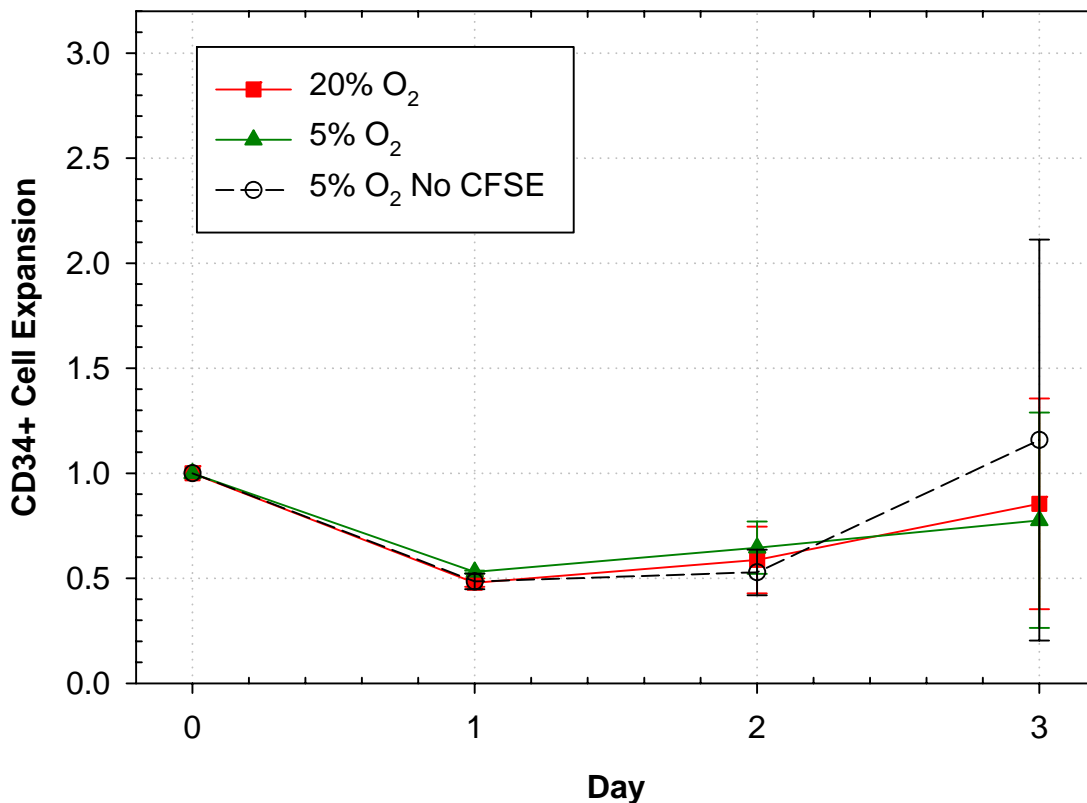


**Figure 4.3.2:** Expansion of CD34<sup>+</sup> cells in three-day cultures. CFSE stained cells (Section 3.4.1.6) were seeded at ~200,000 cells/mL into 24-well plates with serum-free media and 100 ng/mL SCF, 100 ng/mL FL, and 50 ng/mL TPO. Cultures were grown in two different humidified, 5% CO<sub>2</sub> incubators: one with atmospheric oxygen concentration (20% O<sub>2</sub>, squares) and the other with 5% O<sub>2</sub> (triangles); the balance was N<sub>2</sub>. Unstained cells (No CFSE, open circles) were cultured under 5% O<sub>2</sub>. The overall expansion of cells was multiplied by the percentage of CD34<sup>+</sup> cells (determined by flow cytometry) to obtain the number of CD34<sup>+</sup> cells/mL. Expansion was calculated by dividing the number of CD34<sup>+</sup> cells/mL on day X by the initial number of CD34<sup>+</sup> cells/mL. Data shown are the average of two experiments  $\pm$  S.E.M.

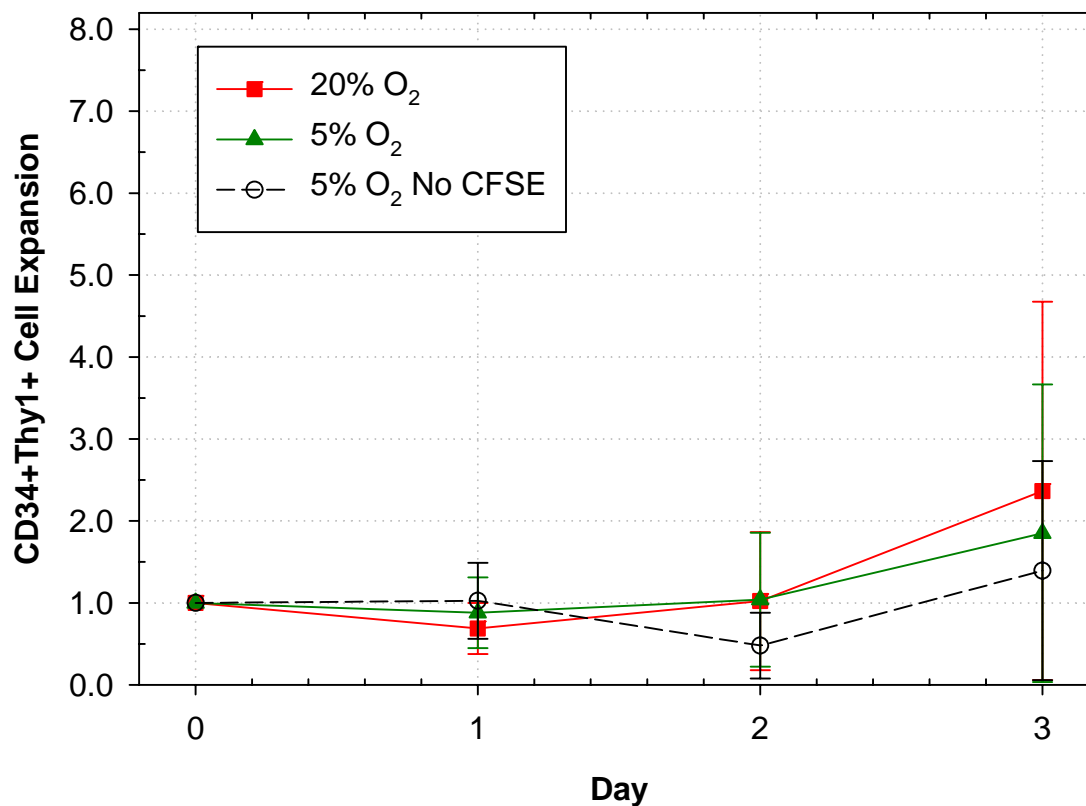


**Figure 4.3.3:** Expansion of CD34+Thy1+ cells in three-day cultures. CFSE stained cells (Section 3.4.1.6) were seeded at ~200,000 cells/mL into 24-well plates with serum-free media and 100 ng/mL SCF, 100 ng/mL FL, and 50 ng/mL TPO. Cultures were grown in two different humidified, 5% CO<sub>2</sub> incubators: one with atmospheric oxygen concentration (20% O<sub>2</sub>, squares) and the other with 5% O<sub>2</sub> (triangles); the balance was N<sub>2</sub>. Unstained cells (No CFSE, open circles) were cultured under 5% O<sub>2</sub>. The overall expansion of cells was multiplied by the percentage of CD34+Thy1+ cells (determined by flow cytometry) to obtain the number of CD34+Thy1+ cells/mL. Expansion was calculated by dividing the number of CD34+Thy1+ cells/mL on day X by the initial number of CD34+Thy1+ cells/mL. Data shown are the average of two experiments  $\pm$  S.E.M.

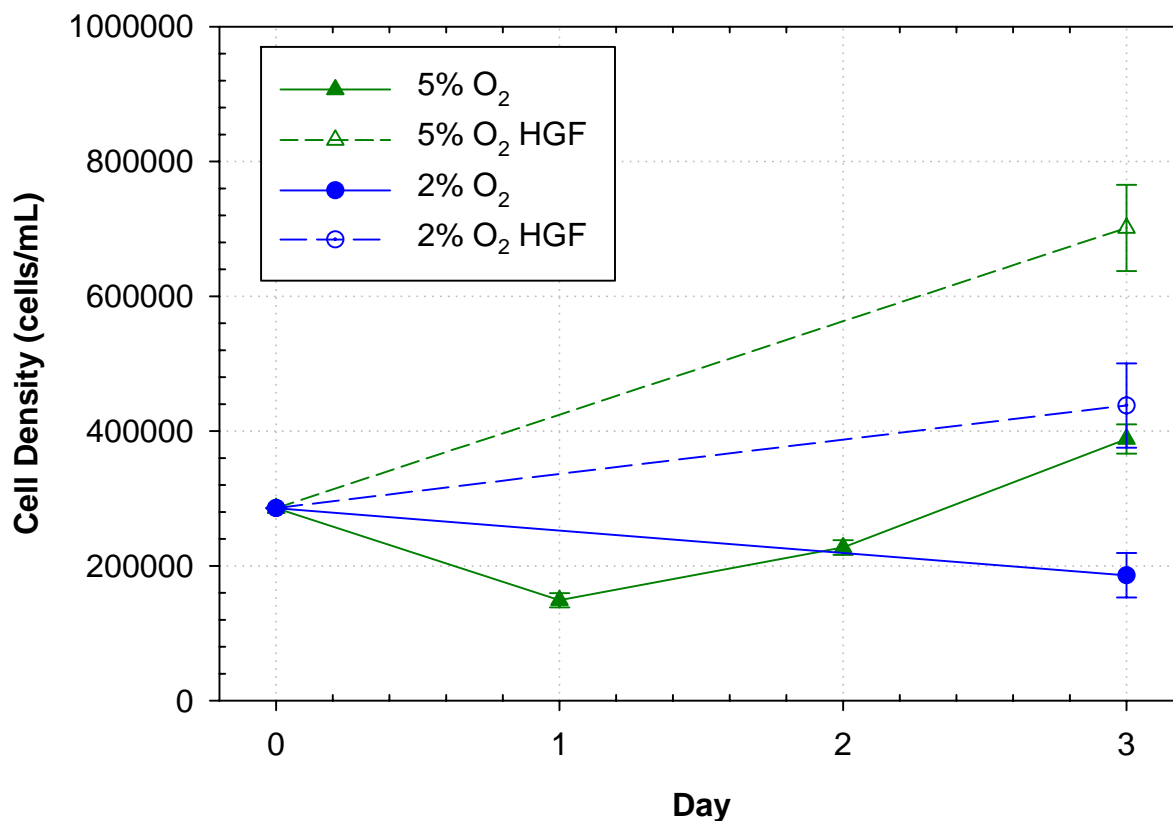


**Figure 4.3.4:** Cell density of BM CD34<sup>+</sup> cells cultured in low oxygen concentration (2%) or elevated growth factor concentrations for three days. Cultures were grown in two different humidified, 5% CO<sub>2</sub> incubators: 5% O<sub>2</sub> (triangles) and 2% O<sub>2</sub> (circles). Cells were seeded at 250,000 cells/mL into 24-well plates with serum-free media and 100 ng/mL SCF, 100 ng/mL FL, and 50 ng/mL TPO (filled symbols) or for elevated levels of growth factors (HGF, open symbols) media contained 300 ng/mL SCF, 300 ng/mL FL, and 150 ng/mL TPO. Sample wells were sacrificed only on day 3 and cell density determined using a Coulter counter. Data shown are the average of replicate samples from a single experiment  $\pm$  S.E.M.

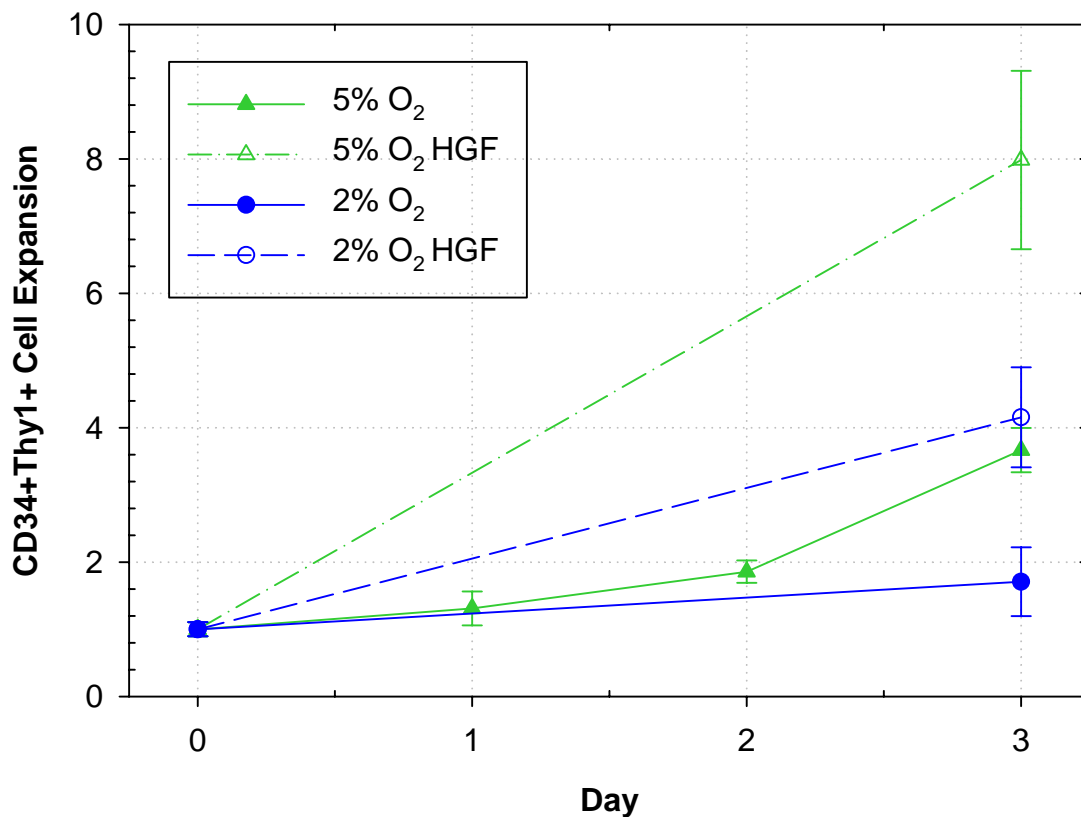


**Figure 4.3.5:** Expansion of CD34+Thy1+ cells in three-day cultures. Cultures were performed as described in Figure 4.3.4. The overall expansion of cells was multiplied by the percentage of CD34+Thy1+ cells (determined by flow cytometry) to obtain the number of CD34+Thy1+ cells/mL. Expansion was calculated by dividing the number of CD34+Thy1+ cells/mL on day X by the initial number of CD34+Thy1+ cells/mL. Data shown are the average ( $\pm$  SEM) of replicate samples from a single experiment.

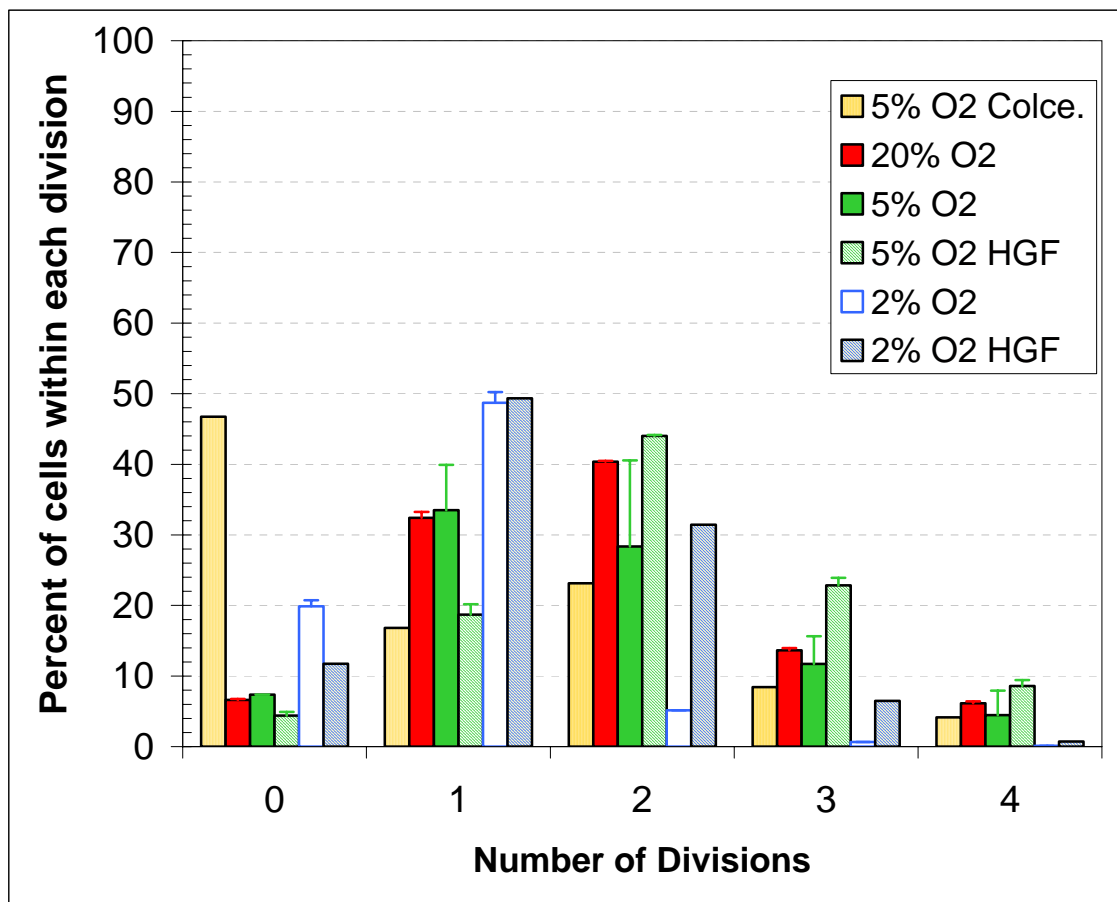


**Figure 4.3.6:** Overall cell division pattern of CD34+ cells cultured for three days as described in Figures 4.3.1 and 4.3.4. Percent of cells that had undergone a given number of cell divisions, tracked with CFSE dye at the end of a three-day experiment. Cells cultured with 0.1  $\mu\text{g}/\text{mL}$  colcemide (vertical stripes) were used a ‘no division’ control. From left to right the series shown are: 5% O<sub>2</sub> with colcemide, 20% O<sub>2</sub> (solid black bars), 5% O<sub>2</sub> (solid grey bar), 5% O<sub>2</sub> with HGF (grey downward diagonal stripes), 2% O<sub>2</sub> (white bars), and 2% O<sub>2</sub> with HGF (lt. grey horizontal stripes). Data shown are the average of replicate samples from a single experiment  $\pm$  S.E.M.

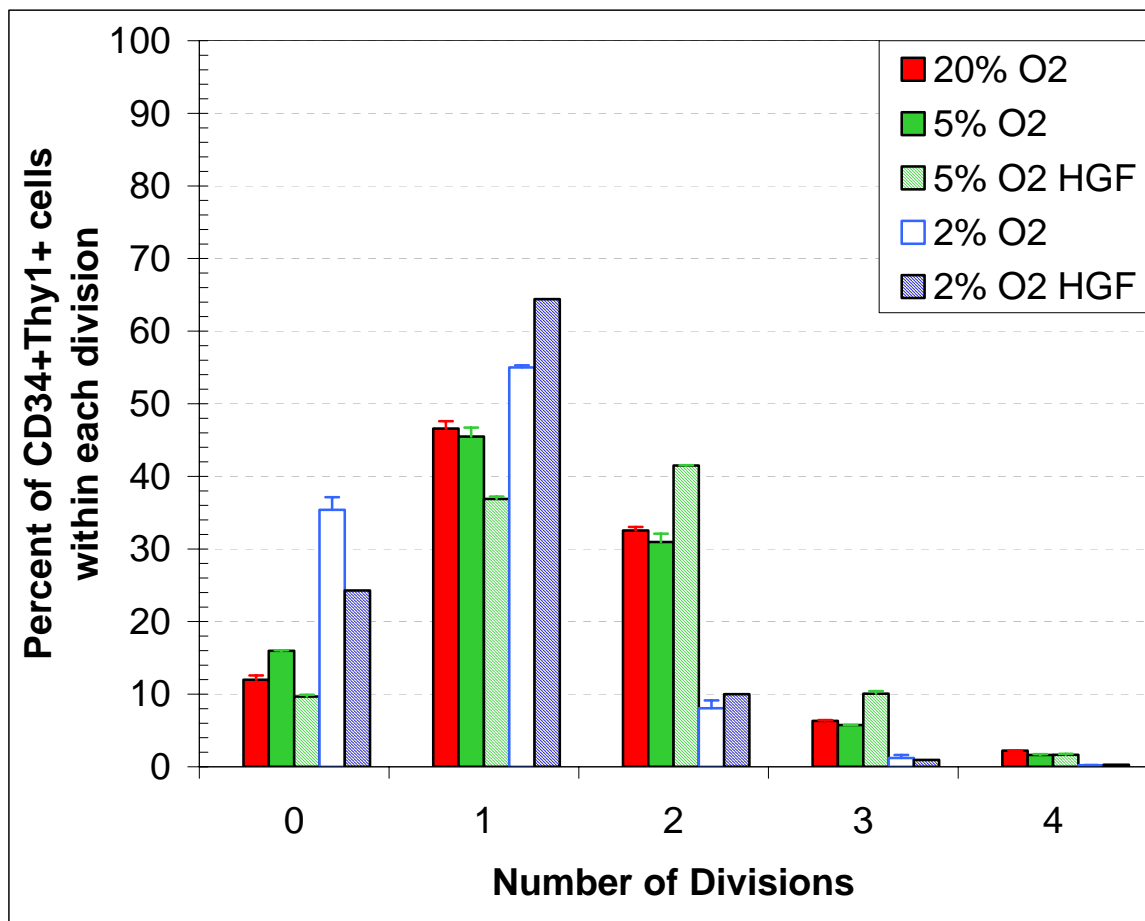


**Figure 4.3.7:** Cell division pattern of CD34+Thy1+ cells cultured for three days as described in Figures 4.3.1 and 4.3.4. Percent of CD34+Thy1+ cells that had undergone a given number of cell divisions, from left to right the series shown are: 20% O<sub>2</sub> (solid black bars), 5% O<sub>2</sub> (solid grey bar), 5% O<sub>2</sub> with HGF (grey downward diagonal stripes), 2% O<sub>2</sub>(white bars), and 2% O<sub>2</sub> with HGF (lt. grey horizontal stripes). Data shown are the average of replicate samples from a single experiment  $\pm$  S.E.M.

#### **4.4 DISCUSSION OF PRIMARY CELL EXPERIMENTS WITH LOW OXYGEN TENSION**

Studies prior to these experiments suggested that culture of HSCs in reduced oxygen tension should improve the expansion of candidate HSCs. Previous studies by our group identified reduced oxygen tension as a key variable in the expansion of committed progenitors [30, 194-196]. Other groups have explored the effects of low oxygen tension on the culture of HSCs [24-29]. Two published reports by Ivanovic and co-workers showed that mouse BM CD34+ cells grown at 1% O<sub>2</sub> maintained stem cell potential (evidenced by repopulating assays), while cultures at 20% O<sub>2</sub> did not [25, 27]. This group also showed that human mPB CD34+ selected cells cultured at 1% O<sub>2</sub> maintained stem cell potential [26]. Similarly, Danet, et al. showed that human BM CD34+ cells cultured at 1.5% O<sub>2</sub> resulted in ~ 6 fold expansion of NOD/SCID repopulating cell compared to cultures at 20% O<sub>2</sub> [29].

The main goal of these experiments was to determine if culture of HSCs in reduced oxygen tension would yield greater expansion of CD34+Thy1+ cells. We hypothesized that cultures at 5% O<sub>2</sub> would maintain the expression of candidate stem cell markers, while undergoing division better than cultures at 20%. However, results from cell division tracking studies showed no significant difference in the ability to retain CD34+Thy1+ expression in cells undergoing division under different O<sub>2</sub> tensions. It is possible that with additional samples we would have been able to show statistically significant differences. However, due to the small differences seen between conditions and the expensive nature of these experiments, this line of research was not continued.

## **CHAPTER 5: STUDIES WITH TPO MIMETIC PEPTIDE AND LIPOPEPTIDES**

### **5.1 INTRODUCTION**

Thrombopoietin (TPO) is an important regulator of primitive HSCs and committed progenitors [9-12, 62, 77, 147, 148, 201]. The interaction between TPO and its receptor, c-Mpl, induces the activation of several signaling pathways, including the JAK/STAT, MAPK, and PI3-K pathways [148, 156, 157]. Studies have shown that the amplitude and duration of TPO-induced activation results in differentiation, proliferation, or protection from apoptosis [202-204]. Using Mpl-transduced BaF-3 cells Millot and coworkers showed that cells with high levels of TPO-stimulated activation resulted in proliferation, while cells with lower activation levels only promoted survival of cells [202]. Matasumura et al. used Mpl-transduced human F-36P cells to analyze the effects of TPO activation of various signaling molecules including STAT1, STAT3, STAT5, and Ras in the MAPK pathway [203]. They showed that TPO-induced proliferation was dependent on STAT5 and Ras activation, and prolonged activation of Ras could lead to megakaryocytic differentiation of F-36P-Mpl cells. The work of Rouyez et al. with Mpl-transduced UT-7 cells (UT-7/Mpl) supports the idea that prolonged activation of ERK leads to megakaryocytic differentiation [204]. They showed that prolonged activation of ERK in TPO-stimulated UT-7/Mpl cells enhanced megakaryocytic differentiation and adding inhibitors of phosphorylation could inhibit differentiation.

There are no reports of studies using immobilized TPO, possibly because TPO is not presented in a membrane-associated or heparin-bound form. Nevertheless, studies with growth factors not naturally displayed as an immobilized ligand have shown differential effects upon immobilization. Ito and coworkers revealed that when insulin—a protein found only in solution

within the body—was artificially immobilized, the stimulation of CHO cells was increased in magnitude and duration as compared to soluble insulin [42]. We hypothesized that immobilization of TPO would improve HSC expansion. To test our hypothesis we used a TPO mimetic peptide (TPOm). TPOm is a peptide identified by Cwirla and coworkers using phage display [43] (see Figure 3.1.1 for a TPOm schematic). This branched peptide dimer binds cMpl and is similar to rhTPO in the promotion of megakaryocyte (Mk) production from human bone marrow CD34+ cells.

To present cells with an immobilized TPOm molecule, the peptide was modified with lipid anchors for incorporation into a hybrid bilayer membrane (HBM). Our group has previously used HBMs to present peptide mimics of cell adhesion molecule (CAM) ligands [47, 184]. To accomplish this, peptide mimics of CAM ligands were conjugated to lipid anchors via a poly(ethylene glycol) (PEG) tether, then incorporated into dipalmitoylphosphatidylcholine (DPPC) vesicles for deposition onto hydrophobic surfaces. Depositing the lipid vesicles on a hydrophobic surface creates a lipid monolayer specifically presenting the CAM ligands. This strategy for immobilizing lipopeptides was extended to the presentation of TPOm. We synthesized two versions of TPOm lipopeptide; the first is linked by a single lipid at the carboxy terminus (TPOm-1L) and the second linked to a lipid at both amine termini of the branched peptide (TPOm-2L) (Figure 3.1.1). These immobilization strategies do not interfere with the bioactivity of TPOm, as shown by cell adhesion and signaling assays using M07e cells. Culture surfaces with TPOm lipopeptides elicit similar activation of ERK1,2 and STAT5 molecules in M07e cells as compared to PEGylated TPOm (TPOm-PEG) and rhTPO.

Several experiments with human CD34<sup>+</sup> selected cells were used to evaluate the effects of immobilized presentation of TPOm in serum-free medium. Setup of these cultures was based on our normal cytokine cocktail of SCF, FL, and TPO. In these experiments TPO was supplied as soluble TPOm-PEG or immobilized TPOm lipopeptides (TPOm-L) presented from HBMs. In these experiments we evaluated the overall expansion and surface marker retention of CD34<sup>+</sup> cells and CD34<sup>+</sup>Thy1<sup>+</sup> cells. Outcomes for soluble and HBM-presented TPOm were similar, indicating that the TPOm presentation method did not affect the ability to retain CD34<sup>+</sup> cells or CD34<sup>+</sup>Thy1<sup>+</sup> cells.

TPO's influence on megakaryocyte differentiation presents an additional opportunity to test the efficacy of immobilized TPOm. In addition to the effects on primitive HSCs, TPO is the primary regulator of megakaryopoiesis and platelet production. TPO influences Mk growth and development by increasing the size and number of Mks, stimulating the expression of Mk-specific markers (such as CD41 and CD61), and promoting the polyploidization (multiple cycles of DNA replication without cell division yielding many copies of DNA within one cell) of committed Mks [147]. Cultures were conducted in serum-free medium using mPB and BM CD34<sup>+</sup> cells stimulated only with TPOm. Cultures supplemented exclusively with TPOm-1L supported Mk maturation, as evidenced by the appearance of polyploid CD41<sup>+</sup> cells after 9 and 12 days of culture. Similar to cytokine cocktail cultures, the method of TPOm presentation did not alter the production of Mks.

## **5.2 RESULTS**

### **5.2.1 Synthesis of TPOm lipopeptides**

Various TPOm peptides were synthesized on several different resins, including Rink amide AM, Chlortrityl, Rink amide PEGA, and PEGA amine resins by Drs. Bi-Huang Hu and Tor W. Jensen [184]. HPLC and MALDI-TOF MS analysis of the resultant products revealed that peptides produced on the PEGA amine resin with HMPB linker yielded the purest product. Peptides synthesized on this resin were used to form two TPOm lipopeptides and a soluble control molecule as described in Materials and Methods (Section 3.1.1). A schematic representation of each molecule is shown in Figure 3.1.1.

### **5.2.2 Activation studies using M07e cells**

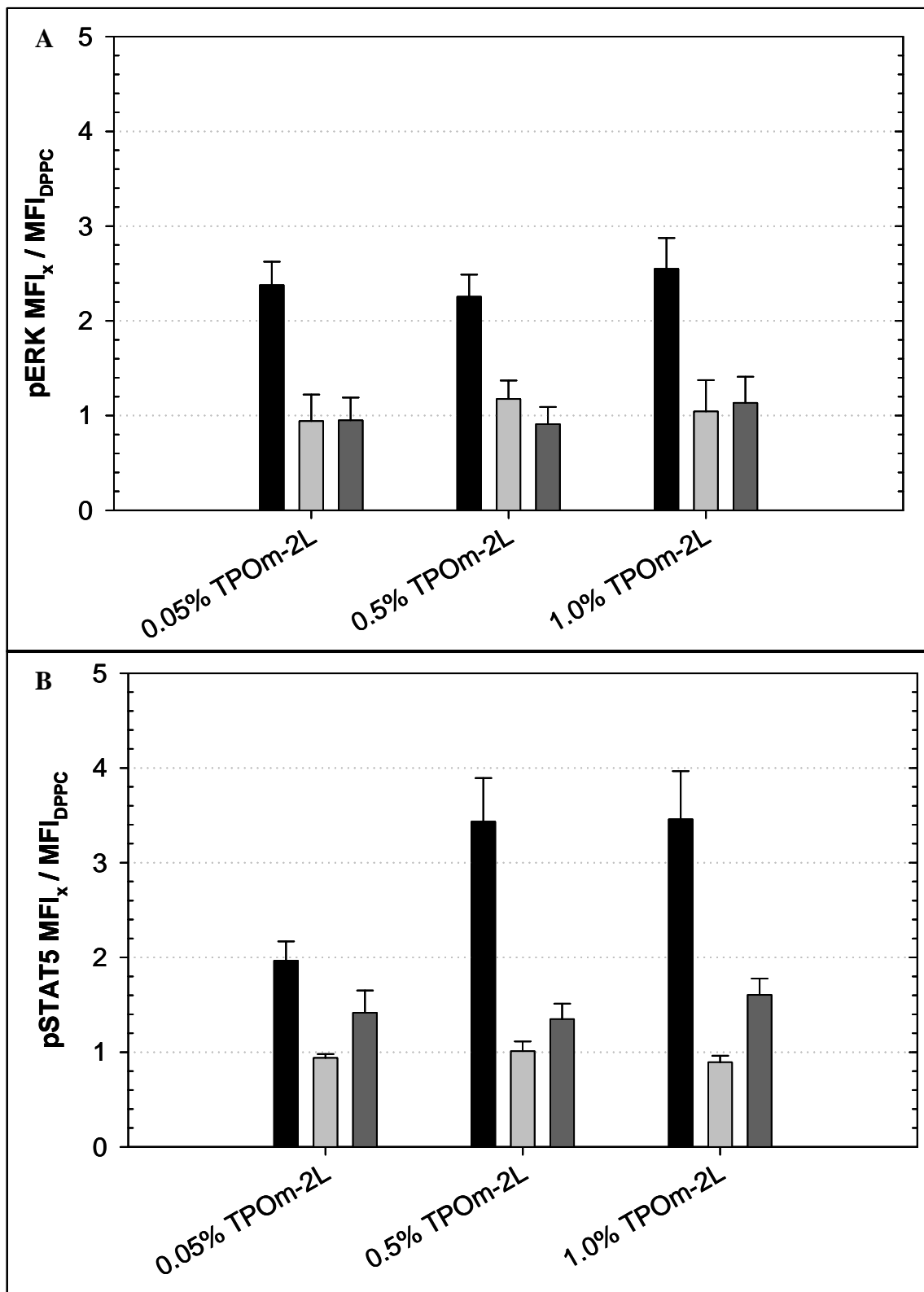
#### **5.2.2.1 Activation of ERK 1,2 and STAT5 with soluble TPOm**

The bioactivity of synthesized TPOm-PEG was examined using a flow cytometric assay adapted to measure phosphorylated ERK 1,2 and STAT5 [190]. The use of whole cells rather than cell lysates differentiates flow cytometric from traditional cell-signaling assays. Cells must be fixed to stop cellular activity and permeabilized to allow antibodies to stain intracellular molecules. Krutzik et al. showed that fixing with paraformaldehyde followed by permeabilization with methanol yielded the greatest separation between stimulated and unstimulated controls [198]. Our experiments indicated that fixing in 2% paraformaldehyde at 4° C yielded the most consistent results. After fixing, cells were permeabilized by the addition of ice cold 90% methanol solution. After rinsing and blocking, cells were stained with antibodies and readied for data acquisition. A more detailed summary of the cell signaling protocol is included in Section 3.4.1.5.

To prepare M07e cells for stimulation assays, exponentially growing cells were washed twice with PBS and placed in growth-factor-free media overnight. Optimization experiments indicate that cell density during overnight growth factor starvation is important. Cells starved at higher density in culture showed increased basal levels of phosphorylated ERK1,2 and STAT5 on DPPC alone, which led to lower relative levels of TPOM mediated stimulation (Figure 5.2.1). In some cases, basal levels were as high as the levels seen upon stimulation, so that differences between stimulated and unstimulated cells were not observed. Optimization experiments also demonstrated that the length of time that starved cells were held at high density—for loading wells in the activation assay—was a key variable. When cells were kept at high densities ( $\geq 1.2 \times 10^6$  cells/mL) for extended periods (~ 35 minutes), basal phosphorylated ERK 1,2 (pERK) and phosphorylated STAT5 (pSTAT5) levels were elevated compared to an aliquot of the same cells sampled at five minutes (Figure 5.2.2).

In activation studies, M07e cells were stimulated for 20 minutes with various concentrations of soluble TPOM-PEG. Figure 5.2.3 shows representative histograms for stimulated cells stained with anti-phospho-STAT5 antibody, anti-phospho-ERK 1,2 antibody, or isotype control antibodies. Phosphorylation of ERK 1,2 and STAT5 increased in a TPOM-dose-dependent manner (Figure 5.2.4). The data are presented as fold-over-isotype to normalize for experiment-to-experiment variation, as discussed in Section 3.4.1.5. TPOM-PEG and recombinant human TPO (rhTPO) stimulated ERK activation to a similar extent when added to growth-factor-starved cells at the same molar dose (Figure 5.2.5).

**Figure 5.2.1:** Effect of cell density during starvation. In three separate experiments M07e cells were removed from growth-factor-containing media and starved overnight at  $0.4 \times 10^6$  cells/mL (black bars),  $1.65 \times 10^6$  cells/mL (lt. grey bars), and  $1.9 \times 10^6$  cells/mL (grey bars). Cells were stimulated in serum-containing media (IMDM + 2.5% FBS) on surfaces with various concentrations of TPOM-2L for 20 minutes and the levels of pERK (**A**) and pSTAT5 (**B**) was measured. Values shown were normalized to DPPC by dividing the average mean fluorescence intensity (MFI) of at least three replicate samples for each condition by the average MFI of at least three replicate DPPC samples ( $\pm$  SD).



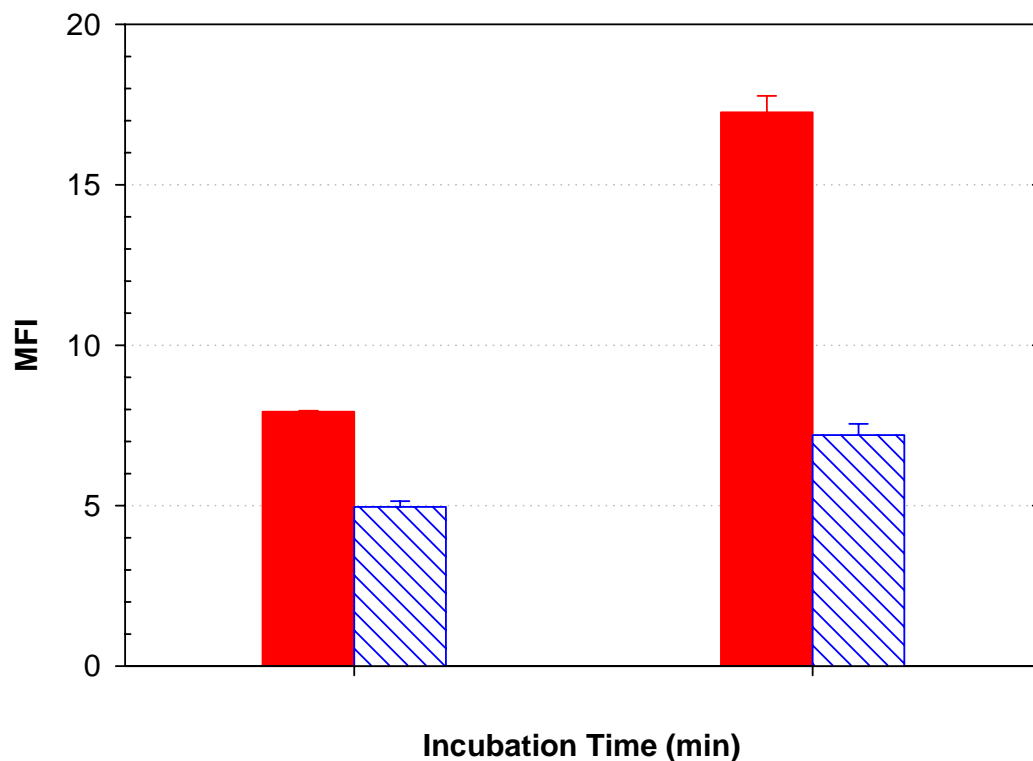


**Figure 5.2.2:** The time starved cells are at high cell density before stimulation affects basal levels in unstimulated cells. Phosphorylation of ERK1,2 (solid bars) and STAT5 (bars with angled bands) for unstimulated M07e cells. Cells were starved overnight and were loaded into TPCS plates at the indicated time points with IMDM + 2.5% FBS in the absence growth factors. Cells were ‘stimulated’ for 20 minutes and processed according to cell signaling protocol (Section 3.4.1.5). The average of two technical replicates is shown from an experiment representative of two repeats.

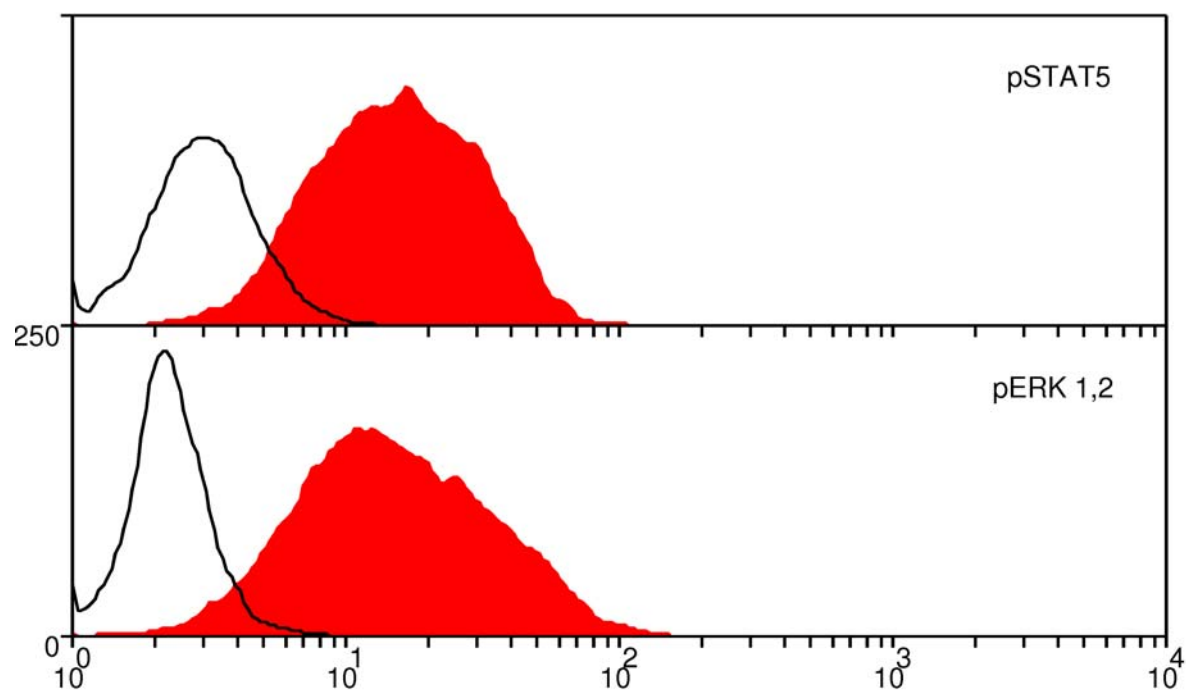


**Figure 5.2.3:** Representative histograms showing typical output from flow cytometric cell-signaling assay. M07e cells were starved overnight and stimulated in serum containing media (IMDM + 2.5% FBS) with 5 nM TPOM-PEG for 20 minutes in TPCS plates and processed according to cell signaling protocol (Section 3.4.1.5). Shown are isotype controls (line) and specific signals for stimulated cells (filled histogram).

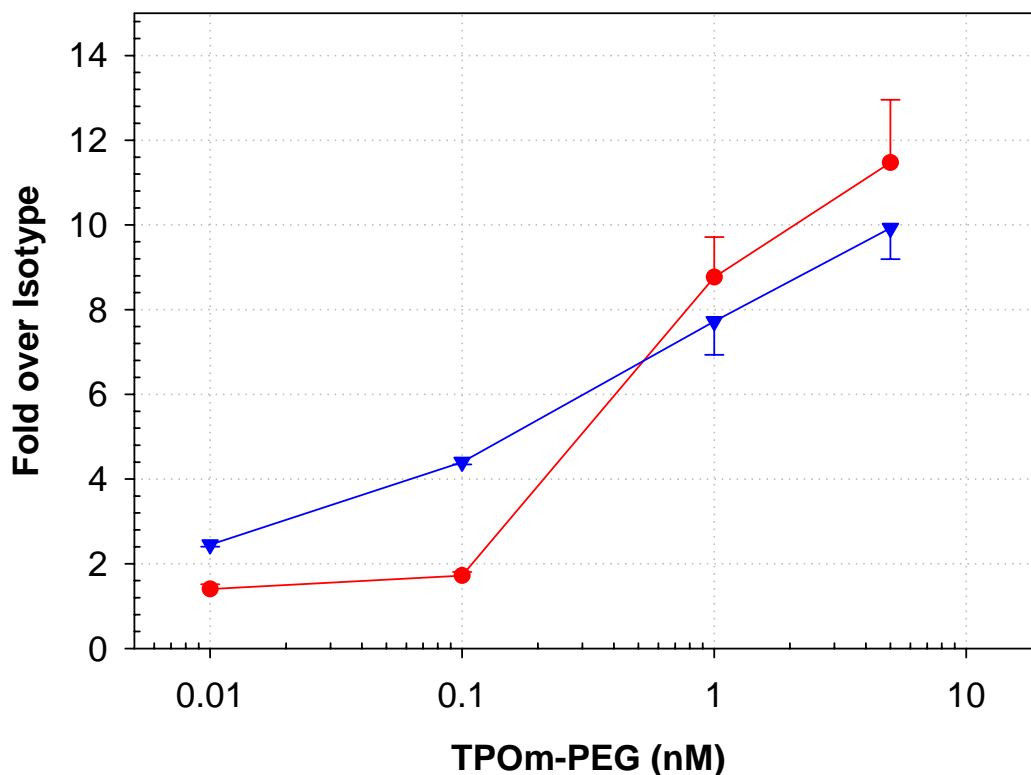


**Figure 5.2.4:** Summary of the phosphorylation of ERK1,2 (circles) and STAT5 (inverted triangles) in M07e cells. M07e cells were starved overnight and stimulated in serum containing media (IMDM + 2.5% FBS) with various concentrations of TPOm-PEG. Cells were stimulated for 20 minutes in TPCS plates and processed according to cell signaling protocol (Section 3.4.1.5). Fold-over-isotype values were calculated by dividing the mean fluorescence intensity (MFI) of a sample by the MFI of an isotype-matched control that was performed on the same day. Data shown is the average ( $\pm$  SEM) for replicate wells for at least four experiments performed on different days.

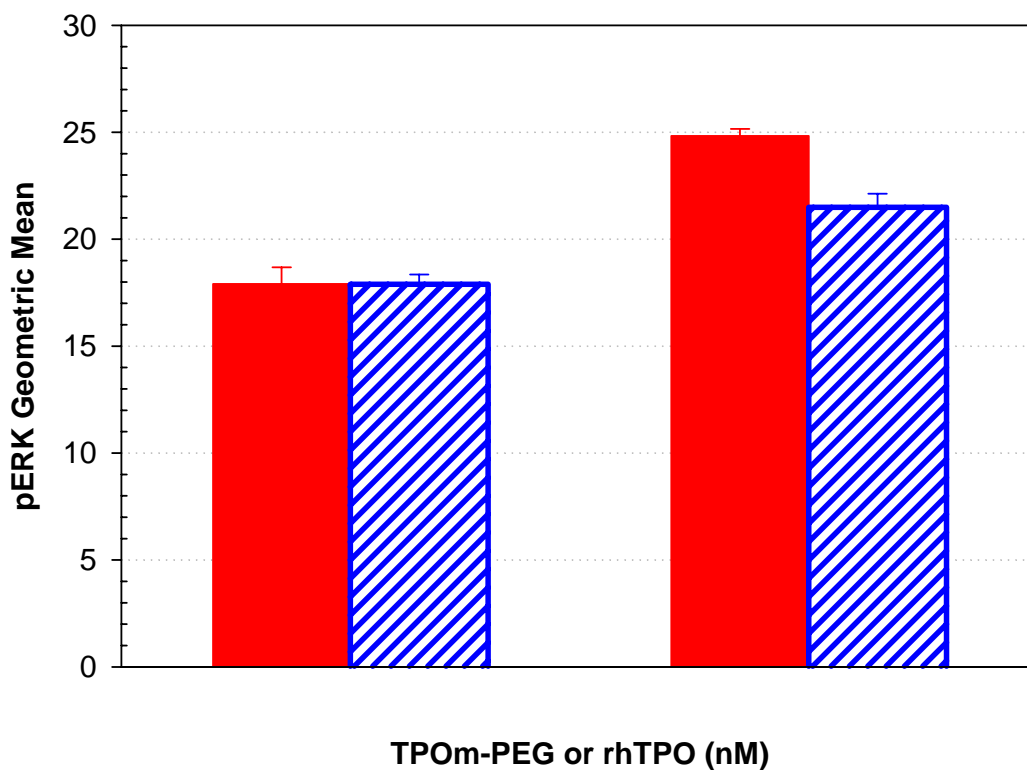


**Figure 5.2.5:** Comparison of ERK 1,2 activation induced by rhTPO and TPOm-PEG in M07e cells. M07e cells were starved overnight and stimulated in serum containing media (IMDM + 2.5% FBS) and stimulated with TPOm-PEG (Solid bars) and rhTPO (stripped bars) at 0.01 and 1.06 nmol/L for 30 minutes. The average of two technical replicates ( $\pm$  SEM) from an experiment representative of three repeats is shown.

### 5.2.2.2 Immobilized TPOM lipopeptides induce activation of STAT5 and ERK 1,2 at similar levels as soluble material

Normal force centrifugation adhesion studies (Section 3.4.2) performed by Shara Dellatore demonstrated a specific interaction between cells and TPOM lipopeptides deposited within the HBM (Figure 5.2.6). This, combined with the active conformation of TPOM-PEG, suggested that TPOM lipopeptides should induce the activation of ERK 1,2 and STAT5. The flow cytometric signaling assay was used to evaluate the ability of TPOM-L in HBMs to induce signal molecule activation. M07e cells were simulated for 20 minutes with various levels of TPOM-1L incorporated within a background of DPPC. As with soluble TPOM-PEG, TPOM-1L induced phosphorylation of both ERK 1,2 and STAT5 (Figure 5.2.7). Dose-dependent activation was not apparent on TPOM-1L surfaces, in contrast to soluble TPOM-PEG. Stimulation of M07e cells on surfaces prepared with just 0.05% TPOM-1L elicited near-maximal levels of pERK and pSTAT5. Maximal activation of ERK 1,2 was similar to that with 5 nM TPOM-PEG. Activation of STAT5 by TPOM-1L did not reach the activation levels produced by 5 nM TPOM-PEG (nine replicates in five experiments,  $p = 0.1$ ). Surfaces incorporating TPOM-2L were not investigated as thoroughly for signaling activity as those incorporating TPOM-1L. However, the experiments performed indicate that TPOM-2L also activates ERK 1,2 and STAT5 (Figure 5.2.8).

To evaluate the kinetic response of M07e cells to TPOM stimulation, time course activation studies were performed. These studies were designed to determine if the TPOM-L surfaces enhanced the duration or intensity of signaling compared to soluble TPOM-PEG. In M07e cells, different TPOM presentation methods did not alter the duration of pERK or pSTAT5 activation (Figure 5.2.9).

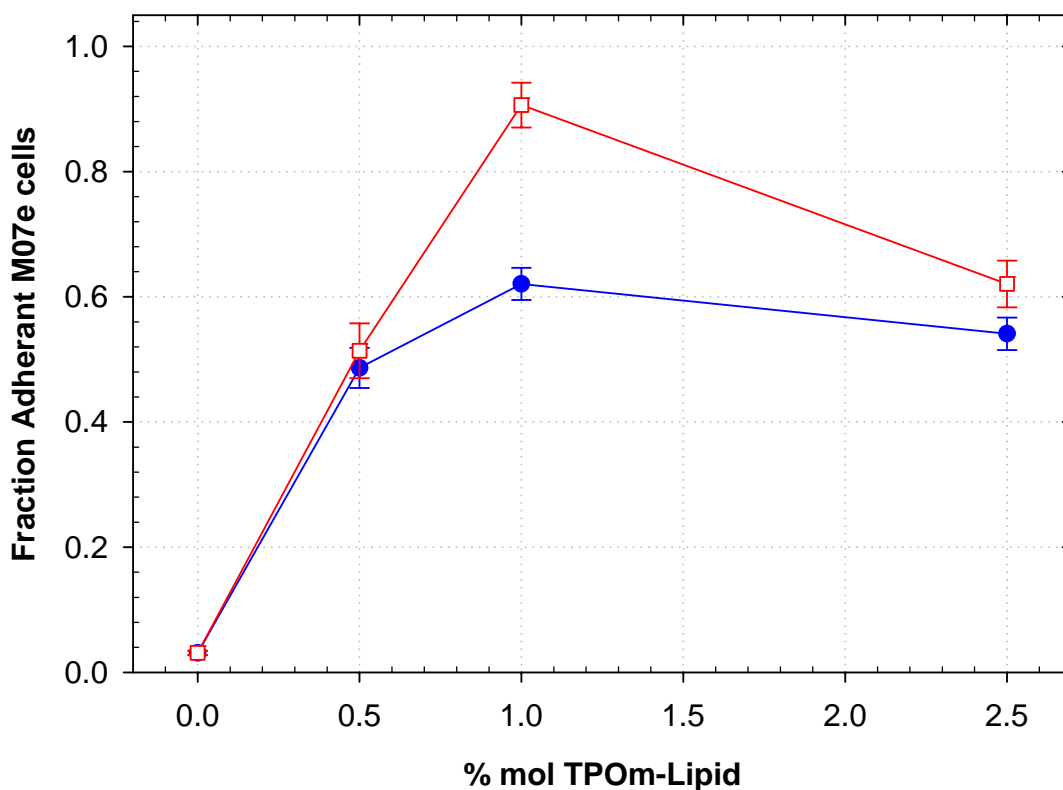


**Figure 5.2.6:** Fraction of M07e cells adherent to TPOm-lipopeptides in HBM.

Exponentially growing M07e cells were stained with CFSE or Calcein AM and the adhesion assay performed as described in Section 3.4.2 on surfaces with various concentrations of TPOm-1L (filled circles) and TPOm-2L (open squares). Metamorph software was used to count the number of cells in each image of particular regions of the cassette both before and after centrifugation. The fraction of adherent cells was calculated by dividing the number of cells in the post-centrifugation images by the number of cells in the pre-centrifugation images. Data shown are the average of at least 18 replicate wells from at least five separate experiments  $\pm$  S.E.M.

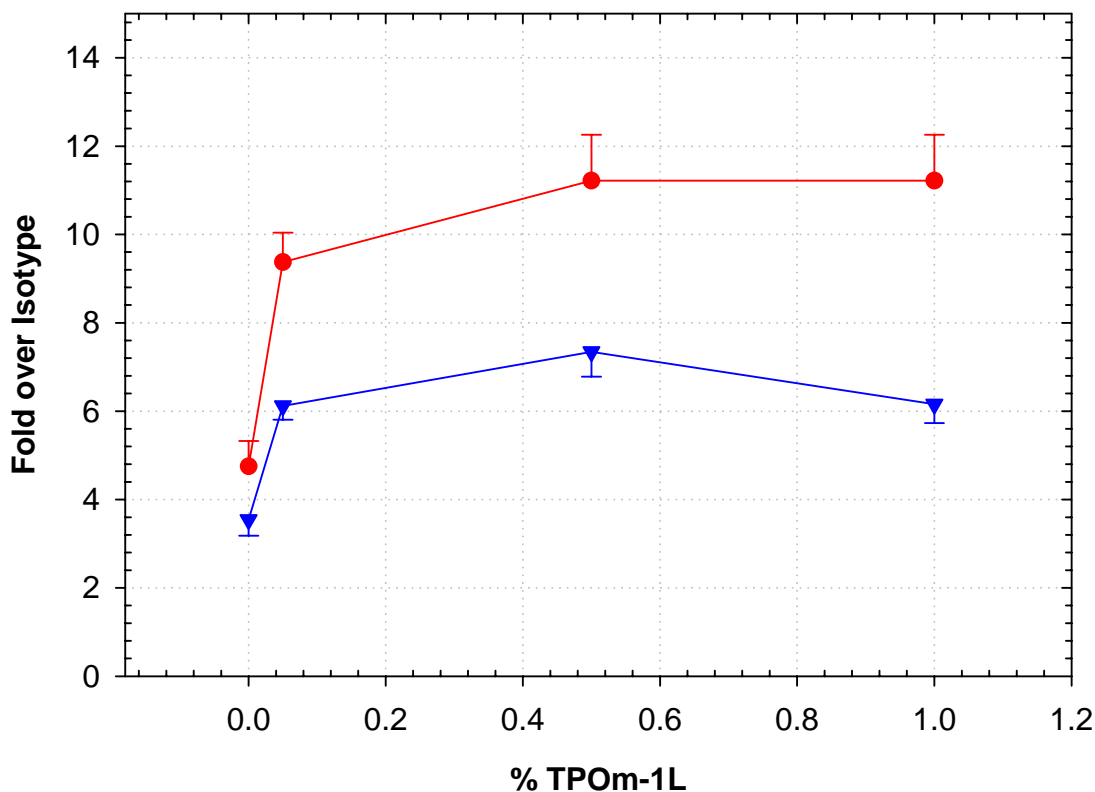


**Figure 5.2.7:** Activation of ERK 1,2 (circles) and STAT5 (inverted triangles) in M07e cells stimulated on DPPC surfaces with various amounts of TPOM-1L. M07e cells were starved overnight and stimulated in serum-containing media (IMDM + 2.5% FBS) for 20 minutes followed by processing according to the cell signaling protocol (Section 3.4.1.5). Fold-over-isotype values were calculated by dividing the mean fluorescence intensity (MFI) of a sample by the MFI of an isotype-matched control that was performed on the same day. Data shown is the average ( $\pm$  SEM) for replicate wells for at least four experiments performed on different days.

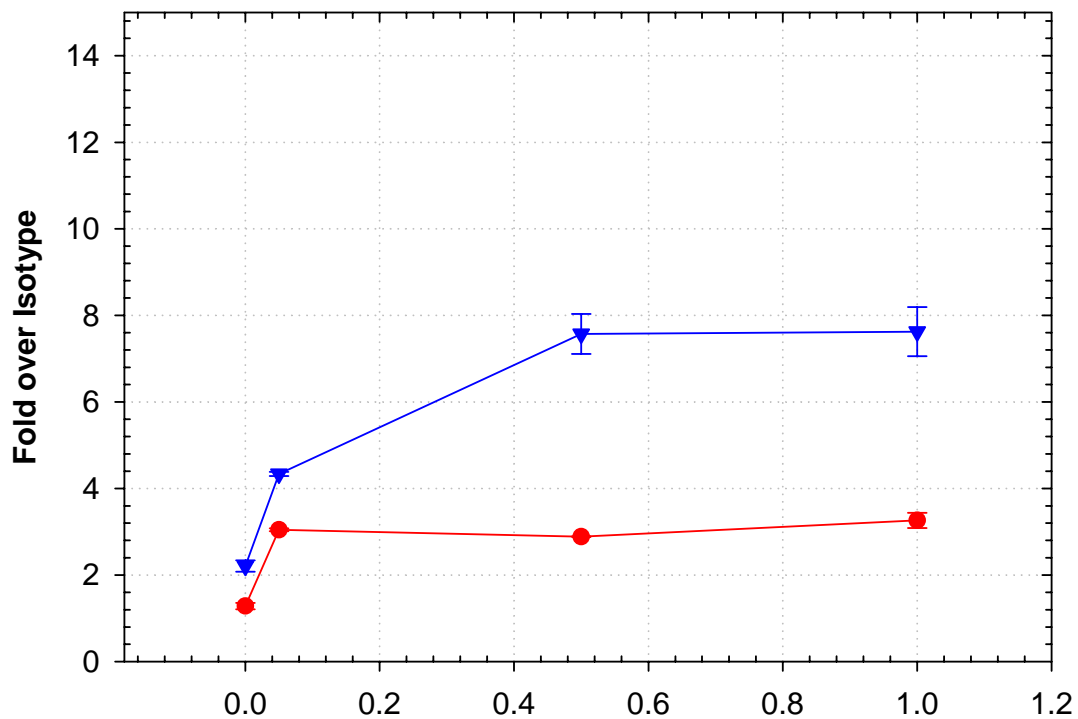
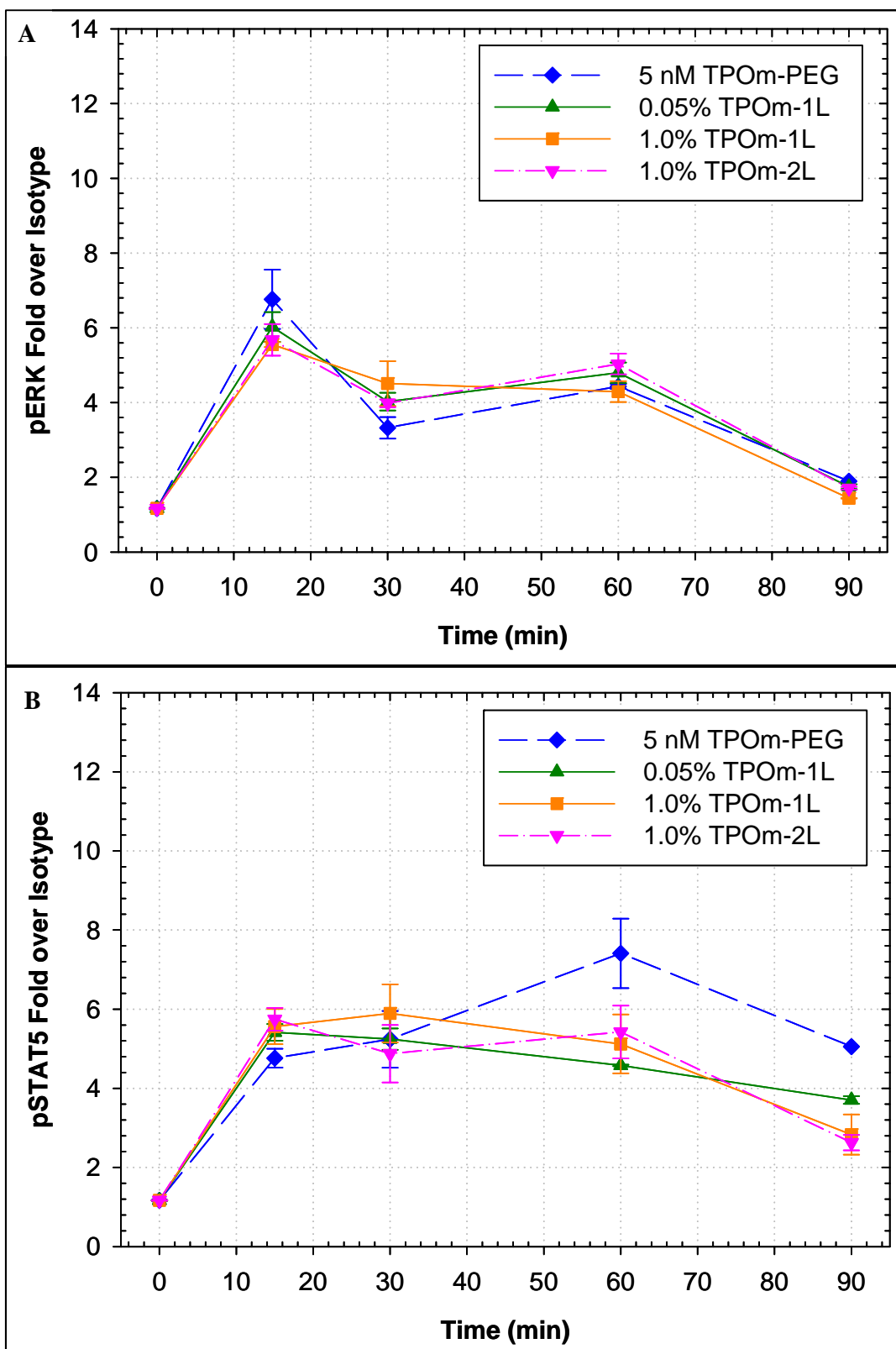


**Figure 5.2.8:** Summary of the activation of ERK 1,2 (circles) and STAT5 (inverted triangles) in M07e cells stimulated on DPPC surfaces with various amounts of TPOm-2L. M07e cells were starved overnight and stimulated in serum containing media (IMDM + 2.5% FBS) for 20 minutes followed by processing according to the cell signaling protocol (Section 3.4.1.5). Shown is the average ( $\pm$  SEM) for replicate wells for at least four experiments performed on different days.

**Figure 5.2.9:** Time course cell signaling activation studies. M07e cells were prepared by overnight starvation followed by stimulation for up to 90 minutes and processed according to cell signaling protocol (Section 3.4.1.5). Cells were stimulated on DPPC surfaces with 5 nM TPOM-PEG (diamond), 0.05% TPOM-1L (triangle), 1.0% TPOM-1L (square), and 0.05% TPOM-1L (inverted triangle). Fold over isotype for the activation of ERK 1,2 (**A**) and STAT5 (**B**) are shown. The average ( $\pm$  SEM) of three wells from a single experiment representative of three repeats are shown.



### 5.2.2.3 Activation of STAT5 and ERK 1,2 is enhanced in M07e cells stimulated by TPOM-1L and SCF

The interaction of TPO and other cytokines (including SCF and FL) is important in the maintenance of primitive HSCs. To ensure that cells could engage HBM-presented TPOM-1L and still interact with other cytokines, M07e cells were stimulated on surfaces with TPOM-1L in the presence of 10 ng/mL SCF. By itself, SCF induces low levels of STAT5 phosphorylation in M07e cells (Figure 5.2.10). Stimulation of M07e cells on TPOM-1L surfaces with soluble SCF enhances the levels of phosphorylated STAT5 beyond that seen with TPOM-1L alone (Figure 5.2.10 compared to Figure 5.2.7). SCF alone induced near high levels of pERK. However, M07e cell stimulation on TPOM-1L surfaces slightly enhanced activation of ERK 1,2 by soluble SCF.

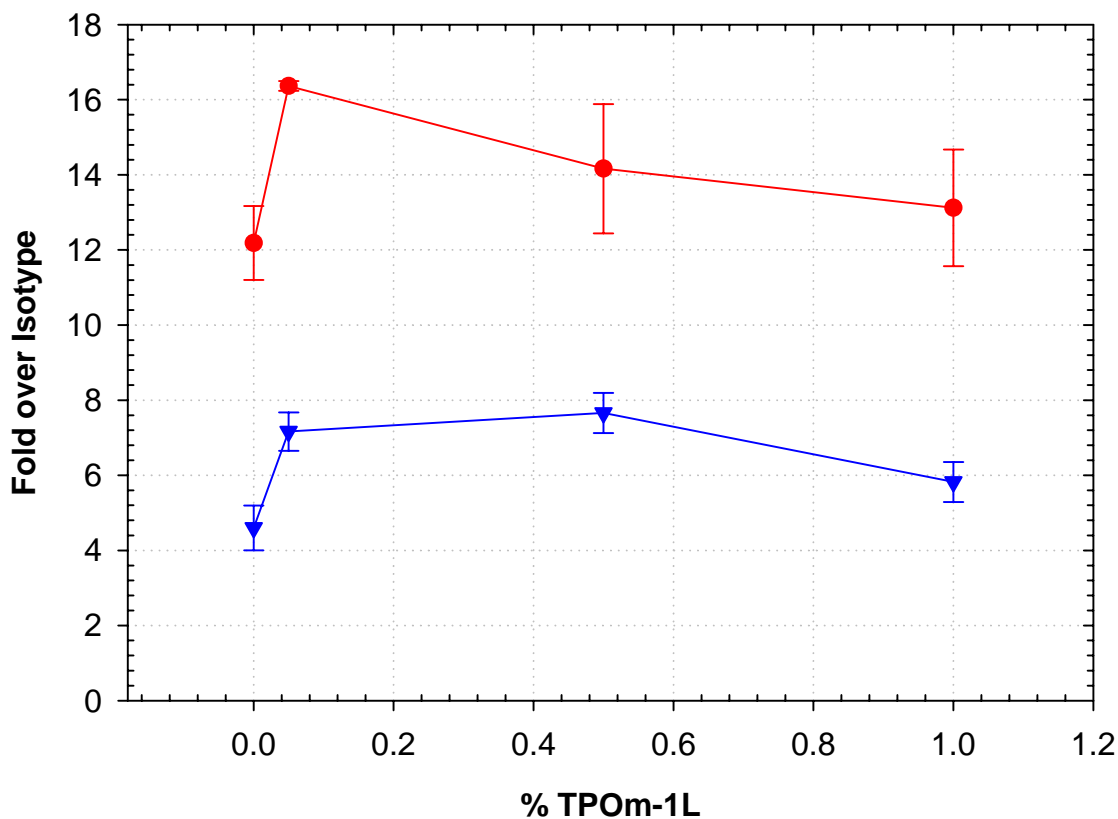


**Figure 5.2.10:** Summary of the activation of ERK 1,2 (circles) and STAT5 (inverted triangles) in M07e cells when stimulated with 10 ng/mL soluble SCF and various amounts of immobilized TPOM-1L. M07e cells were starved overnight and stimulated in serum-containing media (IMDM + 2.5% FBS) for 20 minutes followed by processing according to the cell signaling protocol (Section 3.4.1.5). Shown is the average ( $\pm$  SEM) for replicate wells for at least four experiments performed on different days.

#### 5.2.2.4 Stimulatory effect of carrier lipids

We consistently observed elevated pERK and pSTAT5 levels in M07e cells on unstimulated DPPC controls compared to TCPS controls. To investigate if the increased activation was due to the lipid surfaces, activation studies were conducted with other phosphatidyl choline carrier lipids. Dimyristoylphosphatidylcholine (DMPC) and dioleoylphosphatidylcholine (DOPC) have the same hydrophilic head group, but their different melt transition temperatures alter the fluidity of the HBM. Several activation studies compared unstimulated controls on DPPC, DMPC, and DOPC HBM surfaces to those on TCPS. 'Unstimulated' M07e cells on the three lipid surfaces exhibited similar activation of pERK and pSTAT5. In addition, unstimulated controls on all lipid surfaces showed increased pERK and pSTAT5 levels as compared to TCPS controls (Figure 5.2.11).

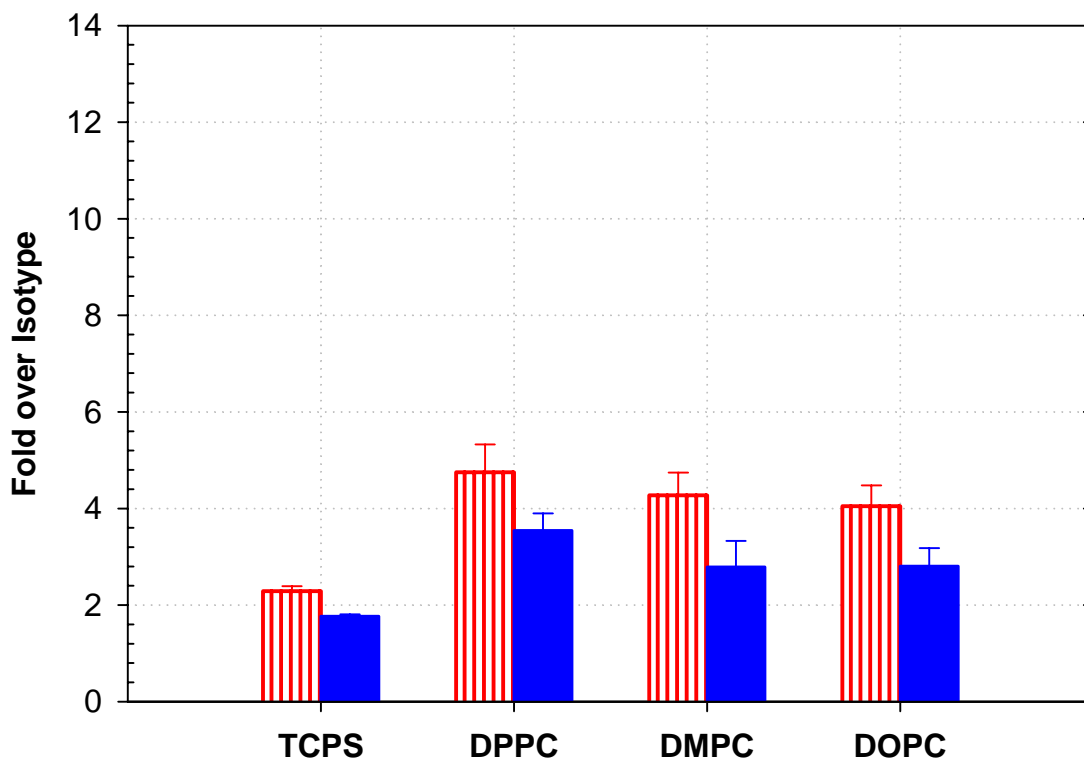
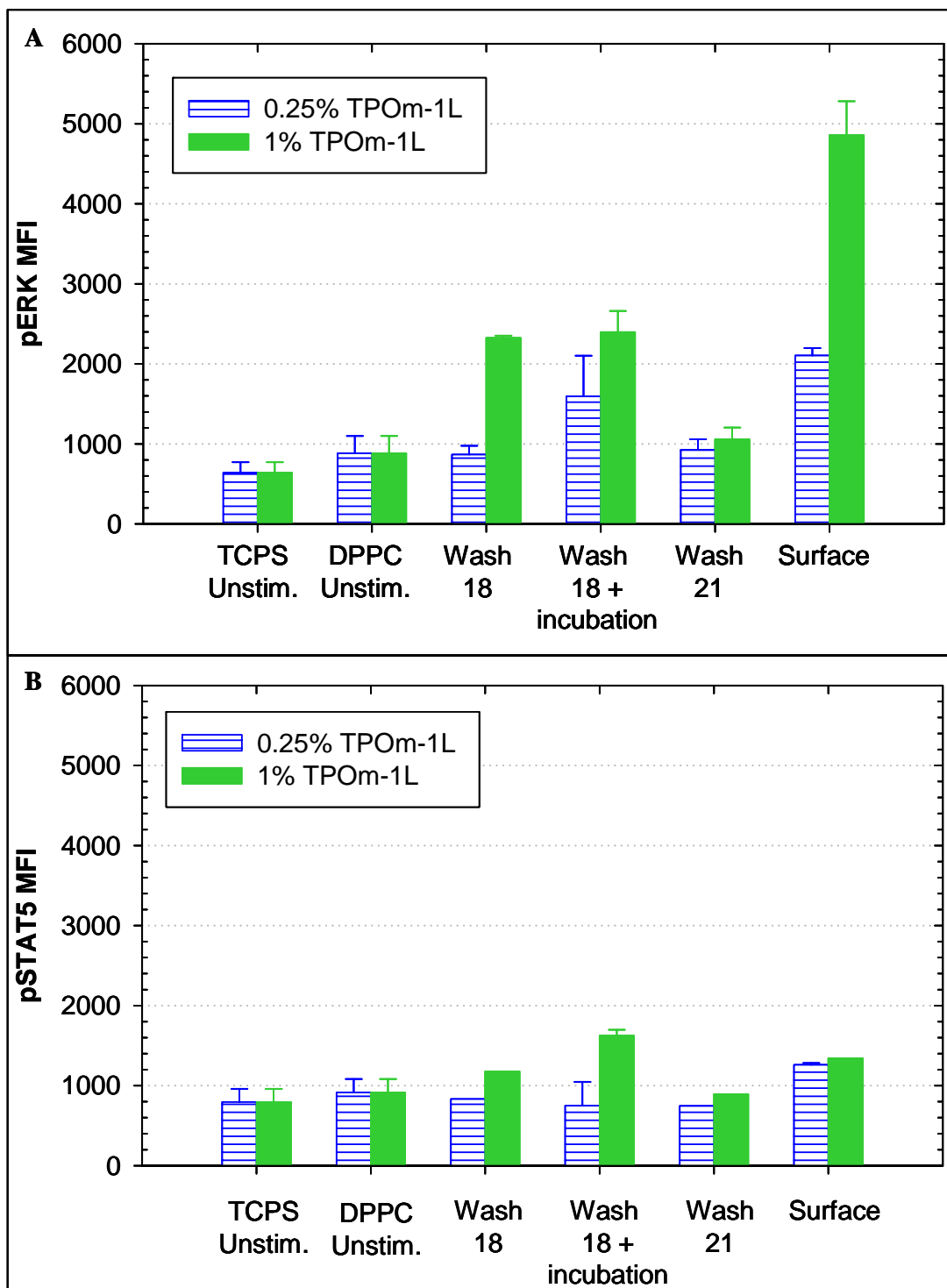


**Figure 5.2.11:** Summary of unstimulated M07e cell activation on various carrier lipids. Phosphorylation of ERK1,2 (vertical striped bars) and STAT5 (solid bars) are shown for M07e cells stimulated on TCPS, DPPC, DMPC, and DOPC surface without growth factors. Cells were prepared as described in Figure 5.2.3 and stimulated for 20 minutes followed by processing according to the cell signaling protocol in Section 3.4.1.5. Data shown are the average ( $\pm$  SEM) for two replicate experiments performed on different days.

#### 5.2.2.5 Release of TPOM-lipopeptides from lipid surfaces

It is possible that TPOM lipopeptides are released from the HBMs during signaling assays and long-term culture. Signaling experiments were conducted to analyze the ability of supernatant from wells prepared with TPOM-1L and TPOM-2L for i stimulate cells. Culture cassettes were prepared normally (Section 3.2.2) and washed by dilution rinses with 18MΩ water 15 times, followed by three dilution rinses with equilibrated media (IMDM + 2.5% FBS). After the final media wash, the top 150 μL of the supernatant was collected, and saved in a TCPS well plate (wash 18). Fresh media was added back to the sampled wells, and the surfaces were incubated for 20 minutes in a humidified, 5% CO<sub>2</sub> incubator at 37° C. The incubation period was chosen to provide a worst case for TPOM-L release during the signaling studies. After the incubation, the top 150 μL of the supernatant was collected (wash 18 + incubation) and surfaces were rinsed with media three additional times. The final rinse was followed by a final collection of a 150 μL supernatant sample (wash 21). Collected supernatants were used to stimulate M07e cells in the standard 20 minute activation assay, and compared to the HBM surfaces from which they came. Some material released during the timeframe of the activation assay, and this increased with the concentration of immobilized TPOM-1L (Figure 5.2.12). However, the activating material in the supernatant could be diluted away using additional rinses. For pERK activation, 1% TPOM-1L surfaces induced substantially greater activation than the released material, while the surface and released material were similar for 0.25% TPOM-1L ( $p = 0.024$  for 1% TPOM-1L and  $p = 0.208$  for 0.25% TPOM-1L, Figure 5.2.12A). Activation of pSTAT5 was much less extensive and the surface induced similar activation as the released material (Figure 5.2.12B).

**Figure 5.2.12:** Levels of pERK (A) and pSTAT5 (B) in M07e cells activated by supernatants removed from surfaces. M07e cells were starved overnight and stimulated in serum-containing media (IMDM + 2.5% FBS) for 20 minutes followed by processing according to the cell signaling protocol (Section 3.4.1.5). Supernatants were collected from 0.25% TPOM-1L surfaces (lined bars) and 1.0% TPOM-1L surfaces (solid bars) prepared normally (Section 3.2.3) by 15 dilution rinses with 18 MΩ water and three dilution rinses with equilibrated serum-containing media. After the final media wash, the top 150 mL of the supernatant was collected, and saved in a TCPS well plate (wash 18). Fresh media was added back to the sampled wells, and the surfaces were incubated for 20 minutes in a humidified, 5% CO<sub>2</sub> incubator at 37 °C. After the incubation, the top 150 mL of the supernatant was collected (wash 18 + incubation) and surfaces were rinsed with media three additional times. The final rinse was followed by a final supernatant collection (wash 21). Data for ‘Surface’ are from M07e cells stimulated on TPOM-1L surfaces after wash 21. The average (± SEM) of two wells from a single experiment representative of two repeats are shown.



### 5.2.3 Cell cultures with TPOM

#### 5.2.3.1 M07e cell culture with TPOM

M07e cell cultures were used to compare cell expansion stimulated by different levels of TPOM-PEG and rhTPO (Table 5.2.1). Growth-factor deprived M07e cells (starved as described in section 3.4.1.5.) were seeded in TCPS 96-well plates and expanded for seven days. TPOM-PEG and rhTPO are similar at low concentrations in their ability to induced similar M07e cell expansion at doses up to 1 nM (Figure 5.2.13). A TPOM-PEG concentration of 0.4 nM gave ~50% of the maximal expansion ( $ED_{50} \sim 0.4$  nM), while the  $ED_{50}$  for rhTPO could not be determined from this experiment.

Primary CD34+ cells are very sensitive to their culture environment [205]. Prior to culturing CD34+ cells, M07e cells were used to evaluate the biocompatibility of our culture cassette for long-term-culture. Cells were monitored for overall expansion and viability for six days. Results from these experiments indicated that the surfaces were biocompatible and potentially suitable for culture with primary CD34+ selected cells (Figure 5.2.14).

**Table 5.2.1:** Concentrations of TPOm-PEG and rhTPO in does response experiment shown in Figure 5.2.13.

	rhTPO (ng/mL)	rhTPO (nM)*	TPOm-PEG (nM)
1	1	0.02	0.1
2	5	0.11	1
3	10	0.21	2.5
4	25	0.53	5
5	50	1.06	10

\*Converted to nM using molecular weight of protein ~ 47,000 g/mol.

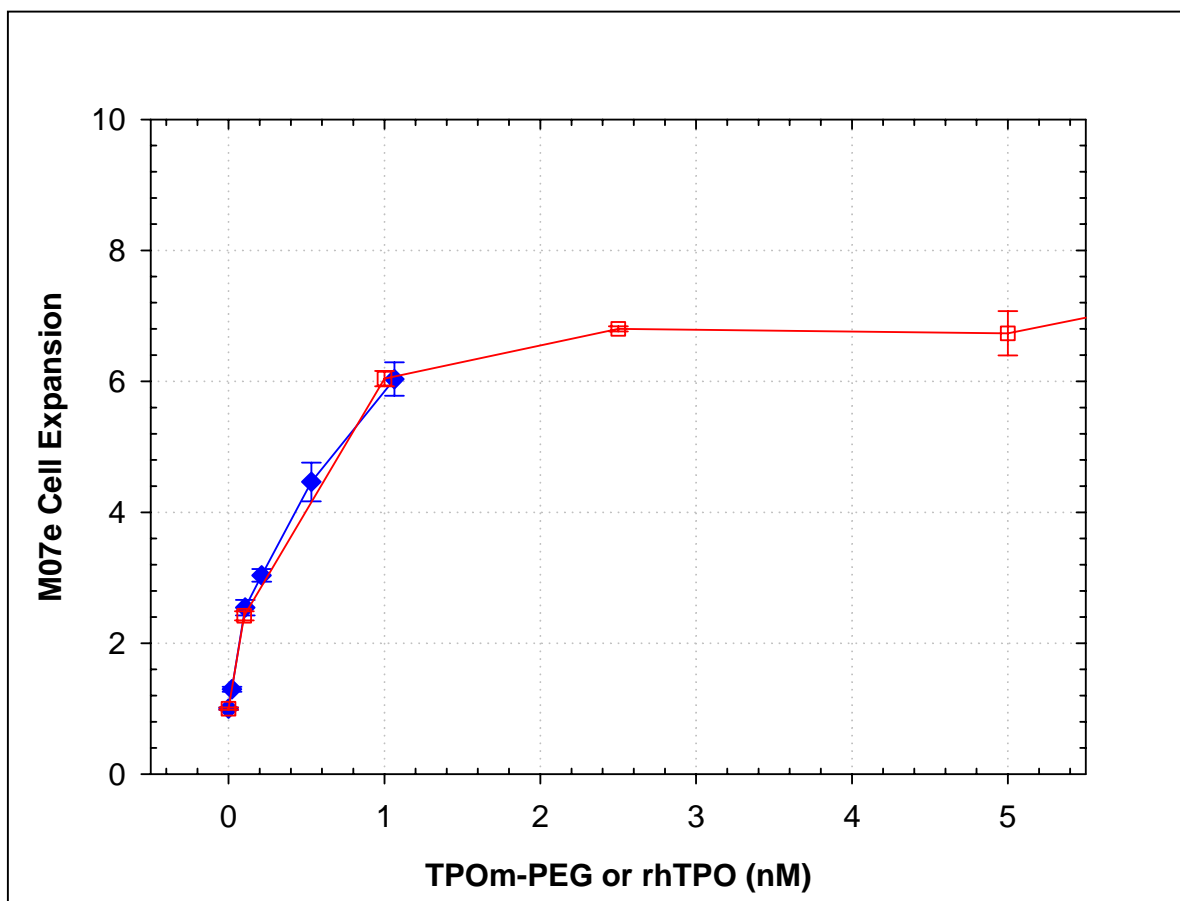


**Figure 5.2.13:** Dose-dependent M07e cell expansion after seven days. M07e cells were cultured with various concentrations of rhTPO (◆) and TPOM-PEG (□). Expansion was calculated by dividing the cell density at day 7 by the seeding density. Data shown are the average of three wells ( $\pm$  SEM) from a single experiment.

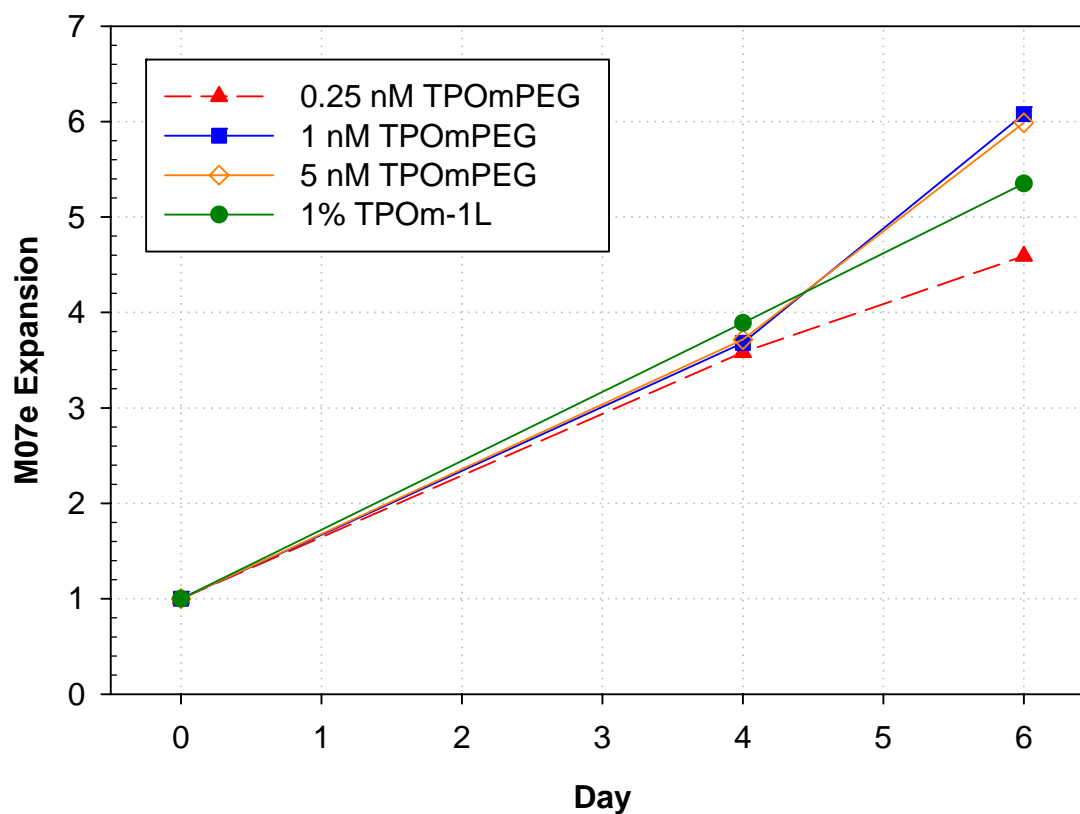


**Figure 5.2.14:** Expansion of M07e cells on lipid surfaces. M07e cells were expanded for six days on DPPC with 1% TPOm-1L (filled circles) or DPPC surfaces with soluble TPOm-PEG at 0.25 nM (filled triangles), 1.0 nM (filled squares), or 5.0 nM (open diamonds). Cells were seeded at  $\sim 180,000$  cells/mL and cultured in a total volume of 100 mL. Expansion was calculated by dividing the cell density at day 6 by the seeding density. Data shown are the average of three wells ( $\pm$  SEM) from a single experiment 6-day biocompatibility experiments.

### 5.2.3.2 Culture of CD34<sup>+</sup> selected cells in cocktail containing SCF and FL

We hypothesize that presenting HSCs with immobilized TPO molecules would enhance overall expansion and maintenance of CD34<sup>+</sup> and CD34<sup>+</sup>Thy1<sup>+</sup> positive cells. To test this hypothesis frozen BM CD34<sup>+</sup> selected cells were cultured in the presence of TPOm-2L for six days. Cells were seeded in serum-free StemPro 34 media with our standard cytokine cocktail of 100 ng/mL SCF, 100 ng/mL FL, and TPO. TPO was provided to the cells in one of three different forms: TPOm-2L in HBM, 5 nM TPOm-PEG on either a DPPC HBM or TCPS, or 50 ng/mL rhTPO in TCPS control well plates (Table 5.2.2). The entire contents of wells were sacrificed on days two, four, and six for analysis of overall expansion and retention of primitive markers CD34 and Thy1. Representative dot plots of cells stained for CD34 and Thy1 expression are shown in Figure 5.2.15. Surfaces with 0.1% and 1% TPOm-2L were similar to soluble TPOm-PEG controls on TCPS and DPPC in overall expansion (Figure 5.2.16A) and maintenance of CD34<sup>+</sup>Thy1<sup>+</sup> cells (Figure 5.2.16B). Additionally, TCPS controls with 50 ng/mL rhTPO could not be distinguished from either version of TPOm when comparing overall expansion or retention of CD34<sup>+</sup> cells or CD34<sup>+</sup>Thy1<sup>+</sup> cells.

A second experiment with primary BM CD34<sup>+</sup> selected cells was performed using TPOm-1L in place of TPOm-2L. Cells were grown in cell culture cassettes or TCPS plates for 6 days. This experiment used our standard cytokine cocktail: 100 ng/mL SCF, 100 ng/mL FL, and TPO—either as 5nM TPOm-PEG or 1% TPOm-1L in HBM. To determine if TPOm had an added effect to the base cytokine cocktail of SCF and FL, a ‘without TPOm’ control was added. IL-3 is known to enhance proliferation of hematopoietic cells, but typically with faster loss of primitive markers. However, a recent report indicated that addition of IL-3 to the SCF, FL, and TPO cytokine cocktail could enhance human BM CD34<sup>+</sup> cell proliferation, while increasing

expansion of primitive LTC-ICs [206]. The addition of IL-3 should promote HSC proliferation and serve as a worst-case scenario to test the retention of CD34+ and CD34+Thy1+ cells. A summary of the different conditions evaluated in this experiment is listed in Table 5.2.3. Cultures were sampled on days two, four, and six for overall expansion and expression of CD34 and Thy1 by sacrificing the contents of culture cassette and TPCS wells. TPOm conditions showed increased overall expansion as compared to TPOm-1L (Figure 5.2.17A). Consistent with our previous findings, and retention of CD34+ cells (DATA NOT SHOWN) and CD34+Thy1+ cells were similar for the various TPOm conditions (Figure 5.2.17B). These results also showed addition of TPOm (soluble or lipid immobilized) did not significantly enhance overall expansion or the ability to retain CD34+ cells (DATA NOT SHOWN) and CD34+Thy1+ cells. Comparison of controls (T-FSTm in Figure 5.2.16 and Figure 5.2.17) shows much lower overall expansion in the second experiment, which was most likely due to donor-to-donor variation. The addition of IL-3 significantly improved overall expansion (Figure 5.2.18A compared to Figure 5.2.17A), while maintaining similar fractions of CD34+ cells (DATA NOT SHOWN) and CD34+Thy1+ cells (Figure 5.2.18B compared to Figure 5.2.17B). As for the case without IL-3, TPOm did not alter CD34+ cell expansion or differentiation.

**Table 5.2.2:** Summary of conditions evaluated in six-day expansion cultures of BM CD34<sup>+</sup> cells with TPOm-2L<sup>a</sup> shown in Figure 5.2.15.

	Name <sup>b</sup>	Background Surface	TPO
1	0.1% 2L-FS	TPOm-2L / DPPC	0.1% TPOm-2L
2	1.0% 2L-FS	TPOm-2L / DPPC	1% TPOm-2L
3	D-FSTm	DPPC	5 nM TPOm-PEG
4	T-FSTm	TCPS	5 nM TPOm-PEG
5	T-FSrhTPO	TCPS	50 ng/mL rhTPO

<sup>a</sup>All conditions in StemPro 34 media with 100 ng/mL SCF and 100 ng/mL FL.

<sup>b</sup>Name derived from the background surface and cytokine cocktail.

Abbreviations used: D = DPPC; T = TCPS; 2L = TPOm-2L; F = Flt-3 Ligand; S = SCF; Tm = TPOm-PEG; 3 = IL-3.

**Figure 5.2.15:** Representative CD34 vs. Thy1 dot plots. Cultures were initiated with CD34+ bone marrow cell in StemPro 34 media and grown on DPPC based surfaces with 100 ng/mL SCF and 100 ng/mL Flt-3 Ligand, and either 5 nM TPOm-PEG or 1% TPOm-2L and grown for six days (**A**). A control with isotype-matched antibodies is shown in (**B**).

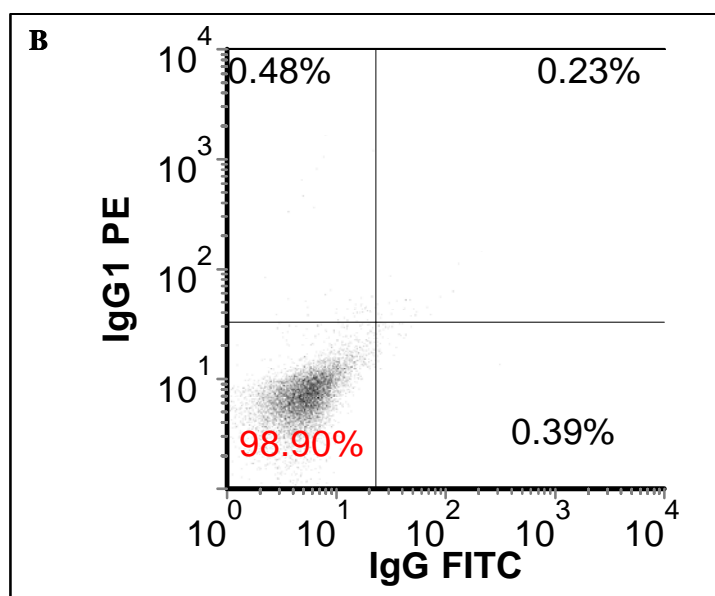
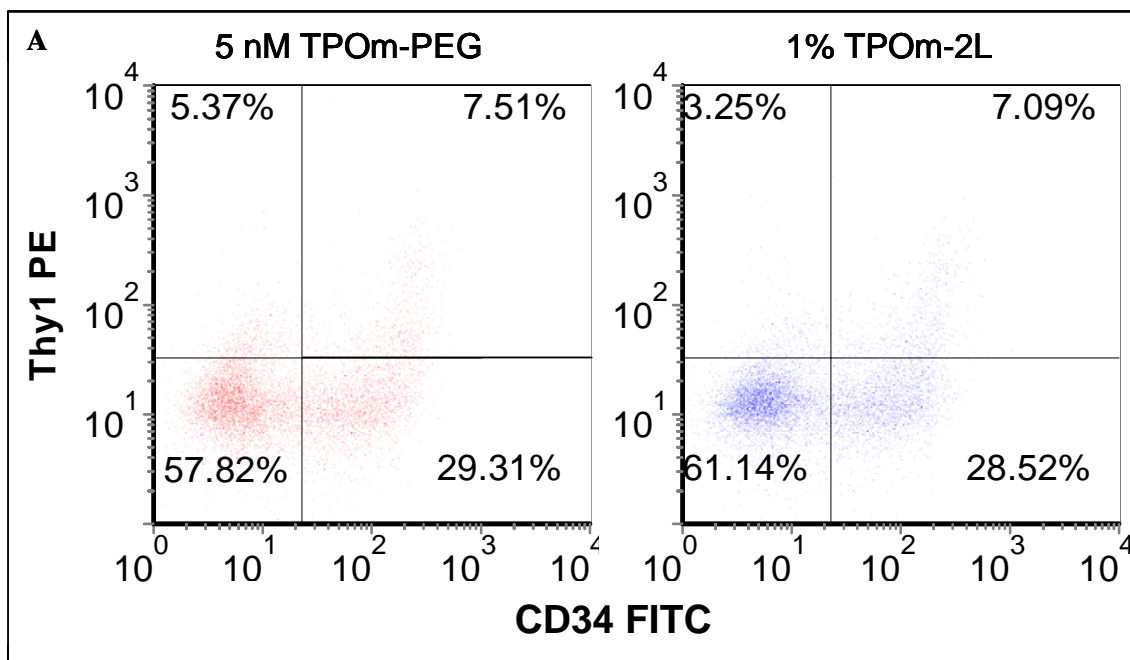


**Figure 5.2.16:** Cell expansion in cultures seeded with CD34+ bone marrow cells.

Cells were cultured in StemPro 34 media with 100 ng/mL SCF and 100 ng/mL Flt-3 Ligand in addition to the TPO. TPO was supplied as either 50 ng/mL rhTPO in TCPS wells (open squares), TPOm-PEG in TCPS wells (open inverted triangle), TPOm-PEG on DPPC surface (inverted filled triangle), 0.1% TPOm-2L (grey diamond), or 1.0% TPOm-2L (filled diamond). Cells were sampled every other day and counted using a Coulter Multisizer for overall expansion (**A**). Overall expansion was calculated by dividing the cell concentration on a given day by the input cell concentration. Cells were also evaluated for expression of surface markers CD34 and Thy1 using a FACScan flow cytometer. The number of CD34+Thy1+ cells was calculated by multiplying the fraction of CD34+Thy1+ cells by overall cell number. The expansion of CD34+Thy1+ cells (**B**) was calculated by dividing the CD34+Thy1+ cells on a given day by the input number of CD34+Thy1+ cells. Conditions are defined in Table 5.2.2.

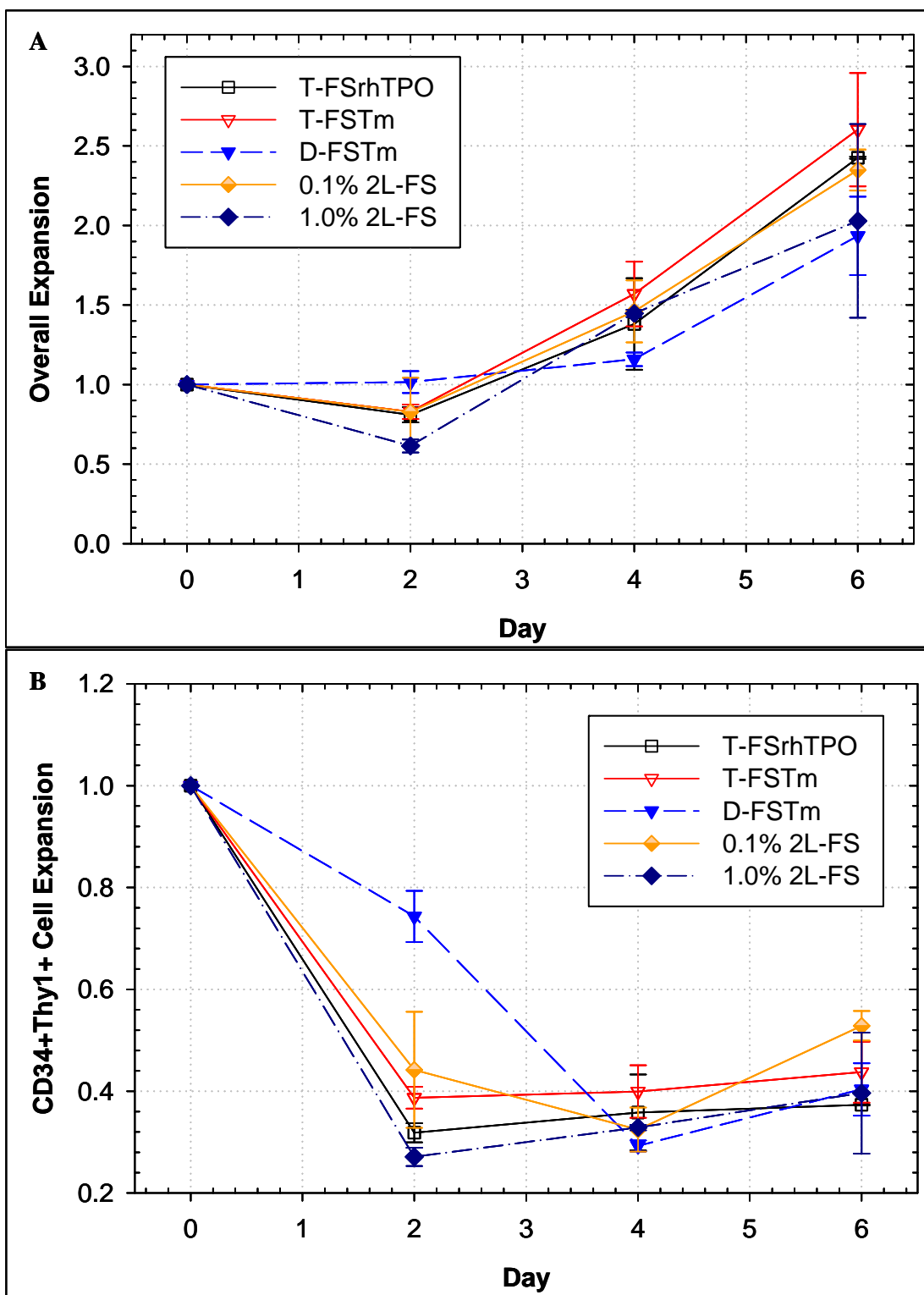


**Table 5.2.3:** Summary of conditions evaluated in six-day expansion cultures of BM CD34+ cells with TPOm-1L <sup>a</sup> Figure 5.2.16 and 5.2.17.

	Name <sup>b</sup>	Background Surface	TPO	Other Cytokines
1	D-FS	DPPC	None	
2	D-FS3	DPPC	None	IL-3 <sup>c</sup>
3	D-FSTm	DPPC	5 nM TPOm-PEG	
4	D-FSTm3	DPPC	5 nM TPOm-PEG	IL-3
5	1L-FS	DPPC	1% TPOm-1L	
6	1L-FS3	DPPC	1% TPOm-1L	IL-3
7	T-FS	TCPS	None	
8	T-FS3	TCPS	None	IL-3
9	T-FSTm	TCPS	5 nM TPOm-PEG	
10	T-FSTm3	TCPS	5 nM TPOm-PEG	IL-3

<sup>a</sup> All conditions in StemPro 34 media with 100 ng/mL SCF and 100 ng/mL FL.

<sup>b</sup> Name derived from the background surface and cytokine cocktail. Abbreviations used: D = DPPC; T = TCPS; 2L = TPOm-2L; F = Flt-3 Ligand; S = SCF; Tm = TPOm-PEG; 3 = IL-3.

<sup>c</sup> 10 ng/mL IL-3

**Figure 5.2.17:** Cell expansion in cultures seeded with CD34+ bone marrow cells. Cells were cultured in StemPro 34 media with 100 ng/mL SCF and 100 ng/mL Flt-3 Ligand for 6 days in TCPS wells (open diamond) or on DPPC coated surfaces (open inverted triangle). TPOm was included in the cytokine cocktail for some conditions: 5 nM TPOm-PEG in TCPS wells (open inverted triangle) or on DPPC surfaces (filled inverted triangles), or as 1.0% TPOm-1L on DPPC surfaces (filled squares). Cells were sampled every other day and counted using a Coulter Multisizer for overall expansion (**A**). Overall expansion was calculated by dividing the cell concentration on a given day by the input cell concentration. Cells were also evaluated for expression of surface markers CD34 and Thy1 using a FACScan flow cytometer. The number of CD34+Thy1+ cells was calculated by multiplying the fraction of CD34+Thy1+ cells by overall cell number. The expansion of CD34+Thy1+ cells (**B**) was calculated by dividing the CD34+Thy1+ cells on a given day by the input number of CD34+Thy1+ cells. Conditions are defined in Table 5.2.3.

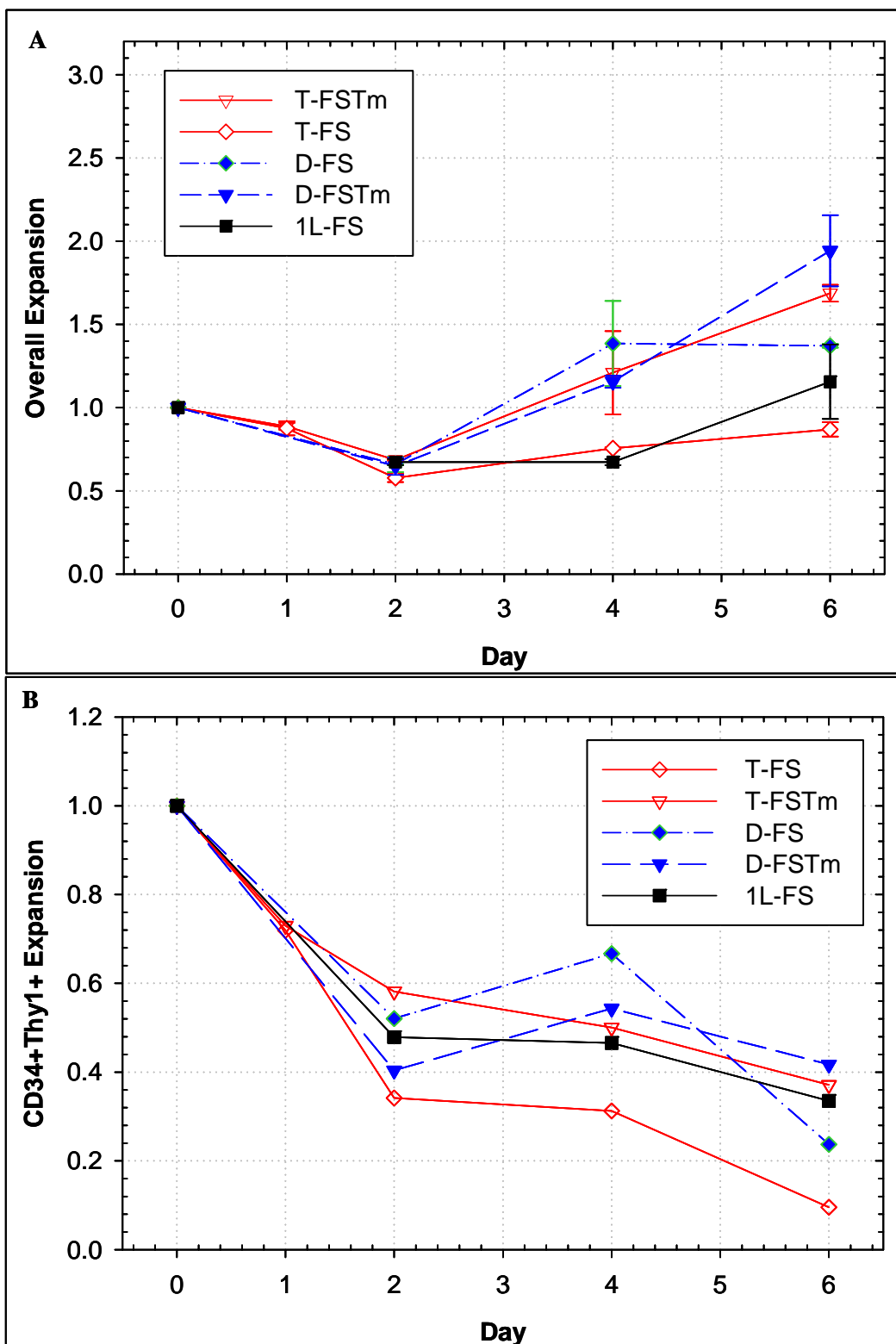
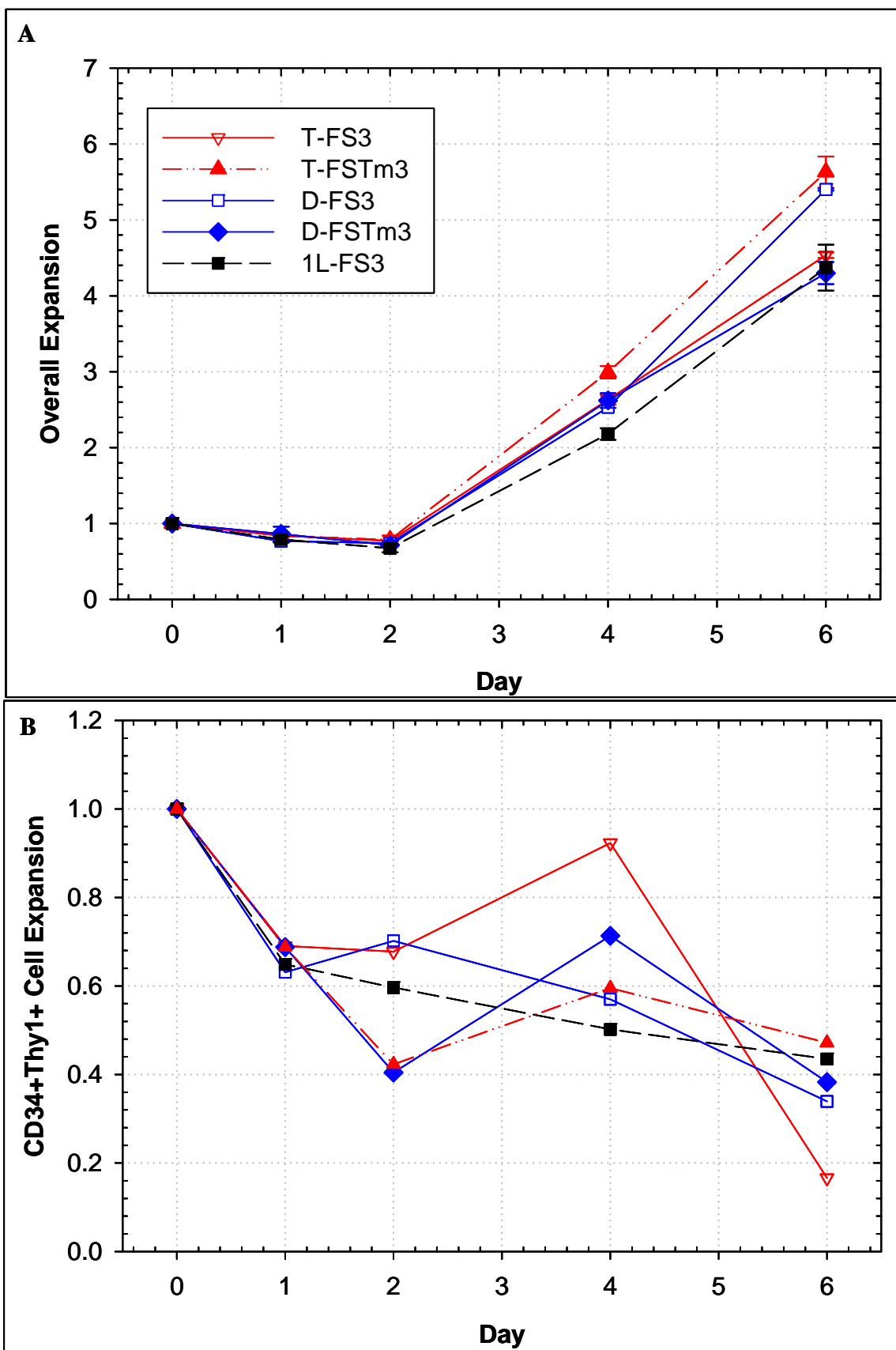
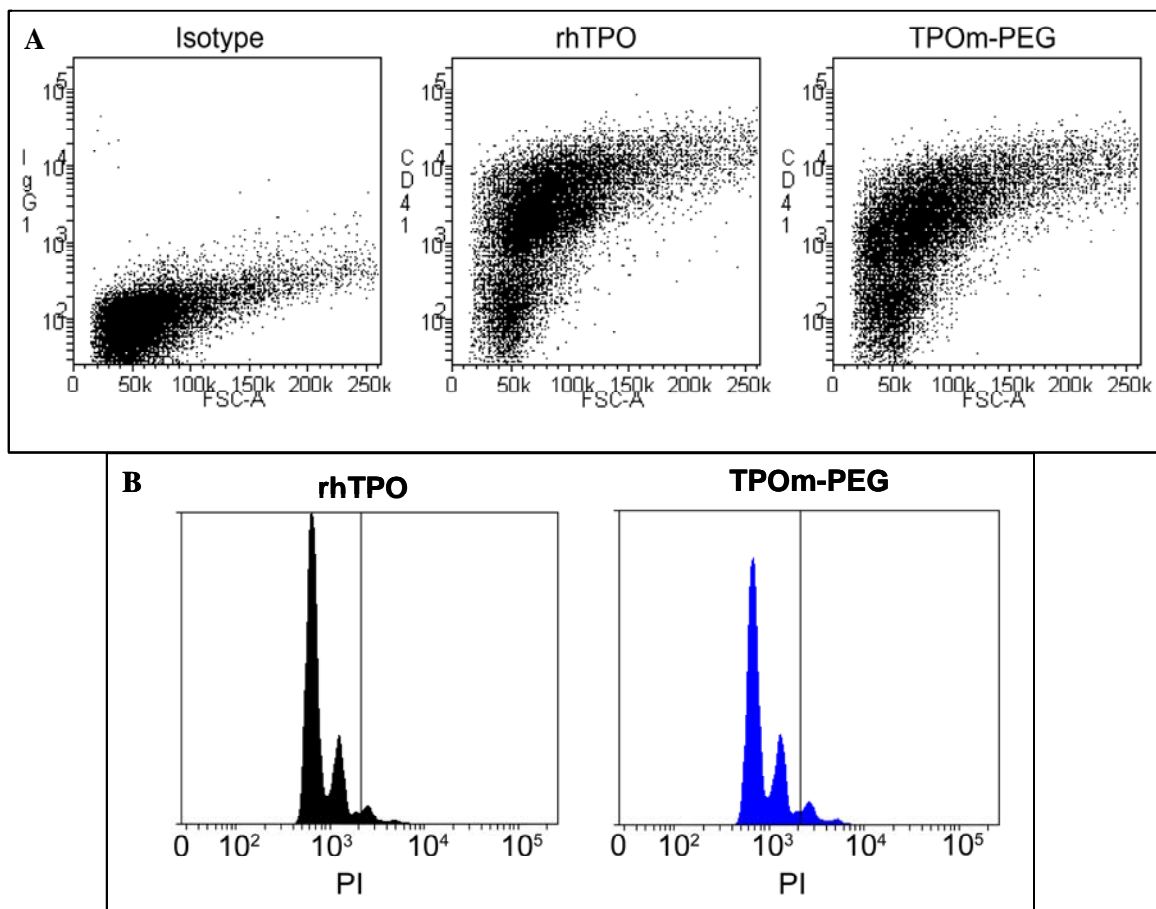


**Figure 5.2.18:** Cell expansion in cultures seeded with CD34+ bone marrow cells under similar conditions as described in Figure 5.2.17 with the addition of 10 ng/mL IL-3. Cells were cultured in StemPro 34 media with 100 ng/mL SCF, 100 ng/mL Flt-3 Ligand, and IL-3 for six days in TCPS wells (open diamond) or on DPPC coated surfaces (open inverted triangle). TPOm was included in the cytokine cocktail for some conditions: 5 nM TPOm-PEG in TCPS wells (open inverted triangle) or on DPPC surfaces (filled inverted triangles), or as 1.0% TPOm-1L on DPPC surfaces (filled squares). Cells were sampled every other day and counted using a Coulter Multisizer for overall expansion (**A**). Overall expansion was calculated by dividing the cell concentration on a given day by the input cell concentration. Cells were also evaluated for expression of surface markers CD34 and Thy1 using a FACScan flow cytometer. The number of CD34+Thy1+ cells was calculated by multiplying the fraction of CD34+Thy1+ cells by overall cell number. The expansion of CD34+Thy1+ cells (**B**) was calculated by dividing the CD34+Thy1+ cells on a given day by the input number of CD34+Thy1+ cells. Conditions are defined in Table 5.2.3.



### 5.2.3.3 Culture of CD34<sup>+</sup> selected cells with only TPOM induces growth of cells with a megakaryocyte phenotype

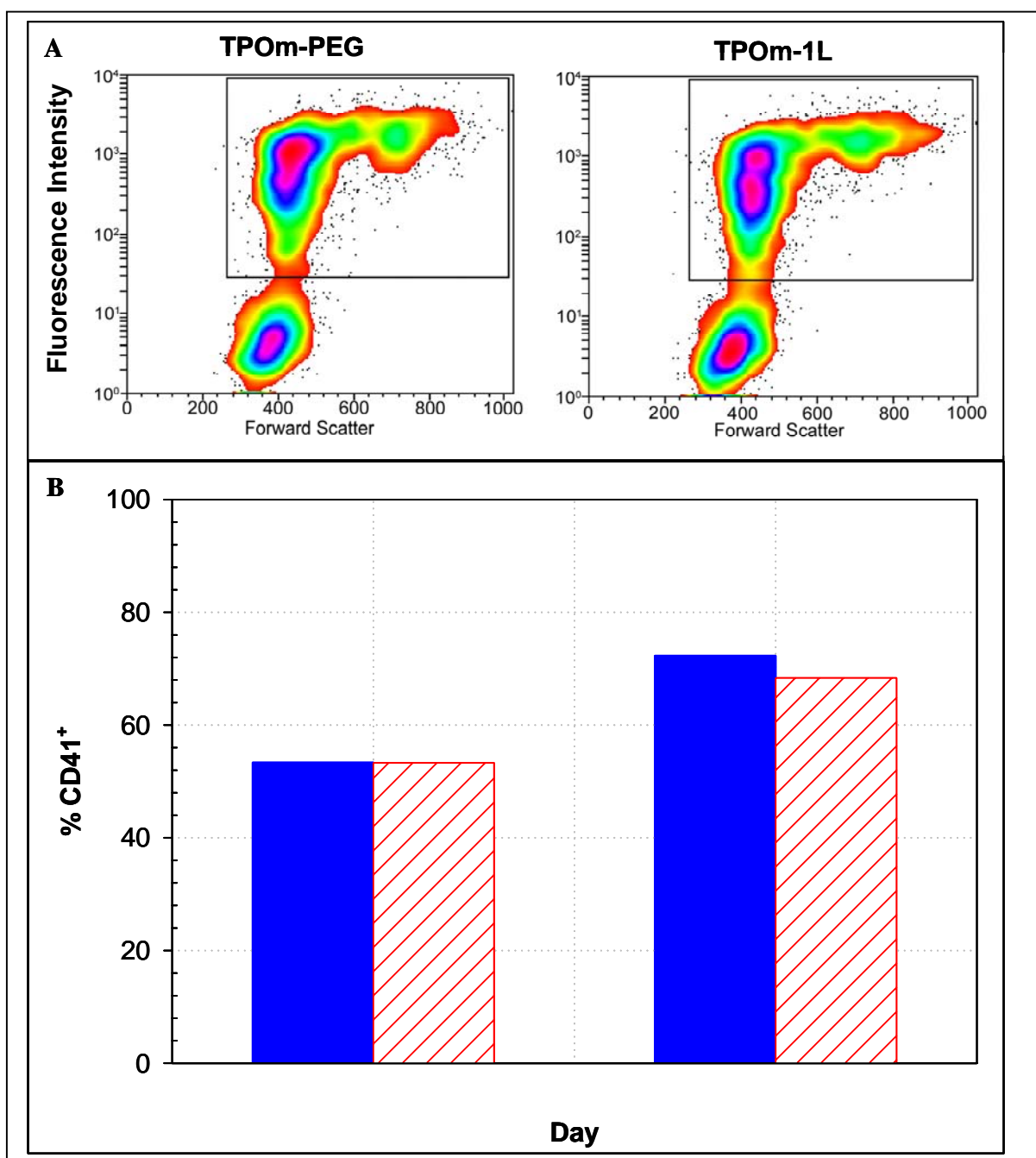
Studies by other groups indicate that mimetic TPO molecules can be as effective in producing Mks from human bone marrow CD34<sup>+</sup> selected cells as rhTPO [43]. Experience in our group has shown that mPB CD34<sup>+</sup> cells cultured with only TPO primarily produce Mks [189]. To test the effectiveness of soluble TPOM-PEG and TPOM lipopeptides, we initiated primary cell cultures stimulated by TPOM only. Separate experiments with frozen mPB CD34<sup>+</sup> cells and BM CD34<sup>+</sup> selected cells yielded similar results, and culture outcomes were similar for TPOM-PEG vs. TPOM-1L. mPB CD34<sup>+</sup> cell cultures were evaluated on day nine and day 11 for characteristics of megakaryocytes—large, polyploid, CD41<sup>+</sup> cells. Control cultures on TCPS surfaces with 5 nM TPOM-PEG or 100 ng/mL rhTPO were similar to each other in terms of CD41<sup>+</sup> cell production and ploidy (Figure 5.2.19). Eleven days after seeding cultures with mPB CD34<sup>+</sup> cells, cells grown in rhTPO were 72.6% CD41<sup>+</sup>, while those grown in TPOM-PEG were 68.4% CD41<sup>+</sup> (Figure 5.2.19A). The production of polyploid cells was also similar with 5.1% and 7.5%  $\geq$  8N for rhTPO and TPOM-PEG, respectively (Figure 5.2.19B). BM CD34<sup>+</sup> cell cultures were evaluated on day nine and day 12 for characteristics of megakaryocytes (Figure 5.2.20). After 12 days of culture, the CD41<sup>+</sup> cell content was similar for TPOM-PEG and TPOM-1L, showing 72.3% and 68.3% CD41<sup>+</sup> cells, respectively (Figure 5.2.20B). The production of polyploid cells was also similar on day 12 for the two versions of TPOM, with 9.4%  $\geq$  8N for TPOM-PEG and 9.1% for TPOM-1L (Figure 5.2.20C). Similar results were observed with BM CD34<sup>+</sup> cells examined on day 12 and mPB CD34<sup>+</sup> cells examined on day 11 (DATA NOT SHOWN).

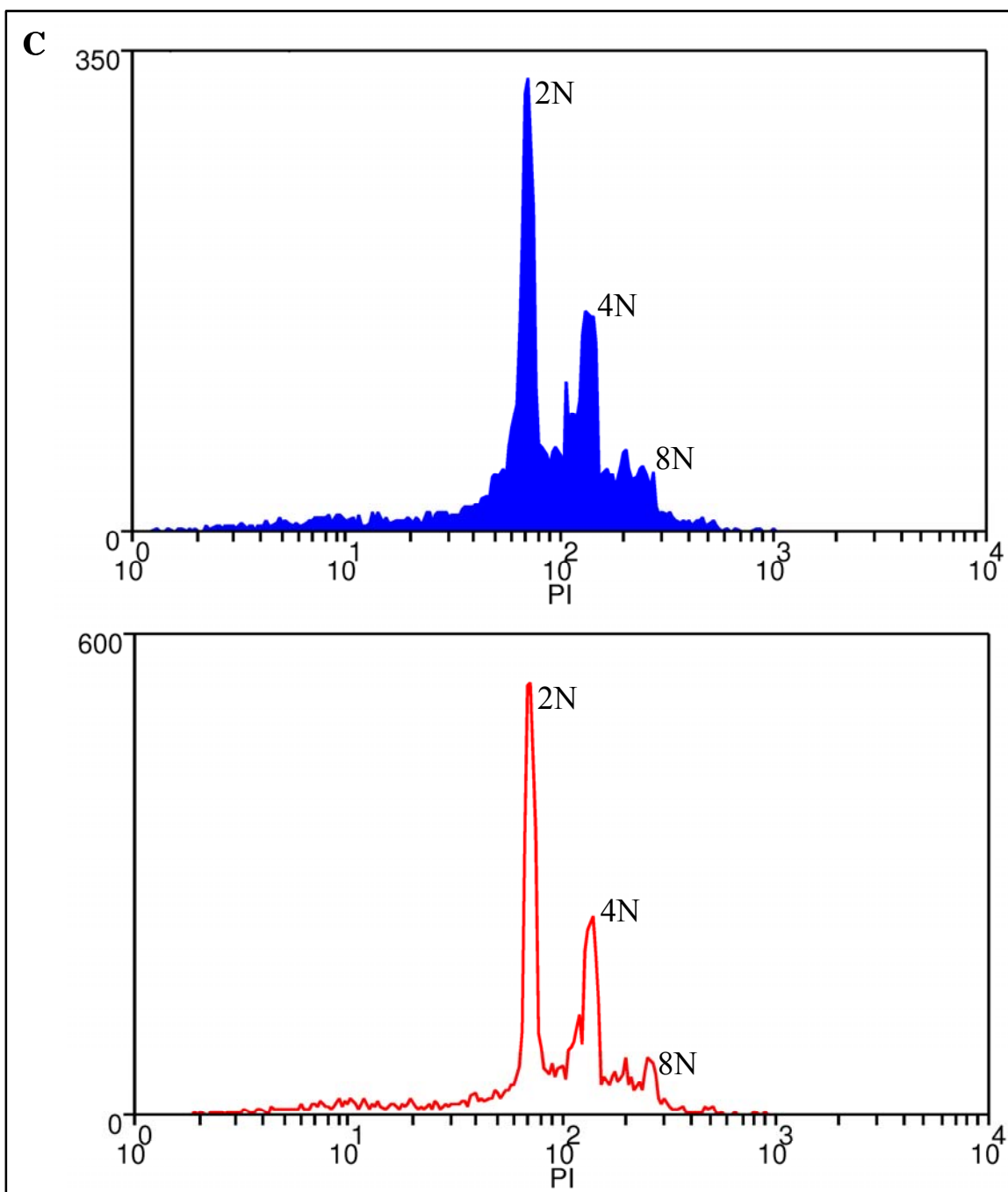


**Figure 5.2.19:** Results from TPO only culture of mPB CD34<sup>+</sup> selected cells on TCPS.

(A) Dot plots of CD41 fluorescence intensity vs. forward scatter on day 11. (B) Ploidy distribution of CD41<sup>+</sup> cells on day 11 for rhTPO and TPOM-PEG.

**Figure 5.2.20:** Results from TPO only culture of BM CD34+ selected cells on lipid-based surfaces. **(A)** Representative % CD41+ cell density plots showing of CD41 fluorescence intensity vs. FSC on day 12 for 5 nM TPOM-PEG and 1% TPOM-1L. **(B)** Summary of % CD41 expression data on days nine and 12. Data shown are the average of two technical replicates from a single experiment. **(C)** Histograms representative of two technical replicates showing the ploidy distribution of CD41+ cells on day 12 for 5 nM TPOM-PEG (top, filled) and 1% TPOM-1L (bottom, open).





## **5.3 DISCUSSION**

### **5.3.1 Synthesis of TPOm**

Modifications of the original TPOm sequence published by Cwirla and coworkers have been previously documented. In three papers, the pharmacokinetics, immunogenicity, and hematological effects of adding high molecular weight poly(ethylene glycol) to the N-terminus of each arm of the dimer were explored [207-209]. Together, these studies show that adding PEG molecules did not alter the ability of the TPOm peptide to promote megakaryopoiesis. These results support our findings that PEG and lipid modification of TPOm does not decrease TPOm activity.

### **5.3.2 Activation of ERK 1,2 and STAT5 with TPOm stimulation**

Upon binding cMpl, TPO induces a cascade of phosphorylation events that result in the activation of several different signaling pathways, including the JAK/STAT pathway and Ras/MAPK pathway [148, 202]. The prolonged stimulation of the MAPK pathway by TPO was previously shown to induce megakaryocyte differentiation [204], while activation of STAT5 is involved in the proliferative response of M07e cells [210]. For these reasons we studied the ability of TPOm molecules to stimulate ERK 1,2 and STAT5 activation. Others have shown that TPO mimetic molecules are capable of upregulating these signaling pathways [177-179, 211-213], but to our knowledge other groups have not studied the activation of cMpl associated signaling pathways using the TPOm peptide sequence developed by Cwirla and coworkers. A different peptide mimetic sequence (LQGCTLRWRAGMC) was developed by Kimura et al. [212]. Using Western blots and electrophoretic mobility shift assays (EMSA), they showed that their TPO mimetic peptide sequence activated JAK2 and STAT5b in Ba/F3-mpl cells. Here we

used a flow cytometric assay to show the activation of ERK 1,2 and STAT5. In this assay, phospho-specific antibodies against ERK 1,2 and STAT5 are used to label fixed and permeabilized whole cells after a 20-minute activation. This assay allowed us to simultaneously determine pERK 1,2 and pSTAT5 levels in the same cells.

We hypothesized that presenting an immobilized TPOM lipopeptide in a HBM surface would increase the amplitude and duration of ERK 1,2 and STAT5 activation, relative to that for soluble TPOM. However, our results showed that TPOM-PEG and TPOM-1L induced a similar magnitude and duration of activated signaling molecules. There are several possible explanations why no differences were observed between soluble TPOM-PEG and HBM-immobilized TPOM-L. It is possible that the similarity resulted from material released from the surfaces. Supernatants collected after the washing process, an incubation step, and three further rinses reveal different information about released material. Collection after washes showed that surfaces were adequately washed, removing residual material from the supernatant before the incubation. However, supernatants collected after a 20-minute incubation showed that material was released from the surface during the signaling studies. TPOM-1L in solution would behave more like soluble TPOM-PEG, and thus kinetics of activation would behave similarly to soluble stimulation. However, even after additional washing, surfaces containing TPOM-1L induced greater pERK activation than the material released prior to the additional washes. This suggests that TPOM-1L in the surfaces also stimulates cMpl-mediated signal transduction.

### **5.3.3 Culture of human CD34+ selected cells with TPOM molecules**

An important aspect of the stem cell niche involves the presentation of cytokines in an immobilized form; either bound to a stromal cell membrane or adsorbed to ECM components

[18]. Others have shown that soluble versus membrane-associated presentation of stem cell factor can significantly alter the production of primitive HSCs [38, 41, 123]. TPO is not expressed as a membrane-bound protein in vivo. However, results with insulin suggest that the benefits of surface localization are not limited to naturally-membrane-bound cytokines. When insulin, was bound to a surface to create an artificial juxtacrine stimulation, fibroblast expansion increased several-fold over that with soluble insulin [214]. We hypothesized that presenting an immobilized TPOm lipopeptide in a HBM surface would enhance HSC expansion. However, we found that the method of TPOm presentation had no significant effect on overall expansion or on the maintenance of CD34+Thy1+ cells. Controls in a follow-up experiment indicated the addition of TPOm did not significantly enhance overall expansion or retention of CD34+Thy1+ cells in cultures with SCF and FL, with or without IL-3. Therefore, further examination of HSC expansion with TPOm was not continued.

## CHAPTER 6: EXPERIMENTS WITH BIOTINYLATED SCF

### 6.1 INTRODUCTION

Many studies have shown that hematopoietic stem cell (HSC) expansion is greater on stromal cell co-cultures than in suspension cultures. A key difference between co-cultures and suspension cultures is the presentation of stem cell factor (SCF). Stromal cells display membrane-associated and soluble forms of SCF, but only the soluble form is presented to cells in suspension cultures. Researchers have shown that membrane-associated and soluble SCF have different physiological roles. *Sl<sup>d</sup>* mice only express soluble SCF and suffer from severe defects in germ-line, hematopoietic, and pigmentation cells [39]. Reintroduction of membrane-associated SCF into *Sl<sup>d</sup>* mice corrected these defects [38]. Furthermore, fibroblasts from *Sl<sup>d</sup>* mice are unable to support the survival of the growth-factor-dependent cell line FDC-P1 [122].

The effects of immobilized SCF and anti-SCF receptor (c-Kit) antibodies have been evaluated in several studies. Kurosawa and coworkers demonstrated that an immobilized monoclonal antibody (YB5.B8) could substitute for SCF as an activator of c-Kit in M07e cells [123]. In its soluble form YB5.B8 inhibited the proliferation of M07e cells, but when immobilized it promoted proliferation and synergized with GM-CSF for M07e cell proliferation. Doherty et al. used a fusion protein combining the cellulose-binding domain of cellulase, Cex, to present immobilized SCF (SCF-CBD) on cellulose surfaces [124]. SCF-CBD surfaces enhanced SCF-dependent proliferation in M07e, TF-1, and mouse B6SutA cell lines as compared to soluble SCF. Additional characterization of SCF-CBD surfaces using B6SutA cells showed extended c-Kit phosphorylation [125]. In contrast to SCF-CBD, an immobilized fusion protein

between IgG<sub>1</sub> and rat SCF (rSCF-IgG<sub>1</sub>) decreased the maximum growth potential of M07e cells, but induced adhesion dependent shape change in factor dependent CS-1 cells [126].

We hypothesized that immobilization of SCF would improve HSC expansion. To test our hypothesis we chemically modified SCF with biotin for display on surfaces coated with biotin-binding molecules. We have explored two different systems to evaluate this hypothesis. The first system was developed by Dr. Dominic Chow and employed the use of commercially available NeutrAvidin-coated plates. NeutrAvidin is an uncharged, deglycosylated version of avidin with similar biotin-binding properties. HSC expansion on immobilized biotinylated SCF surfaces was delayed, but extended as compared to soluble SCF controls. However, large amounts of biotinylated SCF were required for immobilized surfaces to induce M07e cell expansion. Control experiments performed later suggested that biotinylated SCF was continually released from the surface. Therefore, the results could not be attributed directly to immobilized SCF. The second system for biotinylated SCF immobilization was built upon a non-fouling layer of poly(ethylene glycol) (PEG) anchored to the surface via the amino acid 2,4-dihydroxyphenylalanine (DOPA). This system was pioneered in Dr. Phil Messersmith's laboratory. In conjunction with Dr. Rico Gunawan, we have been working to expand the functionality of DOPA-PEG surfaces by specifically presenting molecules important in cell culture applications. To accomplish this goal biotin was conjugated to the end of the PEG-DOPA to form DOPA-PEG-biotin (Figure 3.1.3). Biotinylated SCF could then be specifically displayed on DOPA-PEG-biotin surfaces through an avidin bridge. This approach has the added advantage that we will be able to use our previous work characterizing biotinylated SCF. Characterization of DOPA-PEG-biotin surfaces using M07e cells has shown that immobilized

biotinylated SCF can elicit a specific adhesive interaction, activate ERK 1,2 signaling, and promote cell growth.

## **6.2 RESULTS FOR THE BIOTINYLATION OF SCF**

Biotinylated SCF (biotin-SCF) was prepared using a commercially available crosslinker, sulfo-NHS-LC-biotin (Figure 3.1.4). NHS reacts with primary amines to form a stable amide bond. Thus, the primary amines of lysine and the N-terminus are the principal target of sulfo-NHS-LC-biotin. SCF contains 13 lysine residues (Table 2.4.1).

Sulfo-NHS-LC-biotin was reacted with 200  $\mu$ g SCF (at 0.5 mg/mL) at different biotin-to-protein (BP) molar ratios (2:1, 5:1, 10:1, and 100:1). The extent of biotinylation of the various biotin-SCF constructs was determined using MALDI-TOF MS. The addition of a single biotin to SCF is key to accomplishing the goal of defined orientation. Multiple biotinylations are undesirable since the resulting biotin-SCF could bind to surfaces at multiple points of attachment. SCF biotinylated at a BP ratio of 2:1 showed that a small amount of SCF was modified with a single biotin crosslinker (Figure 6.2.1). As the BP ratio increased to 10:1 the proportion of biotin-SCF became larger, and the fraction of SCF with multiple biotins increased. A BP molar ratio of 100:1 resulted in the addition of several biotins per SCF molecule, with up to five biotins added (Figure 6.2.2). These results indicate that multiple residues are biotinylated as the amount of crosslinker is increased. Under conditions where a single biotin molecule was added to SCF, Dr. Dominic Chow previously determined that lysine residue 31 (K31) was preferentially biotinylated [215]. K31 is located far away from receptor binding and dimerization sites (Figure 6.2.3), thus its biotinylation should not alter bioactivity of SCF.

NHS-esters slowly hydrolyze [216], thus sulfo-NHS-LC-biotin is sensitive to moisture. The repeated use of the same stock reagent can decrease the efficiency of biotinylation (Figure 6.2.4). A BP ratio 2:1 is suggested for fresh material for adding a single biotin to SCF. However, the BP ratio may need to be increased as the stock material ages or with the number of vial openings. The specificity of the reaction is not expected to change with different BP ratios that yield similar final product (single biotinylation of SCF), as hydrolysis of NHS-LC-Biotin removes the active group necessitating the use of a higher BP ratio. The overall extent of biotinylation was determined with a commercially available HABA reagent. Results indicated an average of  $0.25 \pm 0.10$  moles of biotin were added per mole of SCF under conditions where a single biotin was added to SCF.

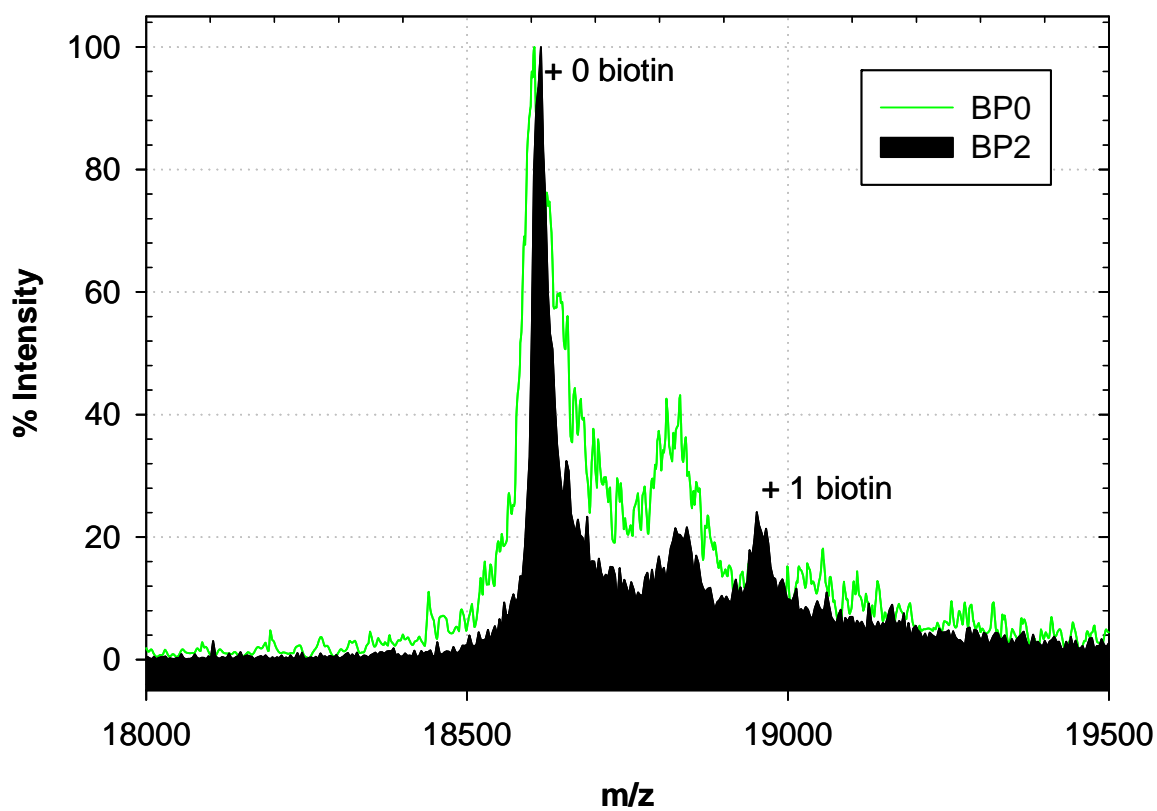


**Figure 6.2.1:** MALDI-MS spectra of SCF biotinylated with sulfo-NHS-LC-biotin at a biotin to protein (BP) ratio of 2:1 (filled), with unbiotinylated SCF (line) as a control.

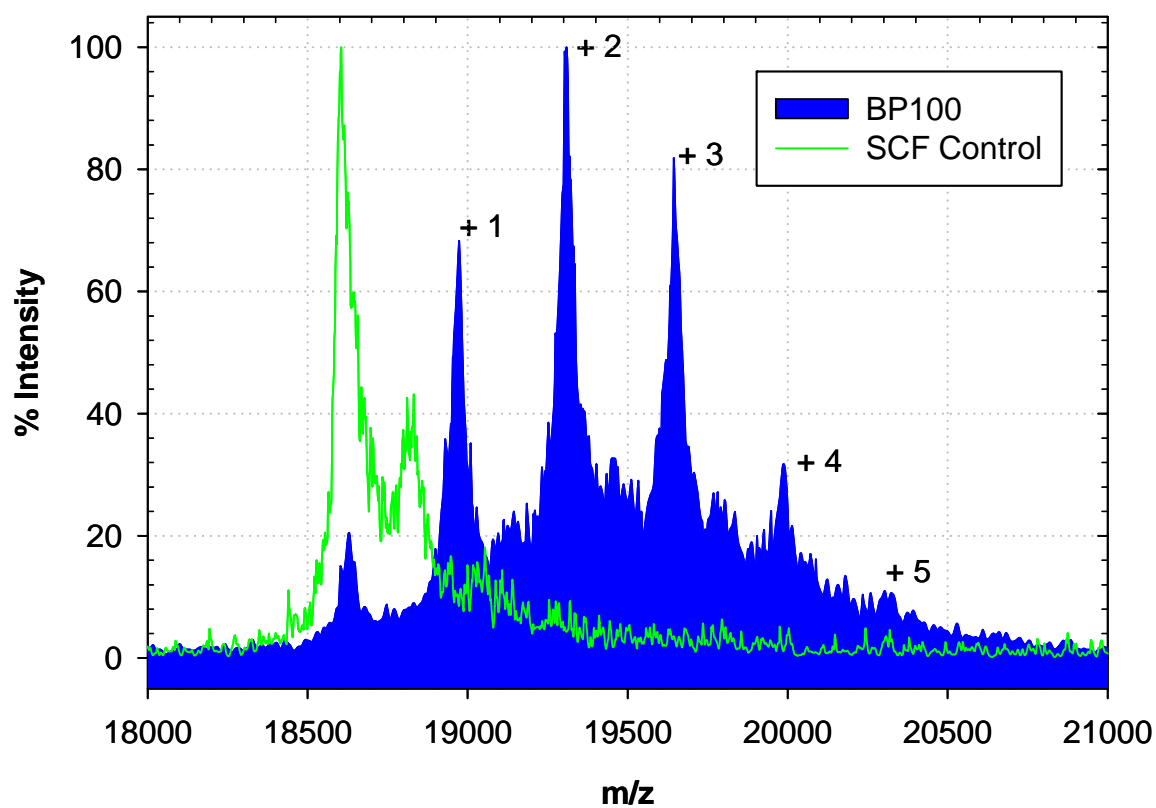


**Figure 6.2.2:** MALDI-MS spectra of SCF biotinylated with sulfo-NHS-LC-biotin at a biotin-to-protein (BP) ratio of 100:1 (filled), with unbiotinylated SCF (line) as a control.

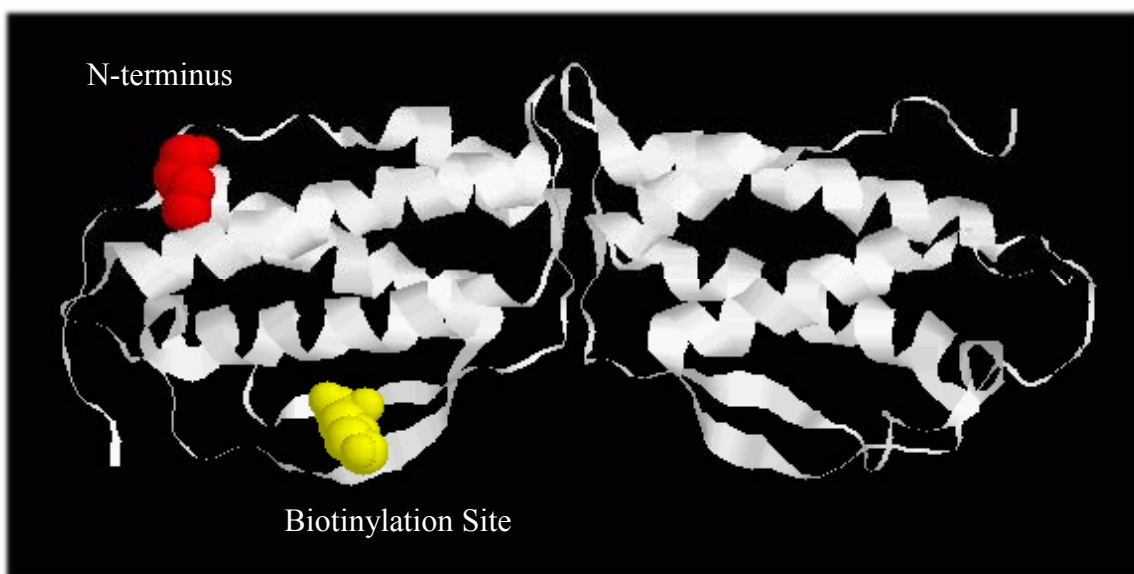


**Figure 6.2.3:** from Dominic Chow's thesis, Figure 4.3 [215]. Location of the amino acid residue biotinylated with a single sulfo-NHS-LC-biotin. Residue location was determined by peptide mapping. Stem cell factor (white) is presented as a dimer. The locations of the N-terminus of SCF and the biotinylated residue are shown for a SCF monomer.

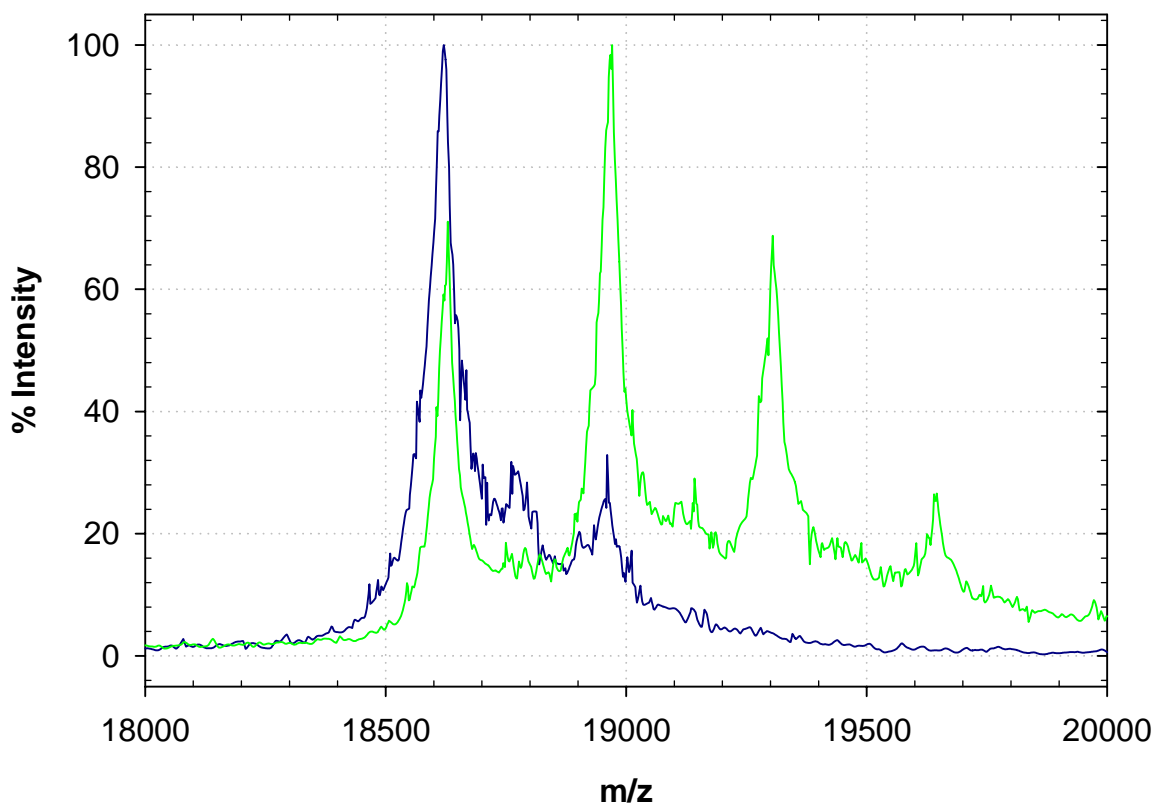


**Figure 6.2.4:** Comparison of MALDI-MS spectra for SCF biotinylated with sulfo-NHS-LC-biotin at a biotin-to-protein (BP) ratio of 10:1. SCF was biotinylated with a fresh stock of sulfo-NHS-LC-biotin (light green line) and compared to biotinylation after the stock vial had been opened seven times (dark blue line).

## **6.3 RESULTS WITH BIOTIN-SCF IMMOBILIZED ON NEUTRAVIDIN-COATED PLATES**

### **6.3.1 Immobilized biotin-SCF on NeutrAvidin-coated plates**

Assistance was provided to Dr. Dominic Chow who performed the majority of the characterization the immobilized biotin-SCF on commercially available NeutrAvidin-coated surfaces [215]. Biotin-SCF loaded into NeutrAvidin-coated wells at a concentration of 10  $\mu\text{g/mL}$  resulted in the immobilization of  $\sim 40$  ng of biotin-SCF per well (Table 6.3.1). M07e cell expansion reached a plateau at 30 ng biotin-SCF per well when immobilized (Figure 6.3.1). In contrast, soluble SCF required only 1 ng/well to reach near-maximal M07e cell expansion. The low potency of immobilized biotin-SCF compared to soluble SCF indicates that the majority of biotin-SCF on the surface was not active, at least until a critical surface density of  $\sim 20$  ng/well was reached. SCF inactivation likely resulted from a combination of non-specific interactions of biotin-SCF with the NeutrAvidin-coated surfaces, causing the protein to denature, and UV sterilization of biotin-SCF-modified surfaces.

**Table 6.3.1:** Biotin-SCF immobilized on NeutrAvidin-coated surfaces.

<b>Immobilization Concentration (<math>\mu\text{g/mL}</math>)</b>	<b>ng/well</b>	<b>ng/cm<sup>2</sup>*</b>
0.1	0.63	1.96
0.4	2.31	7.22
1	7.60	23.76
2	19.82	61.95
4	29.75	92.97
6	34.14	106.67
8	39.94	124.81
10	40.29	125.91
25	60.96	190.50

Surface loading was determined by measuring radioactivity associated with NeutrAvidin-coated surfaces loaded with <sup>125</sup>I-labeled biotin-SCF; from Dominic Chow's thesis [215].

\* ng/cm<sup>2</sup> calculated by dividing ng/well by the surface area per well (0.32 cm<sup>2</sup>).

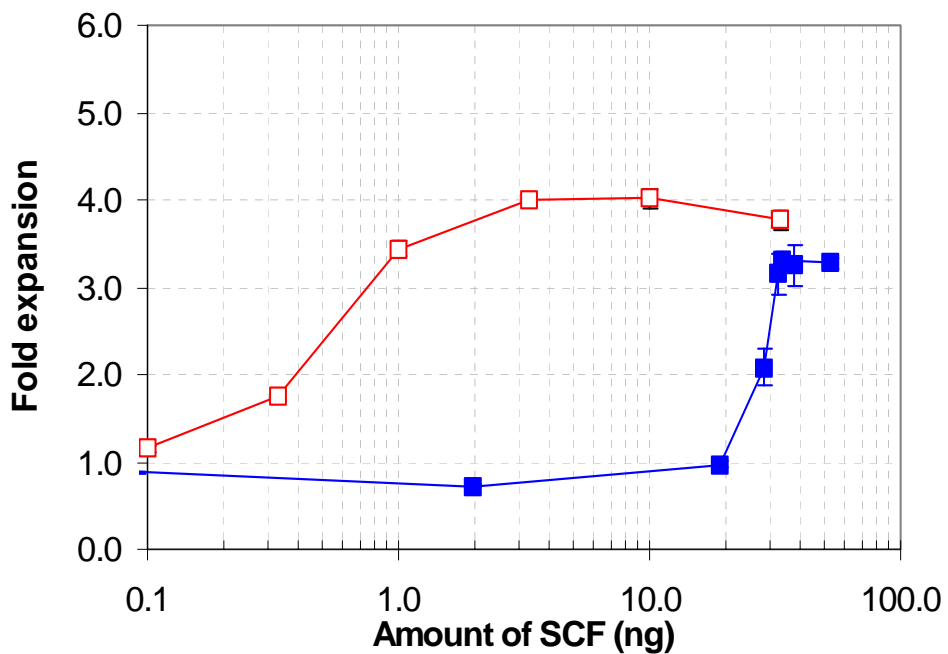


**Figure 6.3.1:** Taken from Dominic Chow's Ph.D. thesis, Figure 5.1. [215]. Proliferation of M07e cells after four day culture on biotin-SCF-modified NeutrAvidin-coated surfaces (filled squares). Cells were seeded at 250,000 cells/mL in a 96-well plate. Controls were comprised of cells seeded onto NeutrAvidin-coated surfaces and supplemented with various amount of soluble SCF (open squares). Data are the average ( $\pm$  SD) of measurements from two wells and each well was counted twice.

### **6.3.2 Adhesion of M07e cells to immobilized biotin-SCF on NeutrAvidin-coated plates**

Dr. Dominic Chow performed adhesion assays to ensure that the M07e cells specifically interacted with biotin-SCF-modified NeutrAvidin-coated surfaces [215]. The number of attached cells on biotin-SCF-modified NeutrAvidin-coated surfaces correlated with the extent of cell proliferation (Figure 6.3.2). Biotin-SCF-modified surfaces that resulted in greater cell M07e cell expansion also showed enhanced levels of cell attachment, up to 40 ng/well. This indicates that biotin-SCF immobilized on surfaces remained active when a sufficiently high dose of material was used to modify NeutrAvidin-coated surfaces. Above 50 ng per well the fraction of attached M07e cells decreased, which may have been due to competitive inhibition from desorbed biotin-SCF. Control NeutrAvidin-coated surfaces treated with soluble SCF exhibited minimal M07e cell adhesion.

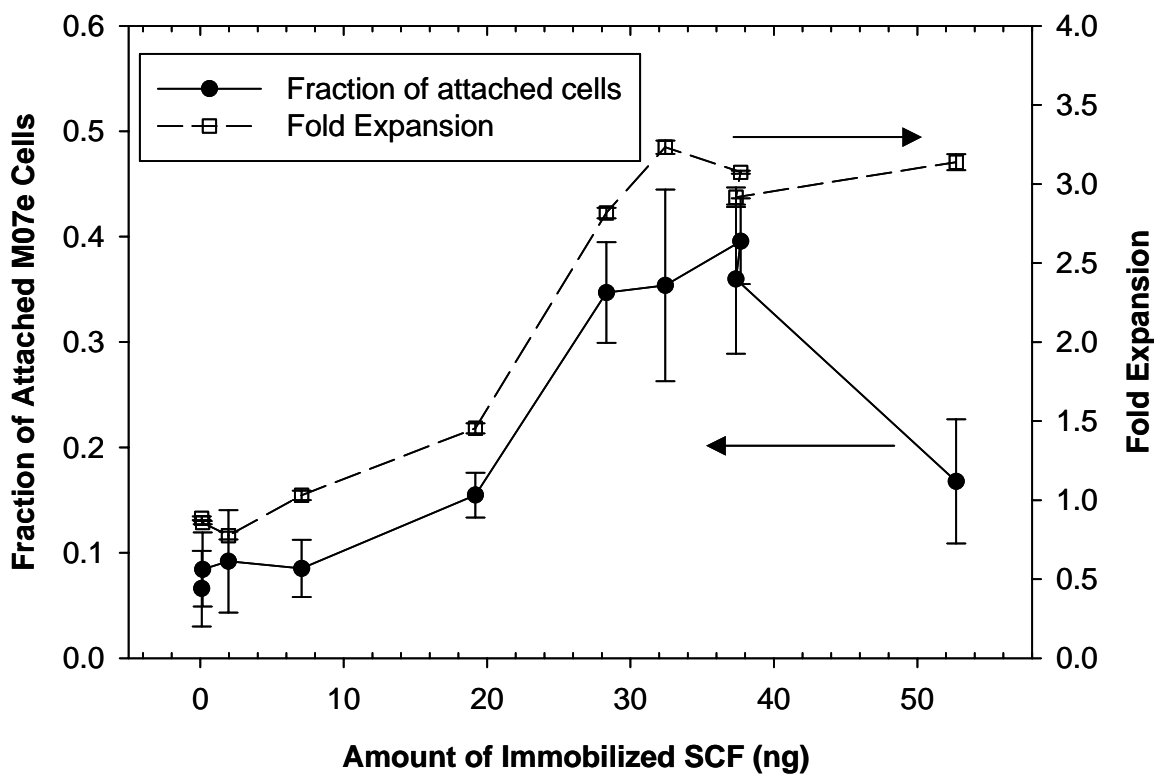


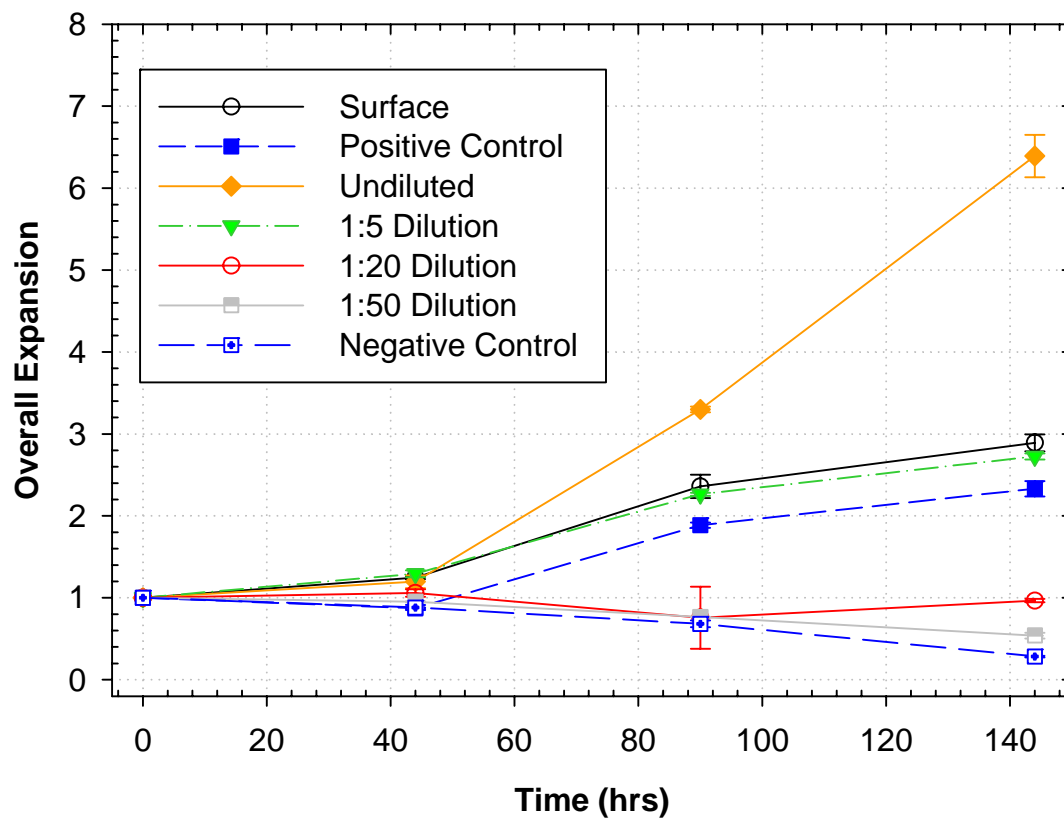
**Figure 6.3.2:** Taken from Dominic Chow's Ph.D. thesis, Figure 5.6. [215]. Fraction of M07e cells attached to NeutrAvidin-coated biotin-SCF-modified surfaces (●). Data shown are the averaged results from three independent experiments, each of which with at least two individual wells. For comparison, the fold-expansion of M07e cells after four days of culture on NeutrAvidin coated biotin-SCF-modified surfaces (□) is shown.

### 6.3.3 Confounding effects due to release of surface-immobilized biotin-SCF

Given the large amount of biotin-SCF immobilized on NeutrAvidin-coated surfaces and the results from adhesion assay, it was possible that a portion of biotin-SCF was releasing from the surface. Desorption of even a small fraction of immobilized SCF could account for the biological effects attributed to immobilized SCF. We (James King and Peter Fuhrken) directly tested the effects of released SCF by culturing M07e cells in media conditioned by overnight incubation on biotin-SCF culture surfaces. For this experiment, biotin-SCF surfaces were prepared under standard procedures (Section 3.2.4) by immobilizing biotin-SCF at 10  $\mu\text{g/mL}$  in NeutrAvidin-coated wells. Wells were rinsed with PBS and sterilized by 30-minute exposure to 254 nm UV light. The wells were then loaded with StemPro 34 media and incubated overnight in the biotin-SCF-modified NeutrAvidin-coated wells. Media from biotin-SCF-modified NeutrAvidin-coated wells were collected and sterile filtered. Media was then used at full strength or diluted in serum-free StemPro 34 media conditioned overnight by NeutrAvidin-coated wells. As a control M07e cells were also cultured on the biotin-SCF-modified NeutrAvidin-coated wells that was used to prepare the conditioned media.

Undiluted conditioned media supported much greater M07e cell growth than control medium supplemented with 5 ng/mL SCF ( $p = 0.002$  at 144 hours, Figure 6.3.3). Even a 1:5 dilution of conditioned medium supported growth similar to that for the positive control ( $p = 0.08$  at 144 hours). A 1:20 dilution maintained input cell numbers and a 1:50 dilution gave a similar response to the negative control medium without SCF. Despite the release of material surfaces remained bioactive, stimulating similar growth as the positive control. However, this was not sufficient to eliminate the confounding effects of released SCF.

**Figure 6.3.3:** Biotin-SCF released from NeutrAvidin-coated wells supports M07e cell growth. Biotin-SCF was immobilized at 10  $\mu\text{g}/\text{mL}$  in NeutrAvidin-coated wells and washed under standard procedures (Section 3.2.4). StemPro 34 media was incubated overnight in the biotin-SCF-NeutrAvidin coated wells. Media from coated wells was collected and syringe filtered using a 0.22  $\mu\text{m}$  filter. Media was then used at full strength (filled diamonds) or diluted at 1 part to 5 parts (inverted triangles), 1:20 (open diamonds), or 1:50 (top filled square) with media conditioned overnight in NeutrAvidin wells and used to culture M07e cells seeded at  $\sim 2.5 \times 10^5$  cells/mL. Fresh StemPro 34 was added to biotin-SCF-modified surfaces and used to culture M07e cells (open circles). Positive (filled squares) and negative (open squares) controls are StemPro 34 conditioned overnight in NeutrAvidin plates with or without the addition of 5 ng/mL soluble SCF, respectively. Results are the average ( $\pm$  SEM) for triplicate wells in a single experiment.



### **6.3.4 Immobilized biotin-SCF on NeutrAvidin-coated plates influence on proliferation and differentiation of CD34+ cells**

Prior to the experiments discussed in the previous section, we tested the effects of immobilized biotin-SCF on the proliferation and differentiation of mPB and BM CD34-selected cells.

Initially, different concentrations of biotin-SCF (1, 10, 20, and 40  $\mu\text{g}/\text{mL}$ ) were used to modify in NeutrAvidin-coated well plates. Cells were seeded in X-Vivo 15 media with 100 ng/mL FL and 50 ng/mL rhTPO at three different seeding densities:  $2.5 \times 10^5$ ,  $1.0 \times 10^5$ , and  $0.4 \times 10^5$  cells/mL. The control condition comprised cells in the same media supplemented with 100 ng/mL soluble SCF in TCPS well plates. Cultures were evaluated on days three, six, and nine for overall expansion, expression of CD34 and Thy1 surface markers, and colony-forming ability.

For a seeding density of  $\sim 250,000$  cells/mL, the growth kinetics for mPB CD34+ cell cultures on NeutrAvidin-coated surfaces treated with 10, 20, or 40  $\mu\text{g}/\text{mL}$  biotin-SCF were very similar. Compared to controls on NeutrAvidin-coated surfaces, the total number of cells in cultures with immobilized SCF at 10, 20, and 40  $\mu\text{g}/\text{mL}$  was higher on days 6 and 9 (Figure 6.3.4). Surfaces immobilized with 1  $\mu\text{g}/\text{mL}$  biotin-SCF had substantially lower cell expansion, likely due to the lower surface density of biotin-SCF. For seeding densities of 250,000 BM CD34+ cells/mL ( $n = 3$ ) and 100,000 cells/mL ( $n = 2$ ), overall cell expansion with soluble SCF was greater than that with immobilized biotin-SCF (NeutrAvidin-coated surfaces modified with 10  $\mu\text{g}/\text{mL}$  biotin-SCF) at day 3 (Figure 6.3.5A). However, cell expansion was similar with both types of SCF by day 6 (Figure 6.3.5B) and expansion on immobilized biotin-SCF was greater than that with soluble SCF by day 9 (Figure 6.3.5C). The declines in CD34+ and CD34+Thy1+ cell percentages during culture were similar for soluble SCF and immobilized biotin-SCF (Figure 6.3.6). The numbers of CFU-GM in cultures with biotin-SCF-modified NeutrAvidin-coated

surfaces were similar to controls with soluble SCF on NeutrAvidin coated surfaces for all days examined (Day 3  $p = 0.264$ , Figure 6.3.7A). The number of BFU-E colonies (Figure 6.3.7B) was also similar for biotin-SCF-modified NeutrAvidin-coated surfaces and soluble SCF controls on NeutrAvidin-coated surfaces on all days except day 3 ( $p = 0.03$ ). Due to the SCF release problems discussed in section 6.3.3 and the similarities seen in expansion and retention of CD34+ cells, this project was put on hold until we recently gained access to a new type of culture surface that allows for immobilization of small amounts of SCF in an active form.

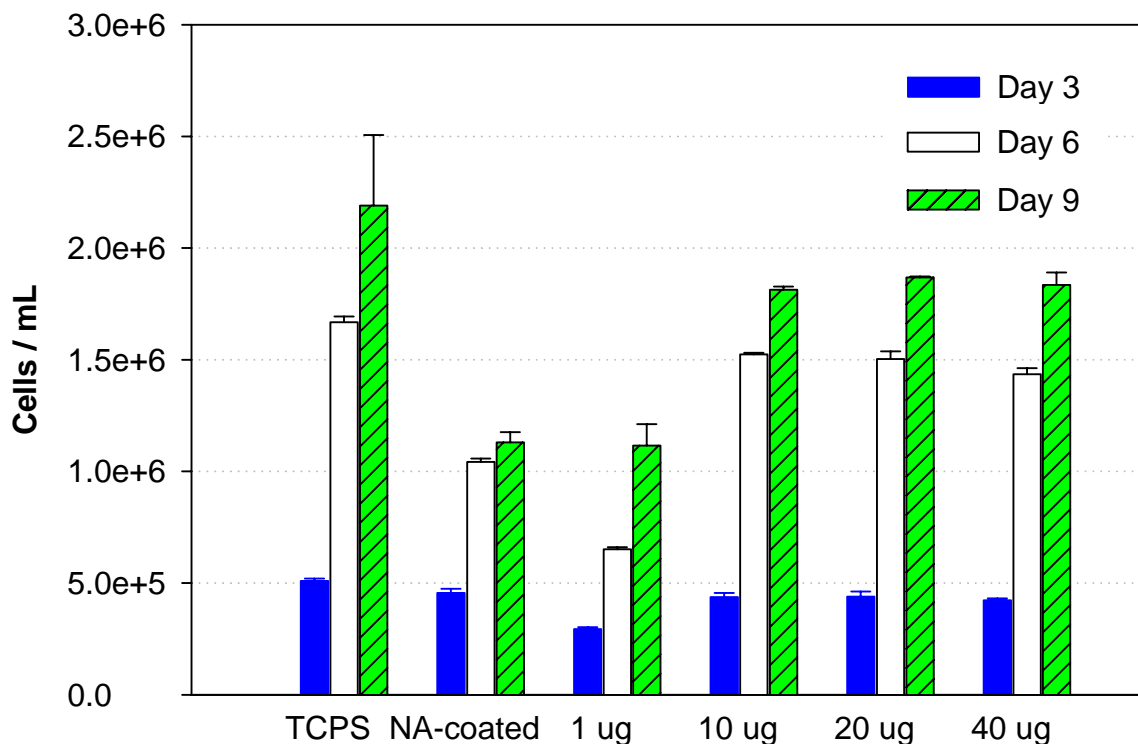
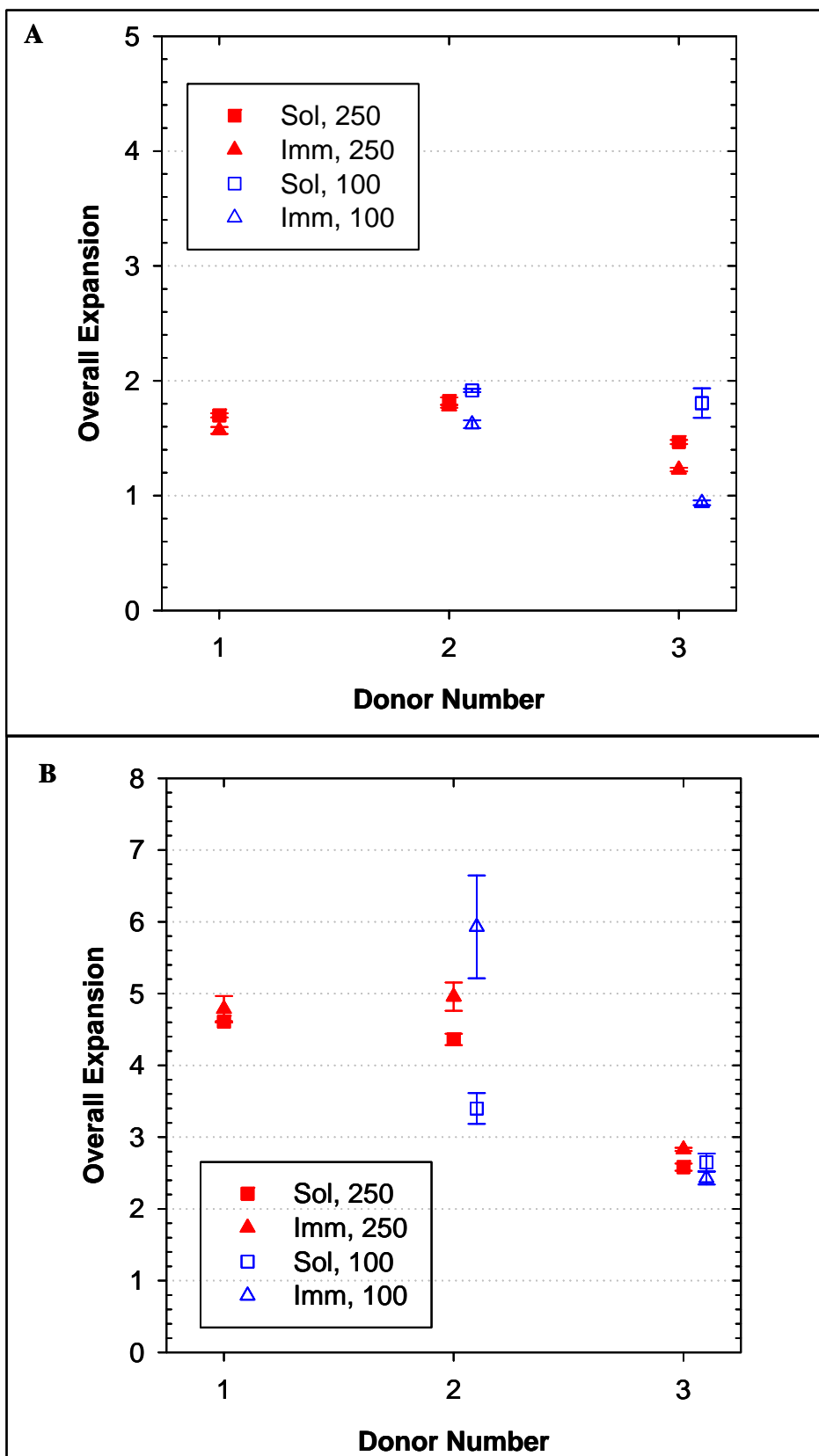


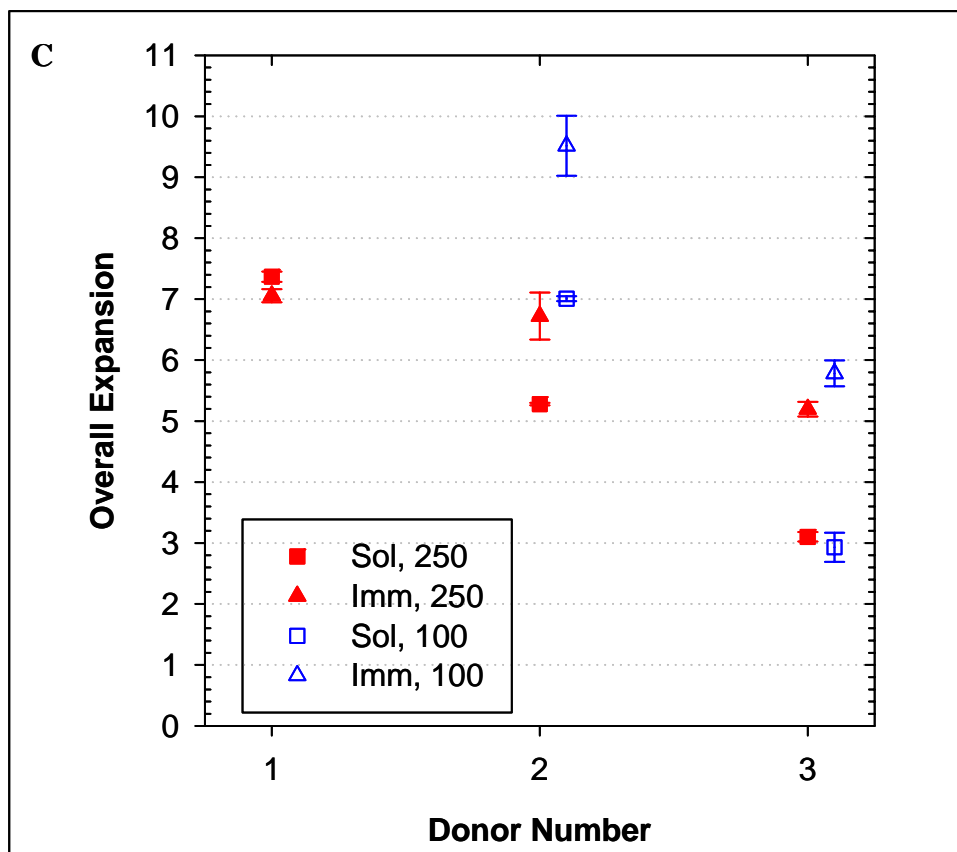
**Figure 6.3.4:** Number of total cells from a culture of mPB CD34+ selected cells.

Cells were cultured for 9 days with biotin-SCF immobilized on NA coated plates in the presence of 100 ng/mL FL and 50 ng/mL rhTPO. SCF was biotinylated with sulfo-NHS-LC-biotin at a BP ratio of 10 and immobilized at various concentrations (1  $\mu\text{g}/\text{ml}$  (1 ug), 10  $\mu\text{g}/\text{ml}$  (10 ug), 20  $\mu\text{g}/\text{ml}$  (20 ug), and 40  $\mu\text{g}/\text{ml}$  (40 ug)).

Controls were cultured on TCPS a NeutrAvidin-coated (NA-coated) surfaces with 100 ng/mL soluble SCF. Data shown are the average of two measurements taken from a single experiment.

**Figure 6.3.5:** Overall expansion of BM CD34+ selected cells. CD34+ cells from three BM samples were evaluated for overall fold expansion using soluble FL and rhTPO, and either soluble SCF (100 ng/mL; squares) or immobilized SCF (10 µg/mL; triangles). Overall expansion was evaluated at days 3 (**A**), 6 (**B**), and 9 (**C**) at the seeding densities of 250,000 cells/ml (filled) and 100,000 cells/ml (open; donor 2 and 3 only). Data points represent the mean  $\pm$  SEM of at least three measurements.





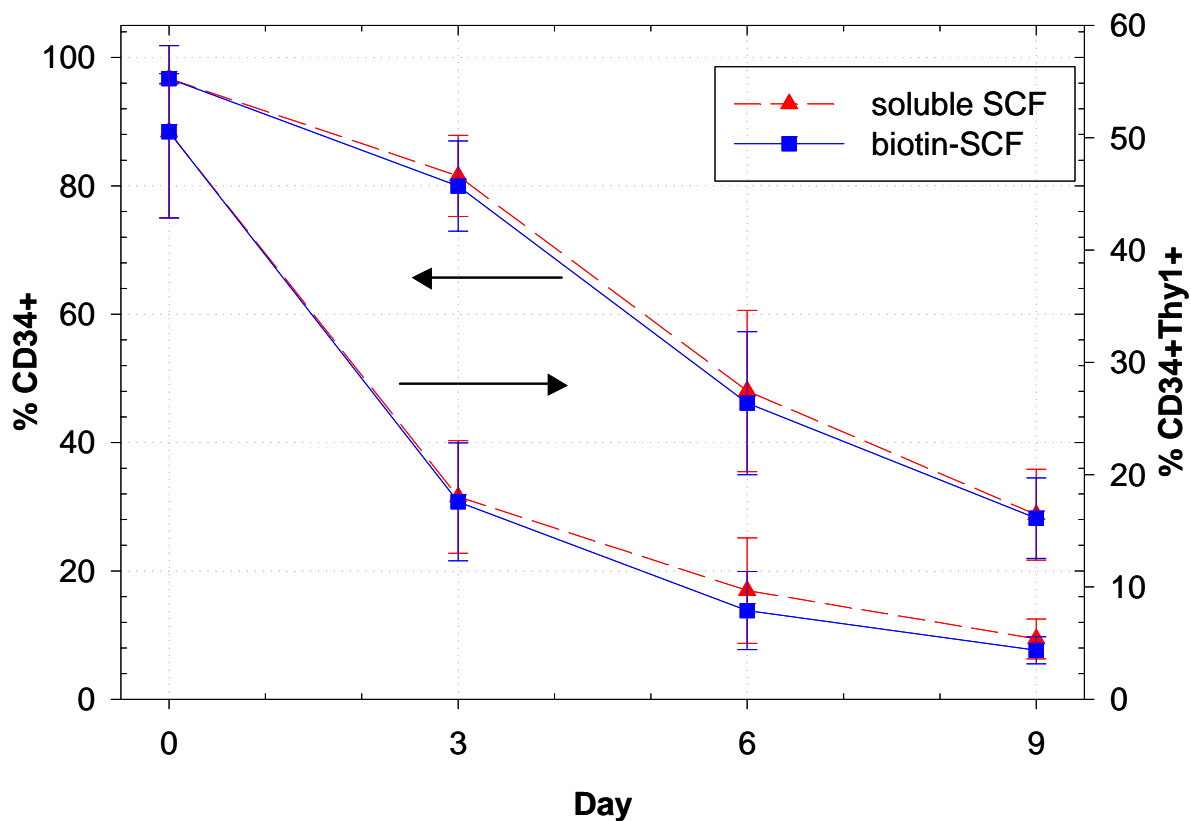
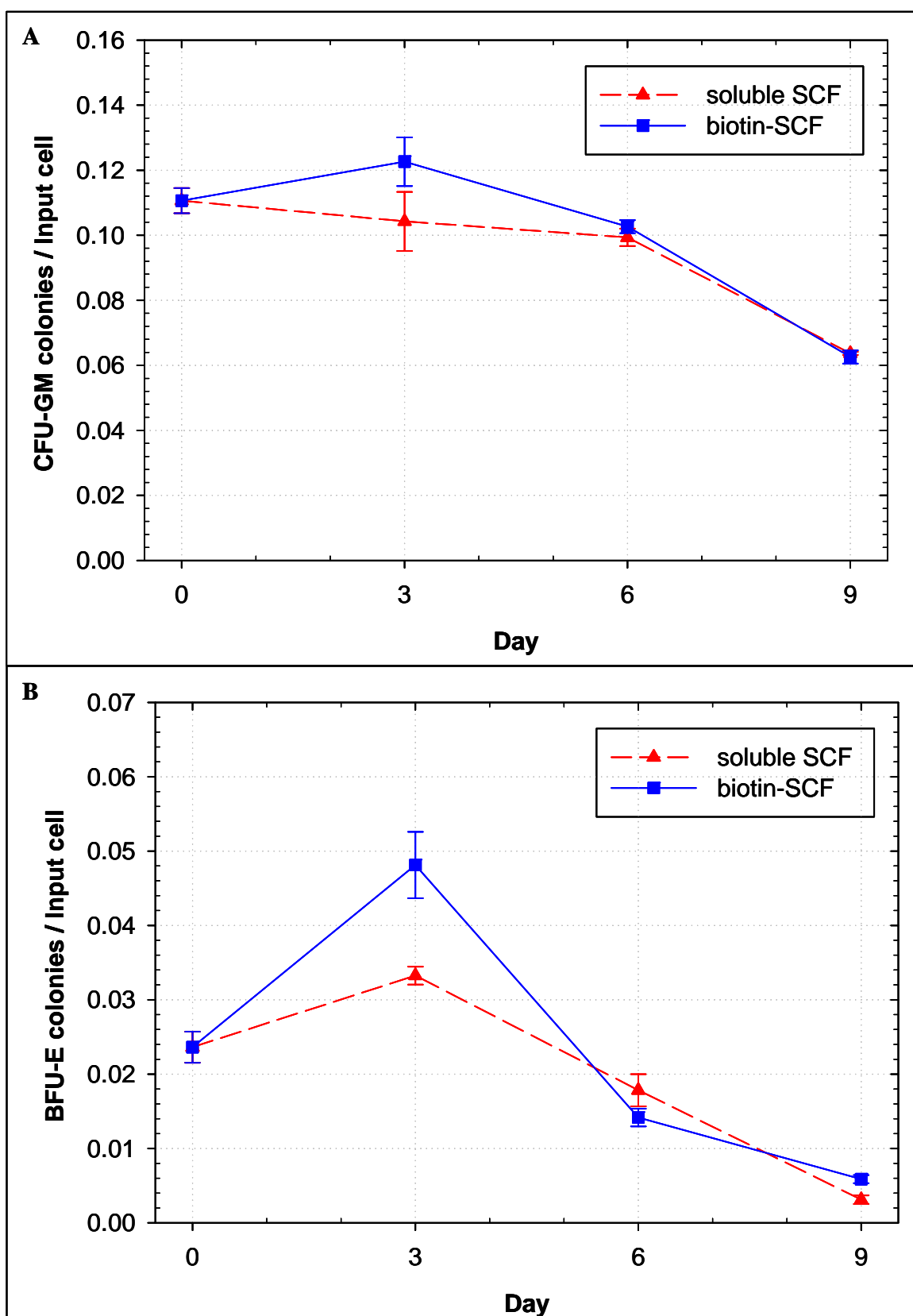


**Figure 6.3.6:** Percentage of CD34+ and CD34+Thy1+ cells from a culture of BM CD34+ selected cells seeded at 250,000 cells/mL. Cells were cultured for 9 days with biotin-SCF immobilized on NeutrAvidin-coated plates in the presence of 100 ng/mL FL and 50 ng/mL rhTPO. SCF was biotinylated with sulfo-NHS-LC-biotin at a BP ratio of 10 and immobilized at 10  $\mu$ g/ml (squares). Cells for controls were cultured on NeutrAvidin-coated surfaces with 100 ng/mL soluble SCF (triangles). Data shown are the average ( $\pm$  SEM) from an experiment representative of four

**Figure 6.3.7:** Number of CFU-GM (A) and BFU-E (B) per input cell. mPB CD34+ cells were cultured for nine days in the presence of FL (100 ng/mL) and TPO (50 ng/mL) on NeutrAvidin-coated surfaces with 100 ng/mL soluble SCF (triangles) or on biotin-SCF-modified NeutrAvidin-coated surfaces (immobilized with 10  $\mu$ g/mL biotin-SCF, squares). Data was calculated by dividing the number of colonies by the input number of cells: day 0 = 1000 cells, day 3 = 2000, day 6 = 3000, and day 9 = 6000. Data shown is the average  $\pm$  SEM of two replicates from an experiment representative two repeats.



#### **6.4 RESULTS FOR DOPA-PEG SURFACES FOR biotin-SCF PRESENTATION**

Due to the SCF release problems discussed in Section 6.3.3, a second culture system for the presentation of immobilized biotin-SCF was developed. This culture system employs poly(ethylene oxide) (PEG) molecules end-functionalized with the amino acid DOPA. DOPA is a major constituent of mussel adhesive proteins; a protein secreted by mussels to anchor to a variety of surfaces [217, 218]. DOPA provides for an adhesive moiety to attach PEG to surfaces in a defined orientation, thus giving the surface its characteristic non-fouling properties. This system was pioneered in Dr. Phil Messersmith's laboratory. On Au- or TiO<sub>2</sub>-coated surfaces, methoxy-terminated-PEG-DOPA<sub>3</sub> (2000 or 5000 MW PEG) molecules greatly reduced non-specific binding of protein and fibroblasts for up to 14 days in culture [171].

Functionalizing both ends of a PEG molecule—one end with three DOPA amino acids and the other with biotin—allows for binding of specific molecules within a background that resists non-specific adhesion. Through an avidin linkage we can bind biotin-SCF in a defined manner. Incorporating a small fraction of DOPA<sub>3</sub>PEG-biotin (DPb; PEG MW = 3400) within a background of DOPA<sub>3</sub>PEG (DP; PEG MW = 2000), we were able to combine the non-fouling nature of a PEG surface with specific presentation of immobilized SCF.

DOPA interacts strongly with TiO<sub>2</sub> [219, 220]. A thin layer of TiO<sub>2</sub> is easy to deposit onto planar surfaces via e<sup>-</sup> beam evaporation and glass microscope slides remain transparent when coated. For these reasons we used TiO<sub>2</sub>-coated microscope slides as the base for our cell culture cassettes. Cell culture cassettes were prepared in a manner similar to cassettes for lipid-based cultures.

#### 6.4.1 Synthesis of DOPA-PEG and DOPA-PEG-biotin

DP was synthesized by Dr. Zhongqiang Liu using a method developed by Dr. Bruce Lee, both from the Messersmith lab. In this synthesis, the amine terminus of methoxy-PEG (2000 MW)-NH<sub>2</sub> serves as an initiator of polymerization for diacetyl protected DOPA-*N*-carboxyanhydride (NCA). The initial molar ratio of DOPA to PEG is tailored for the incorporation of three DOPA amino acids per PEG molecule (Section 3.1.2, [221]). A schematic of DP is shown in Figure 3.1.2. Dr. Bruce Lee adapted the DP polymerization synthesis scheme to produce DPb (Section 3.1.4, [221]). To synthesize DPb, the terminal NHS group of biotin-PEG-NHS (3400 MW PEG) was first converted to a primary amine, which then can be used as a polymer-bound initiator for diacetyl protected DOPA-NCA polymerization. Similar to DP synthesis, the initial molar ratio of DOPA to PEG is tailored for the incorporation of three DOPA amino acids per PEG molecule. A schematic of DPb is shown in Figure 3.1.3.

#### 6.4.2 Characterization of DP and DPb surfaces

Dr. Rico Gunawan characterized different molar ratios of DPb and DP on surfaces formed on TiO<sub>2</sub>-coated surfaces using optical waveguide lightmode spectroscopy (OWLS). OWLS was used to test DPb and DP surfaces for their ability to resist non-specific protein adsorption and specific interaction with streptavidin. Non-specific adsorption of streptavidin was very low for surfaces coated with 100% DP ( $\sim 1 \text{ ng/cm}^2$ , DATA NOT SHOWN) and streptavidin binding to surfaces coated with 10% DPb was 40-fold greater than for DP (DATA NOT SHOWN) [221]. BSA adsorption to surfaces with increasing DPb content was also monitored to determine the level of non-specific adsorption to defect sites that may be present on the surfaces. BSA surface density tended to increase with increasing DPb content, but was very low for all DPb levels

(Figure 6.4.1). Moreover, adding BSA prior to incubation with NeutrAvidin did not alter the specificity or extent of NeutrAvidin binding to surface DPb (DATA NOT SHOWN). This confirmed that the surfaces were non-fouling even when DPb was incorporated.

Streptavidin surface concentration increased linearly with that of DPb (Figure 6.4.1). However, only about 0.1 mole of streptavidin bound per mole of DPb on the surface. This suggests that many of the biotin molecules are buried within the PEG layer and not accessible for binding streptavidin. The low level of streptavidin binding could also be due to preferential adsorption of DP (vs. DPb). However, the absorbance vs. temperature (25°C to 75°C) profiles in cloud point buffer were very similar for DPb, DP, and their mixtures (DATA NOT SHOWN). Thus, the 50°C deposition temperature should not promote closer packing or preferential adsorption of DP on the surface. The linear increase of streptavidin binding to surfaces with increasing DPb content was confirmed with ELISA using HRP-conjugated streptavidin. The ratio of  $0.14 \pm 0.02$  moles of streptavidin-HRP per mole of DPb obtained was similar to the molar ratio of  $0.08 \pm 0.05$  obtained for streptavidin via OWLS (DATA NOT SHOWN).

The dose-dependence of NeutrAvidin adsorption was similar to that for streptavidin (Figure 6.4.2 compared to Figure 6.4.1). The surface concentration of biotin-SCF adsorbed on NeutrAvidin increased linearly with DPb surface concentration and approximately 0.8 moles of biotin-SCF bound to each molecule of NeutrAvidin (Figure 6.4.2). The projected area of a single SCF dimer is  $27.84 \text{ nm}^2$  [116], while the projected area of streptavidin is  $24.75 \text{ nm}^2$  [168]. Thus, steric hindrance should limit the binding of biotin-SCF to NeutrAvidin.

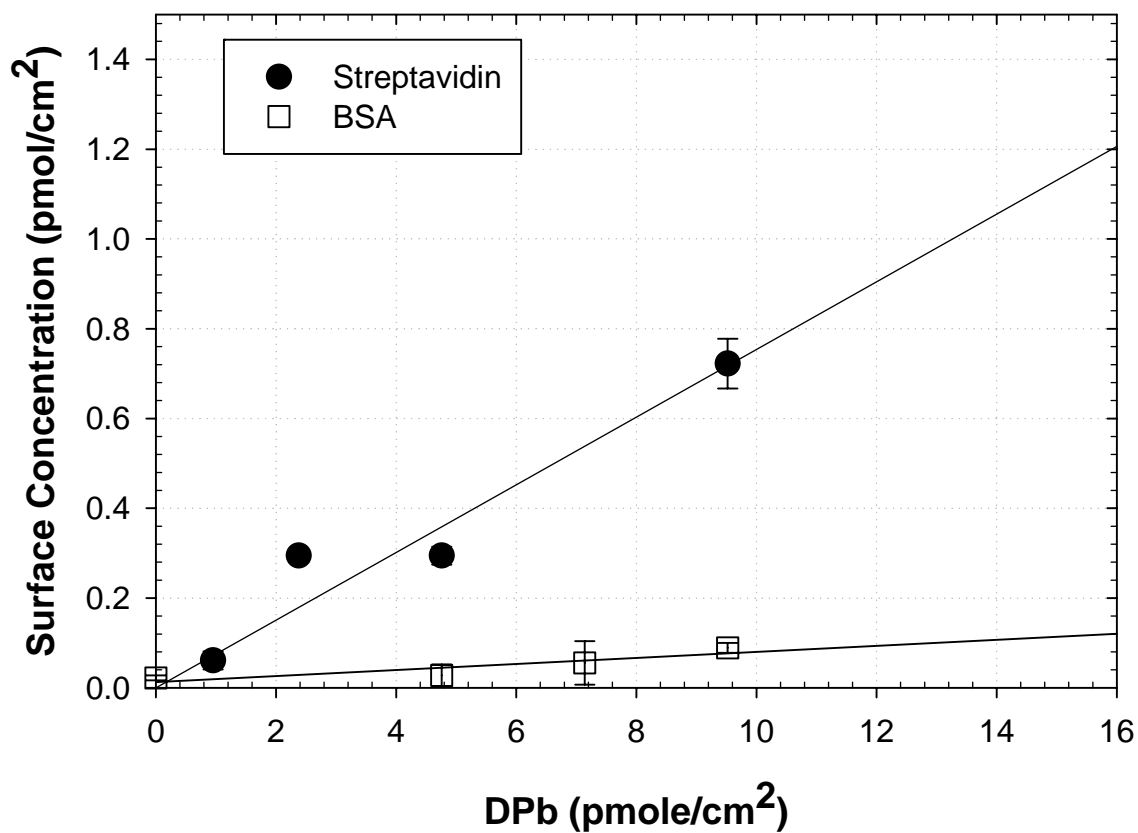


**Figure 6.4.1:** Streptavidin adsorption onto DPb/DP surfaces. OWLS was used to measure the increase in streptavidin (solid circles) and BSA (open squares) surface concentrations with increasing surface concentrations of DPb. Data are presented as the mean ( $\pm$  SD) of at least three experiments. 1 mol% DPb corresponds to a surface density of 0.9 pmole DPb/cm<sup>2</sup>. Data from Dr. Rico Gunawan's characterization of DPb surfaces [15].

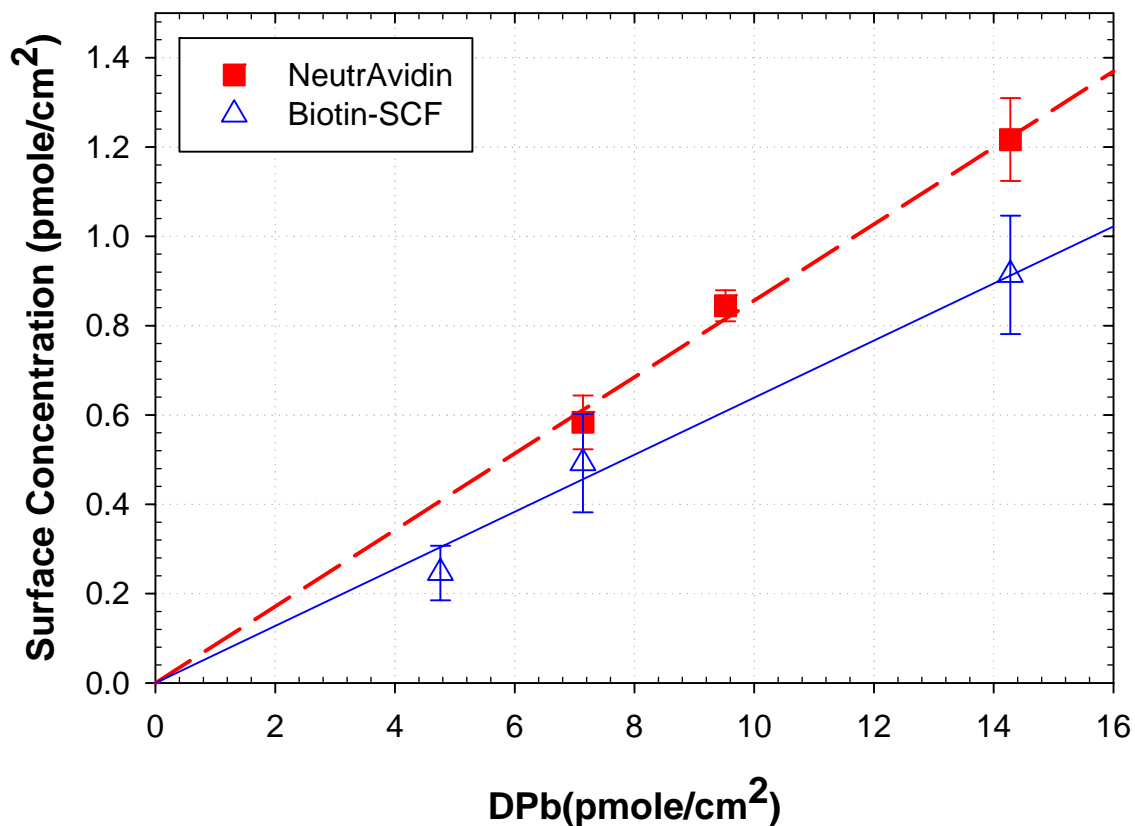


**Figure 6.4.2:** Sequential adsorption of NeutrAvidin (solid squares, dashed line) and biotin SCF (open triangles, solid line) molecules to DPb/DP-coated surfaces was monitored using OWLS. The surface concentrations of NeutrAvidin and biotin-SCF increased linearly with the DPb surface concentration. Data are presented as the mean  $\pm$  SD of three experiments. 1 mol% DPb corresponds to a surface density of 0.9 pmole DPb/cm<sup>2</sup>. Data from Dr. Rico Gunawan's characterization of DPb surfaces [15].

### 6.4.3 biotin-SCF Supports M07e Cell Adhesion and ERK Activation

The bioactivity of immobilized biotin-SCF was demonstrated using both M07e cell adhesion and activation of the ERK signaling pathway. Cells adhered to immobilized biotin-SCF in a DPb-dose-dependent manner (Figure 6.4.3). A plateau of 0.8 was reached between 2.5% and 5% DPb. Pre-incubating M07e cells with soluble SCF showed the specificity of the adhesion. In the pre-incubation step a saturating dose of SCF is used to occupy all available c-Kit molecules. After pre-incubation, the fraction of adherent M07e cells on biotin-SCF-modified 2.5% DPb surfaces was reduced from approximately 0.8 to 0.1 (Figure 6.4.4).

M07e cells simulated for 20 min with biotin-SCF exhibited a DPb-dose-dependent increase in the level of phosphorylated ERK1,2 (pERK) as the surface DPb content was increased from 0% to 1% (Figure 6.4.5). However, pERK levels did not increase further when the DPb content was increased to 2.5%. Thus, the plateau for ERK1,2 activation occurred at a much lower DPb content than that for cell binding. Stimulation of M07e cells with unbiotinylated soluble SCF in control TCPS well plates resulted in a similar level of ERK 1,2 activation for an equivalent amount of total SCF, up to 0.5 ng/well (Figure 6.4.6). Activation of ERK 1,2 with soluble SCF plateaued at a slightly increased level compared to immobilized biotin-SCF, although this increase was not statistically significant ( $p = 0.114$ ).

The activation of STAT5 by DPb-biotin-SCF surfaces was also evaluated using M07e cells. We previously documented that SCF does not induce phosphorylation of STAT5 in M07e cells by itself (Figure 5.2.10), so the fact that biotin-SCF-modified DPb surfaces did not elicit upregulation of pSTAT5 is not surprising (DATA NOT SHOWN). Studies from Drayer et al.

confirm that M07e cells do not phosphorylate STAT5 when stimulated with SCF, but synergistically enhance TPO-mediated STAT5 activation [222].

It should be noted that in order to observe a DPb-dose-dependent increase in ERK phosphorylation, a blocking step before NeutrAvidin addition was necessary. Despite this pre-blocking step, activation induced by DP surfaces treated with NeutrAvidin and biotin-SCF was significantly increased compared to untreated surfaces ( $p < 0.001$ , Figure 6.4.5). The fact that there was no difference in the adhesion assay for treated and untreated DP surfaces suggests that elevated signaling on treated surfaces was due to non-specific binding of biotin-SCF, perhaps to the edges of the wells. Unstimulated control cells 'activated' on DP surfaces not treated with NeutrAvidin/biotin-SCF show similar pERK levels as unstimulated TCPS controls ( $p = 0.433$ , Figure 6.4.4). Pre-blocking cassettes uppers with DOPA<sub>x</sub>Lys<sub>y</sub>-PEG (2000 MW PEG) did not significantly alter the level of activation seen in treated vs. untreated cassettes (DATA NOT SHOWN).

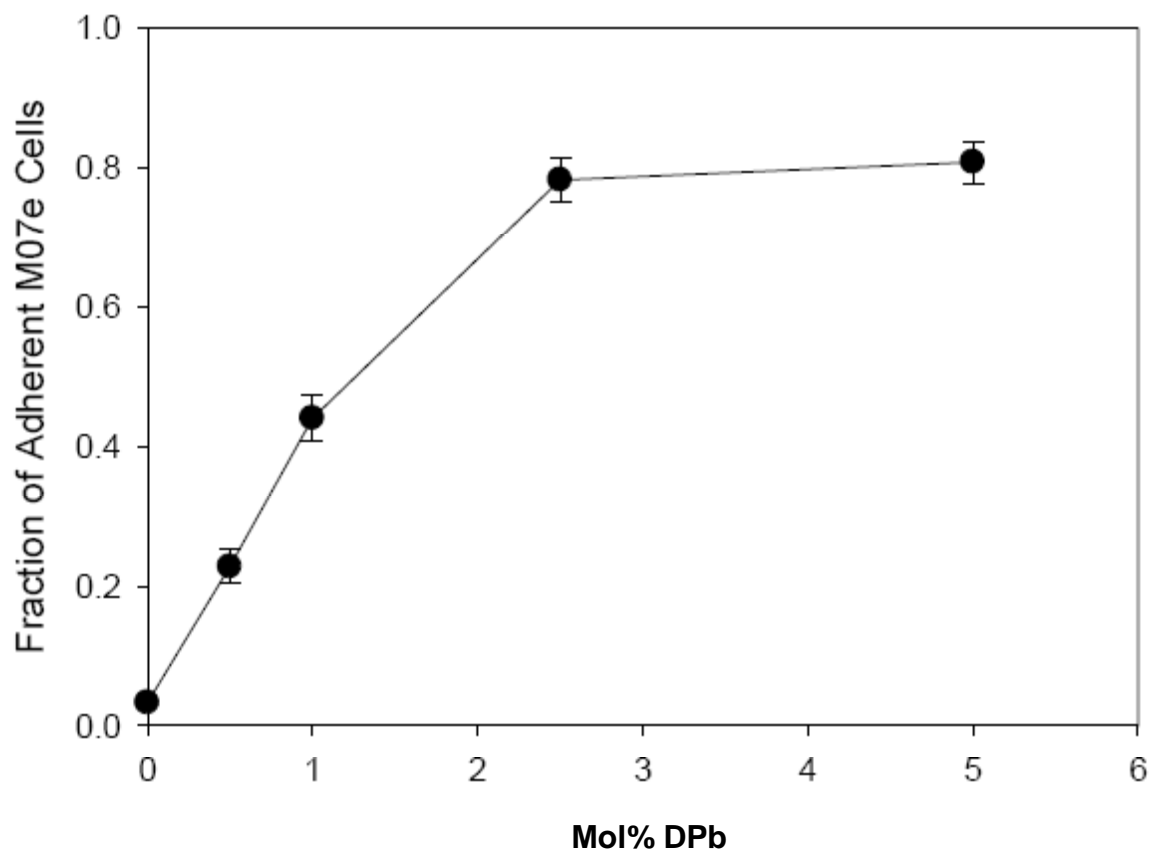


**Figure 6.4.3:** Fraction of M07e cells adherent to biotin-SCF- modified DPb surfaces.

Exponentially growing M07e cells were stained with CFSE or Calcein AM and the adhesion assay performed as described in Section 3.4.2 on surfaces with various concentrations of DPb. To determine the fraction of adherent cells, Metamorph software was used to count the number of cells in each image before and after non-adherent cell removal via normal-force centrifugation. The fraction of adherent cells was calculated by dividing the number of cells in the post-centrifugation images by the number of cells in the pre-centrifugation images. Data shown are the average ( $\pm$  SEM) of at least 18 replicate wells from six separate experiments.

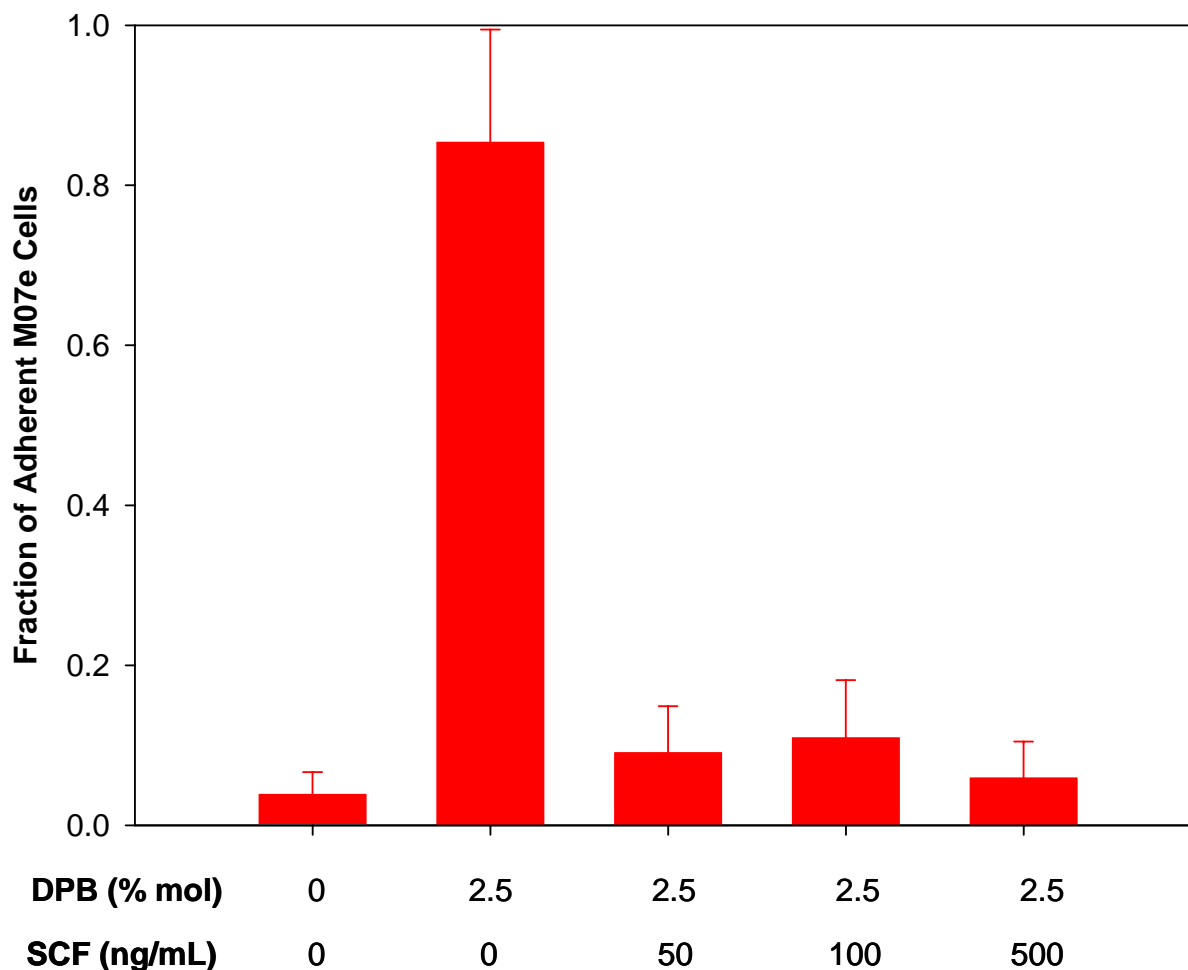


**Figure 6.4.4:** Fraction of M07e cells adherent to to biotin-SCF-modified DPb surfaces.

Exponentially growing M07e cells were stained with CFSE or Calcein AM and pre-incubated with various concentrations of SCF. The cells were used to perform an adhesion assay on surfaces with 2.5% DPb. To determine the fraction of adherent cells, Metamorph software was used to count the number of cells in each image before and after non-adherent cell removal via normal force centrifugation. The fraction of adherent cells was calculated by dividing the number of cells in the post-centrifugation images by the number of cells in the pre-centrifugation images. Data are the average ( $\pm$  SEM) from an experiment representative three repeats.

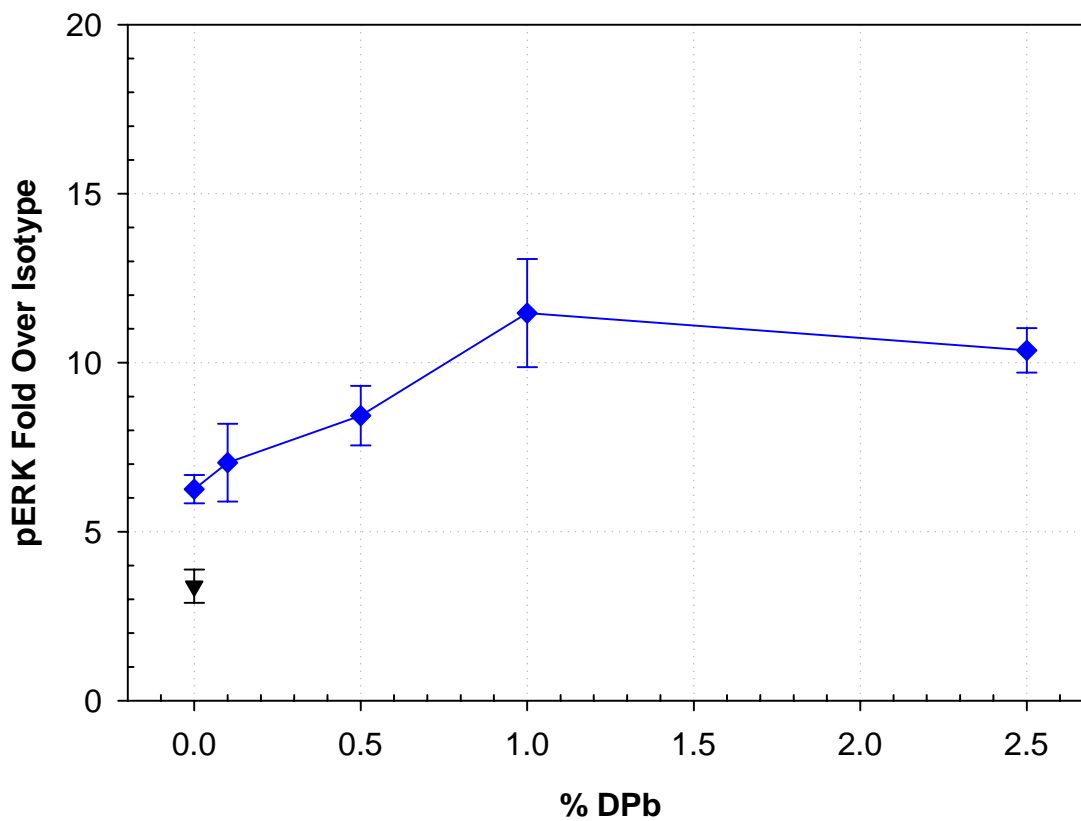
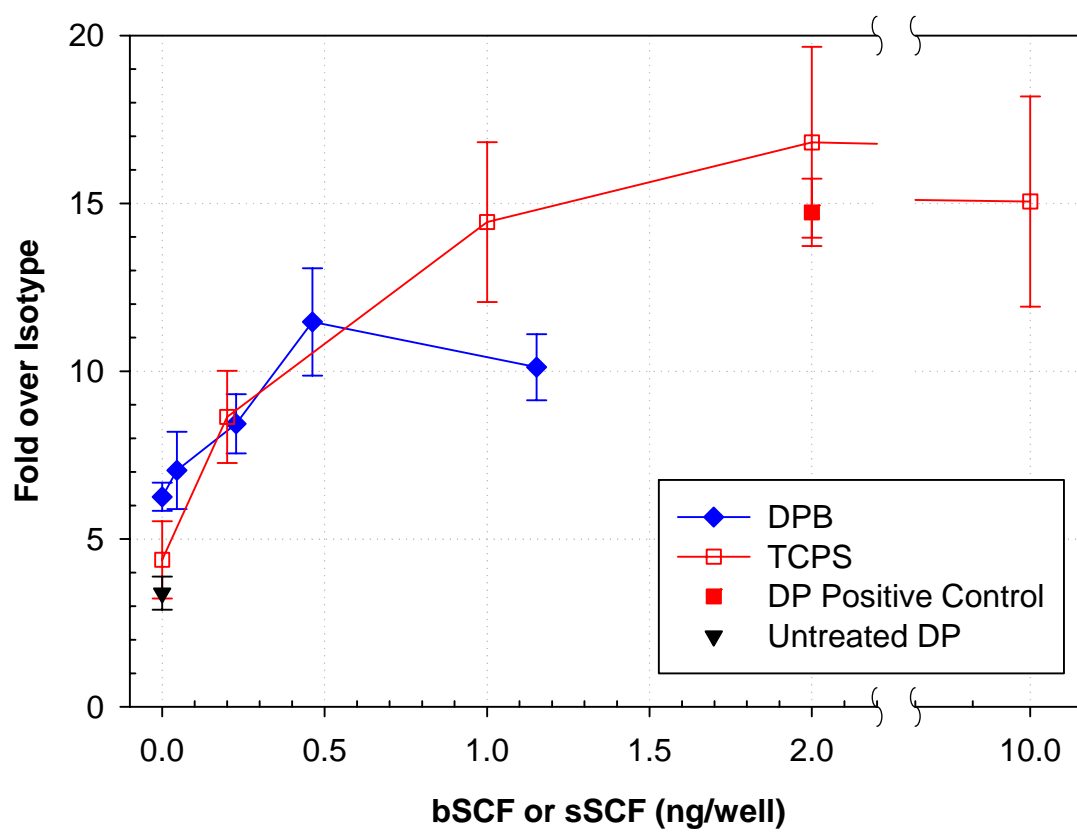


**Figure 6.4.5:** Activation of ERK 1,2 in M07e cells stimulated on biotin-SCF-modified DPb surfaces. M07e cells were starved overnight and stimulated in serum-containing media (IMDM + 2.5% FBS) for 20 minutes followed by processing according to the cell-signaling protocol (Section 3.4.1.5). A DP surface not treated with NA and biotin-SCF was used as an additional negative control (filled inverted triangle). Data presented is the mean  $\pm$  SEM of six activation experiments.

**Figure 6.4.6:** Activation of ERK 1,2 in M07e cells stimulated on biotin-SCF-modified DPb surfaces (filled diamond) and on TCPS control surfaces (open squares) with various amounts of SCF. M07e cells were starved overnight and stimulated in serum-containing media (IMDM + 2.5% FBS) for 20 minutes followed by processing according to the cell-signaling protocol (Section 3.4.1.5). DP controls included a positive control with 10 ng/mL soluble SCF on DP surface (filled square) and a DP surface that was not treated with NA or biotin-SCF (filled inverted triangle). Data for DPb and untreated control are shown in Figure 6.4.5 and re-plotted here with a different x-axis. The ng/well for DPb surfaces were calculated using results from OWLS data (Figure 6.4.2) and ng/well for TCPS surfaces were calculated using the soluble concentration and the medium volume within the well. Data presented represent the mean  $\pm$  SEM of six activation experiments.

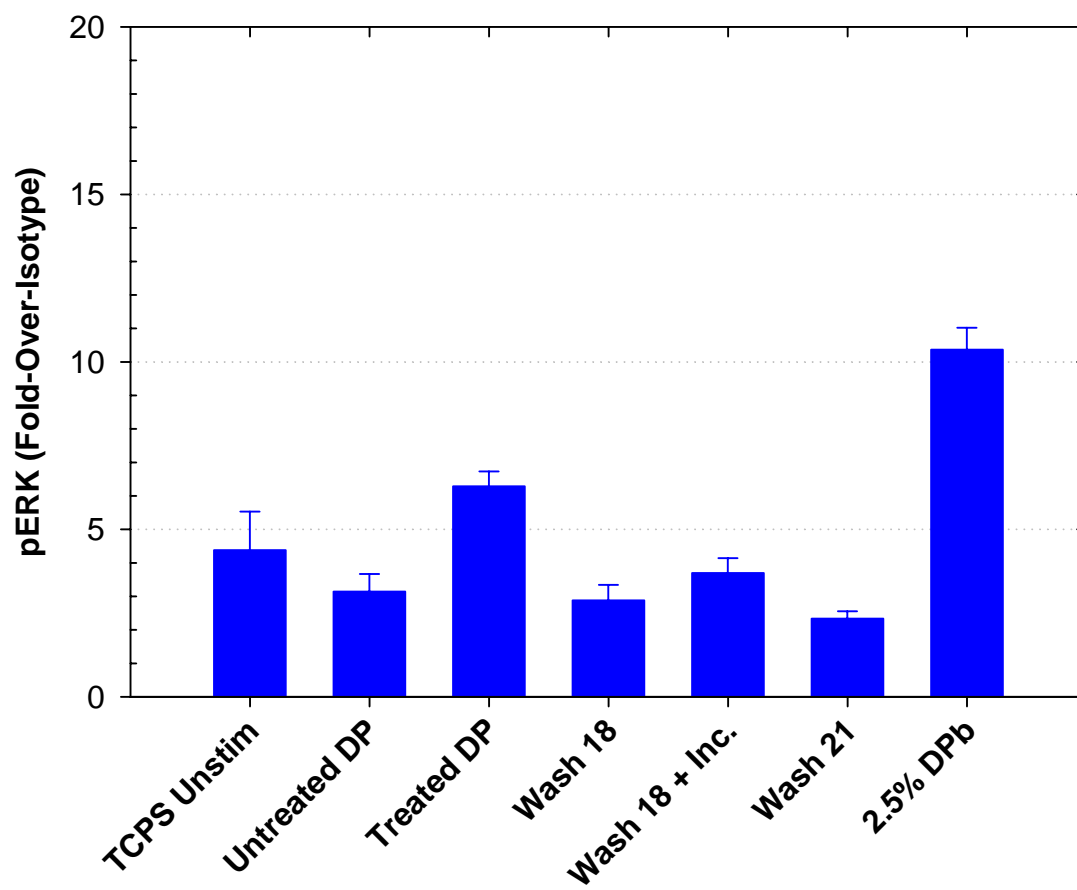


#### **6.4.4 Release of biotin-SCF from DPb surfaces**

##### ***6.4.4.1 Release of biotin-SCF from DPb surfaces analyzed by cell signaling assays***

To test for possible release of biotin-SCF from DPb surfaces we performed activation experiments to analyze medium conditioned with biotin-SCF-DPb surfaces. Surfaces were prepared normally (Section 3.2.5 and 3.2.6) and conditioned medium was collected similarly to that for release studies with TPOm lipopeptides (Section 5.2.2.5): after the final dilution rinse with media (wash 18); after a 20-minute incubation in a humidified, 5% CO<sub>2</sub> incubator at 37° C (wash 18 + incubation); and after an additional three washes (wash 21). A small amount of biotin-SCF was released during the 20-minute incubation time (Figure 6.4.7). However, the level of activation from the released material was significantly less than the activation seen on DP surfaces treated with NeutrAvidin and biotin-SCF. This indicates that material released during the 20 minute incubation was likely due to non-specific adsorption. Importantly, the surfaces induced significantly greater activation than the released material ( $p < 0.001$ ).

**Figure 6.4.7:** ERK 1,2 activation in M07e cells by supernatants removed from 2.5% DPb surfaces. M07e cells were starved overnight and stimulated in serum-containing media (IMDM + 2.5% FBS) for 20 minutes followed by processing according to the cell-signaling protocol (Section 3.4.1.5). Supernatants were collected from surfaces prepared normally (Section 3.2.5 and 3.2.6) by 15 dilution rinses with PBS/1% BSA/0.05% Tween-20 and three dilution rinses with equilibrated serum-containing media. After the final media wash, the top 150 mL of the supernatant was collected, and saved in a TCPS well plate (wash 18). Fresh media was added back to the sampled wells, and the surfaces were incubated for 20 minutes in a humidified, 5% CO<sub>2</sub> incubator at 37° C. After the incubation, the top 150 mL of the supernatant was collected (wash 18 + incubation) and surfaces were rinsed with media three additional times. The final rinse was followed by a final supernatant collection (wash 21). Data for 2.5% DPb are from surfaces after wash 21. Data for TCPS Unstim, Untreated DP, and Treated DP are subset of the data shown in Figure 6.4.3, performed on the same days as the release studies. The average ( $\pm$  SEM) of at least 9 total wells from a four experiments are shown.



#### ***6.4.4.2 Release of biotin-SCF from DPb surfaces analyzed by cultures with conditioned media***

We also directly tested the possibility of biotin-SCF releasing from DPb surfaces by culturing M07e cells in media conditioned by overnight incubation on DPb surfaces modified with biotin-SCF. This experiment was designed to replicate the conditioned media experiments performed with commercially available NeutrAvidin-coated plates (Section 6.3.3). For this experiment, biotin-SCF surfaces were prepared under standard procedures for preparing sterile surfaces (Section 3.2.6). UV-sterilized cassette assembled with TiO<sub>2</sub>-coated glass were modified overnight with a 0.22- $\mu$ m-filtered solution of 2.5% DPb in DP at 50°C. The DPb surfaces and upper portions of the cassette were blocked with a sterile solution of 1% BSA in PBS, followed by treatment with 100  $\mu$ L of a 0.1 mg/mL solution of NeutrAvidin and subsequent addition of 50  $\mu$ L of a 0.01 mg/mL solution biotin-SCF. The wells were rinsed under standard procedures (Section 3.2.6) with 15 dilution washes of PBS and three dilution rinses with StemPro 34 media. After the final rinse, the wells were incubated overnight on the biotin-SCF-modified DPb surfaces. Media from biotin-SCF-modified surfaces were collected and used at full strength or diluted in serum-free StemPro 34 media conditioned overnight by incubation on DP surfaces for the six-day expansion of factor-starved M07e cells in TPCS wells. As a control, M07e cells were also cultured on the biotin-SCF-modified surfaces that were used to prepare the conditioned media.

Similar to the experiment with commercially available NeutrAvidin-coated surfaces, undiluted conditioned media supported greater M07e cell growth than a positive controls (Figure 6.4.8). Growth stimulated by undiluted conditioned media from biotin-SCF modified surfaces significantly enhanced M07e cell expansion as compared to medium (conditioned by DP

surfaces) supplemented with 5 ng/mL SCF ( $p = 0.005$  at 146 hours). Undiluted conditioned media from biotin-SCF modified surfaces also induced greater expansion than that on 2.5% DPb surfaces ( $p = 0.043$  at 146 hours). Despite the release of material, surfaces remained bioactive, stimulating similar expansion after 103 hours of culture ( $p = 0.476$ ) and greater expansion after 146 hours ( $p = 0.009$ ) as compared to the positive control.

Control cultures simulated with soluble SCF were performed concurrently with the conditioned media experiment. The expansion of M07e cells for different levels of soluble SCF stimulation were compared on TCPS and DP surfaces (Figure 6.4.9). For similar concentrations of SCF, M07e cell expansion was similar in TCPS wells and on DP surfaces, providing further validation that DP surfaces are biocompatible. M07e cell expansion on 2.5% DPb surfaces (as shown in Figure 6.4.8) was similar to expansion with 5 ng/mL soluble SCF for the first 103 hours. After 103 hours expansion continued at a similar rate on 2.5% DPb surfaces, while cells stimulated with soluble SCF reached a plateau at 103 hours. This is similar to what was seen with the positive control for the conditioned media experiment (Figure 6.4.12), and indicates that SCF was depleted.

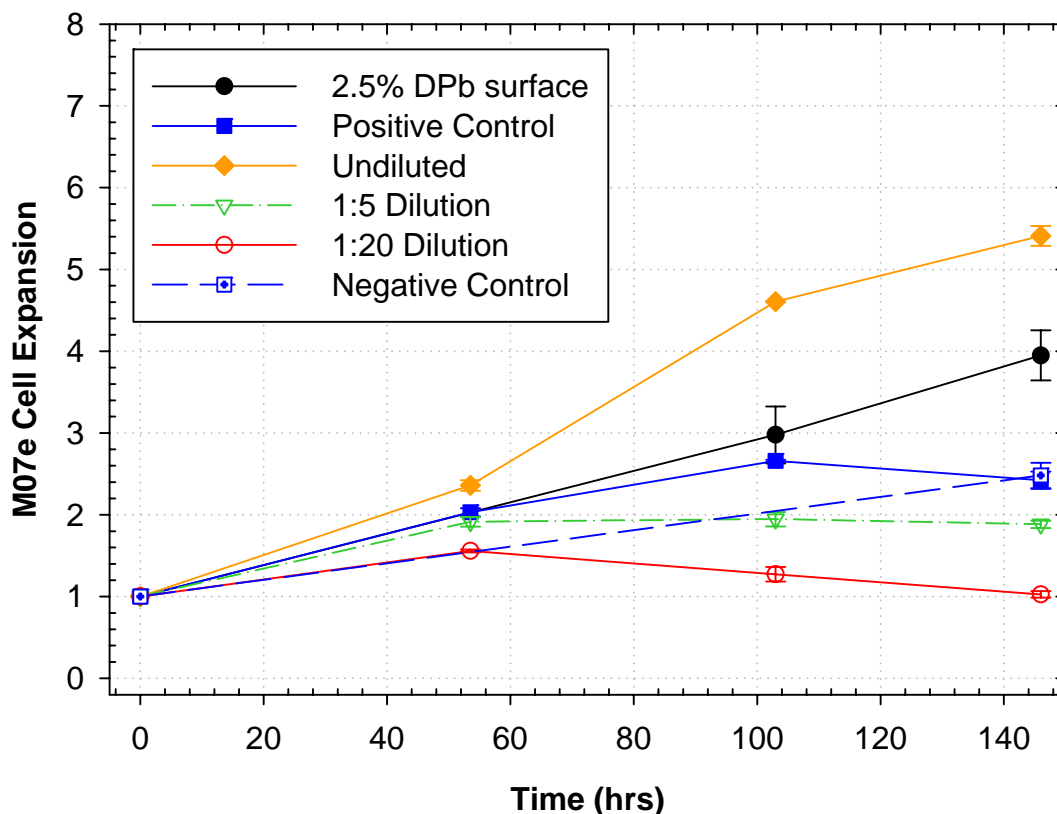
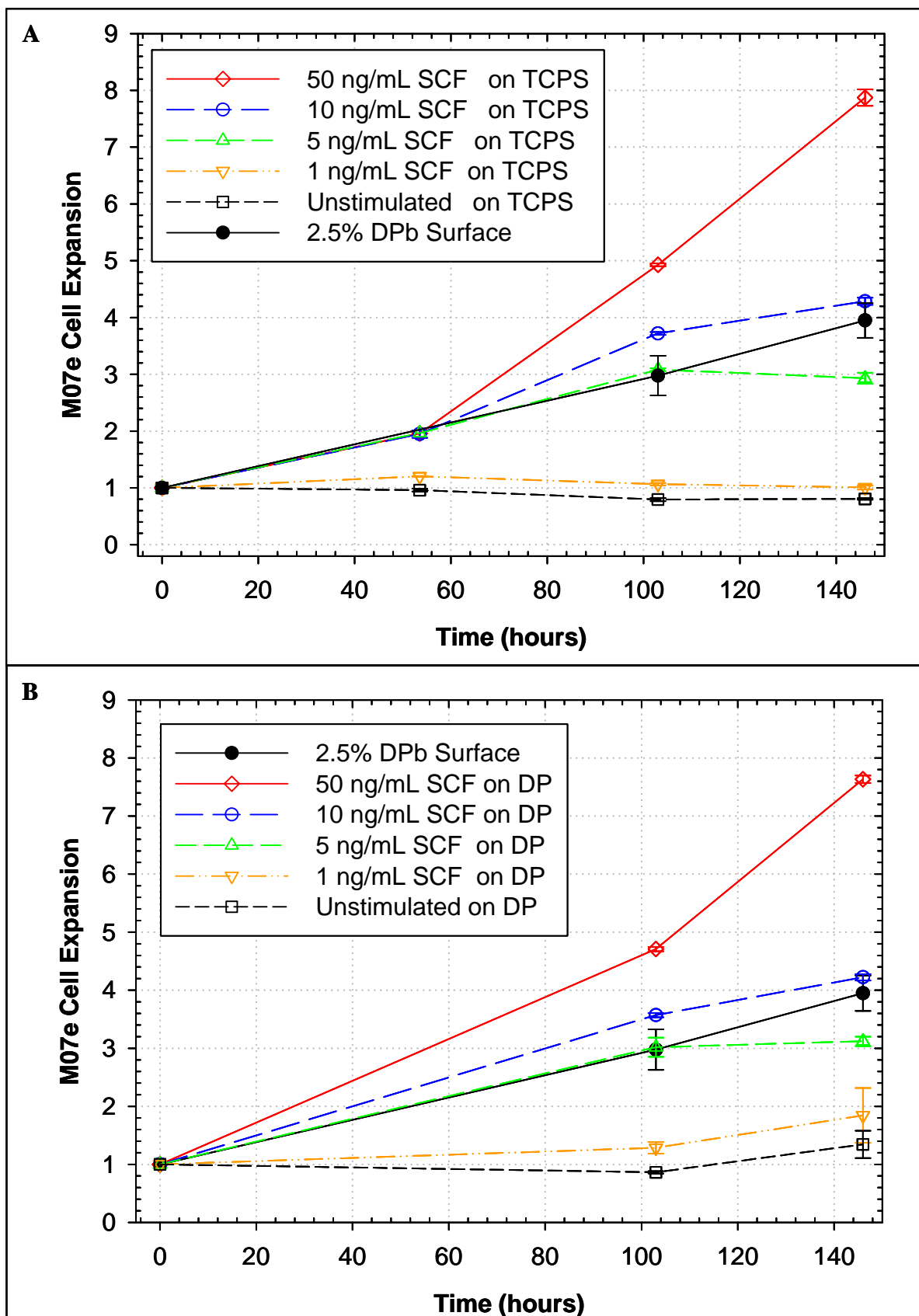


**Figure 6.4.8:** Biotin-SCF released from DPb surfaces. Biotin-SCF was immobilized at 0.01 mg/mL on NeutrAvidin-modified 2.5% DPb surfaces and washed under standard procedures (Section 3.2.6). StemPro 34 media was conditioned by overnight incubation on the biotin-SCF-modified surfaces. Media from biotin-SCF coated wells was collected, then used undiluted (filled diamonds) or diluted at 1 part to 5 parts (inverted triangles), or 1:20 (open circles) with media conditioned overnight on DP surfaces to stimulate M07e cell expansion on TCPS plates. Positive (filled squares) and negative (open squares) controls are StemPro 34 conditioned overnight on DP surfaces with or without the addition of 5 ng/mL soluble SCF. Cells were also cultured on the biotin-SCF-modified surfaces that was used to prepare the conditioned media. Results are the average ( $\pm$  SEM) for triplicate wells in a single experiment.

**Figure 6.4.9:** Dose response for M07e cell expansion in TCPS wells (A) and on DP surfaces (B). Exponentially growing M07e cells were starved overnight and stimulated in StemPro 34 media with different concentration of soluble SCF: 50 ng/mL SCF (open diamonds, solid line), 10 ng/mL SCF (open diamonds, dashed line), 5 ng/mL SCF (open triangles), or 1 ng/mL SCF (inverted, open triangles with dash-dot-dot line). A negative control was comprised of starved M07e cells cultured in StemPro 34 in the absence of additional growth factors (Unstimulated, open squares). M07e cells cultured on 2.5% DPb surface (same data as Figure 6.4.12) are shown for comparison. Data are the average ( $\pm$  SEM) of at least three replicates from a single experiment.



#### 6.4.5 CD34<sup>+</sup> cell cultures on DP and DPb-NeutrAvidin-biotin-SCF surfaces

We hypothesized that presenting HSCs with immobilized SCF would enhance overall expansion and maintenance of CD34<sup>+</sup> and CD34<sup>+</sup>Thy1<sup>+</sup> cells. Primary CD34<sup>+</sup> cells are very sensitive to their culture environment [205], so we first compared overall expansion and retention of CD34<sup>+</sup> and CD34<sup>+</sup>Thy1<sup>+</sup> cells on DP surfaces with those on TCPS control surfaces. Frozen mPB CD34<sup>+</sup> selected cells were seeded in serum-free StemPro 34 media with a cytokine cocktail of 100 ng/mL soluble SCF, 100 ng/mL FL, 50 ng/mL TPO, 10 ng/mL IL-3. Prior to DP modification, TiO<sub>2</sub> surfaces were sterilized by 30 minute exposure to 254 nm UV light. All subsequent treatments of the surfaces were done with sterile technique and all solutions were 0.22- $\mu$ m-filtered to maintain sterility of the surfaces.

Overall cell expansion on DP surfaces followed similar trends as on TCPS, albeit with lower overall expansion (day 4  $p = 0.06$ ; day 6  $p = 0.003$ , Figure 6.4.10A). Cultures on DP and TCPS surfaces also had similar percentages of CD34<sup>+</sup> cells up to day four, but TCPS surface had a significantly higher percentage of CD34<sup>+</sup> cells on day 6 (Figure 6.4.10B). The greater overall expansion and percent CD34<sup>+</sup> cells on TCPS surfaces resulted in significantly greater CD34<sup>+</sup> cell expansion on TCPS as compared to DP surfaces (Figure 6.4.10C). DP and TCPS surfaces had similar percent CD34<sup>+</sup>Thy1<sup>+</sup> cells (Figure 6.4.10B), but decreased overall expansion on DP surfaces resulted in a somewhat smaller number of CD34<sup>+</sup>Thy1<sup>+</sup> cells compared to TPCS (Figure 6.4.10C).

The similar trends in cultures of mPB CD34<sup>+</sup> cells on DP surfaces and TCPS controls gave further indication that DPb surfaces are potentially suitable for culture with primary CD34<sup>+</sup> cells. However, in two cultures with similar DPb surfaces with immobilized biotin-SCF, frozen

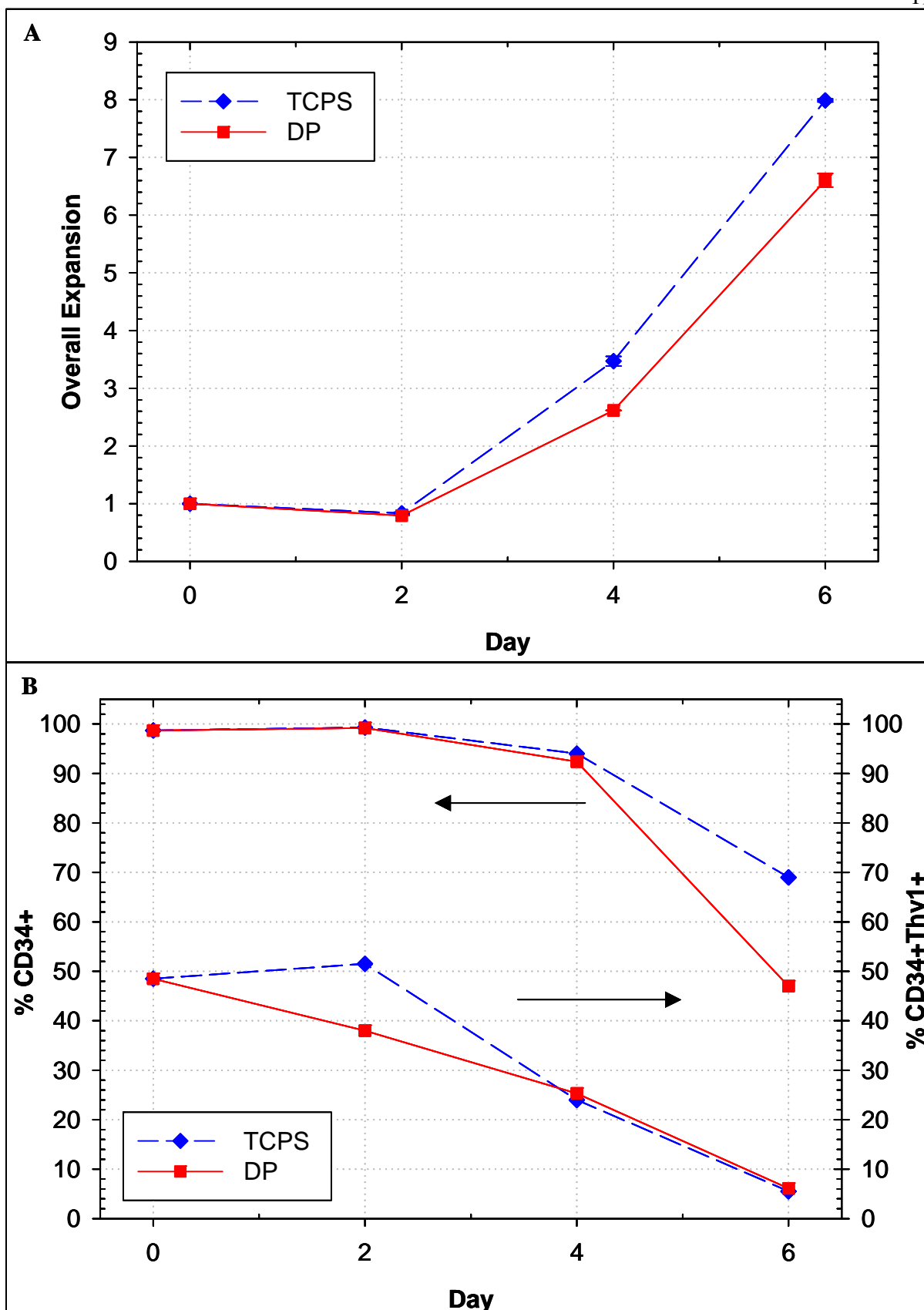
mPB CD34<sup>+</sup> cells showed no overall cell expansion (Figure 6.4.11). Cells were seeded in serum-free StemPro 34 media with a cytokine cocktail of 100 ng/mL FL, 50 ng/mL TPO, and 10 ng/mL IL-3. SCF was provided to the cells via biotin-SCF-modified DPb surfaces or controls with 100 ng/mL soluble SCF. DP surfaces not treated with NeutrAvidin or biotin-SCF showed similar expansion as TCPS controls. In these experiments, preparation of the DP surfaces was similar to DPb surfaces, including similar sterilization, dilution rinses, and media.

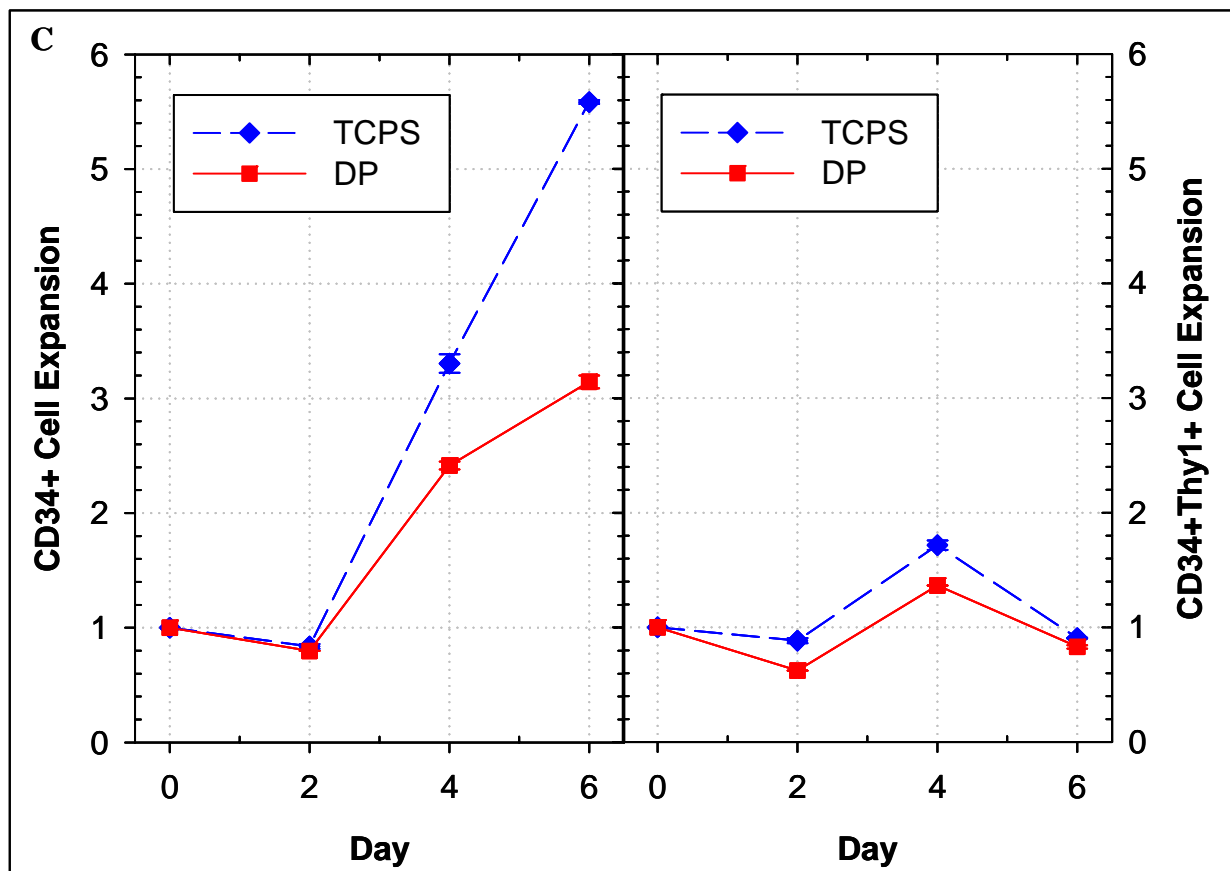
In a second set of experiments, M07e cells were used as a control to evaluate the effects of DP and DPb surfaces. M07e cells cultured on DP surfaces stimulated with 10 ng/mL soluble SCF showed a significant increase in six-day cell expansion as compared to M07e cells cultured on 2.5% DPb modified with biotin-SCF (Figure 6.4.12). While the results were not conclusive, they suggested that either NeutrAvidin or biotin-SCF limited cultures on DPb surfaces.

A follow-up experiment was conducted to test the possible influence of NeutrAvidin and SCF biotinylation on M07e cell expansion. The six-day expansion of M07e cells in TCPS plates was compared for 50 ng/mL soluble SCF, 50 ng/mL soluble biotin-SCF, and 50 ng/mL soluble SCF supplemented with a final concentration of 0.1 mg/mL NeutrAvidin. Comparison of expansion from cultures stimulated by soluble biotin-SCF to soluble SCF should reveal if the biotinylation reaction introduced compounds that negatively regulate cell expansion, but cannot be used for direct analysis of the effect of biotinylation since only 25% of the SCF is biotinylated. The level of NeutrAvidin was selected as a 'worst-case' scenario as this is the concentration used to modify DPb surfaces. Because of the excessive dilution rinses after the addition of NeutrAvidin to DPb surfaces, the number of molecules in wells modified by 100  $\mu$ L of 0.1 mg/mL NeutrAvidin would be much less than the number of molecules per well with this

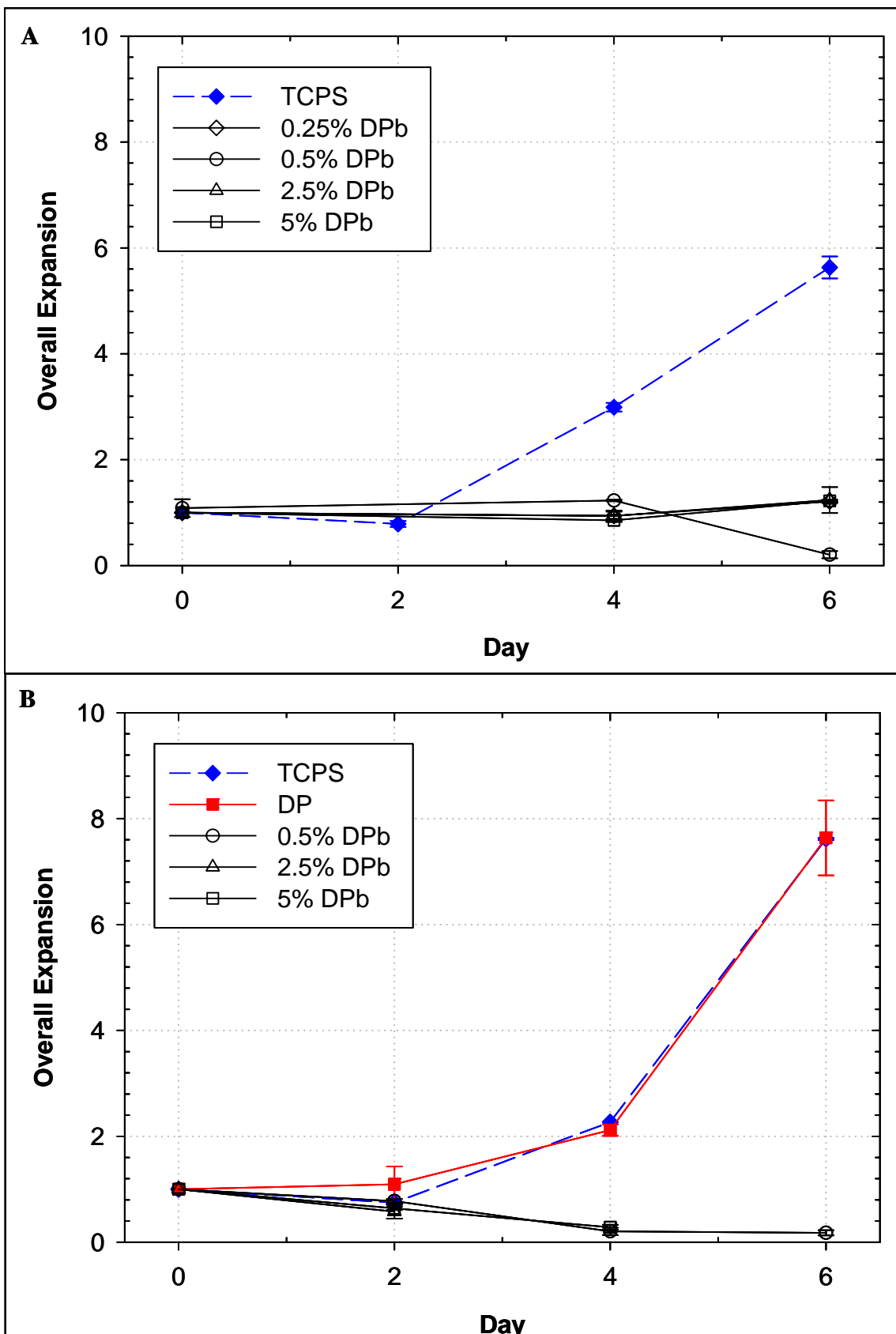
test concentration. M07e cell expansion with SCF was significantly enhanced as compared to biotin-SCF ( $p = 0.003$  at 151 hours) and SCF with soluble NeutrAvidin ( $p < 0.001$  at 151 hours) (Figure 6.4.13). The expansion seen with SCF supplemented with NeutrAvidin was decreased to a level similar to 10 ng/mL soluble SCF ( $p = 0.11$  at 151 hours). This supports the hypothesis that NeutrAvidin is sequestering biotin from the media, thus decreasing cellular expansion. This could be a possible explanation for the poor results seen with primary cell cultures on DPb surfaces. Others within our lab group are currently investigating this hypothesis with NeutrAvidin concentrations similar to those on DPb surfaces. Due to the residual unbiotinylated SCF with biotin-SCF, no conclusive agreements can be made for or against the presence of negatively regulatory molecules or decreased bioactivity due to the biotinylation process.

**Figure 6.4.10:** Expansion and differentiation of mPB CD34<sup>+</sup> selected cells. CD34<sup>+</sup> cells were seeded in StemPro 34 media with 100 ng/mL SCF, 100 ng/mL FL, 50 ng/mL TPO, and 10 ng/mL IL-3. Cells were cultured for six days and evaluated for overall fold-expansion (**A**), percentage of CD34<sup>+</sup> and CD34<sup>+</sup>Thy1<sup>+</sup> cells (**B**), and the expansion of CD34<sup>+</sup> and CD34<sup>+</sup>Thy1<sup>+</sup> cells (**C**) on DP surfaces (filled squares) and in TCPS wells (filled diamonds, dashed line).





**Figure 6.4.11:** Overall expansion for two separate mPB CD34+ selected cell samples on surfaces with various concentrations of DPb modified with biotin-SCF. Cells were seeded in StemPro 34 media with 100 ng/mL FL, 50 ng/mL TPO, and 10 ng/mL IL-3. Data shown is the average  $\pm$  SEM of replicate measurements from two separate experiments.



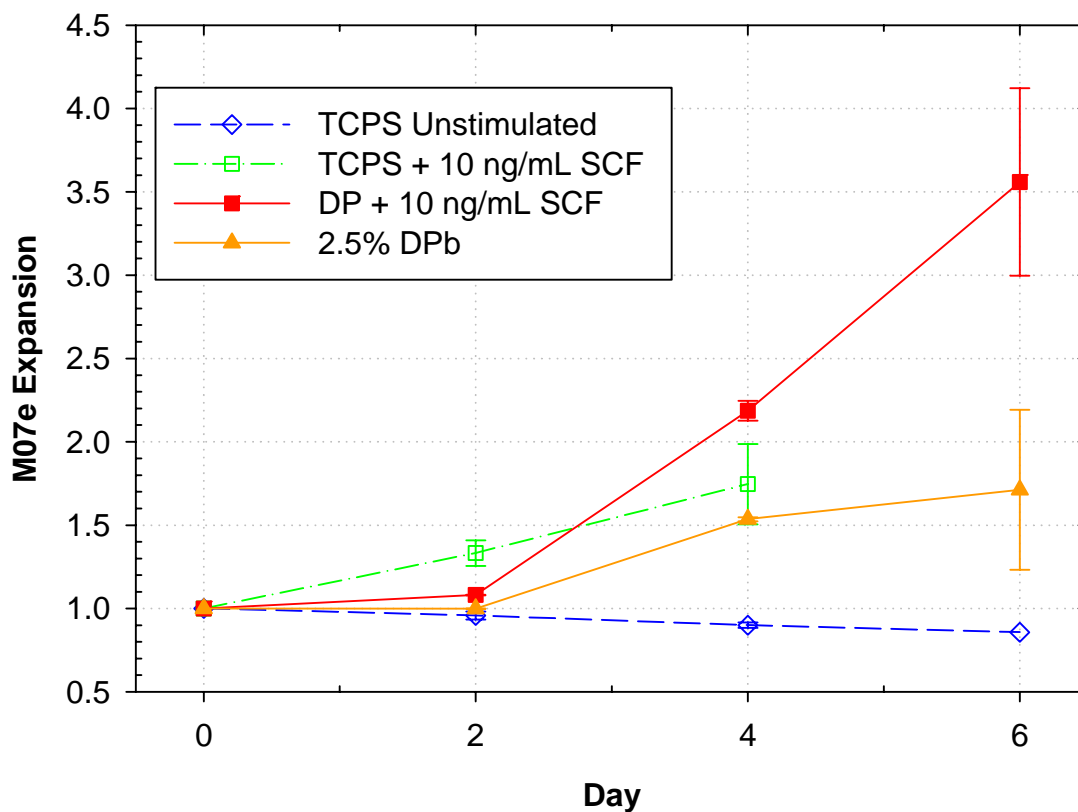


**Figure 6.4.12:** Six-day M07e cell expansion on DPb, DP, and TCPS surfaces. M07e cells were starved overnight and seeded into wells with different methods of SCF presentation: biotin-SCF-modified 2.5% DPb surfaces (filled triangles), DP surfaces with 10 ng/mL soluble SCF (filled squares), or TCPS surfaces with 10 ng/mL soluble SCF (open squares, dot dash line). TCPS wells without growth factors (open diamonds, dashed line) served as a negative control. Data are the average ( $\pm$  S.E.M) of replicate wells from a single experiment.

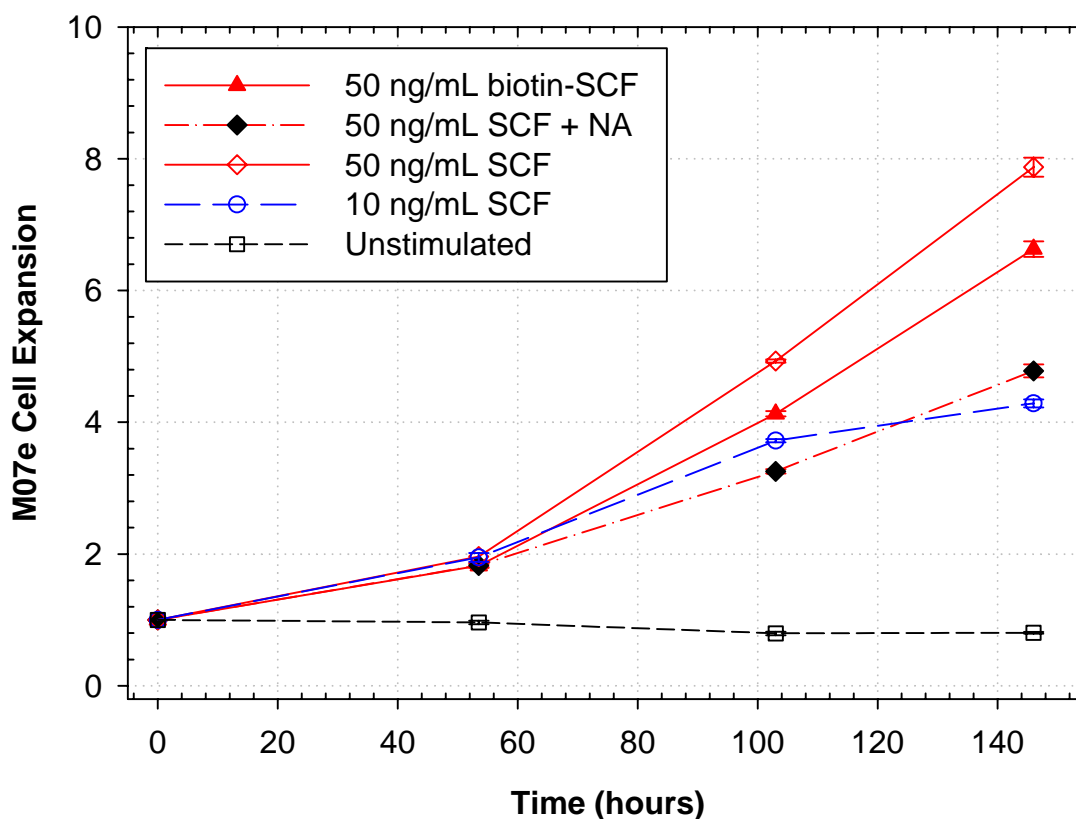


**Figure 6.4.13:** Dose response for M07e cell expansion in wells TCPS. Exponentially growing M07e cells were starved overnight and stimulated in StemPro 34 media with 50 ng/mL biotin-SCF (triangles, solid line), 50 ng/mL soluble SCF with 0.1mg/mL NeutrAvidin (filled diamonds, dash-dot line), 50 ng/mL soluble SCF (open diamonds, solid line), or 10 ng/mL soluble SCF (open diamonds, dashed line). The negative control was comprised of starved M07e cells cultured in StemPro 34 in the absence of additional growth factors (Unstimulated, open squares). Data are the average ( $\pm$  SEM) of at least three replicates from a single experiment.

## **6.5 DISCUSSION**

### **6.5.1 Biotinylation of SCF**

We found the extent of biotinylation of SCF to be highly dependent on the molar ratio of sulfo-NHS-LC-biotin to SCF and the age of the sulfo-NHS-LC-biotin reagent. The number of biotinylation sites per SCF significantly increased with increasing BP ratio. While the extent of biotinylation was lower with a BP ratio of 2:1, this BP ratio repeatedly yielded the addition of a single biotin linker to SCF with fresh reagent. Since the purpose of biotinylating SCF is to specifically present the molecule in a defined orientation, the presence of SCF with multiple biotins is undesirable. For this reason SCF was biotinylated with fresh sulfo-NHS-LC-biotin at a BP molar ratio of 2:1 for cell adhesion, cell signaling, and cell culture assay on DPb surfaces. Evaluation of the biotinylation of SCF revealed that only a portion of the material was biotinylated, leaving the majority of the material unmodified. When used to modify surfaces, unbiotinylated SCF was removed by a series of rinses.

### **6.5.2 Comparison of commercially available NeutrAvidin-coated wells and DPb surfaces**

The preparation of biotin-SCF-modified surfaces was significantly different for DPb and commercially available NeutrAvidin-coated wells. To remove residual, unbound biotin-SCF from NeutrAvidin-coated wells the surfaces were rinsed eight times with 200  $\mu$ L of PBS. After each rinse the entire contents of the well as removed. In contrast, biotin-SCF-modified DPb surfaces were washed via 15 rinses with PBS and three media dilution rinses. Dilution rinses remove only 67% of the liquid within the well (200  $\mu$ L of 300  $\mu$ L) and ensures that once formed the biotin-SCF on the surface never encounters an air-water interface. This minimizes the possibility that the biotin-SCF will be stripped off from the surface.

Another key difference in surface preparation was sterilization. Biotin-SCF-modified NeutrAvidin-coated wells were sterilized by exposure to UV light. This may have contributed the high biotin-SCF loading densities necessary for bioactivity. This is consistent with an experiment showing that by avoiding the 30-minute UV sterilization step the dose-response curve for M07e cell binding and expansion on immobilized SCF shifted to the left (i.e. to lower SCF loading necessary) by approximately three fold (DATA NOT SHOWN). An alternative method was developed to decrease the exposure of proteins to UV sterilization. Prior to biotin-SCF modification, surfaces were sterilized by exposure to UV light. All subsequent treatments of the surfaces were done aseptically. This method was adopted for experiments with DPb surfaces.

Culture of M07e cells in media conditioned by biotin-SCF-modified surfaces showed qualitatively similar results for DPb and commercially available NeutrAvidin-coated surfaces. In both cases the conditioned media supported greater expansion of M07e cells than a positive control with 5 ng/mL soluble SCF. However, quantitatively the DPb surfaces had much less biotin-SCF released from the surfaces; only the 1:5 dilution supported significant M07e expansion with DPb surfaces compared to 1:5 and 1:20 for commercially-available NeutrAvidin-coated plates. It is possible the quantitatively similar results were due to the similarity of the methods used to prepare the conditioned media. The conditioned media was obtained by removal of the entire contents of the wells, which as mentioned above could have removed some biotin-SCF from the surface. Despite the possible removal of material from the surface, biotin-SCF modified surfaces still supported growth indicating that a portion of the biotin-SCF was retained. In a second study of biotin-SCF released from DPb surfaces, activation of ERK from

media conditioned for 20-minutes showed only a very small amount of material was released and this was likely non-specifically bound material.

It is important to note that the amount of biotin-SCF immobilized onto DPb surfaces was similar to the amount of soluble SCF in the well. This is a significant advancement over the commercially available NeutrAvidin-coated wells. On commercially available NeutrAvidin-coated surfaces 20 ng/well biotin-SCF was necessary for ~ 15% of the M07e cells to adhere. The maximum fraction of ~ 0.4 was achieved with about 36 ng biotin-SCF per well. In contrast, at approximately 1.2 ng of biotin-SCF per well on DPb surfaces (2.5% DPb) supported maximal cell adhesion (~ 80 % of cells bound to surface).

### **6.5.3 Cultures on commercially available NeutrAvidin-coated surfaces**

The main problem with commercially available NeutrAvidin-coated surfaces was the requirement of very large amounts of immobilized biotin-SCF to obtain bioactivity. The large amount of material on the surface is problematic since the release of a very small fraction of the immobilized material could mask the effects of SCF immobilization. Given the results from conditioned media studies (Section 6.3.2) it is interesting that the kinetics of overall expansion were different for cultures seeded on ‘immobilized’ biotin-SCF as compared to soluble SCF (Figure 6.3.7). Soluble SCF initially showed increased overall expansion as compared to biotin-SCF immobilized on surfaces, but overall expansion on immobilized SCF was greater than that with soluble SCF after day six. This could be a result of continuous release of large amounts of SCF. Others have investigated the use of very high levels of growth factors and found a preferential expansion of primitive HSCs [199, 223]. Continued release of SCF would be similar to feeding cultures with fresh cytokines. It is also possible that build-up of metabolic by-

products occurred more rapidly due to faster expansion in cultures with soluble SCF, leading to an eventual decline in growth rates.

#### **6.5.4 Characterization of DP and DPb surfaces**

It is not surprising that OWLS studies suggest the ratio of biotin-SCF molecules to NeutrAvidin molecules is less than one. Under the conditions used to modify surfaces, we expect SCF to be associated as a non-covalent homodimer—SCF forms dimers at concentrations greater than 10 ng/mL [113, 115]. The projected area a single SCF dimer is 27.84 nm<sup>2</sup> [116], while streptavidin's projected area is 24.75 nm<sup>2</sup> [168]. Thus, steric hindrance should limit the binding of biotin-SCF to NeutrAvidin.

On DPb surfaces biotin-SCF remained active after immobilization, as evidenced by both M07e cell adhesion and ERK activation. ERK activation by immobilized biotin-SCF was similar to that for soluble SCF until a plateau was reached at 1 mol% DPb. Interestingly, cell adhesion continued to increase with surface DPb content until a plateau was reached at 2.5 mol%. Even with pre-blocking steps, ERK activation induced by DP surfaces treated with NeutrAvidin and biotin-SCF was significantly increased compared to untreated surfaces. This suggests non-specific binding of biotin-SCF to either the cassette upper or directly to the surfaces. Results from signaling studies using conditioned media (20-minute incubation on biotin-SCF modified DPb surfaces) showed low levels of phosphorylated ERK1,2. Activation from surfaces was significantly enhanced compared to the released material indicating that specifically immobilized material elicits much greater activation.

### 6.5.5 Cultures on DOPA-PEG surfaces

Cultures of M07e cells on DPb surfaces and cultures of mPB CD34+ cells on DP surfaces indicated that DPb surfaces are potentially suitable for culture with primary CD34+ cells. However, overall expansion of mPB CD34+ cells has not been observed in two separate experiments. Our results suggest that the presence of NeutrAvidin and/or biotin-SCF are responsible for the lack of expansion, since controls on similarly prepared DP surfaces that were not treated with NeutrAvidin or biotin-SCF supported expansion.

In a follow-up experiment M07e cells were cultured with SCF in StemPro 34 media containing 0.1 mg/mL NeutrAvidin (concentration used in modifying DPb surfaces). Based on one-to-four binding of NeutrAvidin to biotin, 0.1 mg/mL NeutrAvidin would bind approximately 1.63  $\mu\text{g/mL}$  of biotin. The concentration of biotin in StemPro 34 media is 0.013  $\mu\text{g/mL}$ , so it is likely that all the free biotin in the media was associated with NeutrAvidin. Results from this experiment showed that a large dose of NeutrAvidin significantly reduced M07e cell expansion. This suggests that free biotin in the media is being sequestered by NeutrAvidin and is not available to the cells. Biotin is essential for the synthesis of fatty acids. The removal of free biotin could make CD34+ cells reliant upon external sources for fatty acids, thus limiting their expansion potential. OWLS data shows for a 2.5% DPb surface ( $\sim 1.8 \text{ pmol/cm}^2$ , Figure 6.4.2) there are approximately 0.14 pmole NeutrAvidin per  $\text{cm}^2$ . Each well has a surface area of 0.4  $\text{cm}^2$  giving approximately  $3.4 \times 10^{10}$  molecules per well. Each NeutrAvidin molecule could have approximately two of the four biotin-binding sites available (on average 0.8 sites are occupied by biotin-SCF and one site for binding DPb) giving a maximum of  $\sim 7.4 \times 10^{10}$  available biotin-binding sites per well. The concentration of biotin in StemPro 34 media is 0.013 mg/L. We

cultured cells in a volume of 0.175 mL giving a total of  $5.61 \times 10^{12}$  molecules of biotin per well. If all the available biotin-binding sites removed biotin from the media,  $\sim 5.6 \times 10^{12}$  molecules would remain in free solution. Removal of this amount of biotin represents only a 1% reduction in the amount of available biotin. A culture of M07e cells should be performed to confirm the influence of biotin removal. It seems that the removal of this small fraction of biotin should not have such a profound effect on CD34+ cell expansion. However, others have shown that small changes in media composition can have dramatic effects on culture outcomes. For example, chelation of a small concentration of copper in culture of cord blood CD34+ cells significantly enhances expansion and self-renewal [224, 225].

It is also possible that solutions with NeutrAvidin or biotin-SCF could introduce components that negatively affect CD34+ cells. Dialysis required to prepare biotin-SCF is typically performed using non-sterile PBS and NeutrAvidin is not provided in a cell-culture tested format. Either of these could be a source of endotoxin and provide a partial explanation for poor expansion results.

## **CHAPTER 7: CONCLUSIONS AND RECOMENDATIONS**

In this study, three different strategies for improving ex vivo HSC expansion were explored: (1) culture in reduced oxygen tension, (2), presentation of TPO mimetic (TPOm) lipid-peptide (lipopeptide) constructs in a hybrid bilayer membrane (HBM) and (3) immobilization of stem cell factor (SCF) in a defined format for presentation to cells. We hypothesized that by mimicking key components of the in vivo stem cell niche, we could improve ex vivo expansion of HSCs.

### **7.1 STUDIES WITH REDUCED OXYGEN TENSION**

#### **7.1.1 Conclusions**

Three-day cultures of BM CD34+ cells were used to evaluate the influence of reduced oxygen tensions on HSC culture. CD34+ cells cultured under 5% and 20% O<sub>2</sub> exhibited similar overall expansion and retention of CD34+Thy1+ cells. The addition of three-fold greater cytokines to 2% and 5% O<sub>2</sub> cultures significantly enhanced overall expansion and retention of CD34+Thy1+ cells. We hypothesized that a more detailed analysis of cell division—using secondary markers to track the primitive cells—would clarify how reduced oxygen tension alters the maintenance of the most primitive cells. However, our results showed little difference in cell division profiles of CD34+Thy1+ cells cultured under reduced oxygen as compared to normoxia. Therefore, additional studies specifically evaluating how reduced oxygen tension influences culture outcomes were not continued.

#### **7.1.2 Recommendations for future reduced oxygen cultures**

If the work with reduced oxygen cultures was revisited, several additions could improve culture outcomes. To focus on the culture of the candidate HSCs, we chose to monitor cultures for only

the first three days. This was based on our previous work suggesting that after four days in culture the majority of CD34+Thy1+ cells were lost. Reviewing the results in Chapter 4 shows that the small differences in overall expansion were most apparent on the final day of observation. This suggests that extending the evaluation period, perhaps to six days, would allow for larger differences in overall expansion and cell division patterns for different conditions to become more apparent.

In addition to reduced oxygen, HSCs are likely to reside in an area of decreased pH. The interaction of HSCs with osteoblasts at the endosteal surface isolates them from the central sinus. Experimental data shows that pH drops from 7.4 to 7.1 approximately 25  $\mu\text{m}$  from blood vessels in normal subcutaneous tissue [226], and the lowest pH values are observed far away from the central core [227]. To better mimic the in vivo niche reduced pH should also be explored in combination with reduced  $\text{pO}_2$ .

## **7.2 STUDIES WITH TPO MIMETIC MOLECULES**

### **7.2.1 Conclusions**

Using hybrid bilayer membranes (HBMs) to display TPOm lipopeptides, we studied whether or not the immobilized presentation of TPO alters its ability to expand HSCs. There are no reports of studies using immobilized TPO, possibly because TPO is not presented in a membrane-associated or heparin-bound form. By synthesizing TPOm and conjugating it to lipid, we were able to present this molecule in a hybrid bilayer membrane (HBM). HBMs have several advantages, including biocompatibility and oriented presentation of ligands. This allows for the oriented display of the two synthesized versions of TPOm lipopeptides (TPOm-1L and TPOm-2L, collectively TPOm-L) at low loading densities and controlled ratios. We report on the

similar activities of soluble and lipid-immobilized TPOm molecules. Similarity of the two TPOm presentation methods may be a result of material releasing from HBMs. Activation studies with media conditioned by surfaces for 20 minutes induced elevated phosphorylated ERK 1,2 (pERK) in M07e cells, although TPOm-1L surfaces induced even higher levels of activation ERK. Our results with BM and mPB CD34+ cells show that TPOm-L did elicit cellular responses, but they did not provide enhanced expansion of HSCs.

### **7.2.2 Recommendations**

Our findings suggest that TPOm-L in HBMs were equivalent to current methods for retaining primitive HSCs. These findings set the stage for examining synergistic combinations of cytokine mimics and CAM ligands in a defined manner. Cytokines act in cooperation with integrins to alter culture outcomes [228-230]. For example, TPO-induced megakaryopoiesis was blocked with  $\alpha 4\beta 1$  neutralizing antibodies [230]. RGD- and/or LDV-lipopeptides could be co-immobilized with TPOm-L to improve culture outcomes.

Improvements in the long-term stability of the HBMs could also improve culture outcomes and allow for scale-up to large bioprocesses. Elliot Chiakof's lab has produced stabilized, phosphatidylcholine-containing polymeric surface through in situ polymerization of a self-assembled HBMs [231-236]. Microspheres coated with polymerized, Texas Red-labeled lipids maintained uniform fluorescence 40 days after implanting in mice [234]. Once cross-linked, these surfaces could be moved to an air water interface [231]. This capability would allow for more aggressive rinsing protocols and ease washing procedures required for surface preparation. This also may improve long-term culture outcomes, by reducing the effect of

bubbles formed on the well edges. Additionally, this would allow for larger-scale experiments with cultures in suspension bioreactors.

In addition to hybrid bilayer membranes, other systems could be used to present immobilized TPOm. The presentation of a biotinylated TPOm on DOPA-PEG-biotin (DPb) may improve culture outcomes, once the issues with DPb surfaces are resolved (see section 7.3.2). With small changes to the established synthetic methods it would be possible to synthesize DOPA-PEG-TPOm (DP-TPOm) molecules, allowing for the direct incorporation of TPOm into surfaces without the need of an avidin bridge. Incorporating DPb and DP-TPOm into a background of DP would make the surface presentation of multiple ligands easier. Additionally, the covalent linkage of TPOm to the surface should significantly reduce the amount of material released from surfaces; thereby increasing the likelihood of observing differences in cultures with immobilized and soluble TPOm.

### **7.3 STUDIES WITH IMMOBILIZED BIOTIN-SCF ON SURFACES WITH BIOTIN-BINDING MOLECULES**

#### **7.3.1 Conclusions**

We hypothesized that the immobilization of SCF would improve HSC expansion. To test this hypothesis we chemically-modified soluble SCF with a single biotin molecule for immobilization on surfaces coated with NeutrAvidin. Two different culture systems were used to evaluate our hypothesis. The first system used commercially available NeutrAvidin-coated wells. On commercially available NeutrAvidin-coated surfaces large amounts of immobilized biotin-SCF were required to induce M07e cell expansion. HSC expansion on immobilized biotin-SCF surfaces was delayed, but extended as compared to soluble SCF controls. Further investigation suggested that ebiotin-SCF continually released from the surface; therefore, the

results could not attributed directly to immobilized SCF. The majority of these studies used a biotin-to-protein (BP) ratio of 10:1 for the production of biotin-SCF. The fact that we used a BP ratio of 10:1 for these studies should not alter the interpretation/comparison to later studies that used a BP ratio of 2:1. This BP ratio was chosen based on the addition of a single biotin molecule to SCF. Subsequent studies of SCF biotinylation showed that the degree of biotinylation was dependent on the age of the reagent used to modify SCF; consequently different BP ratios could be used with the same overall result.

The second SCF immobilization system used a non-fouling PEG layer anchored to TiO<sub>2</sub>-coated surfaces via 2,4-dihydroxyphenylalanine (DOPA). Biotin was added to the end of DOPA-PEG (DP) molecules for specific presentation of biotin-SCF using an avidin bridge. In conjunction with Dr. Rico Gunawan, DOPA-PEG-biotin (DPb) surfaces were characterized using M07e cells. M07e cells exhibited specific adhesive interaction, activation of ERK 1,2, and promotion of cell growth on biotin-SCF-immobilized DPb surfaces. Two separate experiments have shown that DP surfaces are biocompatible with mPB CD34+ cells and similar to TCPS in overall expansion and retention of CD34+ cells and CD34+Thy1+ cells. However, expansion of mPB CD34+ cells on DPb surfaces has been elusive. Two experiments have shown no overall expansion of mPB CD34+ cells on DPb surfaces with immobilized biotin-SCF. Our results indicate that either NeutrAvidin or biotin-SCF inhibits mPB cell growth, since DP and DPb surfaces were prepared and rinsed with the same solutions.

### **7.3.2 Recommendations for DOPA-PEG-biotin surfaces and biotinylated SCF**

The DPb surfaces used here were sufficient for short-term activation of signaling molecules and adhesion studies with M07e cells. Long-term culture of M07e cells was possible, but in two

separate experiments mPB CD34+ cells cultured on DPb surfaces showed no overall expansion. Primary CD34+ cells are very sensitive to their culture environment [205]. It is possible that free biotin-binding sites on NeutrAvidin removed free biotin from the media, limiting CD34+ cell expansion. Follow up experiments should be conducted to examine this hypothesis in detail. In this experiment M07e cells should be cultured with SCF in StemPro media containing NeutrAvidin and supplemented with various concentrations of free biotin. Biotin should be added at levels above and below the concentration that will be removed from the medium by the added NeutrAvidin. Reduced expansion of M07e cells in conditions where free biotin is limited will help confirm results indicating that sequestration of biotin can lead to reduced CD34+ cell expansion. It is also possible that solutions with NeutrAvidin or biotin-SCF could introduce components that negatively affect CD34+ cells. Dialysis required to prepare biotin-SCF is performed using non-sterile PBS and NeutrAvidin is not provided in a cell-culture tested format. Either of these could be a source of endotoxin or other component and should be tested for growth inhibition to provide a partial explanation for poor expansion results.

M07e cells cultured in media conditioned by biotin-SCF-modified surfaces showed qualitatively similar results for DPb and commercially available NeutrAvidin-coated surfaces. It is possible the quantitatively similar results were due to the similarity of the methods used to prepare the conditioned media. The conditioned media was obtained by removal of the entire contents of the wells, which could have removed some biotin-SCF from the surface. Follow up experiments are suggested to determine if the method of conditioned media collection altered results on biotin-SCF-modified DPb surfaces. In these experiments only the top portion of the media would be removed as the conditioned media. This collection method would be similar to

the dilution rinses used to prepare the surfaces for experiments. This method should be compared directly with surfaces where the entire contents of the well are harvested and used to stimulate M07e cell expansion.

The exploration of ERK 1,2 activation should be expanded to additional cell signaling molecules. Additional analyses should specifically examine the additional pathways that have been shown to have different activation for membrane-associated and soluble SCF. Specifically, the duration of c-Kit tyrosine activation should be evaluated [38, 41]. Studies showed that when stimulated with membrane-associated SCF, c-Kit on M07e cells remained phosphorylated for two hours. In contrast, c-Kit on M07e cells stimulated with soluble SCF returned to basal phosphorylation levels in one hour [41]. Other studies have indicated that PLC- $\gamma$  is required for the differential effect seen in membrane-associated and soluble SCF [92, 141, 142], while others have attributed the differences to sustained and enhanced p38 activation [143]. A more comprehensive analysis of molecules activated by surfaces immobilized with biotin-SCF would help determine the long-term stability of immobilized biotin-SCF.

The lack of difference in HSC expansion with SCF presentation may be improved by changing the system used to culture the cells. In the present system cells interact with a surface and are stimulated with biotin-SCF. If a portion of the material is released from the surface it can immediately interact with cells near the surface and confound results by stimulating the cells as a soluble molecule. Moving to a perfusion-based culture system could resolve some of these issues. Fresh media would constantly be added and removed, thus the concentration of soluble biotin-SCF would be minimized. Additionally, if the cultures were performed in suspension the local high concentration cells (and possibly soluble biotin-SCF) would be removed. Cells in a

stirred suspension may be less likely to immediately interact with soluble biotin-SCF released from surfaces; thus differences between presentation schemes would be easier to observe. The use of suspension-based cultures would require the development of SCF-functionalized microcarriers and methods to remove cells from the microcarriers, but could be a significant advancement.

#### **7.4 OVERALL RECOMMENDATIONS**

The DPb surface can be used in many other applications. This platform was developed as a method to stably present immobilized biotinylated molecules in an active form. Various biotinylated ligands can be incorporated onto surfaces via biotin-binding proteins and varying the molar ratio of DP to DPb easily controls their surface densities. This approach is applicable to a wide variety of substrates due to the DOPA anchor group of the PEG chains.

HSCs express many different cytokine receptors and cell adhesion molecules (CAMs) and show synergistic interactions between multiple receptors [17, 152, 237]. It is likely that improvement of ex vivo culture outcomes would be possible by combining the reduced oxygen tension with immobilized SCF and TPOm to mimic multiple aspects of the niche. The addition of other growth factors and mitogens may also significantly enhance HSC expansion. Reya [238] and Willert [239] demonstrated that Wnt3A with SCF maintains self-renewing mouse BM HSCs with reduced differentiation. Bone morphogenic proteins (BMPs) have been identified as a key component of the HSC niche [66]. Low concentrations of BMP-4 induced human cord blood CD34<sup>+</sup>CD38<sup>-</sup> cell proliferation and differentiation, whereas high concentrations of BMP-4 extended the length of time that NOD/SCID mice repopulating cells could be maintained in ex vivo culture [240]. BMP-4 may also be a candidate for immobilization. Several small molecules

have also recently been identified as candidates to improve the self-renewal and expansion of HSCs including: a copper chelator—tetraethylene pentamine (TEPA) [224, 225], all-trans retinoic acid (ATRA) [241], DNA methylation inhibitor 5-aza 2'-deoxycytidine (5azaD) [242], and DNA deacetylase inhibitors trichostatin A (TSA) [242] and Valproic Acid [243, 244]. Inclusion of a combination of these molecules with presentation of immobilized ligands and soluble cytokines could improve HSC expansion.

**REFERENCES**

1. McAdams, T.A., W.M. Miller and E.T. Papoutsakis, *Hematopoietic cell culture therapies.1. Cell culture considerations*. Trends in Biotechnology, 1996. **14**(9): p. 341-349.
2. Muller-Sieburg, C.E., R.H. Cho, M. Thoman, B. Adkins and H.B. Sieburg, *Deterministic regulation of hematopoietic stem cell self-renewal and differentiation*. Blood, 2002. **100**(4): p. 1302-1309.
3. Bonnet, D., *Haematopoietic stem cells*. Journal of Pathology, 2002. **197**(4): p. 430-440.
4. Boiron, J.-M., B. Dazey, C. Cailliot, B. Launay, M. Attal, et al., *Large-scale expansion and transplantation of CD34+ hematopoietic cells: in vitro and in vivo confirmation of neutropenia abrogation related to the expansion process without impairment of the long-term engraftment capacity*. Transfusion, 2006. **46**(11): p. 1934-1942.
5. *Regenerative Medicine 2006*. August 2006, Department of Health and Human Services.
6. Aschan, J., *Allogeneic haematopoietic stem cell transplantation: current status and future outlook*. British Medical Bulletin, 2006. **77-78**: p. 23-36.
7. Liu, Y., T. Liu, X. Fan, X. Ma and Z. Cui, *Ex vivo expansion of hematopoietic stem cells derived from umbilical cord blood in rotating wall vessel*. Journal of Biotechnology, 2006. **124**(3): p. 592-601.
8. Sanz, M.A., *Cord-Blood Transplantation in Patients with Leukemia -- A Real Alternative for Adults*. The New England Journal of Medicine, 2004. **351**(22): p. 2328-2330.
9. Luens, K.M., M.A. Travis, B.P. Chen, B.L. Hill, R. Scollay, and L.J. Murray, *Thrombopoietin, kit ligand, and flk2/flt3 ligand together induce increased numbers of*

- primitive hematopoietic progenitors from human CD34<sup>+</sup>Thy-1<sup>+</sup>Lin<sup>-</sup> cells with preserved ability to engraft SCID-hu bone.* Blood, 1998. **91**(4): p. 1206-1215.
10. Borge, O.J., V. Ramsfjell, L. Cui and S.E.W. Jacobsen, *Ability of early acting cytokines to directly promote survival and suppress apoptosis of human primitive CD34<sup>+</sup>CD38<sup>-</sup> bone marrow cells with multilineage potential at the single-cell level: Key role of thrombopoietin.* Blood, 1997. **90**(6): p. 2282-2292.
  11. Kobayashi, M., J.H. Laver, T. Kato, H. Miyazaki and M. Ogawa, *Thrombopoietin supports proliferation of human primitive hematopoietic cells in synergy with steel factor and/or interleukin-3.* Blood, 1996. **88**(2): p. 429-436.
  12. Murray, L.J., J.C. Young, L.J. Osborne, K.M. Luens, R. Scollay, and B.L. Hill, *Thrombopoietin, flt3, and kit ligands together suppress apoptosis of human mobilized CD34<sup>+</sup> cells and recruit primitive CD34<sup>+</sup>Thy-1<sup>+</sup> cells into rapid division.* Experimental Hematology, 1999. **27**(6): p. 1019-1028.
  13. Bruno, S., L. Gammaitoni, M. Gunetti, F. Sanavio, F. Fagioli, M. Aglietta, and W. Piacibello, *Different growth factor requirements for the ex vivo amplification of transplantable human cord blood cells in a NOD/SCID mouse model.* Journal of Biological Regulators and Homeostatic Agents, 2001. **15**(1): p. 38-48.
  14. Herrera, C., J. Sanchez, A. Torres, C. Bellido, A. Rueda, and M.A. Alvarez, *Early-acting cytokine-driven ex vivo expansion of mobilized peripheral blood CD34<sup>+</sup> cells generates post-mitotic offspring with preserved engraftment ability in non-obese diabetic/severe combined immunodeficient mice.* British Journal of Haematology, 2001. **114**(4): p. 920-930.

15. Ramsfjell, V., O.J. Borge, L. Cui and S.E. Jacobsen, *Thrombopoietin directly and potently stimulates multilineage growth and progenitor cell expansion from primitive (CD34+ CD38-) human bone marrow progenitor cells: distinct and key interactions with the ligands for c-kit and flt3, and inhibitory effects of TGF-beta and TNF-alpha*. *Journal of Immunology*, 1997. **158**(11): p. 5169-5177.
16. Wilson, A. and A. Trumpp, *Bone-marrow haematopoietic-stem-cell niches*. *Nature Reviews Immunology*, 2006. **6**(2): p. 93-106.
17. Abboud, C.N. and M.A. Lichtman, *Structure of the Marrow and the Hematopoietic Microenvironment*, in *Williams Hematology*, M.A. Lichtman, et al., Editors. 2006, McGraw-Hill, Medical Publications Division: New York.
18. Massague, J. and A. Pandiella, *Membrane-Anchored Growth Factors*. *Annual Review of Biochemistry*, 1993. **62**(1): p. 515-541.
19. Smith, S. and H.E. Broxmeyer, *The Influence of Oxygen-Tension on the Long-Term Growth-In Vitro of Hematopoietic Progenitor Cells from Human Cord Blood*. *British Journal of Haematology*, 1986. **63**(1): p. 29-34.
20. Tavassoli, M. and J.M. Yoffey, *Bone Marrow Structure and Function*. 1983, New York: Alan R. Liss, Inc. 47-64.
21. Chow, D.C., L.A. Wenning, W.M. Miller and E.T. Papoutsakis, *Modeling  $pO_2$  distributions in the bone marrow hematopoietic compartment. I. Krogh's model*. *Biophysical Journal*, 2001. **81**(2): p. 675-684.

22. Chow, D.C., L.A. Wenning, W.M. Miller and E.T. Papoutsakis, *Modeling pO<sub>2</sub> distributions in the bone marrow hematopoietic compartment. II. Modified Kroghian models*. Biophysical Journal, 2001. **81**(2): p. 685-696.
23. Adler, S.S., *Blood Circulation of Bone Marrow*, in *Blood vessels and lymphatics in organ systems*, D.E. Abramson and P.B. Dobrin, Editors. 1984, Academic Press: San Diego. p. 705-719.
24. Cipolleschi, M.G., P. Dellosbarba and M. Olivotto, *The Role of Hypoxia in the Maintenance of Hematopoietic Stem Cells*. Blood, 1993. **82**(7): p. 2031-2037.
25. Ivanovic, Z., B. Bartolozzi, P.A. Bernabei, M.G. Cipolleschi, E. Rovida, P. Milenkovic, V. Praloran, and P. Dello Sbarba, *Incubation of murine bone marrow cells in hypoxia ensures the maintenance of marrow-repopulating ability together with the expansion of committed progenitors*. British Journal of Haematology, 2000. **108**(2): p. 424-429.
26. Ivanovic, Z., P. Dello Sbarba, F. Trimoreau, J.L. Faucher and V. Praloran, *Primitive human HPCs are better maintained and expanded in vitro at 1 percent oxygen than at 20 percent*. Transfusion, 2000. **40**(12): p. 1482-1488.
27. Ivanovic, Z., F. Belloc, J.L. Faucher, M.G. Cipolleschi, V. Praloran, and P. Dello Sbarba, *Hypoxia maintains and interleukin-3 reduces the pre-colony-forming cell potential of dividing CD34<sup>+</sup> murine bone marrow cells*. Experimental Hematology, 2002. **30**(1): p. 67-73.
28. Ivanovic, Z., F. Hermitte, P.B. de la Grange, B. Dazey, F. Belloc, F. Lacombe, G. Vezon, and V. Praloran, *Simultaneous Maintenance of Human Cord Blood SCID-Repopulating*

- Cells and Expansion of Committed Progenitors at Low O<sub>2</sub> Concentration (3%)*. Stem Cells, 2004. **22**(5): p. 716-724.
29. Danet, G.H., Y. Pan, J.L. Luongo, D.A. Bonnet and M.C. Simon, *Expansion of human SCID-repopulating cells under hypoxic conditions*. Journal of Clinical Investigation, 2003. **112**(1): p. 126-135.
30. Cipolleschi, M.G., G. Dippolito, P.A. Bernabei, R. Caporale, R. Nannini, et al., *Severe hypoxia enhances the formation of erythroid bursts from human cord blood cells and the maintenance of BFU-E in vitro*. Experimental Hematology, 1997. **25**(11): p. 1187-1194.
31. Hevehan, D.L., E.T. Papoutsakis and W.M. Miller, *Physiologically significant effects of pH and oxygen tension on granulopoiesis*. Experimental Hematology, 2000. **28**(3): p. 267-275.
32. Mostafa, S.S., W.M. Miller and E.T. Papoutsakis, *Oxygen tension influences the differentiation, maturation and apoptosis of human megakaryocytes*. British Journal of Haematology, 2000. **111**(3): p. 879-889.
33. Koller, M.R., J.G. Bender, E.T. Papoutsakis and W.M. Miller, *Effects of Synergistic Cytokine Combinations, Low Oxygen, and Irradiated Stroma on the Expansion of Human Cord Blood Progenitors*. Blood, 1992. **80**(2): p. 403-411.
34. Koller, M.R., J.G. Bender, E.T. Papoutsakis and W.M. Miller, *Beneficial-Effects of Reduced Oxygen-Tension and Perfusion in Long-Term Hematopoietic Cultures*. Annals of the New York Academy of Sciences, 1992. **665**: p. 105-116.
35. Broudy, V.C., *Stem Cell Factor and Hematopoiesis*. Blood, 1997. **90**(4): p. 1345-1364.

36. Zsebo, K.M., D.A. Williams, E.N. Geissler, V.C. Broudy, F.H. Martin, et al., *Stem-Cell Factor Is Encoded at the Sl-Locus of the Mouse and Is the Ligand for the C-Kit Tyrosine Kinase Receptor*. *Cell*, 1990. **63**(1): p. 213-224.
37. Flanagan, J.G., D.C. Chan and P. Leder, *Transmembrane form of the kit ligand growth factor is determined by alternative splicing and is missing in the Slid mutant*. *Cell*, 1991. **64**(5): p. 1025-1035.
38. Kapur, R., M. Majumdar, X. Xiao, M. McAndrews-Hill, K. Schindler, and D.A. Williams, *Signaling Through the Interaction of Membrane-Restricted Stem Cell Factor and c-kit Receptor Tyrosine Kinase: Genetic Evidence for a Differential Role in Erythropoiesis*. *Blood*, 1998. **91**(3): p. 879-889.
39. Brannan, C.I., S.D. Lyman, D.E. Williams, J. Eisenman, D.M. Anderson, D. Cosman, M.A. Bedell, N.A. Jenkins, and N.G. Copeland, *Steel-Dickie Mutation Encodes a c-Kit Ligand Lacking Transmembrane and Cytoplasmic Domains*. *Proceedings of the National Academy of Sciences of the United States of America*, 1991. **88**(11): p. 4671-4674.
40. Toksoz, D., K.M. Zsebo, K.A. Smith, S. Hu, D. Brankow, S.V. Suggs, F.H. Martin, and D.A. William, *Support of Human Hematopoiesis in Long-Term Bone Marrow Cultures by Murine Stromal Cells Selectively Expressing the Membrane-Bound and Secreted Forms of the Human Homolog of the Steel Gene Product, Stem Cell Factor*. *Proceedings of the National Academy of Sciences of the United States of America*, 1992. **89**(16): p. 7350-7354.
41. Miyazawa, K., D.A. Williams, A. Gotoh, J. Nishimaki, H.E. Broxmeyer, and K. Toyama, *Membrane-bound Steel factor induces more persistent tyrosine kinase activation and*

- longer life span of c-kit gene-encoded protein than its soluble form.* Blood, 1995. **85**(3): p. 641-649.
42. Ito, Y., J. Zheng, Y. Imanishi, K. Yonezawa and M. Kasuga, *Protein-free cell culture on an artificial substrate with covalently immobilized insulin.* Proceedings of the National Academy of Sciences of the United States of America, 1996. **93**(8): p. 3598-3601.
43. Cwirla, S.E., P. Balasubramanian, D.J. Duffin, C.R. Wagstrom, C.M. Gates, et al., *Peptide agonist of the thrombopoietin receptor as potent as the natural cytokine.* Science, 1997. **276**(5319): p. 1696-1699.
44. Winger, T.M., P.J. Ludovice and E.L. Chaikof, *Formation and stability of complex membrane-mimetic monolayers on solid supports.* Langmuir, 1999. **15**(11): p. 3866-3874.
45. Kokkoli, E., S.E. Ochsenhirt and M. Tirrell, *Collective and single-molecule interactions of  $\alpha 5 \beta 1$  integrins.* Langmuir, 2004. **20**(6): p. 2397-2404.
46. Dillow, A.K., S.E. Ochsenhirt, J.B. McCarthy, G.B. Fields and M. Tirrell, *Adhesion of  $\alpha 5 \beta 1$  receptors to biomimetic substrates constructed from peptide amphiphiles.* Biomaterials, 2001. **22**(12): p. 1493.
47. Jensen, T.W., B.H. Hu, S.M. Dellatore, A.S. Garcia, P.B. Messersmith, and W.M. Miller, *Lipopeptides Incorporated into Supported Phospholipid Monolayers Have High Specific Activity at Low Incorporation Levels.* Journal of the American Chemical Society, 2004. **126**(46): p. 15223-15230.
48. da Silva, C.L., R. Goncalves, F. Lemos, M. Lemos, E.D. Zanjani, G. Almeida-Porada, and J.M.S. Cabral, *Modelling of ex vivo expansion/maintenance of hematopoietic stem cells.* Bioprocess and Biosystems Engineering, 2003. **25**(6): p. 365-369.

49. Krause, D.S., *Regulation of hematopoietic stem cell fate*. *Oncogene*, 2002. **21**(21): p. 3262-3269.
50. Gigant, C., V. Latger-Cannard, D. Bensoussan, P. Feugier, P. Bordigoni, and J.F. Stoltz, *Quantitative Expression of Adhesion Molecules on Granulocyte Colony-Stimulating Factor-Mobilized Peripheral Blood, Bone Marrow, and Cord Blood CD34+ Cells*. *Journal of Hematotherapy and Stem Cell Research*, 2001. **10**(6): p. 807-814.
51. Mukhopadhyay, A., T. Madhusudhan and R. Kumar, *Hematopoietic Stem Cells: Clinical Requirements and Developments in Ex-Vivo Culture*. *Advances in Biochemical Engineering/Biotechnology*, 2004. **86**: p. 215-253.
52. Noll, T., N. Jelinek, S. Schmidt, B. Manfred and W. Christian, *Cultivation of Hematopoietic Stem and Progenitor Cells: Biochemical Engineering Aspects*. *Advances in Biochemical Engineering/Biotechnology*, 2002. **74**: p. 111-128.
53. Verfaillie, C.M., *Hematopoietic stem cells for transplantation*. *Nature Immunology*, 2002. **3**(4): p. 314-317.
54. Janssen, W.E. and G.J. Elfenbien, *Mobilization of Peripheral Blood Stem Cells: Are all regiments created equal?* in *Hematopoietic Stem Cells: Biology and Therapeutic Applications*, D. Levitt and R. Mertelsmann, Editors. 1995, Marcel Dekker, Inc.: New York. p. 403-419.
55. Lansdorp, P.M., W. Dragowska and H. Mayani, *Ontogeny-Related Changes in Proliferative Potential of Human Hematopoietic-Cells*. *Journal of Experimental Medicine*, 1993. **178**(3): p. 787-791.

56. Ogawa, M., *Differentiation and Proliferation of Hematopoietic Stem Cells*. Blood, 1993. **81**(11): p. 2844-2853.
57. Andrews, R.G., E.M. Bryant, S.H. Bartelmez, D.Y. Muirhead, G.H. Knitter, W. Bensinger, D.M. Strong, and I.D. Bernstein, *CD34+ marrow cells, devoid of T and B lymphocytes, reconstitute stable lymphopoiesis and myelopoiesis in lethally irradiated allogeneic baboons*. Blood, 1992. **80**(7): p. 1693-1701.
58. Larochelle, A., J. Vormoor, H. Hanenberg, J.C.Y. Wang, M. Bhatia, et al., *Identification of primitive human hematopoietic cells capable of repopulating NOD/SCID mouse bone marrow: Implications for gene therapy*. Nature Medicine, 1996. **2**(12): p. 1329-1337.
59. Danet, G.H., H.W. Lee, J.L. Luongo, M.C. Simon and D.A. Bonnet, *Dissociation between stem cell phenotype and NOD/SCID repopulating activity in human peripheral blood CD34+ cells after ex vivo expansion*. Experimental Hematology, 2001. **29**(12): p. 1465-1473.
60. Tanavde, V.M., M.T. Malehorn, R. Lumkul, Z.G. Gao, J. Wingard, E.S. Garrett, and C.I. Civin, *Human stem-progenitor cells from neonatal cord blood have greater hematopoietic expansion capacity than those from mobilized adult blood*. Experimental Hematology, 2002. **30**(7): p. 816-823.
61. Baum, C.M., I.L. Weissman, A.S. Tsukamoto, A. Buckle and B. Peault, *Isolation of a Candidate Human Hematopoietic Stem-Cell Population*. Proceedings of the National Academy of Sciences of the United States of America, 1992. **89**(7): p. 2804-2808.
62. Young, J.C., K. Lin, G. Hansteen, M. Travis, L.J. Murray, L. Jaing, R. Scollay, and B.L. Hill, *CD34+ cells from mobilized peripheral blood retain fetal bone marrow*

- repopulating capacity within the Thy-1+ subset following cell division ex vivo.*  
Experimental Hematology, 1999. **27**(6): p. 994-1003.
63. Torok-Storb, B., M. Iwata, L. Graf, J. Gianotti, H. Horton, and M.C. Byrne, *Dissecting the Marrow Microenvironment.* Ann NY Acad Sci, 1999. **872**(1): p. 164-170.
64. Nilsson, S.K., H.M. Johnston and J.A. Coverdale, *Spatial localization of transplanted hemopoietic stem cells: inferences for the localization of stem cell niches.* Blood, 2001. **97**(8): p. 2293-2299.
65. Calvi, L.M., G.B. Adams, K.W. Weibrecht, J.M. Weber, D.P. Olson, et al., *Osteoblastic cells regulate the haematopoietic stem cell niche.* Nature, 2003. **425**(6960): p. 841-846.
66. Zhang, J.W., C. Niu, L. Ye, H.Y. Huang, X. He, et al., *Identification of the haematopoietic stem cell niche and control of the niche size.* Nature, 2003. **425**(6960): p. 836-841.
67. Visnjic, D., Z. Kalajzic, D.W. Rowe, V. Katavic, J. Lorenzo, and H.L. Aguila, *Hematopoiesis is severely altered in mice with an induced osteoblast deficiency.* Blood, 2004. **103**(9): p. 3258-3264.
68. Kopp, H.-G., S.T. Avezilla, A.T. Hooper and S. Rafii, *The Bone Marrow Vascular Niche: Home of HSC Differentiation and Mobilization.* Physiology, 2005. **20**(5): p. 349-356.
69. Lichtman, M.A., *The relationship of stromal cells to hematopoietic cells in marrow,* in *Long term bone marrow culture,* D.G. Wright and J.S. Greenberger, Editors. 1984, Alan R. Liss, Inc: New York. p. 3-29.

70. Weiss, L.P., *Functional Organization of the Hematopoietic Tissue*, in *Hematology-Basic Principles and Practice*, R. Hoffman, et al., Editors. 1991, Churhill Livingstone: New York. p. 82-86.
71. Wickramasinghe, S.N., *Human Bone Marrow*. 1975, Oxford: Blackwell Scientific Publications. 60-81.
72. Guyton, A.C. and J.E. Hall, *Textbook of Medical Physiology*. 1996, Philadelphia, PA: W.B. Saunders Company.
73. Yaegashi, K., T. Itoh, T. Kosaka, H. Fukushima and T. Morimoto, *Diffusivity of oxygen in microvascular beds as determined from PO<sub>2</sub> distribution maps*. *American Journal of Physiology-Heart and Circulation Physiology*, 1996. **270**(4): p. H1390-1397.
74. Gref, R., P. Couvreur, G. Barratt and E. Mysiakine, *Surface-engineered nanoparticles for multiple ligand coupling*. *Biomaterials*, 2003. **24**(24): p. 4529-4537.
75. Wineman, J., K. Moore, I. Lemischka and C. Muller-Sieburg, *Functional heterogeneity of the hematopoietic microenvironment: rare stromal elements maintain long-term repopulating stem cells*. *Blood*, 1996. **87**(10): p. 4082-4090.
76. Ulloa-Montoya, F., C.M. Verfaillie and W.-S. Hu, *Culture Systems for Pluripotent Stem Cells*. *Journal of Bioscience and Bioengineering*, 2005. **100**(1): p. 12-27.
77. Piacibello, W., F. Sanavio, A. Severino, A. Dane, L. Gammaitoni, et al., *Engraftment in nonobese diabetic severe combined immunodeficient mice of human CD34<sup>+</sup> cord blood cells after ex vivo expansion: Evidence for the amplification and self-renewal of repopulating stem cells*. *Blood*, 1999. **93**(11): p. 3736-3749.

78. Yao, C.-L., I.M. Chu, T.-B. Hsieh and S.-M. Hwang, *A systematic strategy to optimize ex vivo expansion medium for human hematopoietic stem cells derived from umbilical cord blood mononuclear cells*. *Experimental Hematology*, 2004. **32**(8): p. 720.
79. Muench, M.O., C. Gasparetto and M.A.S. Moore, *The In Vitro Growth of Murine High Proliferative Potential-Colony Forming Cells Is Not Enhanced by Growth in a Low Oxygen Atmosphere*. *Cytokine*, 1992. **4**(6): p. 488-494.
80. Martindale, J.L. and N.J. Holbrook, *Cellular response to oxidative stress: Signaling for suicide and survival*. *Journal of Cellular Physiology*, 2002. **192**(1): p. 1-15.
81. Meagher, R.C., A.J. Salvado and D.G. Wright, *An Analysis of the Multilineage Production of Human Hematopoietic Progenitors in Long-Term Bone-Marrow Culture - Evidence That Reactive Oxygen Intermediates Derived from Mature Phagocytic-Cells Have a Role in Limiting Progenitor-Cell Self-Renewal*. *Blood*, 1988. **72**(1): p. 273-281.
82. Chenais, B., M. Andriollo, P. Guiraud, R. Belhoussine and P. Jeannesson, *Oxidative stress involvement in chemically induced differentiation of K562 cells*. *Free Radical Biology and Medicine*, 2000. **28**(1): p. 18-27.
83. Yang, K.D. and M.F. Shaio, *Hydroxyl Radicals as an Early Signal Involved in Phorbol Ester- Induced Monocytic Differentiation of HL-60 Cells*. *Biochemical and Biophysical Research Communications*, 1994. **200**(3): p. 1650-1657.
84. Studer, L., M. Csete, S.H. Lee, N. Kabbani, J. Walikonis, B. Wold, and R. McKay, *Enhanced proliferation, survival, and dopaminergic differentiation of CNS precursors in lowered oxygen*. *Journal of Neuroscience*, 2000. **20**(19): p. 7377-7383.

85. Lin, Q., Y.-J. Lee and Z. Yun, *Differentiation Arrest by Hypoxia*. Journal of Biological Chemistry, 2006. **281**(41): p. 30678-30683.
86. Ezashi, T., P. Das and R.M. Roberts, *Low O<sub>2</sub> tensions and the prevention of differentiation of hES cells*. PNAS, 2005. **102**(13): p. 4783-4788.
87. Bernaudin, M., Y. Tang, M. Reilly, E. Petit and F.R. Sharp, *Brain genomic response following hypoxia and re-oxygenation in the neonatal rat - Identification of genes that might contribute to hypoxia-induced ischemic tolerance*. Journal of Biological Chemistry, 2002. **277**(42): p. 39728-39738.
88. Hur, E., H.H. Kim, S.M. Choi, J.H. Kim, S. Yim, et al., *Reduction of hypoxia-induced transcription through the repression of hypoxia-inducible factor-1 alpha/aryl hydrocarbon receptor nuclear translocator DNA binding by the 90-kDa heat- shock protein inhibitor radicicol*. Molecular Pharmacology, 2002. **62**(5): p. 975-982.
89. Laderoute, K.R., H.L. Mendonca, J.M. Calaoagan, A.M. Knapp, A.J. Giaccia, and P.J.S. Stork, *Mitogen-activated protein kinase phosphatase-1 (MKP-1) expression is induced by low oxygen conditions found in solid tumor microenvironments - A candidate MKP for the inactivation of hypoxia-inducible stress-activated protein kinase/c-Jun N- terminal protein kinase activity*. Journal of Biological Chemistry, 1999. **274**(18): p. 12890-12897.
90. Wenger, R.H., *Cellular adaptation to hypoxia: O<sub>2</sub>-sensing protein hydroxylases, hypoxia-inducible transcription factors, and O<sub>2</sub>-regulated gene expression*. FASEB Journal, 2002. **16**(10): p. 1151-1162.
91. Fandrey, J., *Hypoxia-Inducible Gene-Expression*. Respiration Physiology, 1995. **101**(1): p. 1-10.

92. Berger, S.A., *Signaling pathways influencing SLF and c-kit-mediated survival and proliferation*. Immunology Research, 2006. **35**(1-2): p. 1-12.
93. Lyman, S.D. and S.E.W. Jacobsen, *c-kit ligand and flt3 ligand: Stem/progenitor cell factors with overlapping yet distinct activities*. Blood, 1998. **91**(4): p. 1101-1134.
94. Huang, E., K. Nocka, D.R. Beier, T.Y. Chu, J. Buck, H.W. Lahm, D. Wellner, P. Leder, and P. Besmer, *The Hematopoietic Growth Factor-KL Is Encoded by the Sl Locus and Is the Ligand of the C-Kit Receptor, the Gene-Product of the W Locus*. Cell, 1990. **63**(1): p. 225-233.
95. McNiece, I.K. and K.M. Zsebo, *The Role of Stem-Cell Factor in the Hematopoietic System*. Cancer Investigation, 1993. **11**(6): p. 724-729.
96. Testa, U., E. Pelosi, M. Gabbianelli, C. Fossati, S. Campisi, G. Isacchi, and C. Peschle, *Cascade transactivation of growth factor receptors in early human hematopoiesis*. Blood, 1993. **81**(6): p. 1442-1456.
97. Hendrie, P.C., K. Miyazawa, Y.C. Yang, C.D. Langefeld and H.E. Broxmeyer, *Mast cell growth factor (c-kit ligand) enhances cytokine stimulation of proliferation of the human factor-dependent cell line, M07e*. Experimental Hematology, 1991. **19**(10): p. 1031-1037.
98. Marziali, G., D. Lazzaro and V. Sorrentino, *Binding of Germ Cells to Mutant Sld Sertoli Cells Is Defective and Is Rescued by Expression of the Transmembrane Form of the c-kit Ligand*. Developmental Biology, 1993. **157**(1): p. 182-190.
99. Hulzinga, J.D., L. Thuneberg, M. Kluppel, J. Malysz, H.B. Mikkelsen, and A. Bernstein, *W/kit gene required for interstitial cells of Cajal and for intestinal pacemaker activity*. Nature, 1995. **373**(6512): p. 347.

100. Kapur, R., E.T. Everett, J. Uffman, M. McAndrews-Hill, R. Cooper, J. Ryder, T. Vik, and D.A. Williams, *Overexpression of Human Stem Cell Factor Impairs Melanocyte, Mast Cell, and Thymocyte Development: A Role for Receptor Tyrosine Kinase-Mediated Mitogen Activated Protein Kinase Activation in Cell Differentiation*. *Blood*, 1997. **90**(8): p. 3018-3026.
101. Wehrle-Haller, B. and B.A. Imhof, *Stem Cell Factor Presentation to c-Kit. IDENTIFICATION OF A BASOLATERAL TARGETING DOMAIN*. *Journal of Biological Chemistry*, 2001. **276**(16): p. 12667-12674.
102. Jin, K., X.O. Mao, Y.J. Sun, L. Xie and D.A. Greenberg, *Stem cell factor stimulates neurogenesis in vitro and in vivo*. *Journal of Clinical Investigation*, 2002. **110**(3): p. 311-319.
103. Motro, B., J.M. Wojtowicz, A. Bernstein and D. van der Kooy, *Steel mutant mice are deficient in hippocampal learning but not long-term potentiation*. *PNAS*, 1996. **93**(5): p. 1808-1813.
104. Copeland, N.G., D.J. Gilbert, B.C. Cho, P.J. Donovan, N.A. Jenkins, D. Cosman, D. Anderson, S.D. Lyman, and D.E. Williams, *Mast-Cell Growth-Factor Maps near the Steel Locus on Mouse Chromosome-10 and Is Deleted in a Number of Steel Alleles*. *Cell*, 1990. **63**(1): p. 175-183.
105. Geissler, E.N., M. Liao, J.D. Brook, F.H. Martin, K.M. Zsebo, D.E. Housman, and S.J. Galli, *Stem cell factor (SCF), a novel hematopoietic growth factor and ligand for c-kit tyrosine kinase receptor, maps on human chromosome 12 between 12q14.3 and 12qter*. *Somatic Cell and Molecular Genetics*, 1991. **17**(2): p. 207-214.

106. Anderson, D.M., D.E. Williams, R. Tushinski, S. Gimpel, J. Eisenman, et al., *Alternate splicing of mRNAs encoding human mast cell growth factor and localization of the gene to chromosome 12q22-q24*. *Cell Growth & Differentiation*, 1991. **2**(8): p. 373-378.
107. Arakawa, T., K.E. Langley, K. Kameyama and T. Takagi, *Molecular-Weights of Glycosylated and Nonglycosylated Forms of Recombinant Human Stem-Cell Factor Determined by Low-Angle Laser-Light Scattering*. *Analytical Biochemistry*, 1992. **203**(1): p. 53-57.
108. Lu, H., C. Clogston, J. Wypych, P. Fausset, S. Lauren, E. Mendiaz, K. Zsebo, and K. Langley, *Amino acid sequence and post-translational modification of stem cell factor isolated from buffalo rat liver cell-conditioned medium*. *Journal of Biological Chemistry*, 1991. **266**(13): p. 8102-8107.
109. Langley, K.E., E.A. Mendiaz, N.L. Liu, L.O. Narhi, L. Zeni, et al., *Properties of Variant Forms of Human Stem Cell Factor Recombinantly Expressed in Escherichia Coli*. *Archives of Biochemistry and Biophysics*, 1994. **311**(1): p. 55-61.
110. Jones, M.D., L.O. Narhi, W.C. Chang and H.S. Lu, *Refolding and oxidation of recombinant human stem cell factor produced in Escherichia coli*. *Journal of Biological Chemistry*, 1996. **271**(19): p. 11301-11308.
111. Arakawa, T., D.A. Yphantis, J.W. Lary, L.O. Narhi, H.S. Lu, et al., *Glycosylated and Unglycosylated Recombinant-Derived Human Stem- Cell Factors Are Dimeric and Have Extensive Regular Secondary Structure*. *Journal of Biological Chemistry*, 1991. **266**(28): p. 18942-18948.

112. Martin, F.H., S.V. Suggs, K.E. Langley, H.S. Lu, J. Ting, et al., *Primary Structure and Functional Expression of Rat and Human Stem-Cell Factor Dnas*. *Cell*, 1990. **63**(1): p. 203-211.
113. Hsu, Y.R., G.M. Wu, E.A. Mendiaz, R. Syed, J. Wypych, et al., *The majority of stem cell factor exists as monomer under physiological conditions*. *Journal of Biological Chemistry*, 1997. **272**(10): p. 6406-6415.
114. Langley, K.E., L.G. Bennett, J. Wypych, S.A. Yancik, X.D. Liu, K.R. Westcott, D.G. Chang, K.A. Smith, and K.M. Zsebo, *Soluble Stem Cell Factor in Human Serum*. *Blood*, 1993. **81**(3): p. 656-660.
115. Lu, H.S., W.C. Chang, E.A. Mendiaz, M.B. Mann, K.E. Langley, and Y.R. Hsu, *Spontaneous Dissociation Association of Monomers of the Human Stem Cell Factor Dimer*. *Biochemical Journal*, 1995. **305**: p. 563-568.
116. Zhang, Z.T., R.G. Zhang, A. Joachimiak, J. Schlessinger and X.P. Kong, *Crystal structure of human stem cell factor: Implication for stem cell factor receptor dimerization and activation*. *Proceedings of the National Academy of Sciences of the United States of America*, 2000. **97**(14): p. 7732-7737.
117. Tajima, Y., E.J. Huang, K. Vosseller, M. Ono, M.A.S. Moore, and P. Besmer, *Role of Dimerization of the Membrane-associated Growth Factor Kit Ligand in Juxtacrine Signaling: The SL17H Mutation Affects Dimerization and Stability---Phenotypes in Hematopoiesis*. *Journal of Experimental Medicine*, 1998. **187**(9): p. 1451-1461.

118. Kapur, R., R. Cooper, X.L. Xiao, M.J. Weiss, P. Donovan, and D.A. Williams, *The presence of novel amino acids in the cytoplasmic domain of stem cell factor results in hematopoietic defects in Steel(17H) mice*. Blood, 1999. **94**(6): p. 1915-1925.
119. Kinashi, T. and T. Springer, *Steel factor and c-kit regulate cell-matrix adhesion*. Blood, 1994. **83**(4): p. 1033-1038.
120. Sasaki, K., K. Ikeda, K. Ogami, J. Takahara and S. Irino, *Cell-to-cell interaction of cytokine-dependent myeloblastic line constitutively expressing membrane-bound stem cell factor abrogates cytokine dependency partially through granulocyte-macrophage colony-stimulating factor production*. Blood, 1995. **85**(5): p. 1220-1228.
121. Krieger, M.S., C. Nissen, C.Y. Manz, D. Toksoz, S.D. Lyman, and A. Wodnar-Filipowicz, *The membrane-bound isoform of stem cell factor synergizes with soluble flt3 ligand in supporting early hematopoietic cells in long-term cultures of normal and aplastic anemia bone marrow*. Experimental Hematology, 1998. **26**(5): p. 365-373.
122. Caruana, G., L.K. Ashman, J. Fujita and T.J. Gonda, *Responses of the murine myeloid cell line FDC-P1 to soluble and membrane-bound forms of steel factor (SLF)*. Experimental Hematology, 1993. **21**(6): p. 761-768.
123. Kurosawa, K., K. Miyazawa, A. Gotoh, T. Katagiri, J. Nishimaki, L.K. Ashman, and K. Toyama, *Immobilized anti-KIT monoclonal antibody induces ligand-independent dimerization and activation of steel factor receptor: Biologic similarity with membrane-bound form of steel factor rather than its soluble form*. Blood, 1996. **87**(6): p. 2235-2243.
124. Doheny, J.G., E.J. Jervis, M.M. Guarna, R.K. Humphries, R.A.J. Warren, and D.G. Kilburn, *Cellulose as an inert matrix for presenting cytokines to target cells: production*

- and properties of a stem cell factor- cellulose-binding domain fusion protein.*  
Biochemical Journal, 1999. **339**: p. 429-434.
125. Jervis, E.J., M.M. Guarna, J.G. Doheny, H. C.A. and D.G. Kilburn, *Dynamic localization and persistent stimulation of factor-dependent cells by a stem cell factor / cellulose binding domain fusion protein.* Biotechnology and Bioengineering, 2005. **91**(3): p. 314-324.
126. Erben, U., E. Thiel and M. Notter, *Differential effects of a stem cell factor-immunoglobulin fusion protein on malignant and normal hematopoietic cells.* Cancer Research, 1999. **59**(12): p. 2924-2930.
127. Qiu, F.H., P. Ray, K. Brown, P.E. Barker, S. Jhanwar, F.H. Ruddle, and P. Besmer, *Primary structure of c-kit: relationship with the CSF-1/PDGF receptor kinase family-- oncogenic activation of v-kit involves deletion of extracellular domain and C terminus.* EMBO Journal, 1988. **7**(4): p. 1003-11.
128. Yarden, Y., W.J. Kuang, T. Yang-Feng, L. Coussens, S. Munemitsu, et al., *Human proto-oncogene c-kit: a new cell surface receptor tyrosine kinase for an unidentified ligand.* EMBO Journal, 1987. **6**(11): p. 3341-51.
129. Olsson, I., U. Gullberg, M. Lantz and J. Richter, *The Receptors for Regulatory Molecules of Hematopoiesis.* European Journal of Haematology, 1992. **48**(1): p. 1-9.
130. Lemmon, M.A., D. Pinchasi, M. Zhou, I. Lax and J. Schlessinger, *Kit receptor dimerization is driven by bivalent binding of stem cell factor.* Journal of Biological Chemistry, 1997. **272**(10): p. 6311-6317.

131. Ashman, L.K., A.C. Cambareri, L.B. To, R.J. Levinsky and C.A. Juttner, *Expression of the YB5.B8 antigen (c-kit proto-oncogene product) in normal human bone marrow*. Blood, 1991. **78**(1): p. 30-37.
132. Papayannopoulou, T., M. Brice, V.C. Broudy and K.M. Zsebo, *Isolation of c-kit receptor-expressing cells from bone marrow, peripheral blood, and fetal liver: functional properties and composite antigenic profile*. Blood, 1991. **78**(6): p. 1403-1412.
133. To, L.B., D.N. Haylock, T. Dowse, P.J. Simmons, S. Trimboli, L.K. Ashman, and C.A. Juttner, *A Comparative Study of the Phenotype and Proliferative Capacity of Peripheral-Blood (PB) CD34+ Cells Mobilized by 4 Different Protocols and Those of Steady-Phase PB and Bone-Marrow CD34+ Cells*. Blood, 1994. **84**(9): p. 2930-2939.
134. Philo, J.S., J. Wen, J. Wypych, M.G. Schwartz, E.A. Mendiaz, and K.E. Langley, *Human stem cell factor dimer forms a complex with two molecules of the extracellular domain of its receptor, kit*. Journal of Biological Chemistry, 1996. **271**(12): p. 6895-6902.
135. Lu, H.S., M.D. Jones, J.H. Shieh, E.A. Mendiaz, D. Feng, P. Watler, L.O. Narhi, and K.E. Langley, *Isolation and characterization of a disulfide-linked human stem cell factor dimer - Biochemical, biophysical, and biological comparison to the noncovalently held dimer*. Journal of Biological Chemistry, 1996. **271**(19): p. 11309-11316.
136. Wandzioch, E., C.E. Edling, R.H. Palmer, L. Carlsson and B. Hallberg, *Activation of the MAP kinase pathway by c-Kit is PI-3 kinase dependent in hematopoietic progenitor/stem cell lines*. Blood, 2004. **104**(1): p. 51-57.
137. Linnekin, D., *Early signaling pathways activated by c-Kit in hematopoietic cells*. International Journal of Biochemistry & Cell Biology, 1999. **31**(10): p. 1053-1074.

138. Radosevic, N., D. Winterstein, J.R. Keller, H. Neubauer, K. Pfeffer, and D. Linnekin, *JAK2 contributes to the intrinsic capacity of primary hematopoietic cells to respond to stem cell factor*. *Experimental Hematology*, 2004. **32**(2): p. 149-156.
139. Weiler, S.R., S. Mou, C.S. DeBerry, J.R. Keller, F.W. Ruscetti, D.K. Ferris, D.L. Longo, and D. Linnekin, *JAK2 is associated with the c-kit proto-oncogene product and is phosphorylated in response to stem cell factor*. *Blood*, 1996. **87**(9): p. 3688-3693.
140. Brizzi, M.F., M.G. Zini, M.G. Aronica, J.M. Blechman, Y. Yarden, and L. Pegoraro, *Convergence of signaling by interleukin-3, granulocyte-macrophage colony-stimulating factor, and mast cell growth factor on JAK2 tyrosine kinase*. *Journal of Biological Chemistry*, 1994. **269**(50): p. 31680-31684.
141. Gommerman, J.L., D. Sitaro, N.Z. Klebasz, D.A. Williams and S.A. Berger, *Differential stimulation of c-Kit mutants by membrane-bound and soluble Steel Factor correlates with leukemic potential*. *Blood*, 2000. **96**(12): p. 3734-3742.
142. Trieselmann, N.Z., J. Soboloff and S.A. Berger, *Mast cells stimulated by membrane-bound, but not soluble, steel factor are dependent on phospholipase C activation*. *Cellular and Molecular Life Sciences*, 2003. **60**(4): p. 759-766.
143. Kapur, R., S. Chandra, R. Cooper, J. McCarthy and D.A. Williams, *Role of p38 and ERK MAP kinase in proliferation of erythroid progenitors in response to stimulation by soluble and membrane isoforms of stem cell factor*. *Blood*, 2002. **100**(4): p. 1287-1293.
144. Kaushansky, K., *Thrombopoietin and the Hematopoietic Stem Cell*. *Annals of the New York Academy of Sciences*, 2005. **1044**(1): p. 139-141.

145. Solar, G.P., W.G. Kerr, F.C. Zeigler, D. Hess, C. Donahue, F.J. de Sauvage, and D.L. Eaton, *Role of c-mpl in Early Hematopoiesis*. Blood, 1998. **92**(1): p. 4-10.
146. Ballmaier, M., M. Germeshausen, S. Krukemeier and K. Welte, *Thrombopoietin Is Essential for the Maintenance of Normal Hematopoiesis in Humans. Development of Aplastic Anemia in Patients with Congenital Amegakaryocytic Thrombocytopenia*. Annals of the New York Academy of Sciences, 2003. **996**(1): p. 17-25.
147. Kaushansky, K., *Thrombopoietin*. The New England Journal of Medicine, 1998. **339**(11): p. 746-754.
148. Geddis, A.E., H.M. Linden and K. Kaushansky, *Thrombopoietin: a pan-hematopoietic cytokine*. Cytokine & Growth Factor Reviews, 2002. **13**(1): p. 61-73.
149. Haznedaroglu, I.C., H. Goker, M. Turgut, Y. Buyukasik and M. Benekli, *Thrombopoietin as a Drug: Biologic Expectations, Clinical Realities, and Future Directions*. Clin Appl Thromb Hemost, 2002. **8**(3): p. 193-212.
150. Hoffman, R.C., H. Andersen, K. Walker, J.D. Krakover, S. Patel, M.R. Stamm, and S.G. Osborn, *Peptide, Disulfide, and Glycosylation Mapping of Recombinant Human Thrombopoietin from Ser1 to Arg246*. Biochemistry, 1996. **35**(47): p. 14849-14861.
151. Kuter, D.J. and C.G. Begley, *Recombinant human thrombopoietin: basic biology and evaluation of clinical studies*. Blood, 2002. **100**(10): p. 3457-3469.
152. Kaushansky, K., *Hematopoietic Stem Cells, Progenitors, and Cytokines*, in *Williams Hematology*, M.A. Lichtman, et al., Editors. 2006, McGraw-Hill, Medical Publications Division: New York.

153. Lok, S., K. Kaushansky, R.D. Holly, J.L. Kuijper, C.E. Lofton-Day, et al., *Cloning and expression of murine thrombopoietin cDNA and stimulation of platelet production in vivo*. *Nature*, 1994. **369**(6481): p. 565.
154. Qian, S., F. Fu, W. Li, Q. Chen and F.J. de Sauvage, *Primary Role of the Liver in Thrombopoietin Production Shown by Tissue-Specific Knockout*. *Blood*, 1998. **92**(6): p. 2189-2191.
155. Kaushansky, K., *Signal Transduction Pathways: An Overview*, in *Williams Hematology*, M.A. Lichtman, et al., Editors. 2006, McGraw-Hill, Medical Publications Division: New York.
156. Drachman, J.G., P. Rojnuckarin and K. Kaushansky, *Thrombopoietin Signal Transduction: Studies from Cell Lines and Primary Cells*. *Methods*, 1999. **17**(3): p. 238.
157. Majka, M., J. Ratajczak, G. Villaire, K. Kubiczek, L.A. Marquez, A. Janowska-Wieczorek, and M.Z. Ratajczak, *Thrombopoietin, but not cytokines binding to gp130 protein-coupled receptors, activates MAPKp42/44, AKT, and STAT proteins in normal human CD34+ cells, megakaryocytes, and platelets*. *Experimental Hematology*, 2002. **30**(7): p. 751-760.
158. Kirito, K., N. Fox and K. Kaushansky, *Thrombopoietin stimulates Hoxb4 expression: an explanation for the favorable effects of TPO on hematopoietic stem cells*. *Blood*, 2003. **102**(9): p. 3172-3178.
159. Kirito, K., N. Fox and K. Kaushansky, *Thrombopoietin Induces HOXA9 Nuclear Transport in Immature Hematopoietic Cells: Potential Mechanism by Which the*

- Hormone Favorably Affects Hematopoietic Stem Cells*. Mol. Cell. Biol., 2004. **24**(15): p. 6751-6762.
160. Lawrence, H.J., J. Christensen, S. Fong, Y.-L. Hu, I. Weissman, G. Sauvageau, R.K. Humphries, and C. Largman, *Loss of expression of the Hoxa-9 homeobox gene impairs the proliferation and repopulating ability of hematopoietic stem cells*. Blood, 2005. **106**(12): p. 3988-3994.
161. Lawrence, H.J., G. Sauvageau, R.K. Humphries and C. Largman, *The role of HOX homeobox genes in normal and leukemic hematopoiesis*. Stem Cells, 1996. **14**(3): p. 281-291.
162. Vijayendran, R.A. and D.E. Leckband, *A Quantitative Assessment of Heterogeneity for Surface-Immobilized Proteins*. Analytical Chemistry, 2001. **73**(3): p. 471-480.
163. Firestone, M.A., M.L. Shank, S.G. Sligar and P.W. Bohn, *Film architecture in biomolecular assemblies. Effect of linker on the orientation of genetically engineered surface-bound proteins*. Journal of the American Chemical Society, 1996. **118**(38): p. 9033-9041.
164. Gaberc-Porekar, V. and V. Menart, *Potential for Using Histidine Tags in Purification of Proteins at Large Scale*. Chemical Engineering & Technology, 2005. **28**(11): p. 1306-1314.
165. Kato, K., H. Sato and H. Iwata, *Immobilization of Histidine-Tagged Recombinant Proteins onto Micropatterned Surfaces for Cell-Based Functional Assays*. Langmuir, 2005. **21**(16): p. 7071-7075.

166. Lata, S. and J. Piehler, *Stable and Functional Immobilization of Histidine-Tagged Proteins via Multivalent Chelator Headgroups on a Molecular Poly(ethylene glycol) Brush*. Analytical Chemistry, 2005. **77**(4): p. 1096-1105.
167. Zhen, G., V. Eggli, J. Voros, P. Zammaretti, M. Textor, R. Glockshuber, and E. Kuennemann, *Immobilization of the Enzyme  $\beta$ -Lactamase on Biotin-Derivatized Poly(L-lysine)-g-poly(ethylene glycol)-Coated Sensor Chips: A Study on Oriented Attachment and Surface Activity by Enzyme Kinetics and in Situ Optical Sensing*. Langmuir, 2004. **20**(24): p. 10464-10473.
168. Huang, N.P., J. Voros, S.M. De Paul and M. Textor, *Biotin-Derivatized Poly(L-lysine)-g-poly(ethylene glycol): A Novel Polymeric Interface for Bioaffinity Sensing*. Langmuir, 2002. **18**(1): p. 220-230.
169. Chilkoti, A. and J.A. Hubbell, *Biointerface Science*. MRS Bulletin, 2005. **30**(3): p. 175-176.
170. Kingshott, P. and H.J. Griesser, *Surfaces that resist bioadhesion*. Current Opinion in Solid State and Materials Science, 1999. **4**(4): p. 403-412.
171. Dalsin, J.L., B.H. Hu, B.P. Lee and P.B. Messersmith, *Mussel adhesive protein mimetic polymers for the preparation of nonfouling surfaces*. Journal of the American Chemical Society, 2003. **125**(14): p. 4253-4258.
172. Dalsin, J.L. and P.B. Messersmith, *Surface modification for protein resistance using a biomimetic approach*. Material Research Society Symposium Proceedings, 2002. **774**: p. 75-80.

173. Vermette, P. and L. Meagher, *Interactions of phospholipid- and poly(ethylene glycol)-modified surfaces with biological systems: relation to physico-chemical properties and mechanisms*. Colloids and Surfaces B: Biointerfaces, 2003. **28**(2-3): p. 153-198.
174. Leckband, D., S. Sheth and A. Halpern, *Grafted poly(ethylene oxide) brushes as nonfouling surface coatings*. Journal of Biomaterials Science -- Polymer Edition, 1999. **10**(10): p. 1125-1147.
175. Kimura, T., H. Kaburaki, S. Miyamoto, J. Katayama and Y. Watanabe, *Discovery of a novel thrombopoietin mimic agonist peptide*. The Journal of Biochemistry, 1997. **122**(5): p. 1046-1051.
176. Duffy, K.J., M.G. Darcy, E. Delorme, S.B. Dillon, D.F. Eppley, et al., *Hydrazinonaphthalene and azonaphthalene thrombopoietin mimics are nonpeptidyl promoters of megakaryocytopoiesis*. Journal of Medicinal Chemistry, 2001. **44**(22): p. 3730-3745.
177. Erickson-Miller, C.L., E. DeLorme, S.-S. Tian, C.B. Hopson, K. Stark, et al., *Discovery and characterization of a selective, nonpeptidyl thrombopoietin receptor agonist*. Experimental Hematology, 2005. **33**(1): p. 85-93.
178. Kimura, T., H. Kaburaki, T. Tsujino, Y. Ikeda, H. Kato, and Y. Watanabe, *A non-peptide compound which can mimic the effect of thrombopoietin via c-Mpl*. FEBS Letters, 1998. **428**(3): p. 250-254.

179. Sakai, R., T. Nakamura, T. Nishino, M. Yamamoto, A. Miyamura, et al., *Xanthocillins as thrombopoietin mimetic small molecules*. *Bioorganic & Medicinal Chemistry*, 2005. **13**(23): p. 6388-6393.
180. Sackmann, E., *Supported Membranes: Scientific and Practical Applications*. Science, 1996. **271**(5245): p. 43-48.
181. Plant, A.L., *Supported Hybrid Bilayer Membranes as Rugged Cell Membrane Mimics*. *Langmuir*, 1999. **15**(15): p. 5128-5135.
182. Hubbard, J.B., V. Silin and A.L. Plant, *Self assembly driven by hydrophobic interactions at alkanethiol monolayers: mechanism of formation of hybrid bilayer membranes*. *Biophysical Chemistry*, 1998. **75**(3): p. 163.
183. Kaladhar, K. and C.P. Sharma, *Supported Cell Mimetic Monolayers and Their Interaction with Blood*. *Langmuir*, 2004. **20**(25): p. 11115-11122.
184. Jensen, T.W., *Controlled High-Affinity Ligand Presentation in Engineered Hybrid Bilayer Membrane Cell Culture Surfaces*, in *Chemical Engineering Department*. 2004, Northwestern University: Evanston, IL. p. 1-257.
185. Fuller, W.D., M.S. Verlander and M. Goodman, *DOPA-containing polypeptides. I. Improved synthesis of high-molecular-weight poly(L-DOPA) and water-soluble copolypeptides*. *Biopolymers*, 1978. **17**(12): p. 2939-2943.
186. Lee, B.P., C.Y. Chao, F.N. Nunalee, E. Motan, K.R. Shull, and P.B. Messersmith, *Rapid Gel Formation and Adhesion in Photocurable and Biodegradable Block Copolymers with High DOPA Content*. *Macromolecules*, 2006. **39**(5): p. 1740-1748.

187. Collins, P.C., L.K. Nielsen, C.K. Wong, E.T. Papoutsakis and W.M. Miller, *Real-time method for determining the colony-forming cell content of human hematopoietic cell cultures*. Biotechnology and Bioengineering, 1997. **55**(4): p. 693-700.
188. Lin, S.Y., J.D. Liu, H.C. Chang, S.D. Yeh, C.H. Lin, and W.S. Lee, *Magnolol suppresses proliferation of cultured human colon and liver cancer cells by inhibiting DNA synthesis and activating apoptosis*. Journal of Cellular Biochemistry, 2002. **84**(3): p. 532-544.
189. Giammona, L.M., P.G. Fuhrken, E.T. Papoutsakis and W.M. Miller, *Nicotinamide (vitamin B3) increases the polyploidization and proplatelet formation of cultured primary human megakaryocytes*. British Journal of Haematology, 2006. **135**(4): p. 554-566.
190. Chow, S., H. Patel and D.W. Hedley, *Measurement of MAP kinase activation by flow cytometry using phospho-specific antibodies to MEK and ERK: Potential for pharmacodynamic monitoring of signal transduction inhibitors*. Cytometry, 2001. **46**(2): p. 72-78.
191. Oostendorp, R.A.J., J. Audet, C. Miller and C.J. Eaves, *Cell division tracking and expansion of hematopoietic long-term repopulating cells*. Leukemia, 1999. **13**(4): p. 499-501.
192. Glimm, H. and C.J. Eaves, *Direct evidence for multiple self-renewal divisions of human in vivo repopulating hematopoietic cells in short-term culture*. Blood, 1999. **94**(7): p. 2161-2168.
193. Arai, F., A. Hirao, M. Ohmura, H. Sato, S. Matsuoka, K. Takubo, K. Ito, G.Y. Koh, and T. Suda, *Tie2/Angiopoietin-1 Signaling Regulates Hematopoietic Stem Cell Quiescence in the Bone Marrow Niche*. Cell, 2004. **118**(2): p. 149-161.

194. Bradley, T.R., G.S. Hodgson and M. Rosendaal, *Effect of Oxygen Tension on Hematopoietic and Fibroblast Cell Proliferation In vitro*. Journal of Cellular Physiology, 1978. **97**(3): p. 517-522.
195. Koller, M.R., J.G. Bender, W.M. Miller and E.T. Papoutsakis, *Reduced Oxygen-Tension Increases Hematopoiesis in Long-Term Culture of Human Stem and Progenitor Cells from Cord Blood and Bone-Marrow*. Experimental Hematology, 1992. **20**(2): p. 264-270.
196. LaLuppa, J.A., E.T. Papoutsakis and W.M. Miller, *Oxygen tension alters the effects of cytokines on the megakaryocyte, erythrocyte, and granulocyte lineages*. Experimental Hematology, 1998. **26**(9): p. 835-843.
197. Lyons, A.B. and C.R. Parish, *Determination of Lymphocyte Division by Flow-Cytometry*. Journal of Immunological Methods, 1994. **171**(1): p. 131-137.
198. Krutzik, P.O. and G.P. Nolan, *Intracellular phospho-protein staining techniques for flow cytometry: Monitoring single cell signaling events*. Cytometry Part A, 2003. **55A**(2): p. 61-70.
199. Zandstra, P.W., E. Conneally, A.L. Petzer, J.M. Piret and C.J. Eaves, *Cytokine manipulation of primitive human hematopoietic cell self-renewal*. Proceedings of the National Academy of Sciences of the United States of America, 1997. **94**(9): p. 4698-4703.
200. Zandstra, P.W., E. Jarvis, C.A. Haynes, D.G. Kilburn, C.J. Eaves, and J.M. Piret, *Concentration-dependent internalization of a cytokine/cytokine receptor complex in human hematopoietic cells*. Biotechnology and Bioengineering, 1999. **63**(4): p. 493-501.

201. Kobayashi, M., J.H. Laver, T. Kato, H. Miyazaki and M. Ogawa, *Recombinant human thrombopoietin (Mpl ligand) enhances proliferation of erythroid progenitors*. *Blood*, 1995. **86**(7): p. 2494-2499.
202. Millot, G.A., W. Vainchenker, D. Dumenil and F. Svinarchuk, *Distinct effects of thrombopoietin depending on a threshold level of activated Mpl in BaF-3 cells*. *Journal of Cell Science*, 2002. **115**(11): p. 2329-2337.
203. Matsumura, I., K. Nakajima, H. Wakao, S. Hattori, K. Hashimoto, et al., *Involvement of Prolonged Ras Activation in Thrombopoietin-Induced Megakaryocytic Differentiation of a Human Factor-Dependent Hematopoietic Cell Line*. *Mol. Cell. Biol.*, 1998. **18**(7): p. 4282-4290.
204. Rouyez, M.C., C. Boucheron, S. Gisselbrecht, I. Dusanter-Fourt and F. Porteu, *Control of thrombopoietin-induced megakaryocytic differentiation by the mitogen-activated protein kinase pathway*. *Molecular and Cellular Biology*, 1997. **17**(9): p. 4991-5000.
205. LaIuppa, J.A., T.A. McAdams, E.T. Papoutsakis and W.M. Miller, *Culture materials affect ex vivo expansion of hematopoietic progenitor cells*. *Journal of Biomedical Materials Research*, 1997. **36**(3): p. 347-359.
206. Srour, E.F., X. Tong, K.W. Sung, P.A. Plett, S. Rice, J. Daggy, C.T. Yiannoutsos, R. Abonour, and C.M. Orschell, *Modulation of in vitro proliferation kinetics and primitive hematopoietic potential of individual human CD34<sup>+</sup> CD38<sup>-/lo</sup> cells in G<sub>0</sub>*. *Blood*, 2005. **105**(8): p. 3109-3116.
207. Case, B.C., M.L. Hauck, R.L. Yeager, A.H. Simkins, M. de Serres, V.D. Schmith, J.E. Dillberger, and R.L. Page, *The Pharmacokinetics and Pharmacodynamics of GW395058*,

- a Peptide Agonist of the Thrombopoietin Receptor, in the Dog, a Large-Animal Model of Chemotherapy-Induced Thrombocytopenia.* Stem Cells, 2000. **18**(5): p. 360-365.
208. De Serres, M., B. Ellis, J.E. Dillberger, S.K. Rudolph, J.T. Hutchins, C.M. Boytos, D.L. Weigl, and R.B. DePrince, *Immunogenicity of Thrombopoietin Mimetic Peptide GW395058 in BALB/c Mice and New Zealand White Rabbits: Evaluation of the Potential for Thrombopoietin Neutralizing Antibody Production in Man.* Stem Cells, 1999. **17**(4): p. 203-209.
209. De Serres, M., R.L. Yeager, J.E. Dillberger, G. Lalonde, G.H. Gardner, et al., *Pharmacokinetics and Hematological Effects of the PEGylated Thrombopoietin Peptide Mimetic GW395058 in Rats and Monkeys After Intravenous or Subcutaneous Administration.* Stem Cells, 1999. **17**(6): p. 316-326.
210. Quentmeier, H., M. Zaborski and H.G. Drexler, *Effects of thrombopoietin, interleukin-3 and the kinase inhibitor K-252a on growth and polyploidization of the megakaryocytic cell line M-07e.* Leukemia, 1998. **12**(10): p. 1603-1611.
211. Inagaki, K., T. Oda, Y. Naka, H. Shinkai, N. Komatsu, and H. Iwamura, *Induction of megakaryocytopoiesis and thrombocytopoiesis by JTZ-132, a novel small molecule with thrombopoietin mimetic activities.* Blood, 2004. **104**(1): p. 58-64.
212. Kimura, T., H. Kaburaki, T. Tsujino, Y. Watanabe and H. Kato, *Signal transduction by the peptide which mimics the activity of thrombopoietin.* Biochemistry and Molecular Biology International, 1998. **44**(6): p. 1203-1209.

213. Duffy, K.J., A.N. Shaw, E. Delorme, S.B. Dillon, C. Erickson-Miller, et al., *Identification of a Pharmacophore for Thrombopoietic Activity of Small, Non-Peptidyl Molecules. 1. Discovery and Optimization of Salicylaldehyde Thiosemicarbazone Thrombopoietin Mimics*. Journal of Medicinal Chemistry, 2002. **45**(17): p. 3573-3575.
214. Liu, S.Q., Y. Ito and Y. Imanishi, *Cell growth on immobilized cell growth factor: I. Acceleration of the growth of fibroblast cells on insulin-immobilized polymer matrix in culture medium without serum*. Biomaterials, 1992. **13**(1): p. 50-58.
215. Chow, D.C., *Effects of Surface-Immobilized Stem Cell Factor on the Differentiation and Proliferation of Hematopoietic Cells*, in *Department of Chemical Engineering*. 2003, Northwestern University: Evanston, Illinois. p. 1-231.
216. Brinkley, M., *A brief survey of methods for preparing protein conjugates with dyes, haptens and crosslinking reagents*. Bioconjugate Chemistry, 1992. **3**(1): p. 2-13.
217. Waite, J.H. and M.L. Tanzer, *Polyphenolic Substance of Mytilus edulis: Novel Adhesive Containing L-Dopa and Hydroxyproline*. Science, 1981. **212**(4498): p. 1038-1040.
218. Waite, J.H. and M.L. Tanzer, *The bioadhesive of byssus: A protein containing L-DOPA*. Biochemical and Biophysical Research Communications, 1980. **96**(4): p. 1554-1561.
219. Dalsin, J.L., L.J. Lin, S. Tosatti, J. Voros, M. Textor, and P.B. Messersmith, *Protein resistance of titanium oxide surfaces modified by biologically inspired mPEG-DOPA*. Langmuir, 2005. **21**(2): p. 640-646.
220. Lee, H., N.F. Scherer and P.B. Messersmith, *Single-molecule mechanics of mussel adhesion*. Proceedings of the National Academy of Sciences of the United States of America, 2006. **103**(35): p. 12999-13003.

221. Gunawan, R.C., J.A. King, B. Lee, P.B. Messersmith and W.M. Miller, *Avidin-Mediated Ligand Presentation Using DOPA-Tethered, Biotinylated Poly(Ethylene Glycol)*. Langmuir, submitted.
222. Drayer, A.L., A.-K. Boer, E.L. Los, M.T. Esselink and E. Vellenga, *Stem Cell Factor Synergistically Enhances Thrombopoietin-Induced STAT5 Signaling in Megakaryocyte Progenitors through JAK2 and Src Kinase*. Stem Cells, 2005. **23**(2): p. 240-251.
223. Ramsfjell, V., D. Bryder, H. Bjorgvinsdottir, S. Kornfalt, L. Nilsson, O.J. Borge, and S.E.W. Jacobsen, *Distinct Requirements for Optimal Growth and In Vitro Expansion of Human CD34+CD38- Bone Marrow Long-Term Culture-Initiating Cells (LTC-IC), Extended LTC-IC, and Murine In Vivo Long-Term Reconstituting Stem Cells*. Blood, 1999. **94**(12): p. 4093-4102.
224. Peled, T., E. Glukhman, N. Hasson, S. Adi, H. Assor, et al., *Chelatable cellular copper modulates differentiation and self-renewal of cord blood-derived hematopoietic progenitor cells*. Experimental Hematology, 2005. **33**(10): p. 1092.
225. Peled, T., E. Landau, J. Mandel, E. Glukhman, N.R. Goudsmid, A. Nagler, and E. Fibach, *Linear polyamine copper chelator tetraethylenepentamine augments long-term ex vivo expansion of cord blood-derived CD34+ cells and increases their engraftment potential in NOD/SCID mice*. Experimental Hematology, 2004. **32**(6): p. 547.
226. Martin, G.R. and R.K. Jain, *Noninvasive Measurement of Interstitial Ph Profiles in Normal and Neoplastic Tissue Using Fluorescence Ratio Imaging Microscopy*. Cancer Research, 1994. **54**(21): p. 5670-5674.

227. Helmlinger, G., F. Yuan, M. Dellian and R.K. Jain, *Interstitial pH and pO<sub>2</sub> gradients in solid tumors in vivo: High-resolution measurements reveal a lack of correlation*. Nature Medicine, 1997. **3**(2): p. 177-182.
228. Kapur, R., R. Cooper, L. Zhang and D.A. Williams, *Cross-talk between  $\alpha_4\beta_1/\alpha_5\beta_1$  and c-Kit results in opposing effect on growth and survival of hematopoietic cells via the activation of focal adhesion kinase, mitogen-activated protein kinase, and Akt signaling pathways*. Blood, 2001. **97**(7): p. 1975-1981.
229. Gotoh, A., A. Ritchie, H. Takahira and H.E. Broxmeyer, *Thrombopoietin and erythropoietin activate inside-out signaling of integrin and enhance adhesion to immobilized fibronectin in human growth-factor-dependent hematopoietic cells*. Annals of Hematology, 1997. **75**(5-6): p. 207-213.
230. Fox, N.E. and K. Kaushansky, *Engagement of integrin  $\alpha_4\beta_1$  enhances thrombopoietin-induced megakaryopoiesis*. Experimental Hematology, 2005. **33**(1): p. 94-99.
231. Liu, H., K.M. Faucher, X.L. Sun, J. Feng, T.L. Johnson, J.M. Orban, R.P. Apkarian, R.A. Dluhy, and E.L. Chaikof, *A Membrane-Mimetic Barrier for Cell Encapsulation*. Langmuir, 2002. **18**(4): p. 1332-1339.
232. Sun, X.L., H. Liu, J.M. Orban, L. Sun and E.L. Chaikof, *Synthesis and Terminal Functionalization of a Polymerizable Phosphatidylethanolamine*. Bioconjugate Chemistry, 2001. **12**(5): p. 673-677.
233. Orban, J.M., K.M. Faucher, R.A. Dluhy and E.L. Chaikof, *Cytomimetic Biomaterials. 4. In-Situ Photopolymerization of Phospholipids on an Alkylated Surface*. Macromolecules, 2000. **33**(11): p. 4205-4212.

234. Wilson, J.T., W. Cui, X.-L. Sun, C. Tucker-Burden, C.J. Weber, and E.L. Chaikof, *In vivo biocompatibility and stability of a substrate-supported polymerizable membrane-mimetic film*. *Biomaterials*, 2007. **28**(4): p. 609.
235. Murphy, M.R., K.M. Faucher, X.-L. Sun, E.L. Chaikof and R.A. Dluhy, *Analysis of photoinitiated polymerization in a membrane mimetic film using infrared spectroscopy and near-IR Raman microscopy*. *Colloids and Surfaces B: Biointerfaces*, 2005. **46**(4): p. 226-232.
236. Marra, K.G., T.M. Winger, S.R. Hanson and E.L. Chaikof, *Cytomimetic biomaterials. I. In-situ polymerization of phospholipids on an alkylated surface*. *Macromolecules*, 1997. **30**(21): p. 6483-6488.
237. Dao, M.A. and C.M. Verfaillie, *Bone Marrow Microenvironment*, in *Hematology: basic principles and practice*, R. Hoffman, et al., Editors. 2005, Elsevier Science Health Science Division.
238. Reya, T., A.W. Duncan, L. Ailles, J. Domen, D.C. Scherer, K. Willert, L. Hintz, R. Nusse, and I.L. Weissman, *A role for Wnt signalling in self-renewal of haematopoietic stem cells*. *Nature*, 2003. **423**(6938): p. 409-414.
239. Willert, K., J.D. Brown, E. Danenberg, A.W. Duncan, I.L. Weissman, T. Reya, J.R. Yates, and R. Nusse, *Wnt proteins are lipid-modified and can act as stem cell growth factors*. *Nature*, 2003. **423**(6938): p. 448-452.
240. Bhatia, M., D. Bonnet, D.M. Wu, B. Murdoch, J. Wrana, L. Gallacher, and J.E. Dick, *Bone morphogenetic proteins regulate the developmental program of human hematopoietic stem cells*. *Journal of Experimental Medicine*, 1999. **189**(7): p. 1139-1147.

241. Collins, S.J., *The role of retinoids and retinoic acid receptors in normal hematopoiesis*. *Leukemia*, 2002. **16**(10): p. 1896-1905.
242. Milhem, M., N. Mahmud, D. Lavelle, H. Araki, J. DeSimone, Y. Sauntharajah, and R. Hoffman, *Modification of hematopoietic stem cell fate by 5aza 2'deoxyctidine and trichostatin A*. *Blood*, 2004. **103**(11): p. 4102-4110.
243. DeFelice, L., C. Tatarelli, M.G. Mascolo, C. Gregorj, F. Agostini, et al., *Histone Deacetylase Inhibitor Valproic Acid Enhances the Cytokine-Induced Expansion of Human Hematopoietic Stem Cells*. *Cancer Research*, 2005. **65**(4): p. 1505-1513.
244. Bug, G., H. Gul, K. Schwarz, H. Pfeifer, M. Kampmann, et al., *Valproic Acid Stimulates Proliferation and Self-renewal of Hematopoietic Stem Cells*. *Cancer Res*, 2005. **65**(7): p. 2537-2541.